UNIVERSITY OF THE WITWATERSRAND, JOHANNESBURG

SCHOOL OF GEOSCIENCES
Faculty of Science

ASSESSMENT OF GROUNDWATER POTENTIAL IN THE EASTERN KALAHARI REGION, SOUTH AFRICA

Presented By: Bronwyn Jonker

Supervisor: Prof. Tamiru Abiye

School of Geosciences

A thesis submitted to the Faculty of Science, University of the Witwatersrand, Johannesburg, in fulfilment of the requirements for the degree of **Master of Science** (Dissertation)

Johannesburg, 2016

DECLARATION

This is to certify that the work contained within this thesis, presented to the University of the Witwatersrand in fulfilment of the requirements for the degree of Master of Science (Dissertation) in Hydrogeology, has been composed entirely by myself and is solely the result of my own work. This is my work in design and execution and all other material contained herein has been duly acknowledged. No part of this thesis has been submitted for any other degree or professional qualification at any other university.

____

Bronwyn Jonker

16/09/2016

____

Date

ACKNOWLEDGEMENTS

A great big thank you to my supervisor, Prof. Tamiru Abiye. Your guidance and constructive feedback during the course of the project is greatly appreciated. Your dedication and passion for this field of geology is truly admired.

I am really impressed with the quality and efficiency of the Department of Water Affairs. My requests for data were always promptly answered. Thank you for making your data available, it is an invaluable service you offer, one that cannot be done without in this field of study.

Thank you to iThemba Laboratories, particularly Mr. Mike Butler, for the processing of my environmental isotope samples. The additional reading that you so kindly suggested and provided proved very useful in trying to understand this field of study.

For all my geophysical and GIS-related maps, acknowledgement goes to the Council for Geoscience. Thank you.

Dr Jeremie Lehmann, a Senior Lecturer at the University of Johannesburg, thank you for putting up with all my GIS related queries, your friendliness and willingness to help is truly appreciated.

The readiness of all the farmers and municipal workers that allowed me access to their farms to sample from their boreholes is also appreciated. Your keen knowledge of the area proved very helpful, placing many unknowns into perspective.

To my wonderful husband, Ernst, and my two fantastic children, Aidan and Liam, a special thank you for the sacrifices that you had to make to see this project to its end. You make a brilliant field team, adding to the fun and excitement of this project.

ABSTRACT

The drought-stricken, eastern Kalahari region of South Africa is a water stressed region that is solely dependent on groundwater for its water supply. This resource is of primary importance in supplying safe drinking water to the inhabitants of both the towns and rural areas within this region, there being no other alternative. This situation can prove precarious, as the poorly understood complexities of the nature and behaviour of groundwater in this region has often led to over utilisation of the resource in some parts. The efficient and sustainable use of groundwater is paramount to ensure the sustainable and equitable development of the region. As such, an attempt was made to contribute to the understanding of the groundwater potential of this region by examining a number of the hydrogeological factors at play.

The total resource potential for the entire study area is estimated at 10,127.29 x 10^6 m^3/a, with the Kalahari aquifer showing the greatest potential in the study area, comprising 50.67 % of the total resource. The storage capability of the Kalahari aquifer (5478.52 x 10^6 m^3) is also impressive, estimated to be more than twice that of the dolomite (2727.99 x 10^6 m^3). This significant storage space of the Kalahari aquifer can allow groundwater recharge to be stored for several decades or even millennia, thereby providing a vital buffer against climate variability. Despite having such great potential, the aquifer is not actively recharged and is often associated with very saline water that is not suitable for human and livestock consumption. As such, although showing the most potential for storage, exploitation of this resource is restricted.

The limestones and dolomites of the Campbell Rand and Schmidtsdrif Subgroups are considered as the most prospective water bearing formations in the study area, largely owing to weathering and karstification processes that have made them prolific aquifers and have aided significantly in their resource potential estimated at approximately 1980.65 x 10^6 m^3/a. Although this area shows potential for higher yielding boreholes (> 5 l/s), this particular aquifer does not display hydraulic continuity, with poor water exchange between compartments, resulting in variations in yield and the amount of recharge available. Unlike the Kalahari, these aquifers cannot sustain abstraction through periods of drought, there being no natural regulation to their outflow, as such, caution has to be exercised over how much of the groundwater can in fact be abstracted from this aquifer.

The weathered granitic rocks of the Archaean basement within the south-central portion of the study area show favourable resource potential (1844.71 x 10^6 m^3/a) and are typically associated with the better quality groundwater in the study area. The groundwater has moderate salinity and is not as “hard” as the water associated with the karstic and Kalahari aquifers. Unfortunately, however, it is this aquifer that is commonly exploited, particularly for intensive irrigated agriculture. Although isotopic evidence suggests the presence of recent recharge, this aquifer receives most of its recharge from

the outcropping areas of the aquifer, with the remaining 70 % of the area being overlain by thick deposits (> 15 m) of Kalahari sediment, which retain a large amount of the recharge from where it is lost by evapotranspiration. As such, if this aquifer is to be utilised sustainably and its use ensured for future generations, stricter controls need to be placed on the volume of water abstracted, particularly by irrigated agriculture.

Aquifers with the least potential in the study area generally comprise the fractured basement rocks of the Kraaipan - Amalia greenstone belt, with a resource potential of 26.45 x 10^6 m^3/a, and the fractured sedimentary rocks of the Asbestos Hills Subgroup, with a resource potential of 108.33 x 10^6 m^3/a. While these aquifers offer poor prospects of securing large volumes of groundwater, with the groundwater being primarily confined to their fracture systems, these aquifers offer some of the best recharge areas within the study area. Their isotopic signature seems to suggest that recharge is taking place from the surrounding high ground, where surface and structural controls are responsible for the regional hydraulic continuity. Under favourable conditions, these aquifers may also recharge the adjacent karstic and granitic aquifers, where local structures enable limited lateral and vertical displacement.

Overall, the calculated groundwater storage and resource potential within the study area satisfies a large proportion of the water demand in the eastern Kalahari region of South Africa. If each aquifer could be sustainably utilised, a considerable volume of water could be abstracted at an assurance of supply similar to that of surface water. The emphasis, however, is placed on “sustainable exploitation”, as groundwater in this region is also vulnerable to quality degradation and over-exploitation. This often stems from the poorly understood nature of groundwater and the hydrogeological factors at play in the region. The key challenge, therefore, relates to the effective management of the resource, with all role players involved in this complex system working together to achieve the goal of maintaining the quality of the water and ensuring that it is used sustainably, protecting it for future generations.

TABLE OF CONTENTS

DECLARATION I
ACKNOWLEDGEMENTS II
ABSTRACT III
TABLE OF CONTENTS V
LIST OF FIGURES VIII
LIST OF TABLES XII
APPENDICES XIV
ABBREVIATIONS XV

1. INTRODUCTION 1
1.1 Background Review 1
1.2 Aims and Objectives 2
2. METHODOLOGY 4
2.1 Collation of Available Data 4
2.2 Hydrogeological Review 4
2.2.1 Storativity/Specific Yield Determinations 5
2.2.2 Aquifer Thickness Calculations 5
2.3 Groundwater Quality Assessment 6
2.3.1 pH 7
2.3.2 Temperature 7
2.3.3 Electrical Conductivity 7
2.3.4 Total Dissolved Solids 7
2.3.5 Total Hardness, Chloride and Nitrate (NO_3+NO_2-N) 8
2.3.6 Dissolved Oxygen (DO) 8
2.3.7 Bacterial Analysis 8
2.3.8 Biological Oxygen Demand (BOD) 9
2.4 Hydrochemical Assessment of the Groundwater 10
2.5 Measurement of Environmental Isotopes 10
2.5.1 Groundwater Sampling 11
2.5.2 Stable Isotope Analysis ($^{2}H/^{1}H$ and $^{18}O/^{16}O$) 11
2.5.3 Tritium Analysis 12
2.6 Quantification of Recharge 12
2.7 Storage and Resource Potential Calculations 14
2.7.1 Groundwater Storage Calculations 14
2.7.2 Groundwater Resource Potential Calculations 14
2.7.3 Groundwater Availability and Exploitation Estimation 15

3. THE PROJECT AREA 16
3.1 Location, Topography and Drainage 16
3.2 Climate 20
3.3 Vegetation and Land Use 20
4. GEOLOGICAL REVIEW 23
4.1 Granitoid Complexes 23
4.2 Kraaipan - Amalia Greenstone Belt Assemblages 25
4.3 Ventersdorp Supergroup 27
4.4 Transvaal Supergroup - Griqualand West Basin 27
4.5 Molopo Farms Complex 32
4.6 Olifantshoek Supergroup 32
4.7 Morokweng Impact Structure 34
4.8 Karoo Supergroup 34
4.9 Kalahari Sequence 35
4.10 Structural Review 40
5. HYDROGEOLOGICAL REVIEW 45
5.1 Geologically Defined Hydrogeological Units 45
5.1.1 Fractured Basement Aquifers (volcanic and meta-sedimentary) 45
5.1.2 Fractured and Weathered Crystalline Basement Aquifers 48
5.1.3 Fractured Sedimentary Rocks 48
5.1.4 Karstified Sedimentary Rocks 49
5.1.5 Intergranular Sedimentary Rocks 52
5.2 Storativity/Specific Yield 53
5.3 Groundwater Level and Saturated Aquifer Thickness 55
5.3.1 Unconfined, Intergranular Sedimentary Aquifers 55
5.3.2 Fractured and Weathered Aquifers 59
6. GROUNDWATER QUALITY 65
6.1 pH 65
6.2 Temperature 69
6.3 Electrical Conductivity 71
6.4 Total Dissolved Solids 73
6.5 Total Hardness 74
6.6 Chloride 75
6.7 Nitrate (NO_3+NO_2-N) 79
6.8 Dissolved Oxygen (DO) 80
6.9 Bacterial Analysis 82
6.10 Biological Oxygen Demand (BOD) 84
7. GROUNDWATER HYDROCHEMISTRY 86
7.1 Results 86

7.2 Discussion ... 90
8. ENVIRONMENTAL ISOTOPE ANALYSIS ... 92
8.1 Results ... 92
8.1.1 Stable Isotope analysis ($^{2}H/^{1}H$ and $^{18}O/^{16}O$) ... 92
8.1.2 Tritium Analysis ... 93
8.2 Age Relationships ... 95
8.3 Origin ... 96
8.4 Geology and Aquifer Connectivity ... 98
8.5 Recharge ... 101
9. GROUNDWATER POTENTIAL ... 105
9.1 Groundwater Storage ... 105
9.2 Recharge ... 119
9.2.1 Mean Annual Precipitation (MAP) ... 119
9.2.2 Concentration of Chloride in Rainfall and Groundwater ... 119
9.2.3 Chloride Mass Balance Calculation and Discussion ... 122
9.3 Groundwater Potential ... 126
9.3.1 Groundwater Resource Potential ... 126
9.3.2 Groundwater Availability and Exploitation ... 128
9.3.2.1 Fractured Basement Volcanic Aquifers ... 130
9.3.2.2 Fractured and Weathered Crystalline Basement Aquifers ... 131
9.3.2.3 Fractured Sedimentary Rocks ... 132
9.3.2.4 Karstified Sedimentary Rocks ... 134
9.3.2.5 Intergranular Sedimentary Rocks ... 135
10. DISCUSSION ... 138
10.1 Fractured Basement Aquifers (volcanic and meta-sedimentary) ... 138
10.2 Fractured and Weathered Crystalline Basement Aquifers ... 139
10.3 Fractured Sedimentary Aquifers ... 140
10.4 Karstic Aquifers ... 141
10.5 Intergranular Sedimentary Aquifers ... 142
11. CONCLUSIONS AND RECOMMENDATIONS ... 144
12. REFERENCES ... 147
13. APPENDICES ... 162

LIST OF FIGURES

Figure 3.1: Locality map showing the area of study relative to the South African provincial boundaries 16

Figure 3.2: The relatively flat and subdued topography of the eastern Kalahari. The hills in the background belong to the Asbestos Hills Subgroup which protrudes above the surrounding topography......... 17

Figure 3.3: Digital elevation model of the study area 18

Figure 3.4: The Lower Vaal Quaternary drainage areas within the region, showing the associated drainage pattern.. 19

Figure 3.5: The Molopo River in flood (February 2014) showing the abundance of vegetation occurring along the river channel 21

Figure 4.1: Sub-Kalahari geological map of the region (Data sourced from Haddon, 2005) 24

Figure 4.2: Flat, whaleback pavement of granite outcropping within the study area, with the inset showing an exposure of fresh granite 25

Figure 4.3: Highly deformed banded iron stone from the Kraaipan greenstone belt 26

Figure 4.4: Stratigraphy of the Ventersdorp Supergroup (after van der Westhuizen *et al.*, 2006).................... 28

Figure 4.5: Outcropping amygdaloidal lava of the Allanridge Formation 29

Figure 4.6: Stratigraphy of the Transvaal Supergroup (Griqualand West Basin) within the study area (after Erikson et al., 2006).. 30

Figure 4.7: Dolomite, limestone and chert layers from the Campbell Rand Subgroup 31

Figure 4.8: Banded iron stone from the Asbestos Hills Subgroup 31

Figure 4.9: Stratigraphy of the Olifantshoek Supergroup within the study area (after Moen, 2006) 33

Figure 4.10: A typical tillite deposit comprising boulders and cobbles (drop stones) which were dropped from floating ice into a melt water lake environment 35

Figure 4.11: Kalahari isopach map of the region (Data sourced from Haddon, 2005)...................................... 36

Figure 4.12: Typical stratigraphy of the Kalahari Supergroup within the study area (after Haddon, 2005) 38

Figure 4.13: The red clays of the Budin Formation overlying the poorly sorted gravels of the Wessels Formation (after Haddon, 2005) 39

Figure 4.14: An exposed section of calcrete within a river cutting 39

Figure 4.15: Total magnetic intensity map of the study area (Data sourced from the Council for Geoscience) 41

Figure 4.16: Gravity map of the study area (Data sourced from the Council for Geoscience) 42

Figure 5.1: The five aquifer storage types identified within the study area (Sub-Kalahari geological data sourced from Haddon, 2005) 46

Figure 5.2: The faulted and fractured amygdaloidal lavas of the Ventersdorp Supergroup exposed at surface 47

Figure 5.3: The faulted and fractured meta-sedimentary (BIF) rocks of the Kraaipan - Amalia greenstone belt. Note the vertical fractures typically associated with this hydrogeological unit. 47

Figure 5.4: Highly weathered and fractured granite typically occurring at shallow depths beneath the Kalahari sand cover 48

Figure 5.5: Fractures typically occurring along the bedding planes of the sedimentary units of the Asbestos Hills Subgroup, which is exposed along a resistant ridge stretching across the study area 49

Figure 5.6: Dissolution features observed along the fractures of exposed dolomite 50

Figure 5.7: The numerous faults and dykes encountered within the study area, superimposed over the sub-Kalahari geology (Structural and geological data sourced from Haddon, 2005; Aeromagnetic data sourced from the Council for Geoscience) 51

Figure 5.8: Jointing of the sandstones of the Eden Formation, with calcretisation of some of the weathered sandstone having taken place (after Haddon, 2005) 52

Figure 5.9 (A): Geological cross section A – B (Lithological data sourced from the Department of Water Affairs and the Council for Geoscience) 56

Figure 5.9 (B): Geological cross section B – C (Lithological data sourced from the Department of Water Affairs and the Council for Geoscience) 57

Figure 5.9 (C): Geological cross section D – E (Lithological data sourced from the Department of Water Affairs and the Council for Geoscience) 58

Figure 5.10 (i): Strike density graphs for the (A) Kraaipan – Amalia greenstone terrane (B) granite basement 60

Figure 5.10 (ii): Strike density graphs for the (C) Karst and (D) Fractured sediments (Transvaal) 61

Figure 5.10 (iii): Strike density graphs for the (E) Transvaal andesites and (F) Olifantshoek quartzites 62

Figure 5.10 (iv): Strike density graph for the (G) Dwyka tillite 63

Figure 6.1: The position of samples collected relative to the sub-Kalahari geology 66

Figure 6.2: pH map of the study area relative to the sub-Kalahari geology (Data sourced from DWAF NGANET) 68

Figure 6.3: Groundwater temperature map of the study area relative to the Kalahari isopach map (Data sourced from DWAF NGANET) ... 70

Figure 6.4: Electrical conductivity map relative to the (A) sub-Kalahari geology (B) Kalahari isopach map (Data sourced from DWAF NGANET) ... 72

Figure 6.5: Hardness map relative to the sub-Kalahari geology (Data from DWAF NGANET) ... 76

Figure 6.6: Chloride map of the study area relative to the sub-Kalahari geology (Data sourced from DWAF NGANET) ... 77

Figure 6.7: A plot of Na against Cl concentrations of groundwater in the region (R^2 of 0.82) relative to the line representing 1:1 Na:Cl ... 78

Figure 6.8: Nitrate map of the study area relative to the sub-Kalahari geology (Data sourced from DWAF NGANET) ... 81

Figure 6.9: Biological oxygen demand over time for those samples collected within the study area ... 85

Figure 7.1: The chemistry data (Piper) relative to the Quaternary drainage regions and the sub-Kalahari geology (Chemistry data sourced from DWAF NGANET) ... 87

Figure 7.2: The chemistry data (Piper Diagram) characteristic of the eastern portion of the study area ... 88

Figure 7.3: The chemistry data (Piper Diagram) characteristic of the central portion of the study area ... 89

Figure 7.4: The chemistry data (Piper) characteristic of the northern and western portion of the study area .. 90

Figure 8.1: Plot of the environmental isotope data on a $\delta^{18}O$ versus δD graph, relative to both the Local and Global Meteoric Water Lines ... 94

Figure 8.2: Plot of $\delta^{18}O$ versus Tritium for the samples collected ... 94

Figure 8.3: Plot of $\delta^{18}O$ versus δD for the samples collected, linked to the various aquifer types ... 99

Figure 8.4: The frequency distribution of $\delta^{18}O$ values in the project area relative to the various lithological units encountered ... 100

Figure 8.5: Potential areas of recharge based on the environmental isotope data collected for the region ... 102

Figure 9.1: The percent by volume held in storage by the respective hydrogeological units ... 107

Figure 9.2 (A): 0 – 30 m Aquifer storage map. Crosshatched areas are not saturated at this specific depth interval ... 108

Figure 9.2 (B): 30 – 60 m Aquifer storage map. Crosshatched areas are not saturated at this specific depth interval 109

Figure 9.2 (C): 60 – 90 m Aquifer storage map. Crosshatched areas are not saturated at this specific depth interval 110

Figure 9.2 (D): 90 – 120 m Aquifer storage map. Crosshatched areas are not saturated at this specific depth interval 111

Figure 9.2 (E): 120 – 150 m Aquifer storage map. Crosshatched areas are not saturated at this specific depth interval 112

Figure 9.2 (F): 150 – 180 m Aquifer storage map. Crosshatched areas are not saturated at this specific depth interval 113

Figure 9.2 (G): 180 – 210 m Aquifer storage map. Crosshatched areas are not saturated at this specific depth interval 114

Figure 9.2 (H): 210 – 240 m Aquifer storage map. Crosshatched areas are not saturated at this specific depth interval 115

Figure 9.3: Distribution of the acquired rainfall data 120

Figure 9.4: Distribution of the groundwater chloride data accessed from the NGANET 121

Figure 9.5: Groundwater recharge surface map relative to the sub-Kalahari geology 123

LIST OF TABLES

Table 5.1: Storativity/Specific yield values assigned to each hydrogeological unit 53

Table 5.2: The 30m interval saturated thicknesses of the Kalahari aquifer 55

Table 5.3: The saturated thicknesses calculated for the various lithological units 63

Table 6.1: The measured physical and chemical parameters of the 19 samples collected 67

Table 6.2: The measured biological parameters of samples collected 82

Table 8.1: Results of the environmental isotopic samples collected 93

Table 9.1: The storage volume calculated for the various lithological units 106

Table 9.2 (A): The storage volume calculated for the various lithological units within the depth interval 0 – 30m 108

Table 9.2 (B): The storage volume calculated for the various lithological units within the depth interval 30 – 60m 109

Table 9.2 (C): The storage volume calculated for the various lithological units within the depth interval 60 – 90m 110

Table 9.2 (D): The storage volume calculated for the various lithological units within the depth interval 90 – 120m 111

Table 9.2 (E): The storage volume calculated for the various lithological units within the depth interval 120 – 150m 112

Table 9.2 (F): The storage volume calculated for the various lithological units within the depth interval 150 – 180m 113

Table 9.2 (G): The storage volume calculated for the various lithological units within the depth interval 180 – 210m 114

Table 9.2 (H): The storage volume calculated for the various lithological units within the depth interval 210 – 240m 115

Table 9.3: The storage volumes determined for the different lithological units by summing the volumes calculated for each of the 30 m depth intervals 116

Table 9.4: Representative groundwater chloride concentrations for the study area 119

Table 9.5: Recharge values calculated for each of the hydrogeological units identified................................. 124

Table 9.6: Groundwater Resource Potential calculated for each of the hydrogeological units identified within the study area... 127

Table 9.7: Borehole yield and transmissivity values assigned to each hydrogeological unit 128

Table 9.8: The likely availability of accessible groundwater per borehole and per km^2 in each of the hydrogeological domains 129

APPENDICES

Appendix A: (i) Piper, (ii) Durov and (iii) Schoeller graphs for the respective Quaternary drainage regions within the study area……………………………………………………………………………….....163

Appendix B: Historical rainfall data………..……………………………………………………….………………....174

ABBREVIATIONS

BIF	Banded Iron Formation
BOD	Biological Oxygen Demand
CMB	Chloride Mass Balance
DEM	Digital Elevation Model
DO	Dissolved Oxygen
DWAF	Department of Water Affairs and Forestry
EC	Electrical Conductivity
EIG	Environmental Isotope Group
GIS	Geographical Information System
GMWL	Global Meteoric Water Line
GPS	Global Positioning System
LMWL	Local Meteoric Water Line
MAP	Mean Annual Precipitation
NGANET	National Groundwater Archive Network
NGIS	National Groundwater Information System
PLMWL	Pretoria Local Meteoric Water Line
SACS	South African Committee for Stratigraphy
SAWS	South African Weather Service
SMOW	Standard Mean Ocean Water
SRTM	Shuttle Radar Topography Mission
TDS	Total Dissolved Solids
TTG	Tonalite, Trondhjemite, Granodiorite
TU	Tritium Units
TWQR	Target Water Quality Range
USGS	United States Geological Survey

1. INTRODUCTION

Along the northern fringes of South Africa is the parched, semi-arid Kalahari, a vast region of sand and bush characterised by precipitation patterns that are unfavourably distributed in space and time, with high rates of evaporation. These conditions may be considered extreme, even challenging to those living in the region, yet the Kalahari remains a wilderness that is capable of sustaining life.

Groundwater is the precious commodity that remains the fundamental resource in allowing for life in this punishing environment. The agricultural sector, as well as growing urban and rural populations in the region, are solely dependent on this scarce resource as it is the only accessible water supply in the region. Given this, the efficient and sustainable use of groundwater is paramount to ensure the sustainable and equitable development of the region. Water resource management issues of this region, therefore, need to be given priority and properly managed by all stakeholders, particularly by the authorities and users. This can only be achieved by understanding the surface catchment and the hydrogeological nature of the underlying groundwater reserve.

An understanding of the limited groundwater resources of the region has proved to be difficult as the hydrogeology of the region is poorly understood. Failure of boreholes is common and there is little or no monitoring of groundwater levels and quality. This project, therefore, proposes to contribute to the understanding of the groundwater potential of this region by examining a number of hydrogeological factors at play. The geology of the region, structural controls, water quality and recharge history are among the most important controlling factors that were examined in order to determine the potential of the region with respect to the groundwater reserves. Characterisation of the groundwater reserve in relation to lithology, structures and other factors that control groundwater occurrence and quality is an important step towards sustainable development of the region.

1.1 Background Review

Drought has been the phenomena of great concern throughout the continent of Africa, because of the devastating effects it has inflicted on the local communities (Opere *et al*., 2003). The eastern Kalahari region of South Africa is no exception and is a recent example of one of those vulnerable areas to be severely affected by drought during the last few years (2012 – 2016), with many of the towns and villages in the area faced with water restrictions, including the farmers in the area who have complained of boreholes drying up. A need was expressed both by farmers and local communities for an understanding of the hydrogeological processes at work in the area, given that the water supply in this semi-arid region is purely dependent on the groundwater reserve.

While a literature review of groundwater studies in semi-arid areas returned a wealth of information regarding various aspects of groundwater science, many of these studies were carried out in semi-arid

Botswana and Namibia (Stephenson *et al*., 2003; Xu and Beekman, 2003). In addition, many of the previous studies, which have contributed significantly to the understanding of factors influencing groundwater potential in semi-arid areas, have largely focussed on a single influencing factor, such as recharge, reserve estimation, isotope analysis etc. (Stephenson *et al*., 2003; Xu and Beekman, 2003). The influence of a number of these different hydrological features on the groundwater potential in the eastern Kalahari region of South Africa is a topic that has not been well addressed. In light of understanding the groundwater potential of the area, it was decided to embark upon a study that would integrate all of this existing research and possibly contribute to the knowledge base of the area.

1.2 Aims and Objectives

Groundwater potential depends on many hydrogeological factors including surface and bedrock lithology, structures, slope steepness and morphology, drainage density, climate, soil and land use. Although the previous studies have contributed significantly to the understanding of the groundwater potential of semi-arid areas, many of the studies have been site specific, largely restricted to the Kalahari of Botswana. The main objective of this study is to apply this wealth of knowledge to the eastern Kalahari region of South Africa, in an attempt to better understand the processes at play, adding to the knowledge base of the region and potentially contributing to the better and more responsible utilisation of this valuable resource.

Knowledge and understanding of the extent and size of the catchment area, as well as the geological events are important for groundwater investigations. Given this, the first step in understanding the groundwater potential of the area will be to provide a basic description of the geomorphology and geology of the region. In particular, the structural and chemical nature of the regional geology will be established and the role it has on the underlying groundwater assessed. This assessment should determine if the Kalahari in this region has the potential to host suitable groundwater reserves or if deeper aquifers need to be exploited.

The assessment of groundwater quality is another major step towards defining the groundwater potential of the region, as well as ensuring the sustainable use and management of the resource. As such, the main objective of the proposed study is to identify the existing water quality problems. The groundwater of this semi-arid region is notoriously associated with its high salt content, largely due to the high rates of evaporation in the area. An understanding of the water quality should assist in quantifying the impacts on consumption and agricultural purposes, in addition to creating awareness on how to better use, manage and protect the groundwater without adversely affecting its future quality.

The desire to better manage limited water resources, as is the case in this semi-arid region, calls for reliable recharge estimation. An understanding of site recharge behaviour is of great importance and goes beyond estimating the average proportion of rainfall entering a given aquifer. As such, this project aims to provide a model that describes the location, timing and probable mechanisms of recharge in the region, in addition to providing estimates of recharge rates based on climatic, topographic, land use and land cover, soil and vegetation types, geomorphological and hydrogeological data. Such a quantification of recharge should provide an ultimate measure of the extent of the reserve and the long-term sustainability of the resource.

Armed with the above information, the next objective in the process will be to delineate groundwater bearing units, including probable structural and geological dependant reserves. An understanding of the controls on the groundwater potential of the area is useful to regulate and optimize water use without adversely impacting water resource for future use.

2. METHODOLOGY

In order to meet with the objectives outlined above, a number of research strategies were employed to ensure that enough and adequate empirical data was gathered for a successful research project.

2.1 Collation of Available Data

The initial stages of the project involved a collation of available historical data for the area, such as borehole logs, geophysical surveys, borehole piezometer readings, water chemistry, rainfall etc. Both the Council for Geoscience and the Department of Water Affairs have historical databases that were made available for this study. The archived data and geophysical maps of the Council of Geoscience were procured upon request, whereas that of the Department of Water Affairs was accessed through the internet via their NGANET website. Many of the farmers also willingly shared information regarding the local rainfall patterns and geology of the area from boreholes that they themselves had drilled.

This historical information, coupled with Geographical Information System (GIS) techniques, assisted in determining the extent and size of the catchment area from a digital elevation model (DEM). Accurate catchment boundaries are necessary for water resource management. They have been considered to be one of the most important areal reporting units in environmental decision making (Oksane and Sarjakoski, 2005), because they play a functional role in integrating the chemical, biological and physical processes within their boundary (Moore, 1993).

Collation and review of the existing literature on the geology of the region also proved fundamental. Combined with a series of geological maps of the region, as supplied by the Council of Geoscience, as well as an archive of borehole data detailing boreholes that were drilled in the area, with many specifying the lithological units that were intersected upon drilling, an adequate knowledge of the sub-surface geology of the region was gained. Integrated with field reconnaissance investigations and local geophysical surveys of the region, notably the aeromagnetic and gravity surveys conducted by the Council of Geoscience, an understanding of the sub-surface structures was also obtained. This allowed for the inference of prospective areas of groundwater potential and the generation of an appropriate conceptual model for these proposed aquifers.

2.2 Hydrogeological Review

An understanding of the geomorphology and geology of the Kalahari Basin, as well as the sub-Kalahari geology and structure, is vital to the understanding of the groundwater potential of the region. The interplay of various geological and geomorphological factors gives rise to complex hydrogeological environments with innumerable variations in aquifer transmissivity, effective porosity, saturated thickness of aquifers and groundwater recharge (MacDonald *et al*., 2012). The determination of some of these aquifer characteristics for each of the hydrogeological environments identified are detailed below.

2.2.1 Storativity/Specific Yield Determinations

Direct measurements of storativity/specific yield proved to be very scarce. As such, general information on the storativity/specific yield of a lithological unit was obtained from the analysis of pump tests that were conducted in the study area. Where not available in existing literature, proxies for these parameters were used, with the flow and storage characteristics of known lithologies being compared and related to those lithological units occurring in the study area.

2.2.2 Aquifer Thickness Calculations

There are various approaches put forward to estimate aquifer thickness, each of which have dealt with the problem of limited information in different ways. In general, the determination of saturated thickness depends on whether or not an aquifer has a fairly well defined base or not. In cases where the base of the aquifer is fairly well defined, such as unconfined, unconsolidated aquifers with distinct boundaries at their bases and those that have a fairly distinct interface between the weathered zone and the underlying fresh rock, estimating aquifer thickness does not pose a big problem. However, in many fractured environments, such as that present in the study area, it has proven difficult to define what constitutes and estimates the "average saturated thickness" of the different aquifer systems. The saturated thickness of the aquifer at any given location, through which groundwater can move, will be controlled by the depth down to which 'open', water-bearing fractures (joints) occur, as well as their geometry (aperture, length and density), frequency and interconnectivity, assuming that the matrix is practically impermeable (DWAF, 2006).

Unconfined, Intergranular Sedimentary Aquifers: The Kalahari intergranular sedimentary aquifer is one such example of an unconfined aquifer for which the saturated thickness could easily be estimated. The Kalahari isopach map of Haddon (2005) provides a detailed distribution of the Kalahari sequence and its associated thickness throughout the study area. Using this isopach map, in addition to the cross sections generated for the region, the average saturated thickness for each 30 m depth interval was determined by calculating the difference in elevation between that particular depth interval and the water table.

It must be noted that acquiring the necessary water level data proved challenging, given that the monitoring of most boreholes by DWAF was discontinued after 1994. Nevertheless, an average water level was calculated for each sampling/monitoring point over the time monitored.

Fractured and Weathered Aquifers: When calculating the saturated thickness for the fractured and weathered aquifers in the study area, another approach to that of unconfined aquifers had to be adopted. While the calculation for saturated thickness remained the same, the depth at which the permeability and storage coefficient of the aquifers are considered to have decreased substantially (aquifer base) from that part of the aquifer which contained the bulk of readily accessible and exploitable groundwater, was largely unknown. In an attempt to determine the aquifer base, groundwater strike information from the National Groundwater Archive (NGANET) of the Department of Water Affairs was used. In particular, Vegter (1995) and Seymour (1996) observed that there are distinct water strike density profile curves for the various types of secondary aquifers, the statistical analysis of which provides a reasonable, indirect method of deriving the base of the fractured aquifers. Once determining the base of the aquifer, the saturated thickness of each aquifer can then be determined by calculating the difference between the aquifer base depth and the rest water level.

The water strike information extracted from the NGANET, recorded in metres below ground level, was divided into the various hydrogeological units, with 'strike density profiles' being generated for each hydrogeological unit. In particular, the number of water strikes (S) within each consecutive 5 m interval below the ground level was determined, with the number of boreholes (N) passing through a particular 5 m depth interval being calculated. The strike density (SD) per 5 m depth interval was calculated as follows: $SD = S / N$, with the value being plotted against the relative depth interval. The resultant "strike density" curves were visually analysed and the 'base of the aquifer' for each unit defined, in metres below ground surface, as the point at which the strike density initially approaches zero. It must be noted that this depth to base of the aquifer does not imply that no water-bearing fractures are likely to occur below this level, but rather refers to the zone in which the bulk of the readily available and exploitable groundwater is stored (DWAF, 2006).

2.3 Groundwater Quality Assessment

A total of 19 samples were collected from different locations spread across the eastern Kalahari region, the position of which was recorded with a handheld GPS (Global Positioning System) unit. Samples were collected in sterilised glass containers directly from each of the borehole's outlet pipes after the borehole had been purged for longer than 30 minutes. Many of these samples were analysed in the hydrogeological laboratory of the University of the Witwatersrand for their biological properties (Bacteria and Biological Oxygen Demand), however, most of the physical and chemical parameters of the groundwater samples were measured on site. The physical and chemical parameters measured on site include temperature, pH, electrical conductivity, total dissolved solids and dissolved oxygen, each of which was measured using multi-probe equipment provided by the University of the Witwatersrand. In certain cases, this information was combined with the vast archive of water quality data from the NGANET database, also administered by the Department of Water Affairs, in an attempt to facilitate interpretation of the results.

2.3.1 pH

The pH of each sample was determined using a Multi-Parameter MM40 pH meter. Prior to use, immediately before the first measurement of the day, the portable pH meter was calibrated against two pH buffer solutions of known, fixed pH (7.0 and 4.01). During calibration, the instrument was adjusted according to the manufacturer's instructions so that the meter read the correct pH value for that buffer based on the field temperature. Care was taken to rinse the electrodes with de-ionised water, gently blotting them dry with soft tissue paper, before transferring the electrode from one solution to the next. Prior to inserting the electrode into the sub-sample for measurement, the electrode was also rinsed with de-ionised water and gently blotted dry. Upon measurement, the electrode was inserted into the glass container and stirred gently while waiting for the reading to stabilize. The pH was subsequently recorded to the nearest 0.01 units

2.3.2 Temperature

A digital thermometer, incorporated into the pH meter discussed in Section 2.3.1, was used to measure the temperature of the groundwater. The temperature of the water was recorded to the nearest 0.1 ^{o}C while the thermometer was immersed in the sub-sample.

2.3.3 Electrical Conductivity

The electrical conductivity of each sample was measured using an electrode that was incorporated into the pH meter discussed in Section 2.3.1. The electrical conductivity of water was measured and recorded as the reciprocal of the resistance measured between two parallel metal plates in the electrode at a specified temperature of 25 ^{o}C. As with the pH electrode, the electrical conductivity electrode was also calibrated immediately before the first measurement of the day against two standard aqueous solutions of known, fixed electrical conductivity (7.0 and 4.01 µS/cm). Subsequent to calibration, the electrical conductivity of each sub-sample was measured and recorded in milliSiemen per centimetre (mS/cm) or microSiemen per centimetre (µS/cm). All measurements were later converted to the International System of Units (SI), which reports conductivity in milliSiemen per metre (mS/m).

2.3.4 Total Dissolved Solids

The same electrode was used to measure the total dissolved solid content of the water samples. It must be noted that this portable measuring tool that is used primarily during field work, essentially provides an indication of the salinity of the groundwater. The total dissolved solids content of the water was recorded to the nearest 1 mg/l while the electrode was immersed in the sub-sample.

2.3.5 Total Hardness, Chloride and Nitrate (NO_3+NO_2-N)

The concentration of calcium, magnesium and other polyvalent metallic cations, which largely determine the hardness of water, were sourced from the NGANET database, administered by the Department of Water Affairs. Similarly, chloride concentration and the combined concentration of nitrate (NO_3), the most common oxidation state of nitrogen, nitrite (NO_2) and nitrogen within the groundwater were also sourced from the NGANET database. Values in the NGANET database were recorded to the nearest 0.01 mg/l.

2.3.6 Dissolved Oxygen (DO)

The dissolved oxygen (DO) concentration of each sample was measured using a DO meter, which makes use of a polarographic system that consists of two metal electrodes surrounded by an electrolyte (Wood 1981; APHA 1998). The actual DO measurement of the sample water was done once the meter/electrode system had been calibrated. This procedure consisted of preparing the electrode, by filling the cap with a solution of potassium chloride to ensure that the membrane tip of the electrode was kept moist, and then calibrating the electrode by using a sample of known DO content. Upon completion of calibration, the membrane was cleaned with de-ionised water and the DO measurements performed by inserting the electrode into the sub-sample. The DO concentration was recorded to the nearest 0.01 mg/l once the reading had stabilised.

2.3.7 Bacterial Analysis

To ensure that the microbiological quality of the groundwater proved representative of the underlying aquifer, samples were collected directly from each of the borehole's outlet pipes after the borehole had been purged for longer than 30 minutes. Samples were collected in glass containers that had been sterilised in an oven at 170 ^{O}C for 30 minutes. When collecting the water sample from the outlet pipe, some of which extended for a few metres in length, the bottle was held under the discharge pipe, with care being taken not to touch the sides of the outlet pipe. Each bottle was filled, with some air space being left behind, and the cap replaced, again taking extreme care not to contaminate the inside of the cap or bottle. The filled bottles were stored on ice and in darkness in a cooler bag to ensure that the bacteria remained viable (alive) yet did not multiply (grow in numbers) between the time of sampling and time of analysis. Given the vast distances that needed to be travelled to collect the samples, the samples did not reach the laboratory for analysis within 24 hours. The maximum holding time for obtaining realistic results is 48 hours (Weaver *et al*., 2007), however, given the demanding logistical constraints, this was not achieved and the results obtained must be treated with caution.

The membrane filtration (MF) technique (Millipore, HANG 47 mm) was used for the isolation and enumeration of three indicator organisms, namely *Escherichia coli, Enterobacter Aerogens* and *Proteus Mirabilis* from all the water samples. One hundred millilitres (100 ml) of sample water was filtered through 0.45 μm pore size GN-6 Metricel membrane filters, held in a stainless steel filtration unit that used a negative pressure vacuum. Samples were then transferred to 45 mm Petri plates containing various selective, nutrient-rich media (m-Endo agar) for the recovery of each indicator group. Each of these plates was incubated for 24 hours at 37 ^{o}C. After the incubation period, all of the typical colonies grown on the filters (m-Endo agar plates – metallic sheen and pink-red colonies) were recorded as presumptive counts for the estimation of colony forming units per 100 millilitre (cfu/100 mℓ).

2.3.8 Biological Oxygen Demand-5 (BOD_5)

Of the 19 sampling sites spread across the eastern Kalahari region, only 11 of these sites were selected for BOD_5 analysis. Samples were collected directly from each of the borehole's outlet pipes after the borehole had been purged for longer than 30 minutes. Samples were collected in 500 ml plastic bottles that were dry and clean. Each bottle was filled, with some air space being left behind, and the cap replaced, taking extreme care not to contaminate the inside of the cap or bottle. The filled bottles were cooled immediately after having being taken by storing the bottles on ice in a dark, plastic container. As with the bacterial samples, vast distances needed to be travelled to collect the samples and the samples did not reach the laboratory for analysis within 6 hours. The maximum holding time for obtaining realistic results according to the OxiTop ® operating manual is 6 hours. Given the demanding logistical constraints, this was not achieved and the results obtained must, therefore, be treated with caution.

The biological oxygen demand of each water sample was measured using the OxiTop ® system over a 5 day period (BOD_5) at 20 ^{o}C. Given the expected BOD_5 range of 0-40 mg/ℓ, a corresponding sample volume of 432 ml, according to the manufacturer's instructions, was used for each analysis. This measured solution was transferred into a brown graduated measuring flask with a capacity of 510 ml and a threaded neck. The brown glass is believed to prevent the possible growth of algae. A magnetic stirrer was inserted into each of the brown flasks, which when placed on a stirring platform in which separate alternating electromagnetic fields are generated, a stirring system was induced. This ensured that the material under test was thoroughly mixed during the entire duration of the measurement so as to accelerate the exchange of oxygen and to prevent deficiency in the measurement sample. A rubber sleeve, into which two sodium hydroxide pellets were placed, was inserted into each of the brown sample bottles, taking care that the pellets did not make contact with the sample. An OxiTop ® measuring head was screwed tightly on each sampling bottle, the rubber sleeve ensuring the necessary sealing of the system. Each of the OxiTop ® measuring heads were synchronised with the OxiTop ® controller, which communicates via an infrared interface, and the measurement started. The controller performed all of the sample management including data storage and graphical evaluation, with the control system recording 360 measured values per sample during the course of the 5 days. Once complete, the measured BOD_5 data, which was expressed in mg/l, was conveniently transmitted to a PC.

2.4 Hydrochemical Assessment of the Groundwater

Given the indisputable advantages of assessing groundwater chemistry, it proved essential to identify the existing hydrochemical signature of the groundwater in this region. This was achieved by extracting chemical analyses from the NGANET archive, which is administered by the Department of Water Affairs. A significantly large amount of data was obtained from this site, which proved exceedingly difficult to interpret when exported into tables of numbers. In order to facilitate the interpretation of the hydrochemical data, the NGIS/CHART application, also managed by the Department of Water Affairs, was used to present this numerical data graphically using Piper, Durov and Schoeller diagrams (Appendix A). When extracting this hydrochemical data from the NGIS/CHART archive, the data was grouped into its respective Quaternary drainage regions, as defined by the Department of Water Affairs. This portion of the eastern Kalahari comprises ten such Quaternary drainage regions, namely 41B, 41C, 41D, 41E, 41F, 41G, 41H, 41K, 41L and 41M, extending from the east to the west of the study area. As such, ten graphs of each type (Piper, Durov and Schoeller) were generated for the study area (Appendix A), each of which are representative of a specific Quaternary drainage region.

2.5 Measurement of Environmental Isotopes

Environmental isotope samples were also collected from selected sites during the sampling programme mentioned above and sent to iThemba Labs, an accredited isotope laboratory, for analysis. In semi-arid areas, the quantification of groundwater recharge is one of the key challenges in determining the long-term sustainability of a resource as recharge rates are generally low in comparison with average annual rainfall or evapotranspiration, and thus difficult to determine precisely (Beekman and Xu, 2003). Although there are numerous methods for recharge estimation (Xu and Beekman, 2003), each with their own advantages and limitations, the “isotope snapshot” approach appears the most attractive in principle. The environmental isotope method embraces the measurement of isotope ratios of the elements making up the water molecule (^{18}O, ^{2}H and ^{3}H), elements which are subject to environmental processes and, therefore, change (Abiye, 2013). Not only do the variations in their isotopic composition assist in determining the origins and ages of different water bodies (Levin and Verhagen, 2013), it has the most potential to forecast groundwater recharge based on the relationship between rainfall, abstraction/evapotranspiration and interconnectivity of water resources, information that can be built into a groundwater management plan at the inception of exploitation (Verhagen, 2003; Abiye 2013).

2.5.1 Groundwater Sampling

In order to employ this method of analysis it proved necessary to sample the groundwater at different locations spread across the eastern Kalahari region. A total of 19 samples (KAL001 – KAL 019) were collected from boreholes that provided water for domestic and drinking use to both farmers and rural settlements, with one rainfall sample also collected (KAL020). The position of each sample was recorded with a handheld GPS (Global Positioning System) unit.

To ensure that the groundwater sampled proved representative of the underlying aquifer, samples were collected directly from each of the borehole's outlet pipes after the borehole had been purged for longer than 30 minutes. Samples were collected in clean 5 litre plastic bottles that were held directly under the discharge pipe and rinsed with the same water prior to sampling. Each bottle was filled to the top, with very little air space being left behind, and the cap replaced, taking extreme care that the bottle was sealed tightly to avoid isotope fractionation through evaporation or diffusive loss of water vapour, and/or isotope exchange with the surroundings. The filled bottles were stored in the dark, in large plastic containers until the samples were delivered to the iThemba Laboratories.

2.5.2 Stable Isotope Analysis ($^{2}H/^{1}H$ and $^{18}O/^{16}O$)

Some 10 – 20 ml of water from each sample was analysed for their stable isotope compositions in the laboratory of the Environmental Isotope Group (EIG) of iThemba Laboratories, Gauteng. The equipment used for stable isotope analysis consisted of a Thermo Delta V mass spectrometer that was connected to a Gasbench, the former of which was able to separate atoms or rather ions with different mass and measure their relative abundances. Since the introduction of water in the mass spectrometer had to be avoided, the $^{18}O/^{16}O$ and D/H ($^{2}H/^{1}H$) ratios of the water samples had to first be transferred to a more suitable gas, in this case carbon dioxide and hydrogen, respectively. As such, prior to analysis, CO_2 was equilibrated with each water sample in about twenty hours, with equilibration time for the water sample with hydrogen being approximately 40 minutes. Laboratory standards, calibrated against international reference materials, were also analysed with each batch of samples (Butler *et al*., 2015).

Analytical results are not reported as concentrations, but instead are commonly expressed as relative isotope ratios of the less frequent to the abundant isotope changes of a sample, presented in the common delta-notation:

$$\delta^{18}O\ (‰) = \left[\frac{(^{18}O/^{16}O)_{sample}}{(^{18}O/^{16}O)_{standard}} - 1\right] X\ 1000$$

which applies to D/H ($^2H/^1H$), accordingly. These delta values are expressed as per mil (parts per thousand: abbreviated as ‰) deviation relative to a known standard, in this case standard mean ocean water (SMOW) for $\delta^{18}O$ and δD. The analytical precision is estimated at 0.2 ‰ for O and 0.8 ‰ for H (Butler *et al*., 2015).

2.5.3 Tritium Analysis

Water from each of the samples collected were also analysed for Tritium (Hydrogen-3) content at the iThemba Laboratories, Gauteng. The samples were distilled and subsequently enriched by electrolysis. The electrolysis cells consisted of two concentric metal tubes, which were insulated from each other. The outer anode, which was also the container, comprised stainless steel, while the inner cathode comprised mild steel with a special surface coating. Some 500 ml of the water sample, having first been distilled and containing sodium hydroxide, was introduced into the cell. A direct current of some 10–20 ampere was then passed through the cell, which was continuously cooled due to the heat generated during sample processing. After several days, the electrolyte volume was reduced to some 20 ml. This volume reduction of some 25 times produces a corresponding tritium enrichment factor of about 20. Samples of standard known tritium concentration (spikes) were also run in one cell of each batch to check on the enrichment attained (Butler *et al*., 2015).

For liquid scintillation counting, samples were prepared further by directly distilling the enriched water sample from the now highly concentrated electrolyte. Approximately 10 ml of the distilled water sample was mixed with 11 ml Ultima Gold and placed in a vial in the analyser and counted in 2 to 3 cycles of 4 hours. The tritium levels of each water sample were expressed in TU, Tritium units, which represents a $^3H/^1H$ ratio of 10^{-18}. Detection limits are usually in the order of 0.2 TU for enriched samples (Butler *et al*., 2015).

2.6 Quantification of Recharge

The quantification of recharge is increasingly given attention in the management of groundwater, particularly in this semi-arid region where the average rainfall is generally low and the evapotranspiration rates high. To ensure the long-term sustainability of this resource, it is essential that the groundwater recharge be estimated. One of the challenges, however, is that there are numerous factors that influence recharge, which are associated with a high degree of spatial and temporal variability and most often high levels of uncertainty. As such, recharge is difficult to determine precisely, with a wealth of recharge estimation methods being available for semi-arid areas, each with their own limitations. While it is understood that confidence in recharge estimates improves when applying a multitude of methods, given the project objectives and the availability of data, it was decided to use the Chloride Mass Balance (CMB) method for recharge estimations. This method was applied across the study area, so as to determine if quantitative estimates of recharge could be defined for different geological formations and/or aquifers.

Recharge was calculated using the basic Chloride Mass Balance formula described by Bean (2003):

$$R = (Cl_p / Cl_{gw}) * MAP$$

Where	R	= recharge (mm/a)
	MAP	= Mean Annual Precipitation (mm/a)
	Cl_p	= chloride in rain (mg/l)
	Cl_{gw}	= chloride in groundwater (mg/l)

The Chloride Mass Balance method is based on the assumption of conservation of mass between the input of atmospheric chloride (rainfall) and the chloride flux in the subsurface (Beekman and Xu, 2003), given that chloride is a conservative tracer. This method of recharge estimation assumes that the various chloride concentrations have resulted from natural, hydrological and evaporative processes. As such, no chloride was added by dissolution of aquifer material, from salts contained within the aquifer matrix, or has entered the aquifer via pollution (DWAF, 2006). The percentage of rainfall entering the groundwater, representing average annual recharge, can, therefore, be derived from the ratio of the chloride concentration in rainfall relative to that of groundwater (Bredenkamp *et al*, 1995). This method does not include all the factors determining groundwater recharge, however, it does include the main factors. These main factors, namely mean annual precipitation, chloride in rainfall and chloride in groundwater and the acquisition of the necessary data are discussed below.

Mean Annual Precipitation: Knowledge of the rainfall patterns and the amount of rainfall that has fallen in the study area proved essential, given that this information is critical to the quantification of recharge. As such, historical rainfall patterns were accessed from local farmers and the Department of Water Affairs (Appendix B). Of the four historical rainfall datasets acquired, two were accessed from the Department of Water Affairs, while the other two were sourced from local farmers.

Chloride in Groundwater: Reliable (accurate laboratory analysis) and spatially representative chloride concentration data in groundwater is essential to enable assessment of recharge. Such data was accessed from the NGANET archive, administered by the Department of Water Affairs.

Chloride in Rainwater: Reliable, time-related chloride data for all of the rainfall stations in the area would have also proved valuable, however, such data does not exist. Within South Africa there is a lack of rainwater chloride concentration data. The currently accepted concentration of chloride in rainfall for the study area is approximately 0.80 mg/l. This is based on the chloride concentrations that were extracted from the rainfall chloride map created during the GRAII study of South Africa (DWAF, 2006). This value of 0.80 mg/l was also calculated by relating rainfall chloride to MAP and geographical setting, using the same formula as that used during the GRAII study (DWAF, 2006).

2.7 Storage and Resource Potential Calculations

Only once the recharge history of the region was modelled, coupled with the geological model of the region and chemical analysis of the groundwater, did it prove possible to determine the potential of this region to host significant groundwater reserves. Particular emphasis was placed on which of the lithological units showed the greatest potential to host groundwater reserves based on their effective porosity, saturated thickness and areal extent. High resolution airborne magnetic and gravity data, as supplied by the Council for Geoscience, was also able to assist in establishing the influence of geology and structures on the groundwater potential in the region. This was combined with available yield data for each lithological unit, which allowed for the generation of a groundwater potential map of the area.

2.7.1 Groundwater Storage Calculations

The groundwater storage for each hydrogeological unit was determined by multiplying the saturated aquifer thickness (Δh) and its surface area (A) by its effective porosity/specific yield (S):

$$\text{Groundwater Storage, } V = \sum A\ S\ \Delta h$$

The estimation of effective porosity/specific yield and saturated thickness are discussed in Section 2.2.1 and 2.2.2, respectively, with the surface area of each aquifer being estimated from the available hydrogeological and geological maps and reports.

2.7.2 Groundwater Resource Potential Calculations

The groundwater potential of an aquifer is largely determined by the storage capacity and recharge rate of the aquifer, with an aquifer of sufficient storage able to support a discharge rate equal to the long-term recharge rate (Vegter, 1995). Given this, the Groundwater Resource Potential was calculated using largely these two parameters in a basic water-balance approach refined by the Department of Water Affairs (DWAF, 2006). It must be noted that the value calculated provides an estimate of the maximum volume (m^3) of groundwater that is potentially available for abstraction on an annual basis under pristine aquifer conditions (**i.e. no abstraction)** and normal rainfall conditions.

$$\text{Resource Potential} = R_e + (S_v / D_i) - B_f$$

Where R_e = Mean Annual Potential Recharge (m^3 / year) – Output of Section 9.2

S_v = Mean Volume of Water stored in Aquifer (m^3) – Output of Section 9.1

D_i = Drought Index – Output of Harvest Potential (Baron *et al*., 1998).

B_f = Mean Annual contribution to River Baseflow – Negligible

The drought index was calculated using the “Rainfall Reliability” factor of Baron *et al*. (1998), which is equal to the 20th Percentile / Median annual rainfall, the inverse of which reflects the expected length of a drought. An average “Drought Index” of 1.40 was used for the project area, the calculation of which can be viewed in Appendix B. The mean annual contribution to river baseflow was regarded as negligible in this semi-arid area, where all of the rivers are ephemeral.

2.7.3 Groundwater Availability and Exploitation Estimation

While the Groundwater Resource Potential provides an impressive estimate of the maximum volume of groundwater that is potentially available for abstraction on a sustainable basis in the study area, the feasibility of abstracting this water is limited by many factors, the main being the physical attributes of each aquifer. In particular, the magnitude of transmissivity (the permeability of the rocks integrated over thickness) affords a notion about the ease at which a hydrogeological unit can transmit groundwater through its interstices (Holland, 2012). Values of transmissivity, however, are scarce and its surrogate, borehole yield, is commonly used as a decisive factor for groundwater-abstraction possibilities. Borehole yield not only provides an indication of the capacity of a borehole to deliver water, it also provides an indication of the rate at which the aquifer is able to deliver water to that borehole. As such, boreholes must be sized and situated to match the nature and transmissivity of the aquifer, with their distribution suitably spaced to capture all of the available water in the aquifer, without exceeding its recharge, lowering its piezometric head below a critical depth or causing undesirable changes in water quality (Baron *et al*., 1998).

Direct measurements of transmissivity and borehole yield for each of the aquifers types identified proved impossible, given the scope of the project. As such, a number of pumping tests throughout the study area were analysed and used to determine a range of possible values for each identified hydrogeological domain (based on lithology); as well as the various structural features present within the study area.

3. THE PROJECT AREA

3.1 Location, Topography and Drainage

Situated in the far western portion of the North West Province (Figure 3.1), the eastern Kalahari basin of South Africa stretches northward from just north of the Orange River into Botswana. In particular, the area of study is situated directly west of the town of Mafeking and some 260 km west of Johannesburg, between latitude 25°15′S and 27°01′S and longitude 22°20′E and 25°22′E (Figure 3.1), covering an area of 50937.59 km^2. Quaternary Government map sheets which partially cover the area of study include 2522 (Bray), 2524 (Mafeking), 2622 (Morokweng) and 2622 (Vryburg).

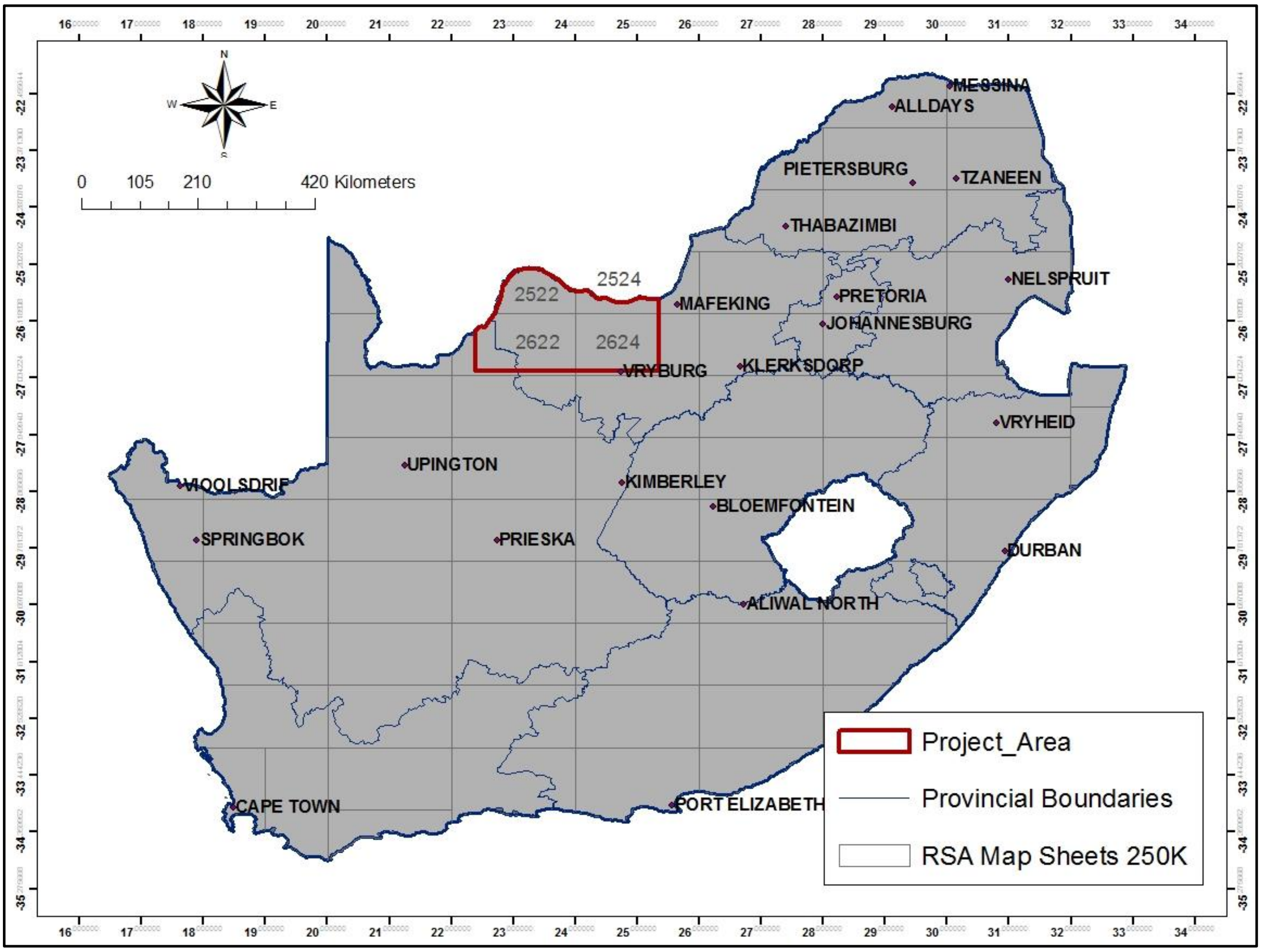

Figure 3.1: Locality map showing the area of study relative to the South African provincial boundaries

Located on the southern African plateau the area is largely covered by sand and the topography is subdued and relatively flat (Figure 3.2), with an average elevation of between 900 to 1200 m above sea level (Figure 3.3). The elevation decreases slightly from the water divide in the south at a surface elevation of approximately 1320 m to the lowest depression, the Molopo River, 220 km to the north at an elevation of 1010 m. The most prominent feature in the study area is a low southwest to northeast curving ridge of the Asbestos Hills Subgroup (Griqualand West Basin), which is 30 – 40 m higher than the surrounding topography (Figure 3.2 and Figure 3.3). The collated, 30 m resolution digital elevation model (DEM) displayed in Figure 3.3 originates from the Shuttle Radar Topography Mission (SRTM) dataset acquired by the United States Geological Survey (USGS), which can be freely downloaded from the internet.

Figure 3.2: The relatively flat and subdued topography of the eastern Kalahari. The hills in the background belong to the Asbestos Hills Subgroup which protrudes above the surrounding topography (Picture by Bronwyn Jonker)

Situated within the Lower Vaal Management area, eleven Quaternary drainage regions cover or partially cover the area of study (Figure 3.4). The drainage pattern is dispersed and dendritic, with low tributary bifurcation ratios that are more deeply incised at the headwater branches (Figure 3.4). This is largely due to the fact that all of the rivers are ephemeral, with storm water draining by sheet flow during short-lived flooding events. Although some flow features follow a structurally controlled direction, most of the rivers flow north westwards, ultimately converging with the Molopo River. Towards the western portion of the study area, the rivers converge to form a westward flowing river, which runs parallel to the Molopo River to the north (Figure 3.4). Some depressions also occur towards the northern part of the study area, which probably reflects poor drainage conditions during wet paleo-climatic periods with high groundwater tables. Extensive calcrete and silcrete duricrust precipitates are found along these depressions, which are produced by subsurface leaching of the feldspathic matrix and removal and precipitation of calcite (De Vries *et al*., 2000).

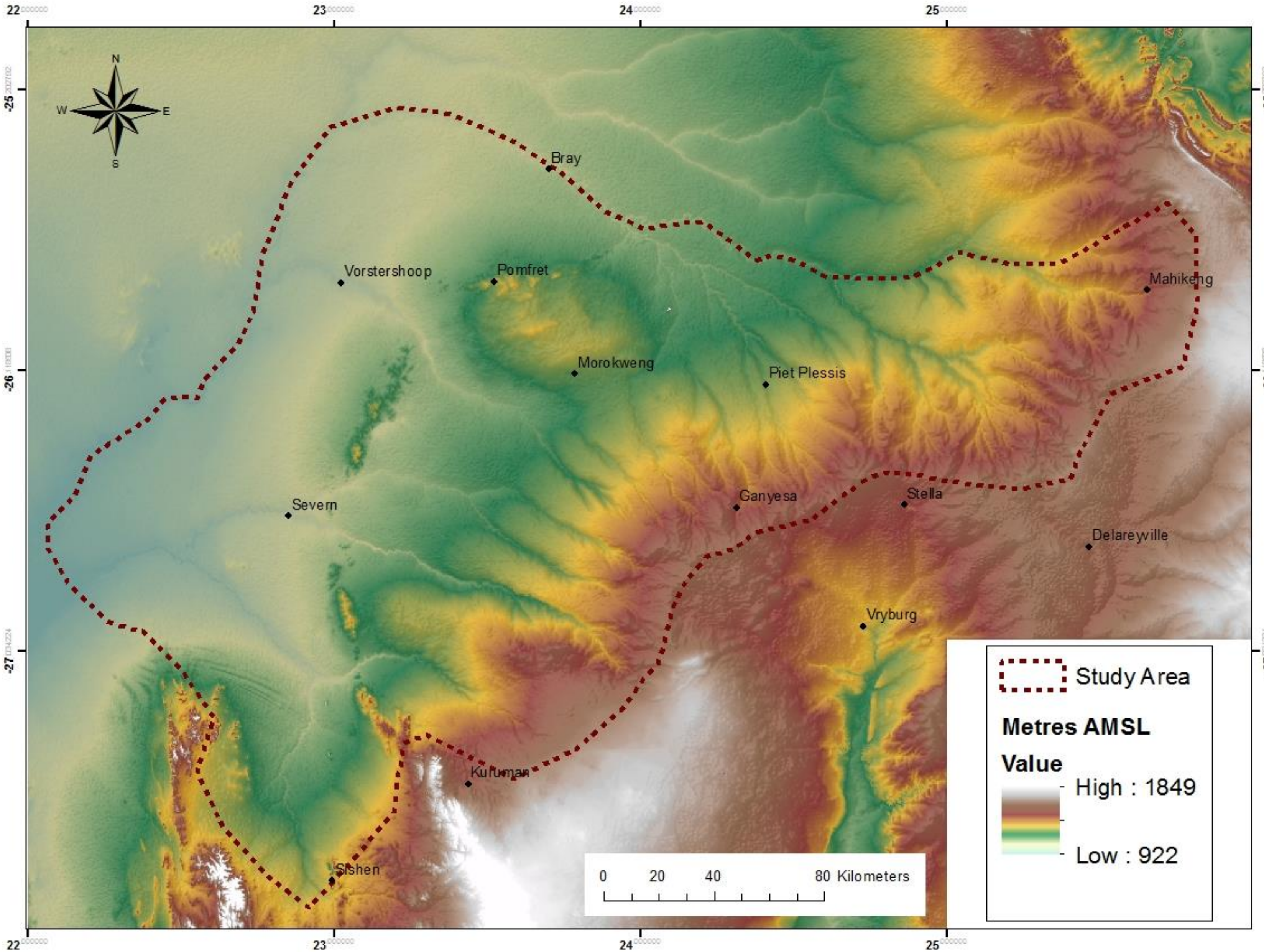

Figure 3.3: Digital elevation model of the study area

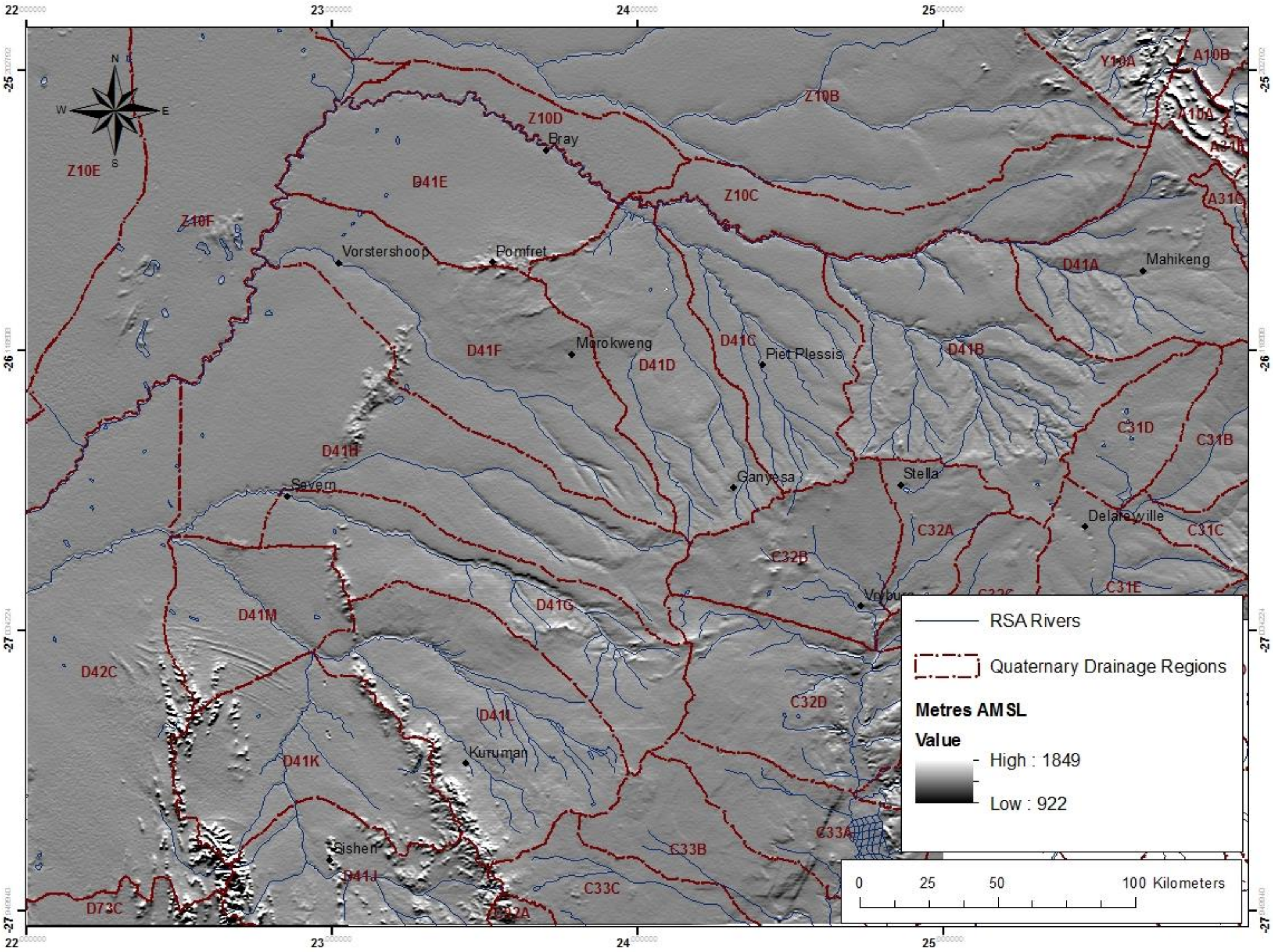

Figure 3.4: The Lower Vaal Quaternary drainage areas within the region, showing the associated drainage pattern

3.2 Climate

The climate of the eastern Kalahari region of South Africa may be described as temperate, with summer temperatures ranging from a minimum of 7 °C to a maximum of 37 °C. Rainfall in this region is seasonal, with a mean annual rainfall of approximately 400 mm falling almost entirely during the summer season between October and April (Appendix B). Potential evaporation rates in this semi-arid region range from 1960 mm to 2100 mm per annum, exceeding annual precipitation (Tessema *et al*., 2014).

The summer rainfall pattern in this semi-arid region manifests itself as intermittent events, separated by long periods of sub-average rainfall depths, a consequence of the diverse atmospheric and geomorphological controls over the Southern African subcontinent (Van Wyk *et al*., 2012). Most rainfall events occur as convective thunderstorms, driven by super-heated ground-surface conditions, which are of limited areal extent and relatively short duration. Rainfall amounts of 10 to 30 mm are common during such high intensity - short duration events, with the convection system usually covering a 3 to 8 km diameter footprint during its rainout phase, but may track a random pathway for several kilometres (Van Heerden and Hurry, 1992). Depending on the regional synoptic conditions, several local convectional systems may develop during periods of high atmospheric moisture loads, initiating extraordinary downpours (> 100 mm < 24 h) over short periods (Van Wyk *et al*., 2012).

Occasionally, large-scale frontal systems bring heavy, widespread rains for periods ranging from one to several days. Such an occurrence is usually associated with one rainout event in the order of 50 to 80 mm or even higher, with the total rainfall depth being as high as 200 to 300 mm. It has been shown that such episodic wet periods, consisting of up to 8 consecutive days, may contain falls that contribute to almost 45% to 60% of the total annual rainfall of an area (Van Wyk *et al*., 2012). These extraordinary events often initiate significant groundwater recharge events which may initiate aquifer storage-recharge (Van Tonder and Bean, 2003).

3.3 Vegetation and Land Use

The eastern Kalahari region supports rather dense vegetation, allowing for the classification of the Kalahari as a bush and tree savannah, with alternating grassland biomes (Figure 3.2). In particular, there is a predominance of Kalahari deciduous Acacia thornveld (open savannah of *Acacia erioloba* and *Acacia haematoxylin,* as well as desert grasses) and shrub bushveld in this portion of the Kalahari. The occurrence of these shrubs and trees is largely determined by the availability of deeper soil moisture for their more extensive root systems. Generally, those areas associated with bedrock outcrop are sparsely vegetated, with greater abundance of shrubs and trees occurring along river channels (Figure 3.5) and pans, along dykes and along the edge of scree slopes surrounding ridges.

By contrast, the rocky soil associated with the dolomite of the Ghaap Plateau are conducive to Tarchonanthus veld (Van Veelen *et al*., 2009).

Figure 3.5: The Molopo River in flood (February 2014) showing the abundance of vegetation occurring along the river channel (Picture by Bronwyn Jonker)

Most of the land in the study area is under natural vegetation, which is largely utilised as natural grazing to feed an array of animals, mostly cattle, game and to a lesser extent sheep and goats. Much of this land is owned by commercial stock farmers, with large portions of state/tribal owned land in the central and western portions of the study area predominantly supporting subsistence farming activities. The grass cover in these areas is dramatically degraded during periods of low rainfall, largely owing to overgrazing and poor planning.

The absence of high physiographic differences and the presence of fertile soil in parts of the study area also make it agriculturally rich and ideal for crop farming. Areas of cultivation are largely found in the Louwna, Tosca and Stella areas, with farming also taking place in some areas close to the Molopo River. Central irrigation pivots are predominantly used in the cultivation of crops, with irrigated areas ranging in size from 10 to 30 hectares. Water for irrigation is solely sourced from the groundwater.

The towns of Vryburg, Mafeking and Kuruman represent the only significant urban areas within or in close proximity to the area of interest, while scattered rural settlements and small towns supporting mining activities abound. In particular, there is large-scale mining activity in the vicinity of Sishen and Hotazel, on the outer edges of the catchment area, where manganese ore, iron ore, tiger's eye and crocidolite (blue asbestos) are mined. As far as can be established, other than this mining activity, there are no other major industries that operate within this portion of the study area.

4. GEOLOGICAL REVIEW

The Kalahari Group of sediments conceals over 3600 million years of Earth's history, masking a long and diverse history of geological events that occurred prior to the deposition of the Kalahari Group (Haddon, 2005). This section of the Kaapvaal Craton constitutes an almost complete record of the evolution of this portion of the continental lithosphere, with the underlying rocks representing almost every time period from the Archaean to the Cretaceous (Figure 4.1). The geological and tectonic evolutionary events that have shaped this portion of the Craton have strongly influenced and collectively defined the hydrological nature of this area, giving rise to complex hydrogeological environments with innumerable variations in aquifer transmissivity, effective porosity, saturated thickness and groundwater recharge (MacDonald *et al*., 2012). Fundamental to this research, therefore, was a collation and review of the existing literature on the geology of the region. This was integrated with field reconnaissance investigations and local geophysical surveys to provide a brief overview of the geological events that are preserved beneath the Kalahari sand cover.

4.1 Granitoid Complexes

Despite the extensive cover of Kalahari Group sediments, a variety of granitic rocks are exposed sporadically throughout the south-eastern portion of the study area, characteristically associated with the Mesoarchaean Kraaipan - Amalia Group of rocks (Figure 4.1). Outcrops within the area are restricted to a few highly weathered outcrops in stream beds that cut into the flattish terrane of sand and calcrete cover; water storage pits; trenches and, rarely, as flat whaleback pavement exposures (Figure 4.2).

Outcrops are characterised by the abundance of variably fractured granitoids, among which gneissic tonalitic, trondhjemitic and granodioritic (TTG) compositions are dominant. On the basis of field, petrological, geochemical and isotopic characteristics, a threefold subdivision was recognised by Anhaeusser and Walraven (1999). The three types of granitoid rocks include (i) foliated tonalitic and trondhjemitic leucogneisses and migmatites, with the oldest of these gneisses giving an age of ca. 3008 Ma; (ii) fine- to medium grained, grey or pink, homogeneous or, in places, weakly foliated, massive granitoids, as well as cross-cutting pegmatitic dykes and veins, with ages ranging from ca. 2915 to 2879 Ma; and (iii) massive, coarse grained, homogeneous, pink, granite-adamellite dated at 2791 ± 8 Ma (Poujol *et al.*, 2002).

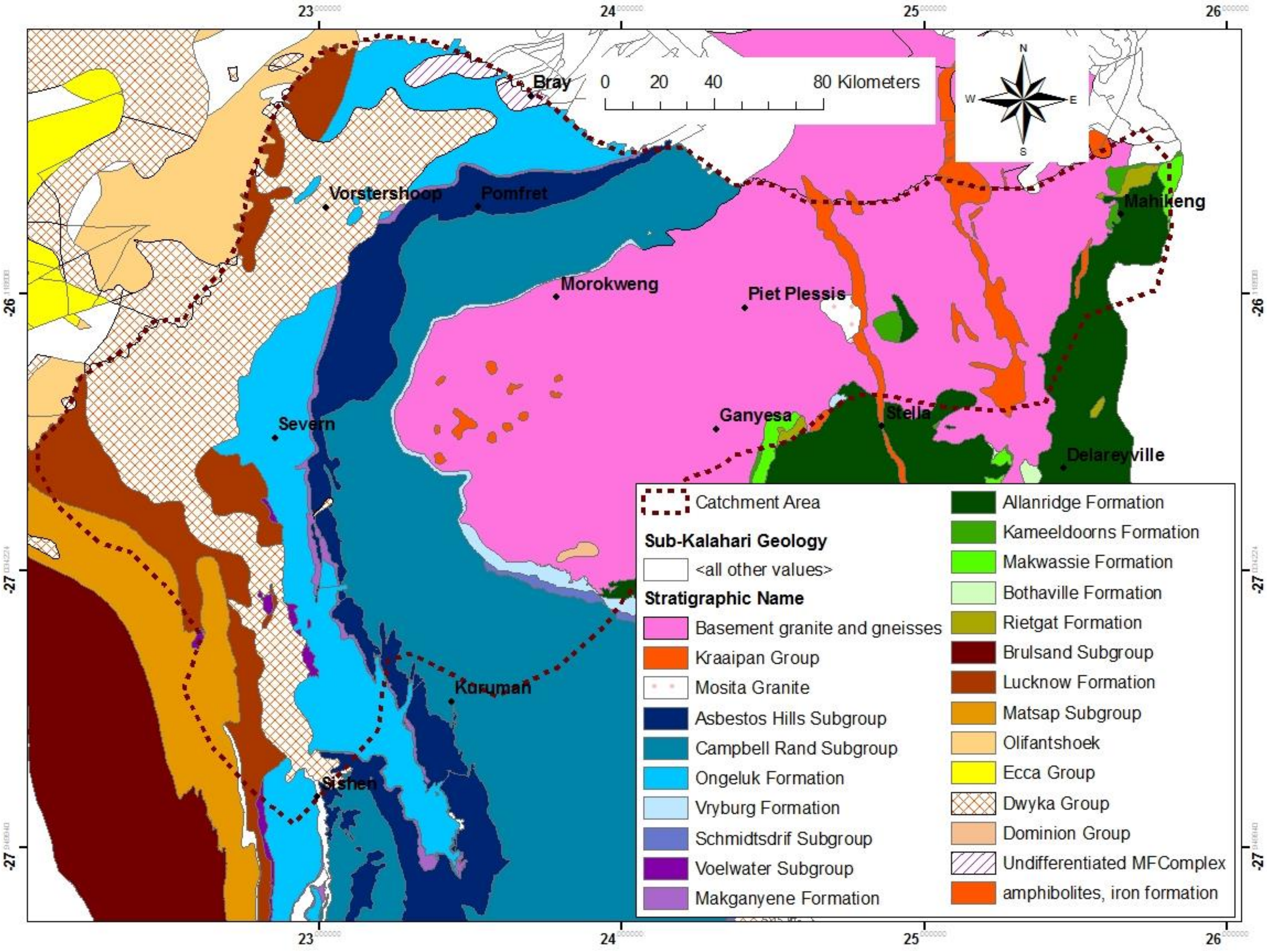

Figure 4.1: Sub-Kalahari geological map of the region (Data sourced from Haddon, 2005)

Figure 4.2: Flat, whaleback pavement of granite outcropping within the study area, with the inset showing an exposure of fresh granite

4.2 Kraaipan - Amalia Greenstone Belt Assemblages

The Kraaipan - Amalia Group of rocks emerge as narrow inliers of outcrop along the eastern edge of the study area, emerging from beneath the blanket of younger Tertiary to Recent Kalahari sediments. The Kraaipan - Amalia rocks crop out sporadically over a distance of approximately 250 km, from southern Botswana in the north to the Amalia - Schweizer-Reneke - Christiana areas in the south (Figure 4.1). They outcrop as low ridges or koppies of resistant steeply dipping beds of chemically precipitated sediments and clastically reworked chemical precipitates, which provide variation in the otherwise monotonous landscape (SACS, 1980, Jones and Anhaeusser, 1991; Anhaeusser and Walraven, 1997, 1999).

Anhaeusser and Walraven (1997, 1999) have described the Kraaipan - Amalia granite-greenstone terrane in terms of a northern and a southern domain. Both regions have a strong regional north-south trend, which is well displayed by the shape of the various greenstone belts and also corroborated by geophysical observations. The Kraaipan rocks in the northern domain are restricted to three, narrow, approximately north-south trending sub-parallel belts, separated by various granitic, gneissic and migmatitic rocks. By contrast, the southern domain (Amalia greenstone belt) is represented by only one greenstone belt sliver also flanked by various granitoid rocks (SACS, 1980; Anhaeusser and Walraven, 1997, 1999). The regional distribution of these four belts are depicted in Figure 4.1. Sporadic greenstone occurrences have also been recorded in exposures west of the Amalia belt (Anhaeusser and Walraven, 1997, 1999), where remnants of volcano-sedimentary rocks are preserved within the granitoid gneisses (Hunter *et al*., 2006).

In general, the Kraaipan - Amalia greenstone belts consist mainly of metamorphosed mafic volcanic rocks and interlayered ferruginous and siliceous metasediments (mainly banded iron formations, jaspilites and ferruginous cherts; Figure 4.3). The volcanic rocks of the Kraaipan - Amalia greenstone terrane consist mainly of massive and, in places, pillowed tholeiitic and andesitic basalts and tuffs. These rocks have been largely metamorphosed and hydrothermally altered to schistose amphibolites and amphibole-chlorite-epidote schists, which are only rarely exposed in the study area. Iron formations (magnetite quartzites, banded ferruginous cherts, jaspilites, and iron formation breccias) are the main Archaean rock types exposed throughout the Kraaipan - Amalia region and are locally intensely deformed and contain gold-sulphide mineralisation in places (SACS, 1980; Jones and Anhaeusser 1991, Zimmermann, 1994).

Figure 4.3: Highly deformed banded iron stone from the Kraaipan greenstone belt

4.3 Ventersdorp Supergroup

The rocks of the Kraaipan - Amalia Group, as well as that of the granitoids, are unconformably overlain to the east and southeast of the study area by subhorizontal Ventersdorp Supergroup lavas of ca. 2.71 Ga (Figure 4.1). This succession of Ventersdorp Supergroup volcanic rocks blanket the Archaean basement between Delareyville in the south and Mafeking in the north.

The Ventersdorp Supergroup comprises the Klipriviersberg Group at the base, followed by the Platberg Group, the sedimentary Bothaville Formation and the volcanic Allanridge Formation (Figure 4.4; Van der Westhuizen *et al*., 2006). Only some of these groups and formations, particularly those in the upper portions of the stratigraphic column, namely the Platberg Group and Allanridge Formation, are present on the edges of the study area.

The Klipriviersberg flood basalts, which extruded during a period of extensional tectonics confined to the Witwatersrand basin, were followed by the deposition of clastic/chemical sediments and bimodal volcanism of the Platberg Group during a period of extensional block faulting, which resulted in graben formation. The pene-contemporaneous extrusion of lava and clastic sedimentation in the grabens and fault troughs produced an interfingering succession of sedimentary, volcanic and pyroclastic rocks (Keyser, 1998).

By the end of Platberg time, faulting and graben filling were virtually complete and the Bothaville Formation was deposited in shallow depressions on a gently undulating Platberg surface. The Bothaville Formation consists primarily of quartzite and/or white, pink or brown conglomerate. The Allanridge Formation has a structurally conformable relation with the underlying Bothaville Formation and consists mainly of dark-green amygdaloidal lava (Figure 4.5), light-green-grey porphyritic lava and pyroclastic rocks (Keyser, 1998; Van der Westhuizen, 2006).

4.4 Transvaal Supergroup - Griqualand West Basin

The period from ~2.65 Ga to ~ 2.6 Ga saw the development of proto-basins for the Transvaal Supergroup (Eglington and Armstrong, 2004). Occupying a large proportion of the sub-Kalahari floor in the central part of the study area are rocks belonging to the Transvaal Supergroup (Figure 4.1), with the most prominent feature in the study area being a southwest to northeast curving ridge of the Asbestos Hills Subgroup, which is 30 - 40 m higher than the surrounding topography (Figure 3.2).

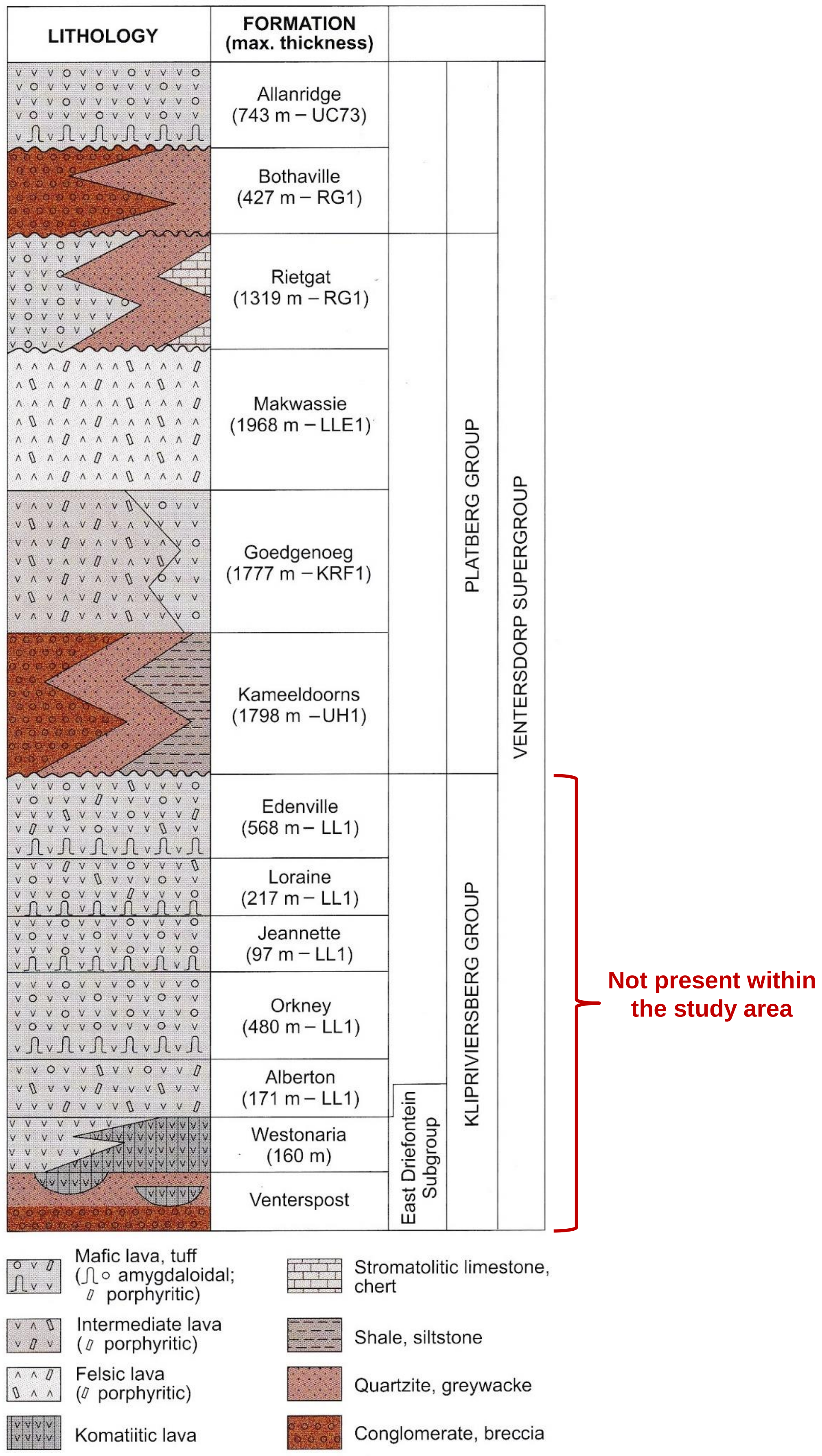

Figure 4.4: Stratigraphy of the Ventersdorp Supergroup (after van der Westhuizen *et al*., 2006)

Figure 4.5: Outcropping amygdaloidal lava of the Allanridge Formation

The basal unit of the Transvaal Supergroup in the Griqualand West Basin is the Vryburg Formation (Figure 4.6), which directly overlies the Archaean granitoids in the central part of the study area. It locally exhibits a basal, transgressive conglomerate, with quartzites, shales and subordinate stromatolitic carbonates passing up in places into basaltic to andesitic amygdaloidal lavas dated at 2642 ± 3 Ma (Walraven and Martini, 1995; Eriksson *et al*., 2006).

Overlying the Vryburg Formation, the Ghaap Group is subdivided, in stratigraphic order (Figure 4.6), into the Schmidtsdrif, Campbell Rand and Asbestos Hills Subgroups (Erikson *et al*., 2006). The Schmidtsdrif Subgroup consists largely of a lower unit of platform carbonates, often characterised by stromatolites, carbonate sands and oolites (Beukes, 1979; Altermann and Siegfried, 1997), and an upper unit of shales, tuffites and BIF-like cherts (Eriksson *et al*., 2006). The Campbell Rand Subgroup, estimated to be 1600 m thick and covering a very large area on the sub-Kalahari geological map (Figure 4.1), consists of dolomite, limestone and chert, with characteristic wavy laminated stromatolites (Grobbelaar *et al.*, 1995; Altermann and Siegfried, 1997; Erikson *et al.,* 2006; Figure 4.7). The Asbestos Hills Subgroup, conformably overlying the Campbell Rand Subgroup comprises banded iron-formation (Figure 4.8), jaspillite, shale and siltstone, which are ferruginised in places, forming irregular bodies of high- to low-grade iron ore (Hälbich *et al.*, 1993).

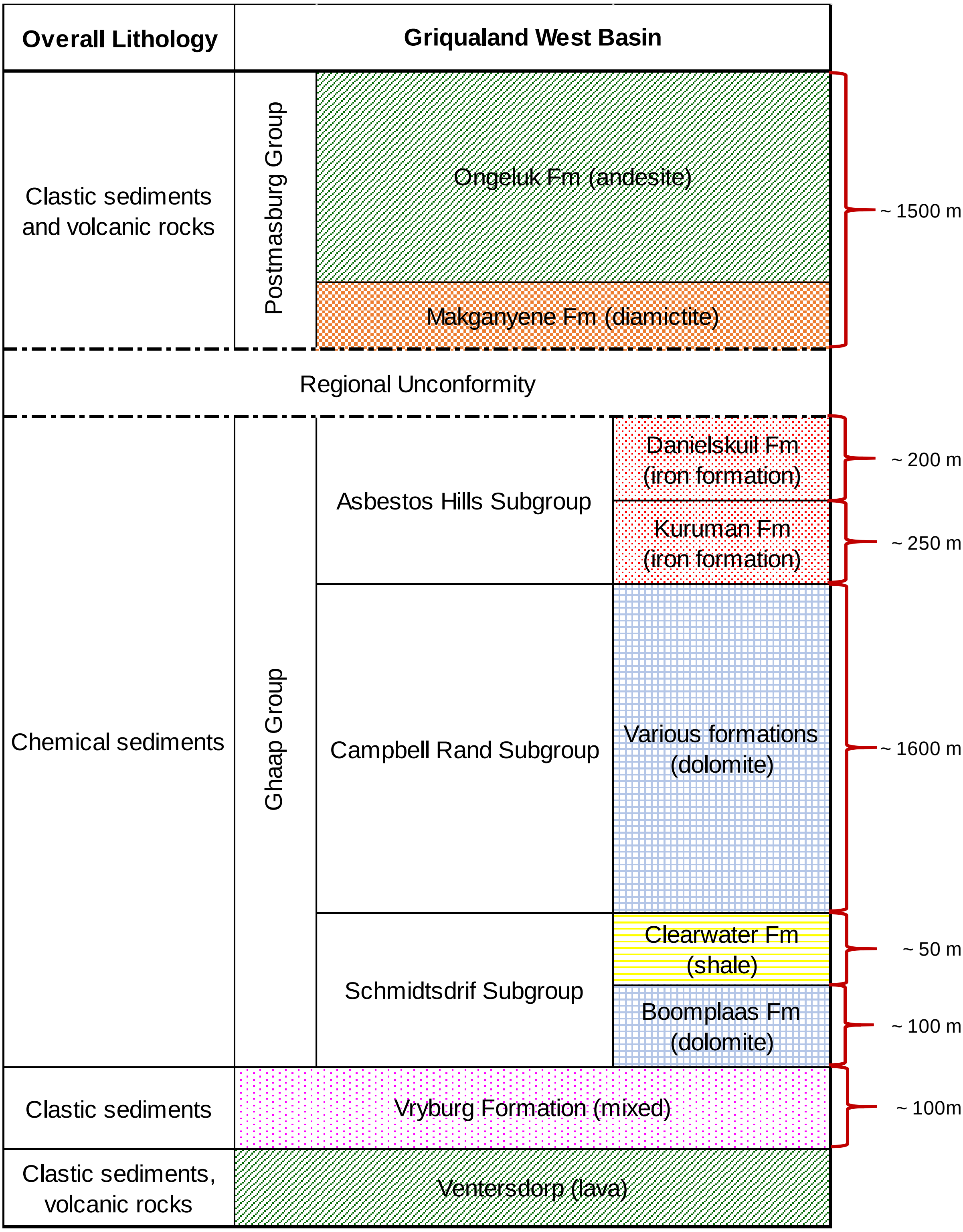

Figure 4.6: Stratigraphy of the Transvaal Supergroup (Griqualand West Basin) within the study area (after Erikson et al., 2006)

Figure 4.7: Dolomite, limestone and chert layers from the Campbell Rand Subgroup

Figure 4.8: Banded iron stone from the Asbestos Hills Subgroup

Cutting deeply down into the underlying Ghaap Group are the basal diamictites of the Makganyene Formation, which together with the overlying mafic lavas (tholeiitic basaltic andesitic lavas) of the Ongeluk Formation and the manganiferous rocks of the Hotazel Formation together constitute the Postmasburg Group (Erikson *et al.,* 2006).

4.5 Molopo Farms Complex

The Molopo Farms Complex, a large layered intrusion of approximately 13000 km^2 in area, is believed to be genetically related to the Bushveld Complex (Gould *et al.*, 1987; Anhaeusser, 2006), with Pb/Pb ages of 2055 Ma (Hartzer, 1998) placing it in the same time frame as that of the Bushveld Complex. It is an elongated (NE – SW), elliptical form that is largely situated in southern Botswana, but extends southwards into the immediately adjacent parts of South Africa near Bray on the Molopo River (Figure 4.1). The complex is completely covered by up to 220 m of Kalahari Group sediments and was initially delineated by a regional geophysical survey (Anhaeusser, 2006).

The Complex consists of a lower Ultramafic Sequence (900 m thick) comprising a succession of harzburgite, pyroxenite and minor dunite, and an overlying Mafic Sequence (1000 – 1500 m thick) consisting of an upwardly fractionated sequence of norites and gabbros (Gould *et al.,* 1987; Reichardt, 1994). Post-emplacement tilting and faulting due to the Kheis orogeny have resulted in considerable sub-vertical displacement and segmentation of the body and host country rocks. Strongly fractionated, ultramafic-mafic sill- or dyke-like offshoots also appear to be a common feature of the Complex, and can be distinguished petrologically from younger dolerite sills and dykes encountered in the area (Reichardt, 1994; Anhaeusser, 2006).

4.6 Olifantshoek Supergroup

Straddling the western margin of the study area are the lower arenaceous sediments and basic lavas of the Olifantshoek Supergroup (Figure 4.1), which form a prominent north-trending mountain range from the vicinity of the Boegoeberg Dam northwards to the Korannaberg, where they are progressively covered by thicker successions of Kalahari Group sediments (Moen, 2006). The sub-Kalahari geological map of Haddon (2005; Figure 4.1) shows remnants of Olifantshoek Supergroup lithologies near Mokopong on the Molopo River, extending further northward into Botswana.

The entire Supergroup consists essentially of interbedded shale, quartzite and basic lava overlain by a thick succession of coarse red and grey quartzite and minor shale (Figure 4.9). The lower lithological units, which form the focus of this study, comprise the Lucknow Formation (the basal Mapedi - Gamagara Formation is absent within the study area), the Hartley-Boegoeberg Dam Formation and the overlying Matsap Subgroup (Figure 4.9). The Lucknow and Hartley Formations consist largely of interbedded shale, quartzite and basic lava, which includes layers of conglomerate and sandstone, that grade into the overlying Matsap Subgroup (Cornell, 1987; Moen, 2006). The reddish-brown arenaceous quartzites and minor shales of the Matsap Subgroup are well developed along the western margin of the study area and are overlain by the quartzites of the Brulsand Subgroup. The latter is largely centred further west of the study area and will not be discussed further in this report.

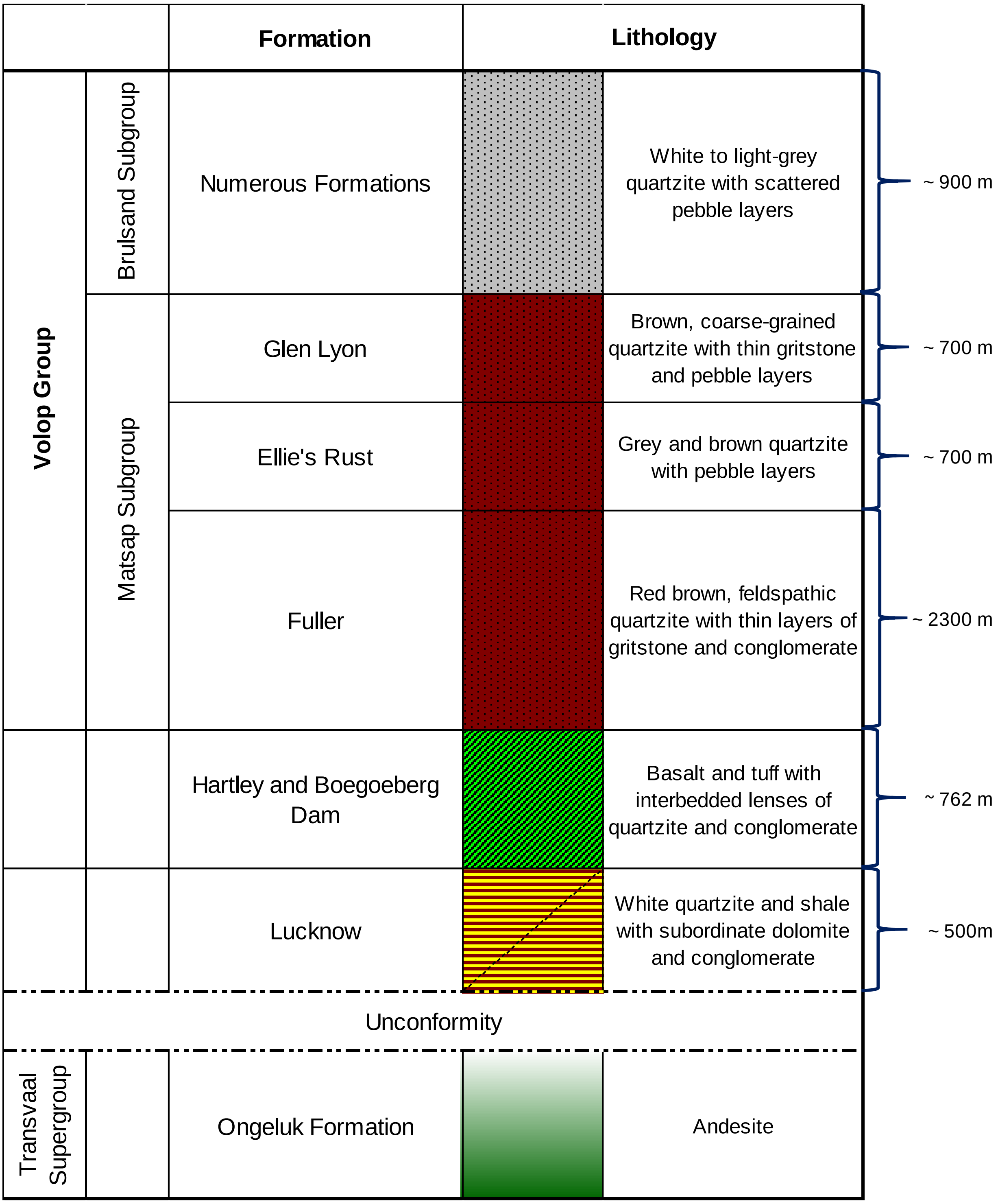

Figure 4.9: Stratigraphy of the Olifantshoek Supergroup within the study area (after Moen, 2006)

Shortly after deposition, rocks of the Olifantshoek Supergroup were involved in low-intensity folding and east-verging, low angle thrusting as part of the Kheis orogeny (Cornell *et al*., 1998; Moen, 2006).

4.7 Morokweng Impact Structure

A large impact structure is centred on a sizeable aeromagnetic anomaly associated with basement granites in the Morokweng region of the study area. Aeromagnetic and gravity images (Figure 4.15 and 4.16) of the Morokweng area have shown the presence of a circular anomaly, roughly 70 km in diameter, beneath the Kalahari sediments (Henkel *et al*., 2002; Reimold *et al*., 2002). Although the surface topography is fairly flat, Kalahari Group isopachs generated by Haddon (2005; Figure 4.11) have also clearly shown a circular feature with anomalous thicknesses of Kalahari Group sediments.

Andreoli *et al*., (1995) investigated drill core from the area and reported finding impact melt rock, as well as shock metamorphic features in the underlying granitoids. The identification of planar deformation features (PDF's) and other shock deformation features (Andreoli *et al.*, 1995; Corner *et al.*, 1996; Hart *et al.*, 1997) and anomalous nickel and iridium concentrations in possible impact melt rocks (Corner *et al.*, 1996; Hart *et al.*, 1997) has enabled interpretation of the feature as a meteorite impact structure.

Drill core from 40 km west of the Morokweng impact crater revealed a thick succession of felsic, granophyric and micropegmatitic granitoids. These intrusive rocks were overlain by an equally thick succession of felsic granophyric volcanics, which were dominated by quartz and feldspars, together with minor biotite and amphibole (Reimold *et al*., 2002). Analysis of this drill core suggested that the maximum crater diameter is less than 80 km (Reimold *et al.*, 2002), which indicates that the central magnetic anomaly delineates the collapsed central uplift of a 70 km wide impact structure capped by impact melt rock.

4.8 Karoo Supergroup

In the study area, the sub-Kalahari geological map shows a trough of Dwyka sedimentary rocks extending southwards from the Botswana border to near the town of Kathu, to the west of Kuruman (Figure 4.1). It is not clear whether this Dwyka trough is a remnant of a much larger covering of tillite in the area, preserved in a subsequent down-faulted graben-like structure that may have been reactivated by the Late Jurassic Morokweng meteorite impact, or if it is limited to a glacial valley which may have been controlled by existing structures (Haddon, 2005).

The Dwyka Group consists of a basal tillite followed by a sequence of shale, siltstone and mudstone, sandstone carbonate lenses and a main tillite (Visser, 1983; Figure 4.10). This glacial sedimentation started in the southern regions of Gondwana in the Late Carboniferous-Early Permian (300-280 Ma), with glaciers eroding high-lying areas and glacial deposits accumulating in fault controlled valleys (Visser, 1989).

The subsequent Karoo Supergroup was deposited in the Karoo - Falklands Basin, part of a retro foreland-arc basin caused by the oblique subduction of the palaeo-Pacific plate. This subduction also resulted in the opening of the Botswana - Zambezi Basin (Visser and Praekelt, 1996). Remnants of these subsequent Karoo Supergroup lithologies are not evident in the study area and are largely centred in the main Karoo and Botswana basins.

Figure 4.10: A typical tillite deposit comprising boulders and cobbles (drop stones) which were dropped from floating ice into a melt water lake environment

4.9 Kalahari Sequence

The geological and tectonic events that have shaped this portion of the craton over the past 3000 Ma, as detailed above, have resulted in a diverse and complex geological setting onto which the Kalahari Group of sediments have been superimposed. In particular, these preceding events have strongly influenced and collectively defined the form and shape of the Kalahari basin, governing the deposition of this extensive, non-marine group of sedimentary rocks in the late Cretaceous and Cenozoic, some 65 - 70 million years ago (Haddon, 2005). Throughout the area the thickest parts of the Kalahari appear to coincide with the occurrence of Dwyka Group rocks, with the deposition of Kalahari Group sediments possibly being controlled by the presence of Dwyka valleys (Partridge *et al*., 2006). Isopachs of the Kalahari Group in the study area show very clearly the presence of large palaeovalley systems where thicknesses of Kalahari Group sediments reach approximately 210 m (Haddon, 2005; Figure 4.11).

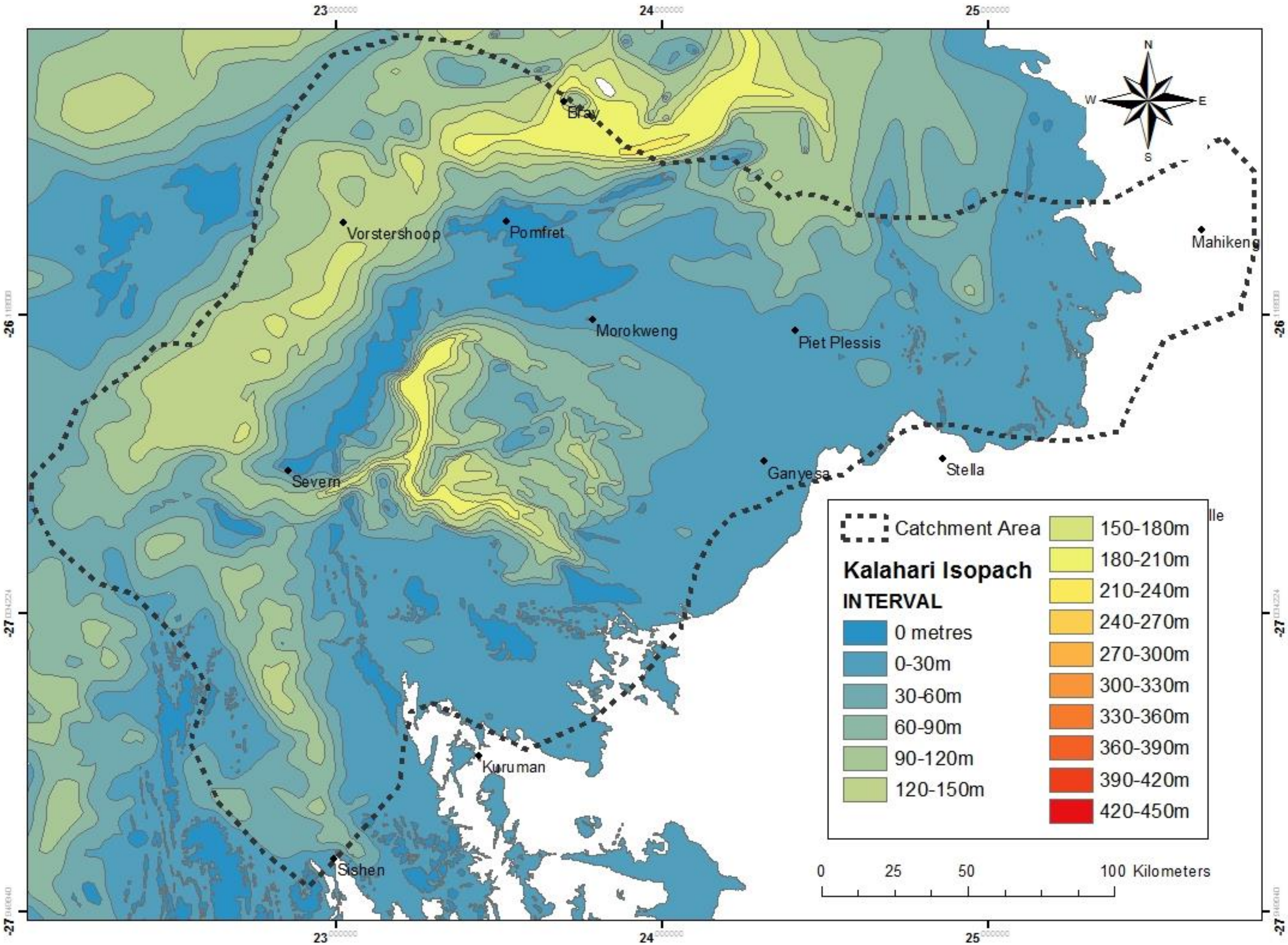

Figure 4.11: Kalahari isopach map of the region (Data sourced from Haddon, 2005)

Palaeovalleys run in a north-south direction between ridges of Olifantshoek and Transvaal Supergroup rocks and link up with a large valley running northeast-southwest along the Botswana border (Haddon, 2005; Partridge *et al*., 2006). In the centre of the map thicker Kalahari sediments fill two deep palaeovalleys that flank the circular Morokweng meteorite impact structure (Figure 4.11), the presence of which is believed to have influenced the deposition of the lower units of the Kalahari Group in this area (Haddon, 2005; Partridge *et al*., 2006). The occurrence of faulting and graben formation in pre-Kalahari rocks also had a strong influence on Kalahari sedimentation, as did the presence of Late Cretaceous drainage systems (Partridge *et al*., 2006).

Due to the limited exposure of Kalahari Group sedimentary rocks, it has proven difficult to define a stratigraphy for the Kalahari Group, with interpretations having to be made from limited borehole data, mine exposures and the few river valleys where the lower formations are exposed. This problem was complicated by the fact that the Kalahari Group of sediments were deposited in a number of small sub-basins, some fault-bounded with syn-depositional movement, which has resulted in a lateral inconsistency of lithological units that can vary within the space of a few kilometres (Haddon, 2005). Nevertheless, it proved possible to recognise a general sequence of lithological units, the description of which is provided below. In general, the Kalahari Group consists of six formations, namely the basal Wessels, overlying Budin, Eden, Mokalanen, Obobogorop and Gordonia Formations (Partridge *et al*., 2006). Figure 4.12 is a schematic stratigraphic column for the Kalahari Group in general and not all the formations shown are present everywhere.

In general, it is believed that the Kalahari basin formed as a response to down-warp of the interior of southern Africa, probably in the Late Cretaceous. The down-warp, along with possible uplift along epeirogenic axes, back-tilted rivers into the newly formed Kalahari basin and deposition of the Kalahari Group sediments began (Haddon and McCarthy, 2005). Initial deposition of basal gravels of the Wessels Formation (Figure 4.13) occurred in the channels of the Cretaceous rivers, with other unsorted gravel beds deposited at the base of scree slopes along the edges of valleys and fault-bounded structures (Haddon and McCarthy, 2005; Partridge *et al.,* 2006). Although this gravel is better developed and thicker in some of the deeper palaeovalleys, it does not occur exclusively in the areas where the Kalahari is at its thickest (Partridge *et al*., 2006). The accumulation of gravels continued as the down-warp of the basin progressed with inter-bedding of the gravel layers with sand and finer sediment carried by the rivers. Thick clay beds comprising largely fine-grained, red and brown calcareous clays of the Budin Formation (Figure 4.13) accumulated in the saline lakes that formed as a result of the back-tilting of rivers (Du Toit, 1954; Bootsman, 1998; Haddon and McCarthy, 2005). Red, brown or, most commonly, yellow sandstones of the Eden Formation were deposited in braided streams inter-fingering with the clays (gradational contact) and covering them in some areas as the shallow lakes filled up with sediment. The sandstones of the Eden Formation are poorly consolidated, with thin pebble layers occurring locally, and become more disaggregated, as well as calcretised and calcified, towards the top (Partridge *et al*.,2006).

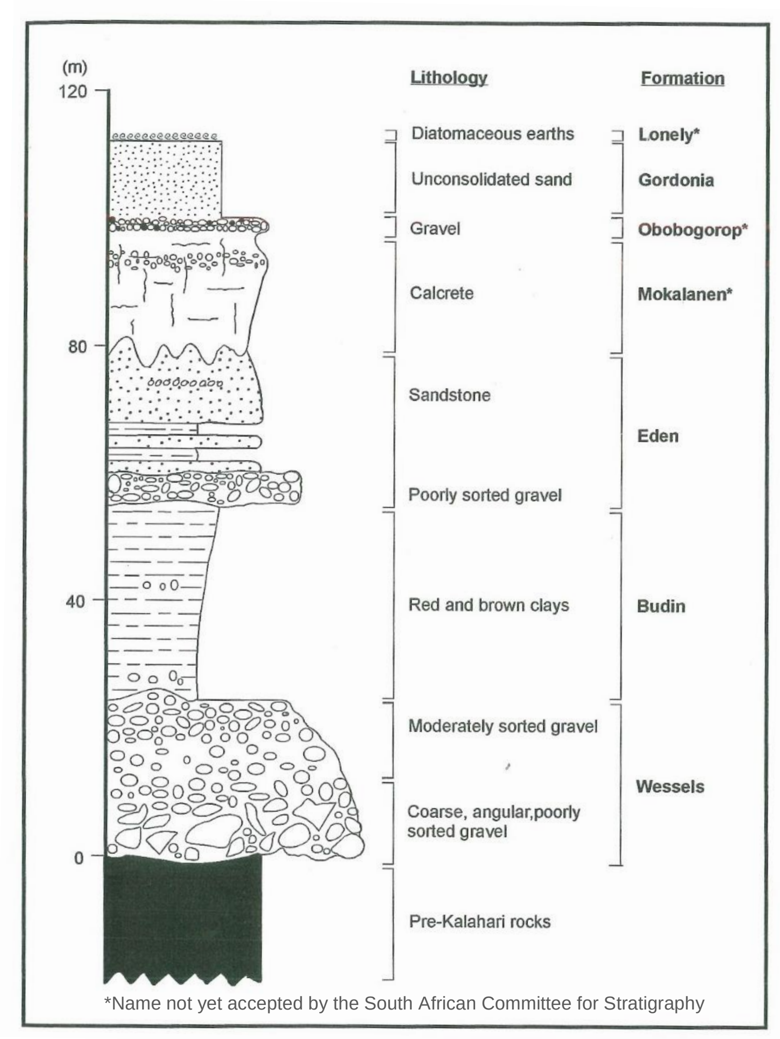

Figure 4.12: Typical stratigraphy of the Kalahari Supergroup within the study area (after Haddon, 2005)

A period of relative tectonic stability during the mid-Miocene saw the silcretisation and calcretisation of older Kalahari Group lithologies. These calcretes are assigned to the Mokalanen Formation and can be divided into a lower, sandy limestone and an overlying conglomerate with a calcareous matrix (Thomas, 1981). Outcrops of these calcretes occur as cliffs along the river valleys (Figure 4.14) and are particularly prominent along the Molopo River and its tributaries (Haddon, 2005). The Mokalanen Formation was deposited under more arid conditions than the underlying fluvial sediments and possibly reflects the interval of global aridification which occurred between 2.8 and 2.6 million years ago (Partridge *et al*., 2006). This period of tectonic stability was followed in the Late Miocene by relatively minor uplift of the eastern side of southern Africa and along certain epeirogenic axes in the interior. More significant uplift that followed in the Pliocene along epeirogenic axes may have elevated Karoo Supergroup and basal Kalahari Group sedimentary rocks above the basin floor where they were exposed to erosion (Haddon and McCarthy, 2005). In particular, the Obobogorop Formation, lying above the calcretes, comprise pebble and boulder clasts believed to have been derived from erosion of Dwyka tillite and, in places, form the cappings of flat erosional remnants (Partridge *et al*., 2006). Eroded sand was washed into the basin where it was reworked and re-deposited by aeolian processes during drier periods, resulting in the extensive red aeolian sands of the Gordonia Formation that cover most of the underlying Kalahari Group of sediments (Haddon and McCarthy, 2005; Partridge *et al*., 2006).

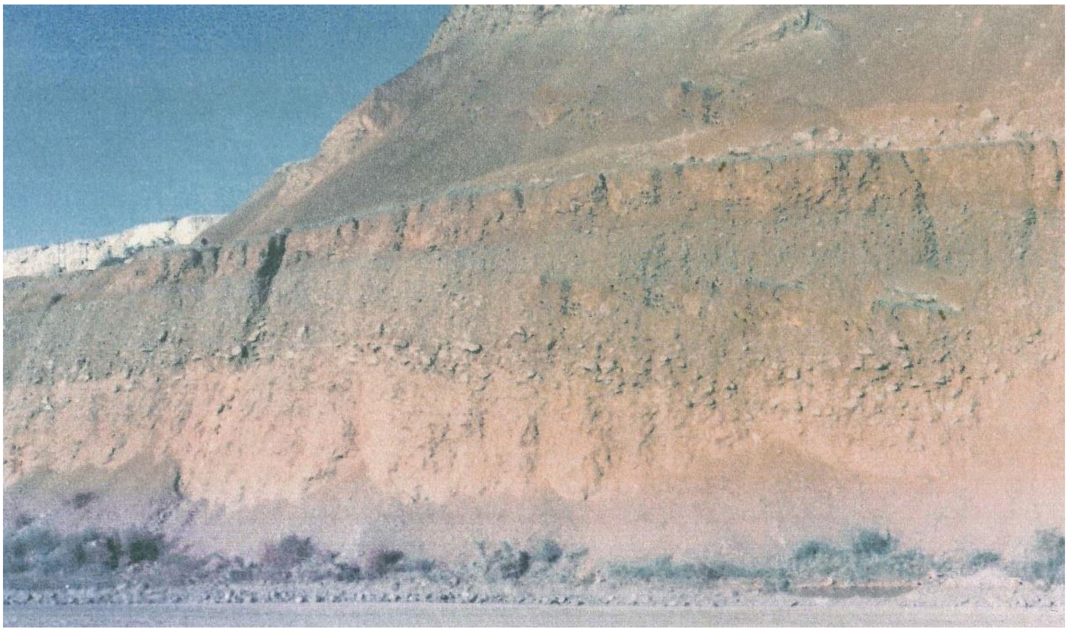

Figure 4.13: The red clays of the Budin Formation overlying the poorly sorted gravels of the Wessels Formation (after Haddon, 2005)

Figure 4.14: An exposed section of calcrete within a river cutting

4.10 Structural Review

In view of the extensive cover of unconsolidated sands, both the sub-Kalahari lithologies and their related structures are poorly exposed on surface, if at all. Structural studies in the area are, therefore, heavily dependent on geophysical methods, coupled with drilling or trenching, to establish critical relationships and the structural nature of the sub-Kalahari geology. Aeromagnetic data, combined with gravity, has proven particularly successfully in detecting fault-related lineaments in sand-covered areas (Reeves and Hutchins, 1982; Tessema *et al*., 2012) and will, therefore, be used for the structural interpretation of the study area.

High-density aeromagnetic and gravity data for the North West Province of South Africa was generated by the Council for Geoscience and was made available on a 250 m and 1000 m line spacing, respectively (Figures 4.15 and 4.16). These revealed a north-south trending Kraaipan - Amalia belt, the highly magnetic nature of which has enabled its extent to be mapped beneath the Kalahari sand cover (Richards, 1979). Further to the south-west, the highly magnetic iron-formations of the Asbestos Hills Subgroup extend north towards the Botswana border where they flank the western side of the Morokweng meteorite impact structure, the latter of which shows up clearly on the magnetic coverage (Figure 4.15). To the west of this, the north-south trending ridges of Olifantshoek Supergroup rocks, which form part of the Kheis Belt, are also noted. Magnetic features to the east of the Kheis belt appear to be more shallow average level magnetic features than the deeply buried, highly magnetic basement to the west of the Kheis Belt (Reeves and Hutchins, 1982; Figure 4.15).

Dykes: A number of strong linear magnetic anomalies cross the study area (Figure 4.15). Owing to the general lack of outcrop, these are interpreted as dykes, with or without fault movement, that are generally near vertical (85 to 90 degrees; Anhaeusser *et al*., 2010). In many cases, these dykes can be linked to various magmatic and volcanic events that have been identified on the craton (Visser, 1956; Hunter and Reid, 1987; Uken and Watkeys, 1997). Within the study area, the dykes display three main trends, namely northeast, east-west and northwest. The northwest-trending dykes are poorly exposed throughout the study area and are magnetically weak. These NW–SE trending dykes are subparallel to the tributaries of the Molopo River (Figure 4.15), which led Tessema *et al*. (2012) to suggest that these dykes intruded the host rock along crustal weak zones, such as faults, which later strongly influenced and guided the development of palaeo-channels along which coarse sediments may have been deposited.

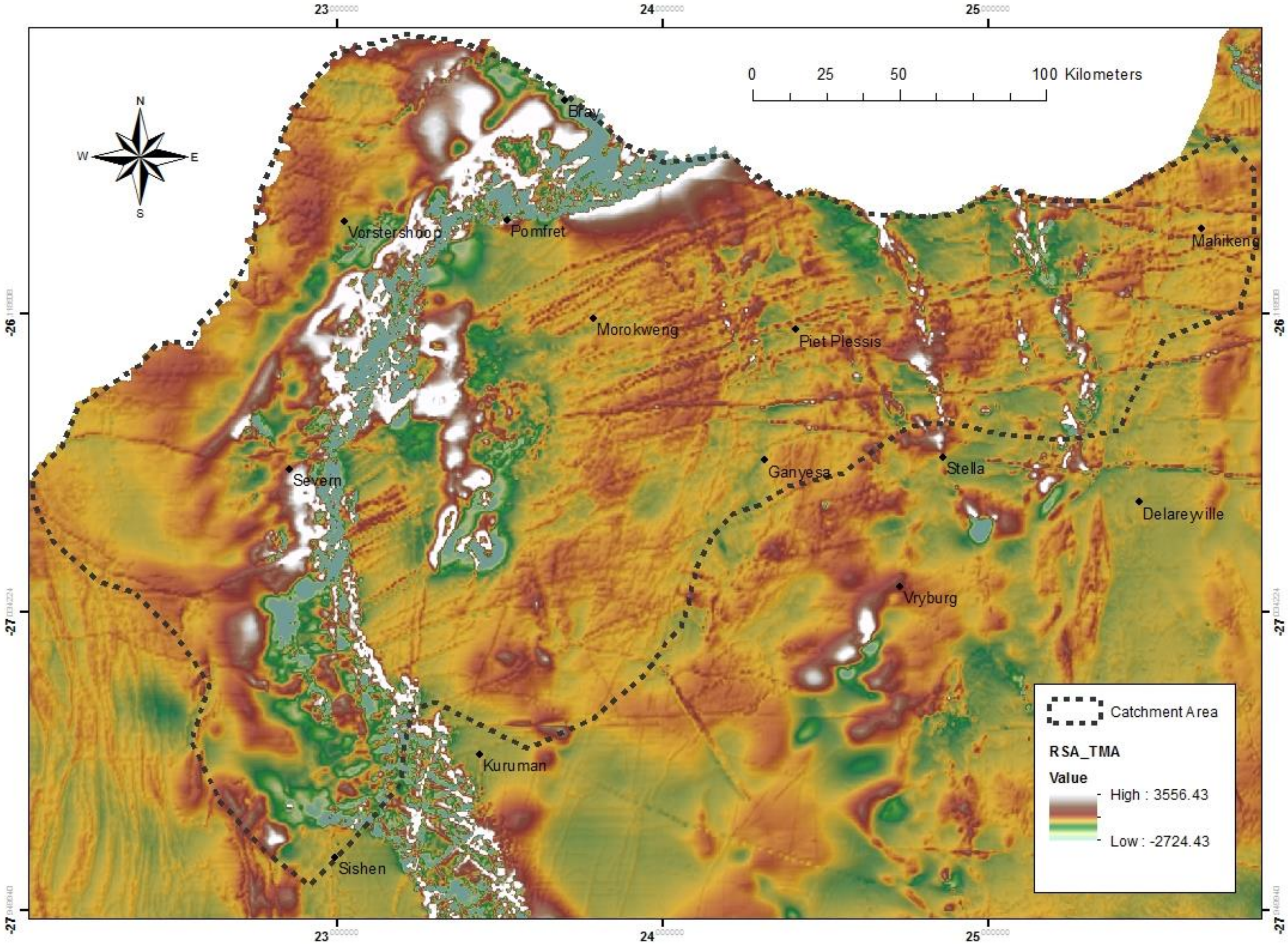

Figure 4.15: Total magnetic intensity map of the study area (Data sourced from the Council for Geoscience)

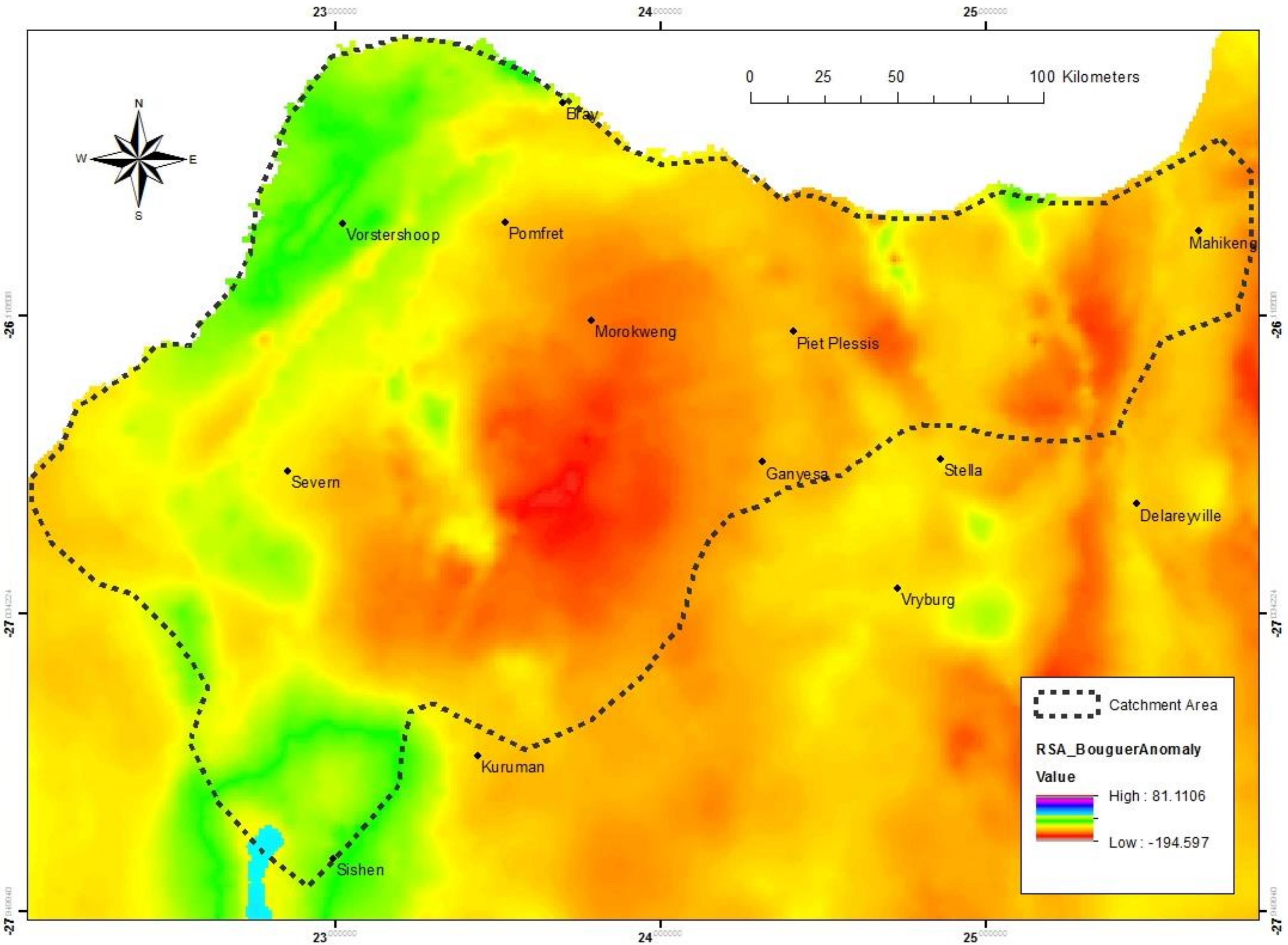

Figure 4.16: Gravity map of the study area (Data sourced from the Council for Geoscience)

The most persistent linear feature in the study area is a southwest to northeast trending dyke swarm, up to 100 km wide, with a strong aeromagnetic signature. These dykes only appear to be present in the bedrock below the Kalahari sediments. To the west of the study area many of these dykes cross the Asbestos Hills Subgroup becoming broader and more fuzzy westward, indicating an increase in depth, before terminating against formations of the Olifantshoek Supergroup (Figure 4.15). Many of these NE–SW trending lineaments are subjected to several structural offsets along strike, confirming multiple phases of deformation. In general, many of the lineaments traverse over a long distance (> 150 km), indicative of the presence of large-scale crustal dilations which were produced during major tectonic events. In particular, these dykes are thought to be linked to the ca. 2700 Ma Ventersdorp rifting event, but also include similar northeast-trending Karoo-age dolerite dykes (Uken and Watkeys, 1997). The youngest dyke event in the study area is represented by the east to west trending dykes, with a strong magnetic lineament that transects the entire study area (Figure 4.15). The east-west trend is thought to represent long regional feeders, which correspond with the long axis of the Bushveld Complex and extends westwards into the Molopo Farms Complex (Anhaeusser, 2006).

While the dykes mentioned above are not as clearly defined in the gravity data as in the magnetic data, the gravity technique has proven successful in delineating areas of different density both within the study area and within the same lithological unit. Quite noticeable on the gravity map (Figure 4.16) is the density low associated with the Morokweng meteorite impact structure. Of more interest, however, are the gravity lows associated with the carbonate rocks of the Campbell Rand Subgroup. Dolomite is known as a good source of underground water, because of its natural subterranean caves and solution channel pathways where large amounts of water can be stored naturally. These underground caves can be remotely detected because they have a lower density than the surrounding solid dolomite and here the gravity technique has been used very successfully to detect possible sinkholes and favourable structures to extract groundwater for domestic consumption. Target selection may be enhanced by the use of magnetic data, which clearly delineates a number of dykes which have compartmentalised the dolomite aquifer into various sub-units (Golder Associates, 2014; Figure 4.15).

Faulting: While more difficult, given the poor exposure, evidence of faulting is also supported on the aeromagnetic images that show several NE-SW and N-S striking lineaments (Figure 4.15). The weakly magnetized N–S striking lineaments are narrow and extend over a few kilometres to tens of kilometres (20 km to 80 km in length), suggesting that they are deeply buried and possibly cut through the host rocks along thrust faults. These N-S striking thrust faults are evident in the Asbestos Hills Subgroup (Figure 5.7), with sections of the iron stones having been thrust from west to east, semi-horizontally into the dolomite of the Campbell Rand Subgroup. By contrast, the NE-SW striking faults in the region are believed to be indicative of normal faults (Golder Associates, 2014). These NE-SW and N-S striking lineaments within the study area are believed to be associated with the late Archaean Ventersdorp Supergroup (Tessema *et al*., 2012). In particular, previous studies (Burke *et al*., 1985, Roering *et al*.,

1990) have noted that extensional faulting accompanied by extrusion of large volumes of Ventersdorp lavas covered large parts of the North West Province, with the maximum thickness of sediments deposited being confined by structural grabens that are bound by N-S striking series of fault systems. These processes were continued during the emplacement of the Bushveld Complex and Pilanesberg alkaline extrusion, which produced a series of normal and strikes-slip fault systems with NE-SW and N-S strike.

It appears that the dominant trends influencing the development of basins and orogenic belts since the Palaeoproterozoic have been oriented in approximately NE-SW and NW-SE directions. Within the study area itself, NE–SW lineaments are displaced by NW–SE striking faults, confirming multiple phases of deformation (Tessema *et al*., 2012). In many cases, the NE orientation is thought to represent the orientation of the rifts that formed, with the NW orientation often representing the faulting perpendicular to the rift orientation. The same NW- and NE-trending structures appear to have been reactivated at various times and during the Phanerozoic were important in controlling initially the lowering of Karoo Supergroup rocks into NE-SW trending grabens, where they were protected from erosion and preserved, and later the Kalahari sedimentation (Haddon, 2005).

5. HYDROGEOLOGICAL REVIEW

The geological and tectonic evolutionary events that have shaped this portion of the Craton (Section 4) have strongly influenced and collectively defined the hydrogeological nature of this area, giving rise to complex hydrogeological environments with innumerable variations in aquifer transmissivity, effective porosity, saturated thickness and groundwater recharge. Fundamental to this research, therefore, was a collation and review of the hydrogeological aspects of the Kalahari and sub-Kalahari geology, the knowledge of which is deemed important in determining the groundwater potential of the region (discussed in Section 9).

5.1 Geologically Defined Hydrogeological Units

Review of the current data, as well as existing national hydrogeological maps, has allowed for the study area to be divided into five aquifer storage types, each of differing hydrogeological characteristics (Figure 5.1). This hydrogeological classification includes fractured basement (volcanic and meta-sedimentary) rocks, weathered crystalline basement, karstic domains, fractured consolidated sedimentary rocks and intergranular consolidated sedimentary rocks.

5.1.1 Fractured Basement Aquifers (volcanic and meta-sedimentary)

Much of the south-eastern portion of the study area (Figure 5.1), which is dominated by the Kraaipan - Amalia greenstone belt and the Ventersdorp Supergroup, is characterised by fractured aquifers. In particular, basic extrusive rocks (andesitic and basaltic lavas; Figure 5.2) and acidic extrusive rocks (rhyolite and quartz porphyry) form the Ventersdorp aquifers, whereas faulted and fractured meta-arenaceous and meta-argillaceous rocks form the Kraaipan - Amalia aquifers (Figure 5.3). Generally, these basement aquifers offer poor prospects of securing groundwater, as they have limited porosity due to the solid nature of the rock and are generally resistant to the development of secondary porosity. Groundwater in such impermeable and hard-rock terranes is primarily confined to available faults, joints, fractures and cross-cutting lineaments (Astier, 1987), the groundwater potential of which is further controlled by the size of the fractures and their interconnectivity.

While it is understood that various rocks (plutonic and volcanic) are permeable along open fissures, the permeability of fissured systems changes and reflects the geological history of the rocks. These older lithological units of the Kraaipan - Amalia and Ventersdorp Supergroups have been exposed to tectonic stress and numerous other geological processes during their vast geological past that have caused changes to the permeability of their fracture systems. In general, younger fracture systems of late tectonic events are often more permeable than those of older ones that may be sealed by secondary minerals (Geyh, 2001). Usually, the width of the fractures and, therefore, their permeability also decreases with increasing depth. The ability of fractures to

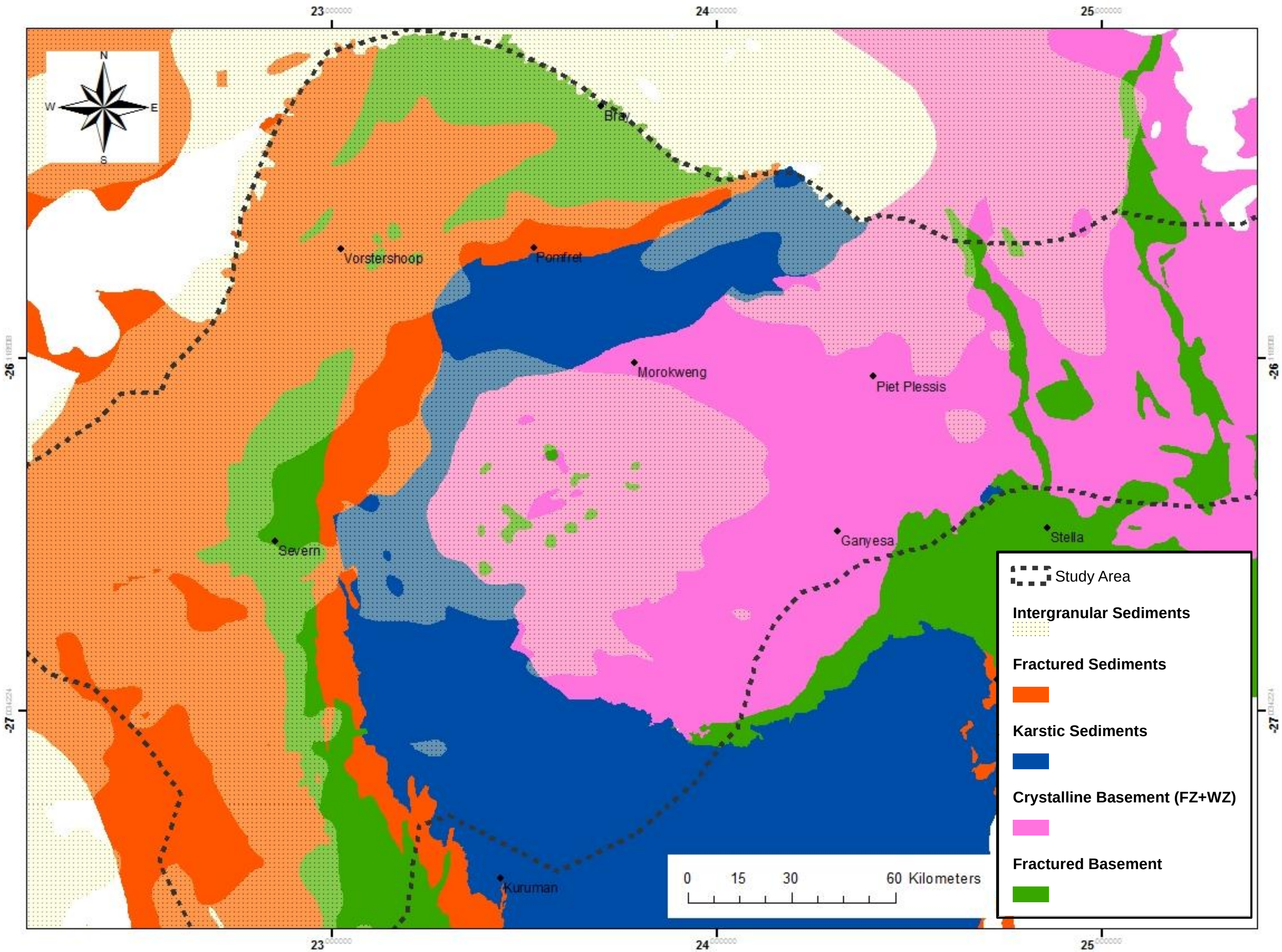

Figure 5.1: The five aquifer storage types identified within the study area (Sub-Kalahari geological data sourced from Haddon, 2005)

act as conduits for groundwater flow are also determined by the degree to which the fractures are interconnected, with fracture connectivity increasing with increasing fracture length and fracture density, hence fracture intersection also increases (Cook, 2003).

Figure 5.2: The faulted and fractured amygdaloidal lavas of the Ventersdorp Supergroup exposed at surface

Figure 5.3: The faulted and fractured meta-sedimentary (BIF) rocks of the Kraaipan - Amalia greenstone belt. Note the vertical fractures typically associated with this hydrogeological unit.

5.1.2 Fractured and Weathered Crystalline Basement Aquifers

The granitic rocks of the Archaean basement within the south-central portion of the study area (Figure 5.1) show poor hydrogeological qualities, as they are generally characterised by very weak parameters of porosity and permeability. The formation of secondary porosity due to weathering, fracturing and jointing are the only means by which this geological formation acquires favourable aquifer character. The grade and depth of weathering is usually a function of climate and mineralogy. Hard plutonic rocks such as granite, which are rich in quartz, are prone to fracturing and mechanical weathering processes, which produce sandy alluvial sediments that are permeable at the surface (Figure 5.4). Weathering may also form open fissures, which are usually permeable down to a certain depth. Within this semi-arid environment, the hydrogeological structures in the crystalline regions are typically characterised by unconfined, shallow groundwater circulation in the zone of weathering and fracturing, which only reaches a depth of some tens of metres (Geyh, 2001).

Figure 5.4: Highly weathered and fractured granite typically occurring at shallow depths beneath the Kalahari sand cover

5.1.3 Fractured Sedimentary Rocks

The Asbestos Hills Subgroup, which comprises banded iron-formation, jaspillite, quartzite, shale and siltstone in a band stretching across the central portion of the study area (Figure 5.1), typically falls under this hydrogeological category. Inclusive are the Dwyka Group of rocks (tillite, shale, siltstone and mudstone) and the Olifantshoek sequence (quartzite, shale and andesite) preserved along the western margin of the study area (Figure 5.1). These rocks have been severely indurated, many ferruginised in places, and have extremely low porosities and primary permeabilities, thereby restricting the occurrence of groundwater. Without the presence of fracture induced secondary permeability (faulting, fracturing and jointing; Figure 5.5) they would at best be considered as aquitards. Where weathering and deformation processes, such as minor folding or the intrusion of dykes, have imparted a secondary permeability, the groundwater abstraction from these aquifers is usually limited (Sami, 1996).

Figure 5.5: Fractures typically occurring along the bedding planes of the sedimentary units of the Asbestos Hills Subgroup, which is exposed along a resistant ridge stretching across the study area

5.1.4 Karstified Sedimentary Rocks

The limestones and dolomites of the Campbell Rand and Schmidtsdrif Subgroups are classified as karstic and are considered as the most prospective water bearing formations in the study area, supporting not only valuable irrigated agricultural activities, but also underpinning the water supply to several towns, including Vryburg. While the primary porosity and hydraulic conductivity of dolomite is poor, weathering and karstification make them prolific aquifers, where the thickness of the deposits allow (Cobbing *et al*., 2014). Carbon dioxide in water dissolves the rock, widens fissures/fractures (Figure 5.6) and creates karst cavities with often very large cross sections (Geyh, 2001). Major structural deformations (faulting) and intrusions (dykes), as well as impervious sedimentary layers (carbonaceous shale and quartzite), within the limestones and dolomites can also divide this hydrogeological unit into semi-autonomous groundwater units or “compartments” (Figure 5.7). These compartments are often used as the basis for hydrogeological characterisation and groundwater management.

Figure 5.6: Dissolution features observed along the fractures of exposed dolomite

While the hydrological characteristics of karstic terrains in general make them well sought after for groundwater exploitation, it must be noted that in the study area the climate is drier and consequently the karst is poorly developed and the residual soil thinner, even absent in places. The dolomites of the Campbell Rand and Schmidtsdrif Subgroups are also rich in insoluble chert as well as Fe and Mn. Apart from features like karren (solution grooves which are commonly separated by sharp ridges; Figure 5.6), the surface morphology is generally not typical of karst, since dendritic networks of valleys and gullies point to the prevalence of surface erosion. This is due to a combination of the high concentration of insoluble impurities in the rock and the semi-arid climate which prevails over most of the karst area (Martini, 2006). It seems that the channel systems are poorly interconnected and partly obstructed by residuals. Shallow phreatic tubes, which rapidly drain the subsurface and are characteristic of the humid karst in purer carbonates, are absent in the Ghaap Plateau karst areas (Martini, 2006).

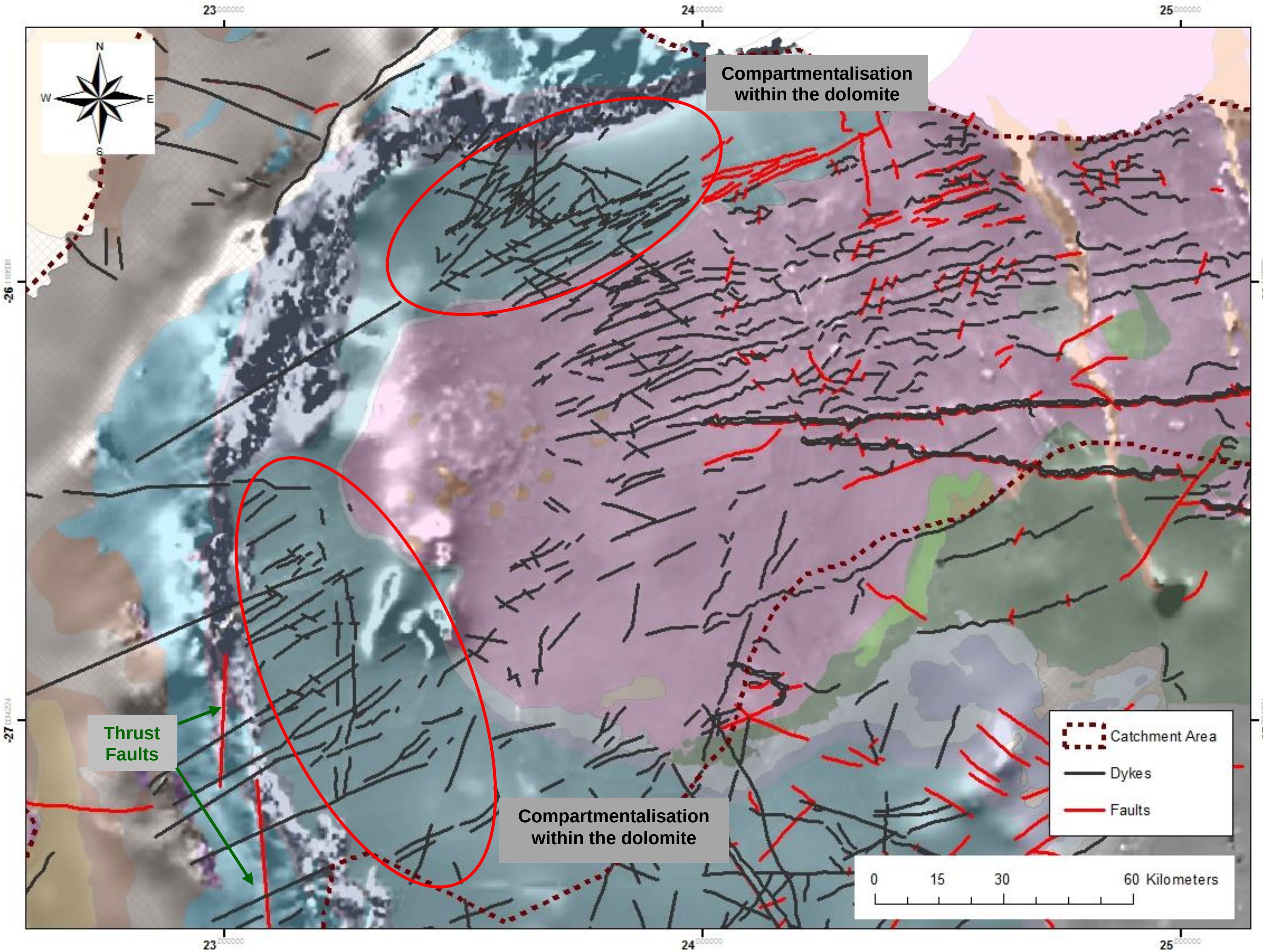

Figure 5.7: The numerous faults and dykes encountered within the study area, superimposed over the sub-Kalahari geology (Structural and geological data sourced from Haddon, 2005; Aeromagnetic data sourced from the Council for Geoscience)

5.1.5 Intergranular Sedimentary Rocks

An intergranular sedimentary aquifer that exhibits the most potential in the study area is that associated with the sandstones of the Eden Formation of the Kalahari Group. This unconfined lithological unit is separated from the basal gravels of the Wessel Formation by the red clays of the Budin Formation, which act as a confining layer. The basal gravel formation, which is largely confined to the deeper palaeo-valleys, and underlying bedrock can be regarded as one aquifer, however, in the absence of the confining Budin Formation clays the upper sandstones of the Eden Formation and the basal gravels, if present, may be regarded as a single hydrogeological unit. This unconfined aquifer is overlain by nodular and hardpan calcrete of the Mokalanen Formation, with the tillite and mudstones of the Dwyka Group serving as an impermeable barrier to the overlying unconfined aquifers of the Kalahari Group.

Usually sandstones are suitable aquifers, often proving to be very efficient aquifers as their porosity and permeability are usually high. Worth mentioning, is the artesian Stampriet aquifer which is located in the Auob Member of the Ecca Group (Alker, 2008; Peck, 2009). Where present, largely in the southwestern portion of the Kalahari Basin (encompassing portions of Botswana, Namibia and South Africa), this aquifer provides much of the groundwater. Unfortunately, remnants of these lower to middle Karoo Supergroup lithologies are not evident in the study area, having possibly been eroded away, with the lower Dwyka Group of rocks forming the only representative of the Karoo Supergroup lithologies.

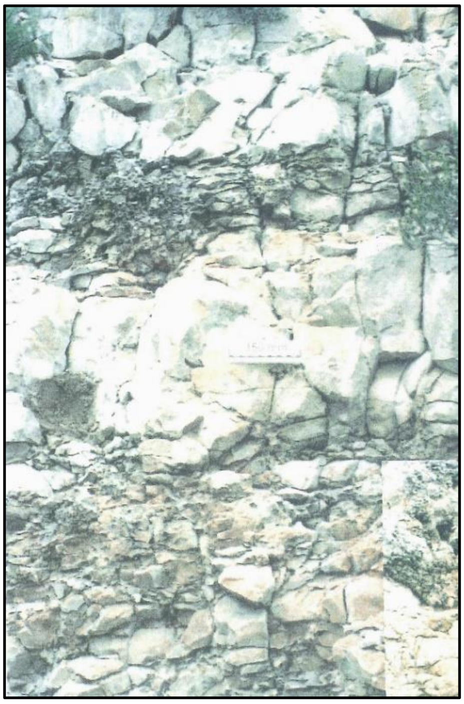

Figure 5.8: Jointing of the sandstones of the Eden Formation, with calcretisation of some of the weathered sandstone having taken place (after Haddon, 2005)

Decisive factors influencing the efficiency of intergranular sedimentary rocks include their grain-size distribution in both the horizontal and vertical directions, rather than the absolute size of their grains and the presence of fine clay particles (Geyh, 2001). From lithological mapping of the area (Haddon, 2005), it has been observed that the sandstones of the Eden Formation comprise inter-fingering layers of clay at its base, with thin pebble layers occurring locally, becoming more disaggregated, as well as calcretised and calcified, towards the top (Partridge *et al.*,2006; Figure 5.8). As such, the permeability of the solid sandstone is low and is not regarded as one of the highest yielding aquifers.

5.2 Storativity/Specific Yield

The complex hydrogeological environments discussed above have innumerable variations in effective porosity and permeability, the knowledge of which is essential for the quantitative calculations of groundwater storage and resource potential of this arid region (Section 9). As such, each of these aquifer storage types were assigned an average storativity/specific yield (See Section 2.2.1). A summary of the storativity/specific yield values assigned to each hydrogeological unit is provided in Table 5.1, with a brief description provided below. The reader, however, is referred to the original literature, referenced in Table 5.1, which details each individual study and the results obtained.

Table 5.1: Storativity/Specific yield values assigned to each hydrogeological unit

Lithostratigraphic Domain	Lithology	Average Storativity/ Specific Yield	Reference
Kalahari, Eden Formation	Sandstone	0.005	Martinelli, 1975 Van Dyk, 2005
Dwyka	Tillite	0.0002	Dondo et al., 2010 DWAF, 2006
Olifantshoek	Quartzites	0.0007	Zhang et al., 2004 DWAF, 2006
Ventersdorp/Transvaal	Andesite/Quartz Porphyry	0.0004	USGS
Transvaal	Shale/BIF	0.0009	Dondo et al., 2010
Transvaal	Dolomite	0.002	Van Dyk, 1993 Van Dyk, 2005
Archaean Crystalline Basement	Granite (Weathered)	0.003	Botha and Bredenkamp, 1992 Nel, 2001
Archaean Crystalline Basement	Granite (Fractured)	0.0002	DWAF, 2006
Kraaipan - Amalia	Meta arenaceous sediments	0.0004	Witthüser et al., 2011

The fractured sedimentary rocks were assigned a low storativity/specific yield, specifically the shales and banded iron formations of the Asbestos Hill Subgroup (Table 5.1). These rocks have been severely indurated, many ferruginised in places, and have extremely low porosities. Without the presence of fracture induced secondary permeability (faulting, fracturing and jointing) the effective porosity of these lithological units would be lower and they would at best be considered as aquitards. The quartzites of the Olifantshoek Supergroup recorded similarly low storativity/specific yield values of 0.0007 (Table 5.1).

Unable to find site specific data for the fractured basement aquifers of the Kraaipan - Amalia greenstone belt, an attempt was made to find a proxy for this storativity value, with the flow and storage characteristics of known lithologies in the Limpopo Province being compared and related to that of the study area. Based on pump test data this lithological unit was assigned a storativity of 0.0004, a value slightly lower than that recorded for fractured sedimentary aquifers (Table 5.1). These rocks have limited porosity and given their vast geological past, there is no doubt that there has been a decrease in the permeability of the fracture system that is present. The basic and acidic extrusive rocks of the Ventersdorp Supergroup, which also form part of the fractured basement aquifers, were assigned a storativity/specific yield of 0.0004 (Table 5.1).

Quite surprising is the effective porosities recorded for the weathered granite basement, values of which have proven to be higher than that of fractured sedimentary and basement aquifers (Table 5.1). It seems that the formation of secondary porosity due to weathering, fracturing and jointing have imparted a favourable character to this aquifer. Similarly, the development of secondary porosity features (fractures and dissolution cavities) within the karstic hydrogeological units have also aided significantly in their exploitation potential, with an effective porosity of 0.002 being assigned to this hydrogeological unit (Table 5.1).

Not surprisingly, the sediments of the Kalahari Group have recorded the best effective porosities within the study area (Table 5.1). While not regarded as one of the highest yielding intergranular aquifers (like Stampriet), largely due to the inter-fingering layers of clay, as well as calcrete, this hydrogeological unit exhibits the most potential in the study area.

As noted in Section 5.1, the structural and tectonic history of a region plays a significant role in determining the behaviour of each aquifer type. While an average storativity/specific yield is given for each aquifer type, it must be noted that the range of variation among so many interdependent and independent factors is so wide that the same aquifer will not always exhibit identical characteristics. Establishing regionally representative values also remains a big challenge, since more often than not, pumping test data is used, and this only covers a small portion of the aquifer under study and may be inaccurate for the remainder of the fractured rock aquifer. Nevertheless, the size of the study area demanded that an average be calculated. A detailed hydrogeological investigation is suggested for any areas of interest, one which should unravel the unique structural controls governing groundwater movement in that particular area.

5.3 Groundwater Level and Saturated Aquifer Thickness

Depending on whether or not an aquifer had a fairly well defined base or not, various approaches were used to estimate aquifer thickness (See Section 2.2.2). A summary of the saturated thicknesses calculated for each hydrogeological unit is provided below.

5.3.1 Unconfined, Intergranular Sedimentary Aquifers

Using the Kalahari isopach map of Haddon (2005; Figure 4.11), in addition to the cross sections generated for the region (Figure 5.9 A, B and C), the average saturated thickness for each 30 m depth interval was calculated, a summary of which is provided in Table 5.2. An average saturated thickness of 57.75 m was calculated for the Kalahari sediments, however, it must be noted that this average was dominated by the thicker and deeper deposits.

Table 5.2: The 30m interval saturated thicknesses of the Kalahari aquifer

Depth Interval (m)	Average Water Level (mbgl)	Base Aquifer (mbgl)	Saturated Thickness (m)
0 - 30 m	17.64	30.00	12.36
30 - 60 m	33.31	60.00	26.69
60 - 90 m	24.33	90.00	65.67
90 - 120 m	82.13	120.00	37.87
120 - 150 m	117.45	150.00	32.55
150 - 180 m	76.29	180.00	103.71
180 - 210 m	80.36	210.00	129.64

When plotting the average water levels calculated for each sampling/monitoring point on the geological cross sections (Figure 5.9 A, B and C) constructed for the study area, it becomes apparent that the depth of the groundwater below the surface is influenced by the thickness of the Kalahari Group of sediments. Shallow water tables occur along watersheds and where the cover of Kalahari Group sediments is thin, and deep water levels occur in areas where the Kalahari Group of sediments are thickest. The thickest portions of the Kalahari Group of sediments (in excess of 180 m) are confined to palaeo-valleys within the region, one running parallel to the Botswana – South African border (adjacent to the Molopo river) and the other enveloping the north-western rim of the Morokweng Impact Structure.

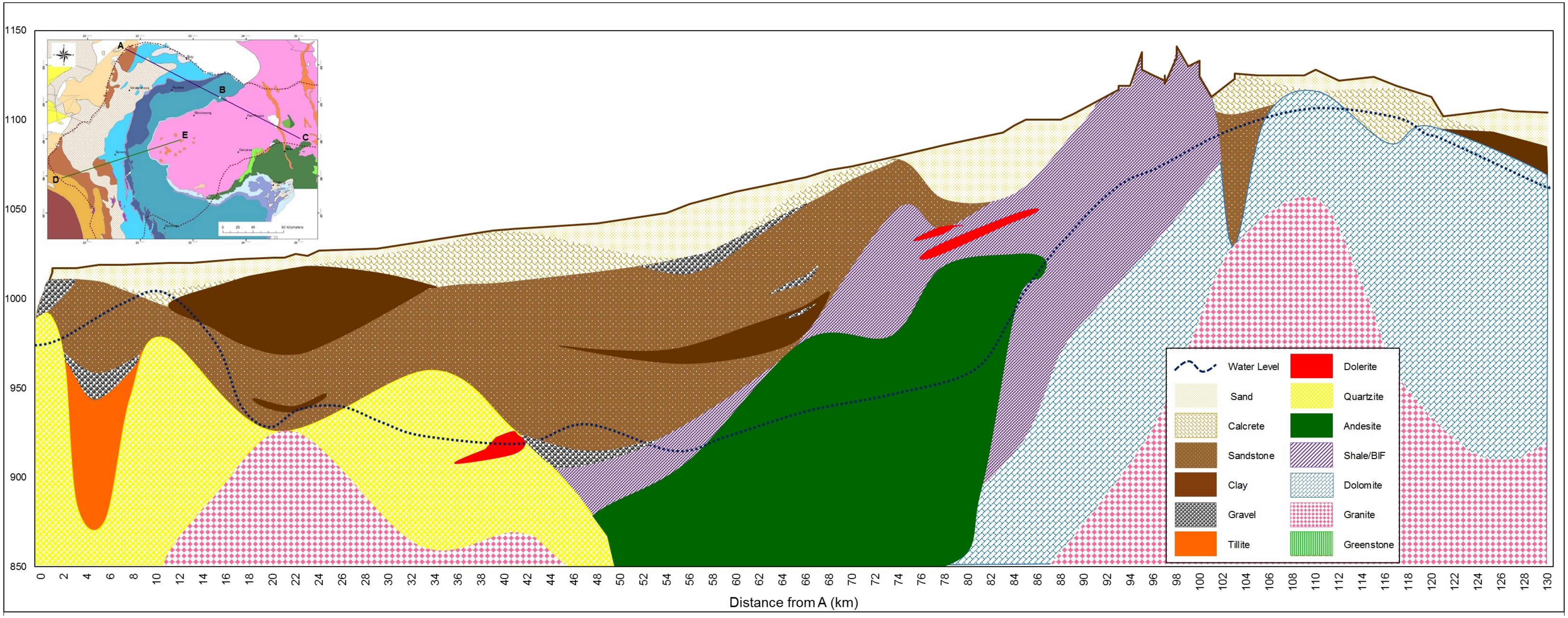

Figure 5.9 (A): Geological cross section A – B (Lithological data sourced from the Department of Water Affairs and the Council for Geoscience)

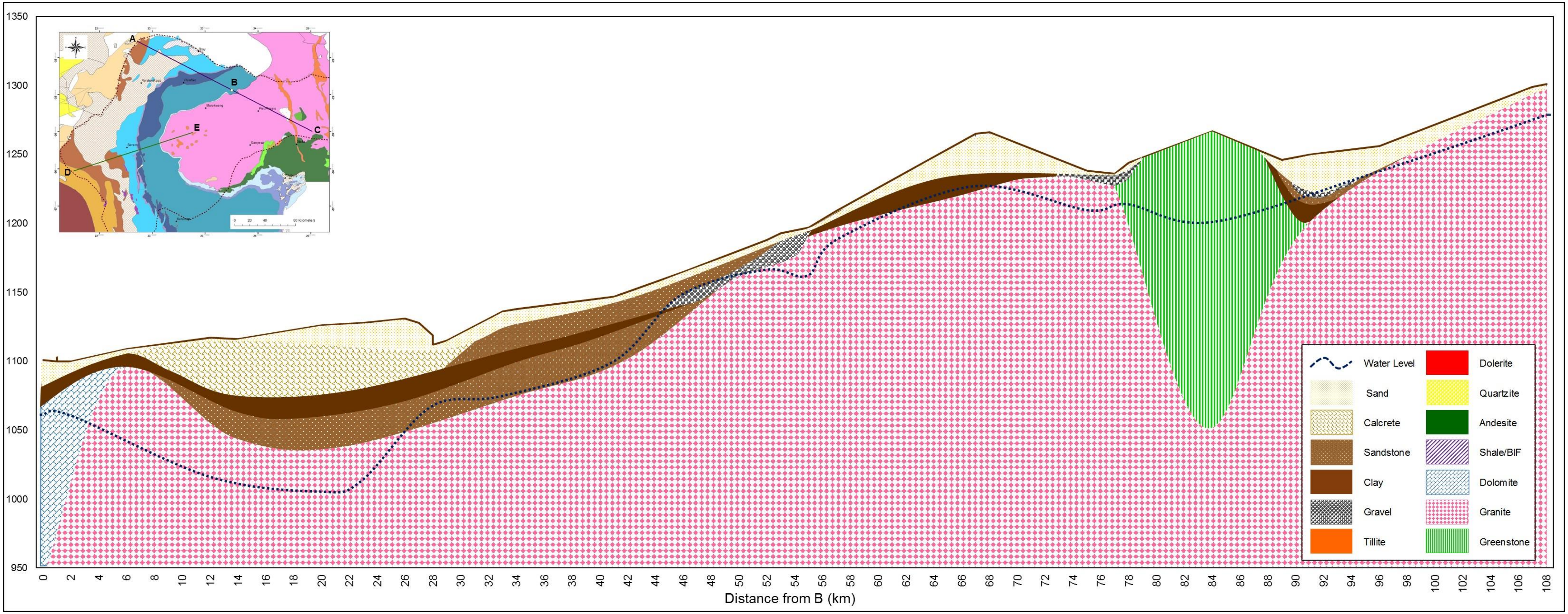

Figure 5.9 (B): Geological cross section B – C (Lithological data sourced from the Department of Water Affairs and the Council for Geoscience)

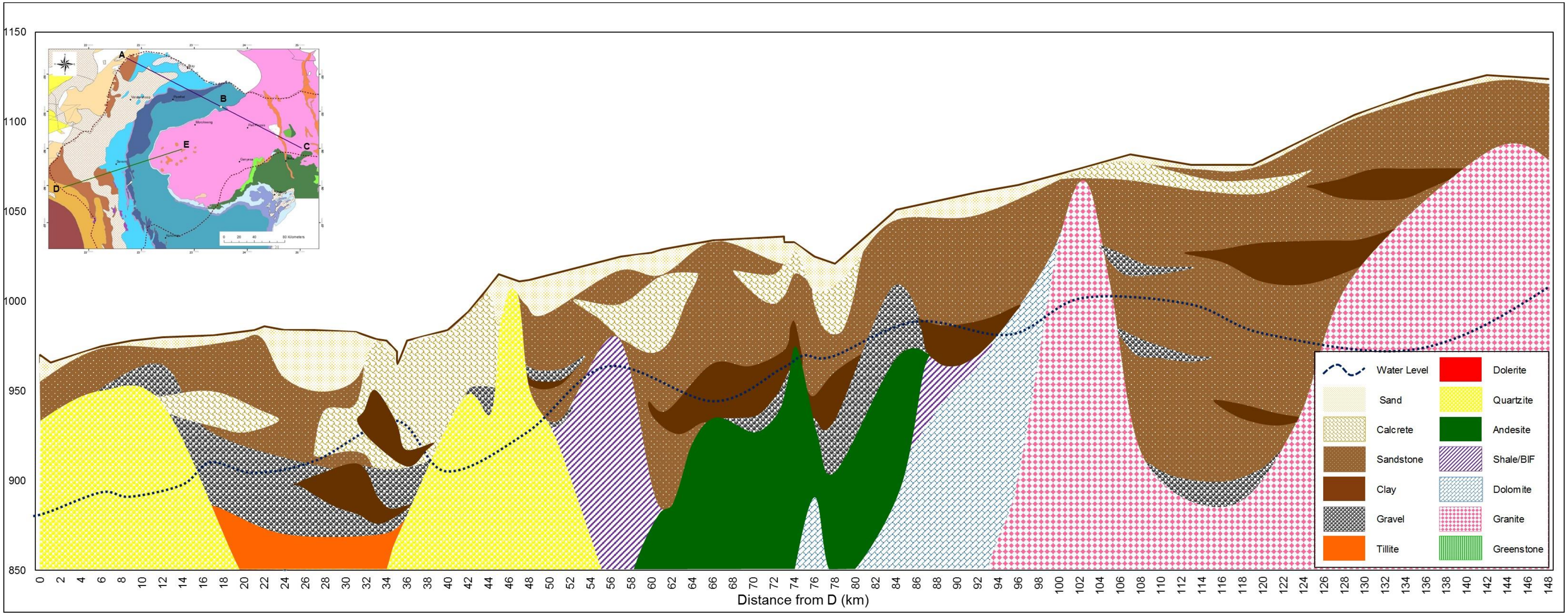

Figure 5.9 (C): Geological cross section D – E (Lithological data sourced from the Department of Water Affairs and the Council for Geoscience)

5.3.2 Fractured and Weathered Aquifers

The water strike information extracted from the NGANET, recorded in metres below ground level, was divided into the various hydrogeological units, with ‘strike density profiles’ being generated (See Section 2.2.2) for each hydrogeological unit (Figure 5.10 A – F). The resultant “strike density” curves are shown below, with the ‘base of the aquifer’ for each unit, in metres below ground surface, provided in Table 5.3.

The strike density graphs vary from region to region, showing the deepest aquifer to be that of the Dwyka Group (Figure 5.10 G), the sediments of which are largely confined to the same palaeo-valley (adjacent to the Molopo river) as that occupied by the thickest portion of the Kalahari Group. Of interest to note when comparing the water strike levels throughout the study area is that most water strike levels in the Archaean granites are shallow, as expected, except for those drilled in the granites and meta-sediments associated with the Morokweng Meteorite Impact crater. This deformation event seems to have had a significant impact on the hydrogeological parameters of this region, with the fractures penetrating much deeper than the structural features usually associated with weathered crystalline basement rocks.

The average saturated thickness calculated for each aquifer is presented in Table 5.3. The fractured basement aquifers typically have a saturated thickness of 75.41 m, which is expected given the nature of these much older lithological units. Their vast geological history and nature of their lithological units (andesite and meta-arenaceous sediments), seem to have restricted the depth to which they and their associated fracture systems are regarded as being permeable. By contrast, the weathered and fractured crystalline basement recorded an average saturated thickness of 61.89 m and 150.0 m, respectively. Note that the saturated thicknesses associated with the Morokweng Impact structure recorded similar values of 120 m, however, no evidence of a weathered zone was noted in this portion of the study area, where the granites are covered by thick Kalahari sediments and the water levels are much deeper (> 90 mbgl).

The strike density graph for the fractured sediments of the Griqualand West sequence indicate an aquifer base at a depth of 205 mbgl (Figure 5.10 D), with a calculated saturated thickness of 140.61 m. However, from the geological cross sections compiled for the area (Figure 5.9 A, B and C), it was noted that these sediments are rarely deeper than 120 m in depth, placing the base of this aquifer at 120 mbgl, with dolomite occurring beneath this depth. As such, it was this depth of 120 mbgl that was used to calculate the saturated thickness of this aquifer unit (Table 5.3), the value of which is estimated to be 55.61 m.

(A)

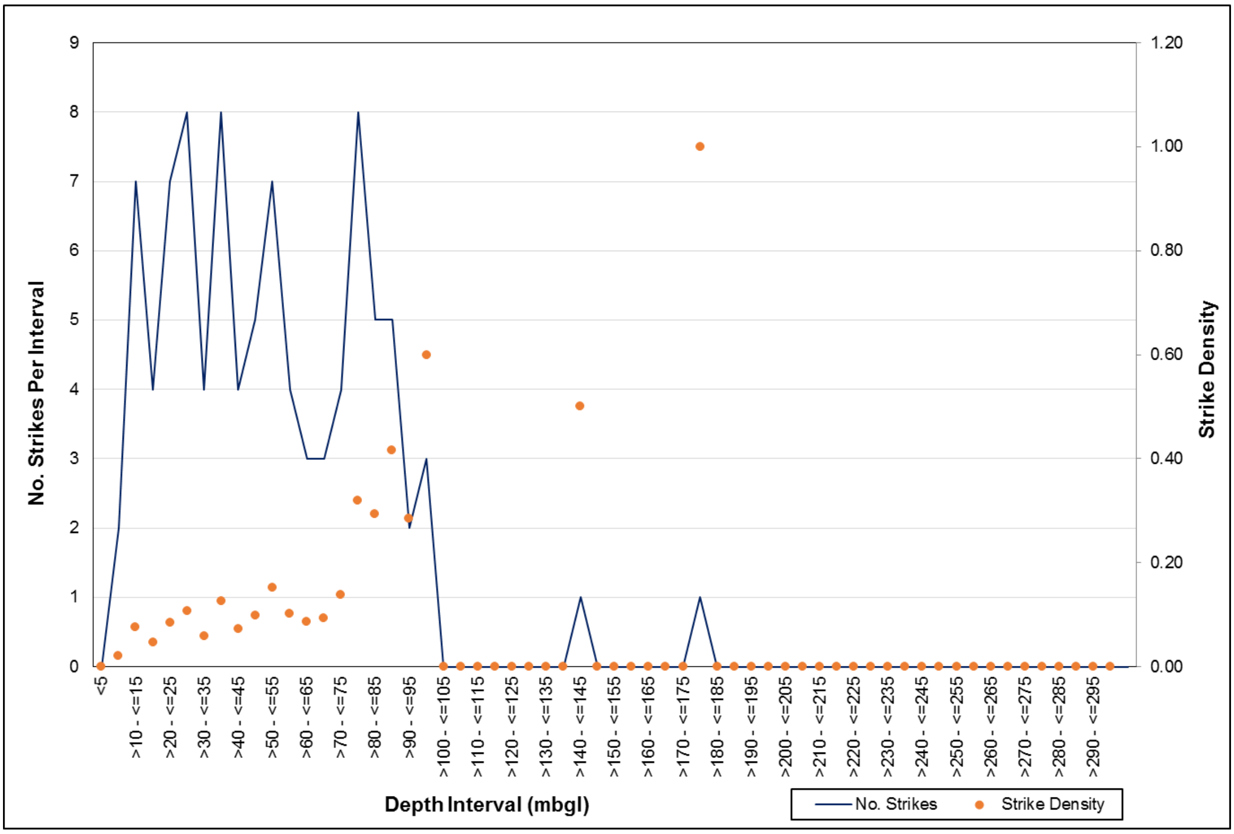

(B)

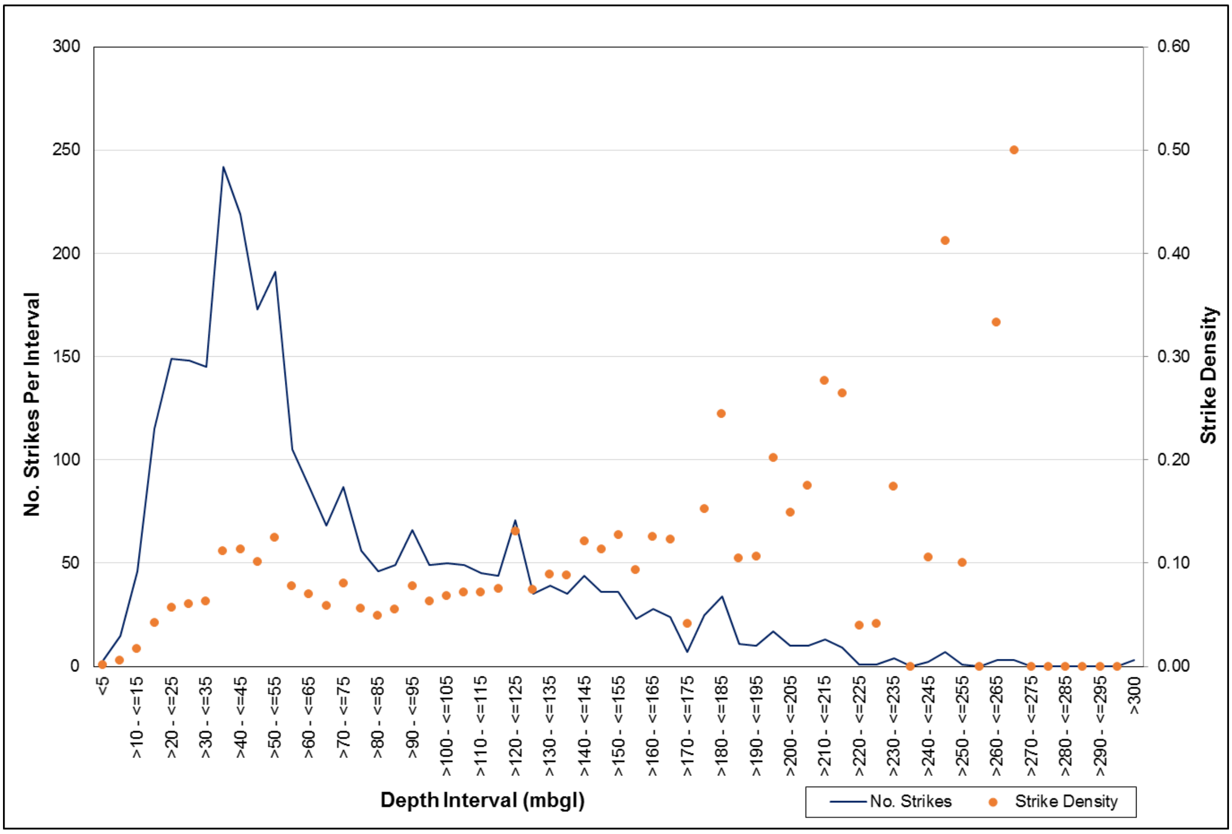

Figure 5.10 (i): Strike density graphs for the (A) Kraaipan – Amalia greenstone terrane (B) granite basement

(C)

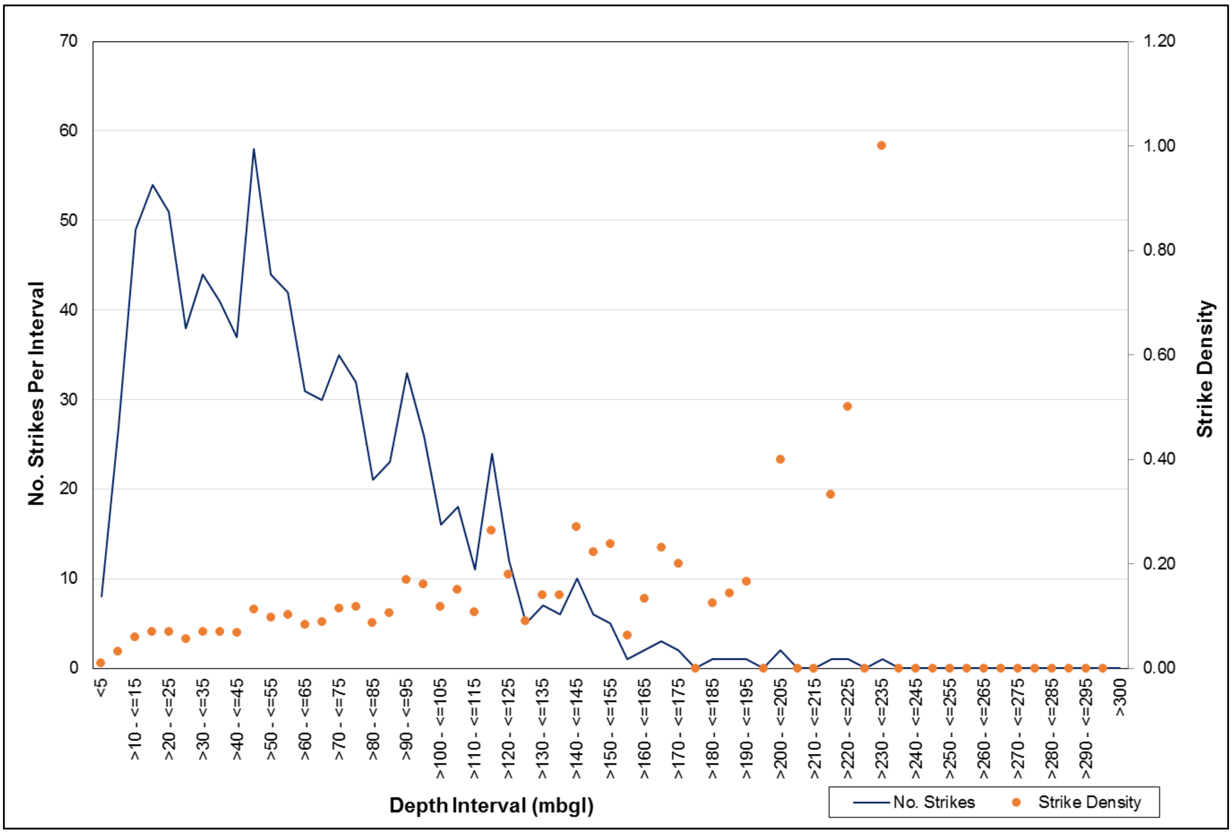

(D)

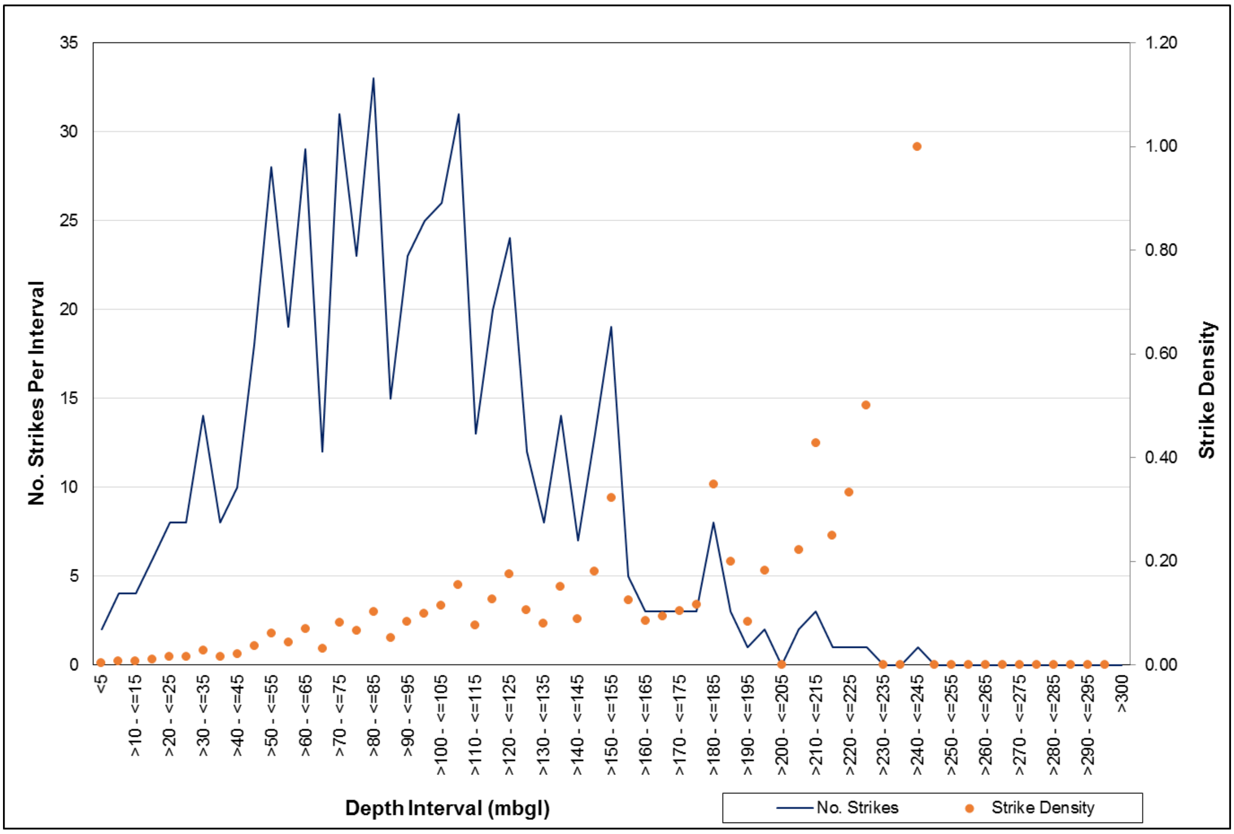

Figure 5.10 (ii): Strike density graphs for the (C) Karst and (D) Fractured sediments (Transvaal)

(E)

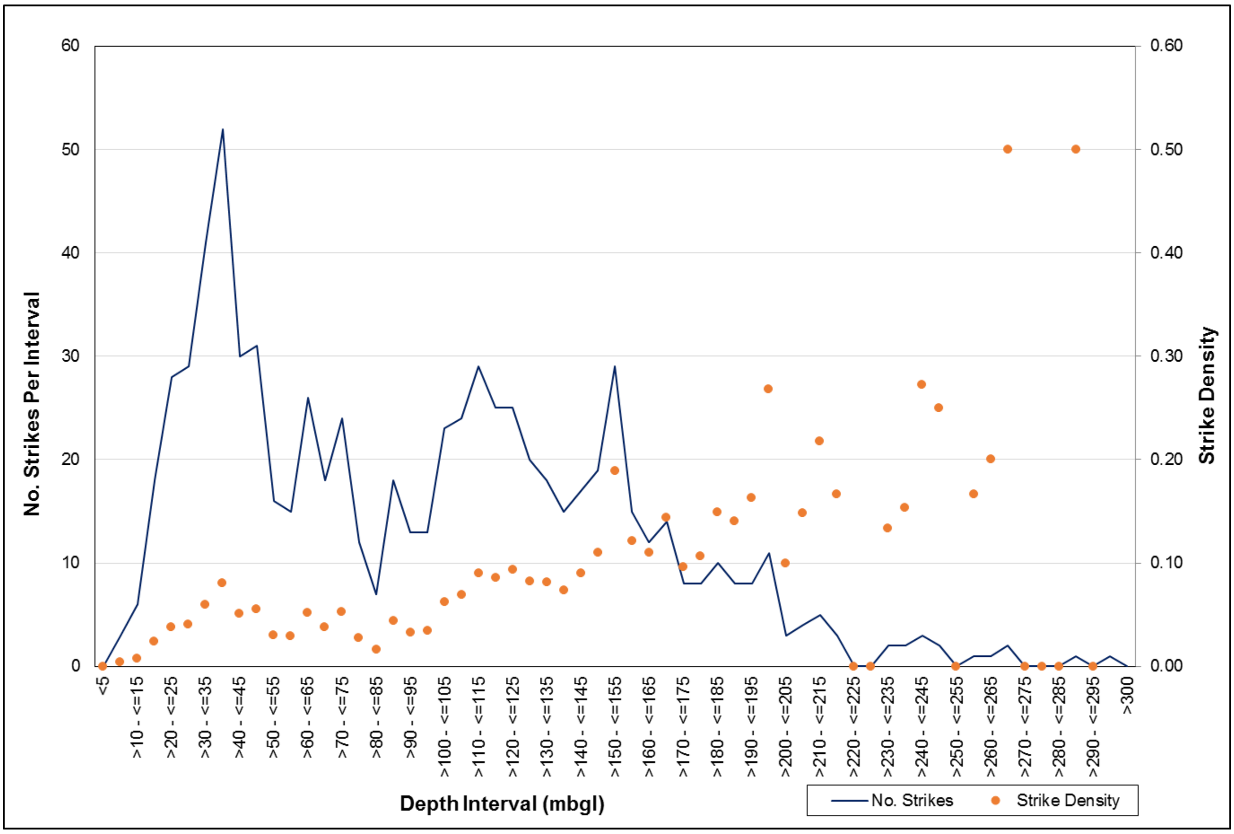

(F)

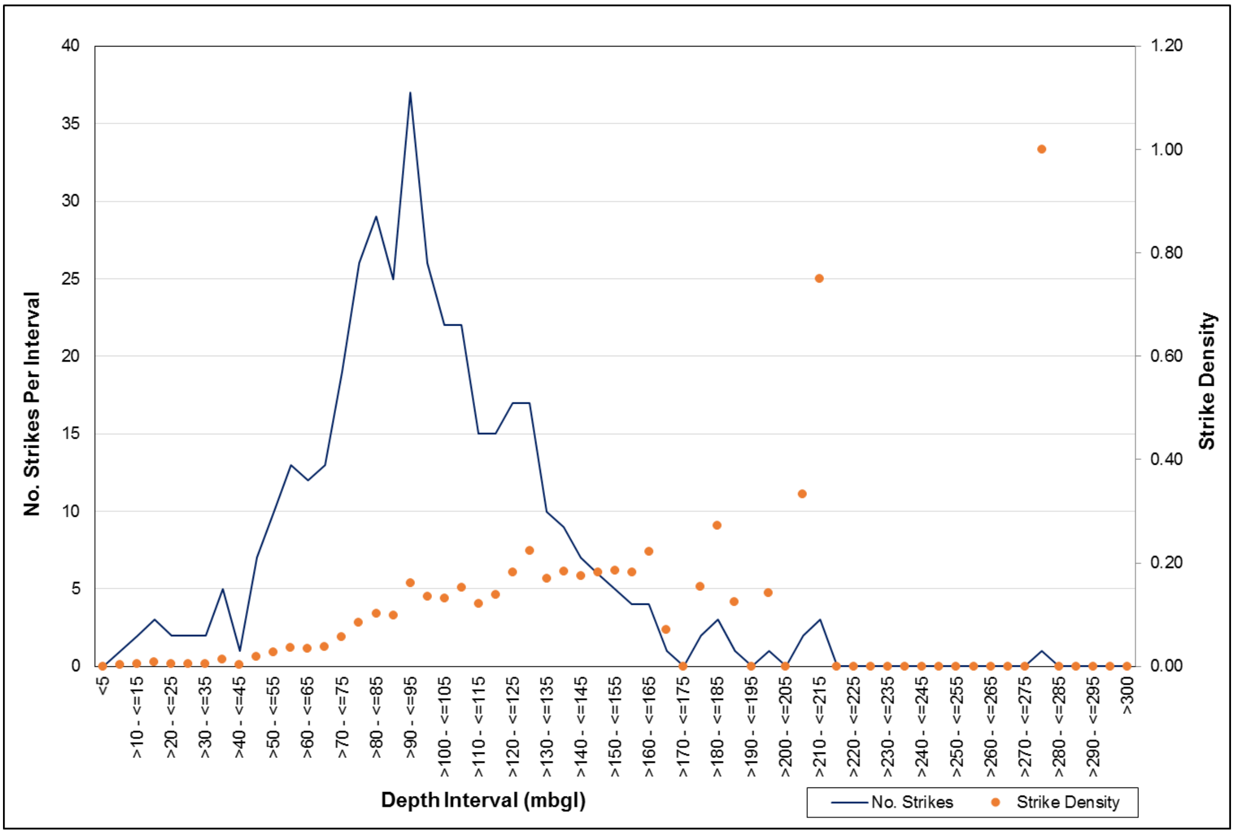

Figure 5.10 (iii): Strike density graphs for the (E) Transvaal andesites and (F) Olifantshoek quartzites

(G)

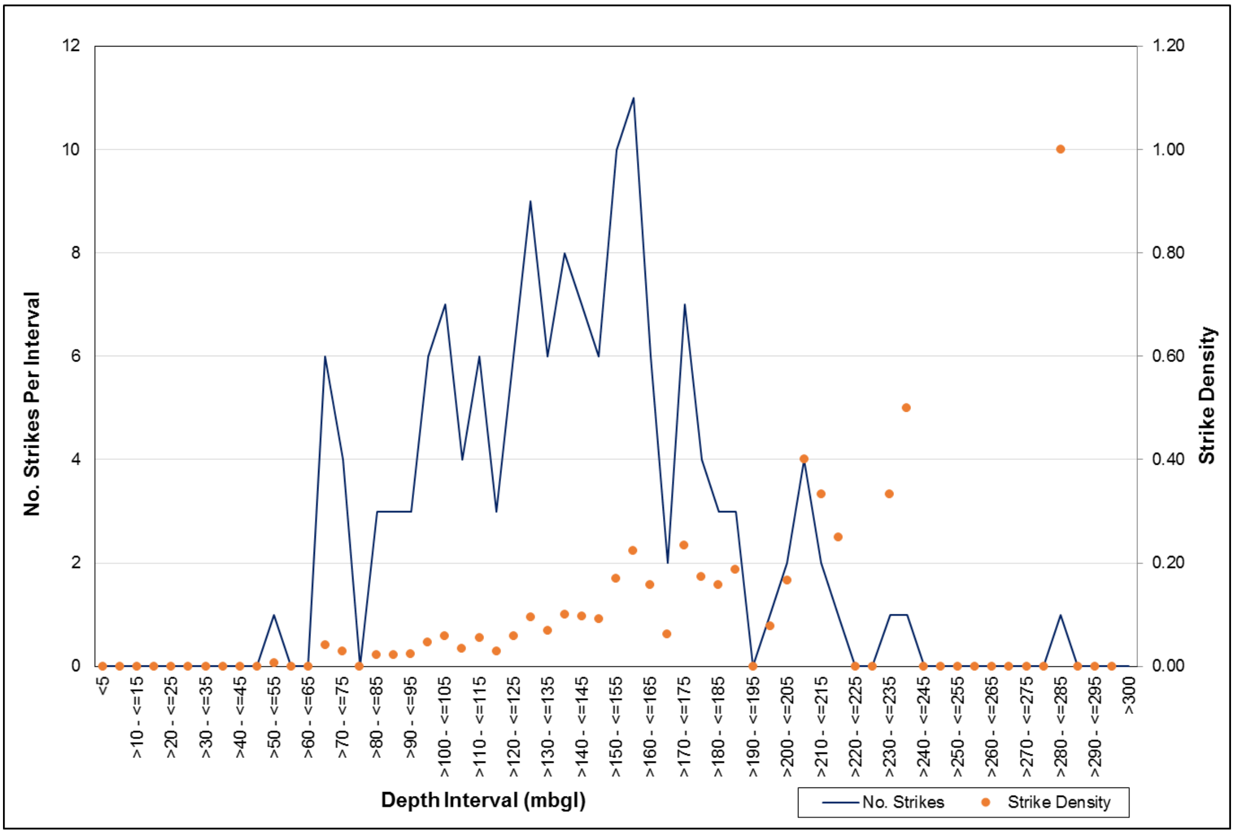

Figure 5.10 (iv): Strike density graph for the (G) Dwyka tillite

Table 5.3: The saturated thicknesses calculated for the various lithological units

Lithostratigraphic Domain	Lithology	Average Water Level (mbgl)	Aquifer Base (mbgl)	Saturated Thickness (m)
Kalahari Group	Sandstone, Shale, Gravel	92.25	150	57.75
Dwyka	Tillite, shale	101.15	225	123.85
Olifantshoek	Quartzites	84.45	175	90.55
Ventersdorp	Andesite/Quartz Porphyry	17.28	45	27.72
Transvaal	Shale/BIF	64.39	120	55.61
Transvaal	Andesite	83.47	225	141.53
Transvaal	Dolomite	25.33	180	154.67
Archaean Basement	Granite (Weathered)	28.11	90	61.89
Archaean Basement	Granite (Fractured)	90.00	240	150.00
Kraaipan - Amalia	Meta-arenaceous sediments	29.59	105	75.41

The quartzites of the Olifantshoek Supergroup recorded an average saturated thickness of 90.55 m. While also being considered as a fractured sedimentary aquifer, the saturated thickness of the Dwyka Group was assessed separately as this aquifer, unlike that of the fractured Griqualand West and Olifantshoek sequences, is seldom utilised. It is largely buried deep beneath the thickest portions of the Kalahari Group of sediments, with few boreholes intersecting this lithological unit. Those holes intersecting the Dwyka Group point to an average saturated thickness of 123.85 m.

The dolomitic aquifer in the central portion of the study area is characterized by an average saturated thickness of 154.67 m. While an average was calculated, it must be noted that this hydrogeological unit also occurs beneath the fractured sedimentary rocks of the Griqualand West sequence, with the unit recording a saturated thickness of 85.0 m between the depths of 120 m and 205 m. It must also be noted that this hydrogeological unit is characterised by numerous compartments, bounded by faults and dolerite dykes, and, as such, each compartment may record its own, varying saturated thickness.

6. GROUNDWATER QUALITY

The term "groundwater quality" describes the physical, chemical, biological and aesthetic properties of water, which determine its fitness for a variety of uses and for protecting the health and integrity of aquatic ecosystems (DWAF, 1996). The South African Water Quality Guidelines, which is regulated by the Department of Water Affairs, is the primary source of information for determining the water quality requirements of different water uses and for the protection and maintenance of the health of aquatic ecosystems. These guidelines are expressed as numerical constants, indicating the Target Water Quality Range (TWQR), which describes what is considered good or ideal water quality, with water quality outside of this prescribed range possibly being harmful to human health. In this study, selected physical properties and the concentration of certain dissolved and suspended materials in the 19 groundwater samples collected (Figure 6.1; See Section 2.3) and those sourced from the NGANET database were analysed and the quality of the groundwater assessed with respect to the Water Quality Guidelines outlined by the Department of Water Affairs.

6.1 pH

The pH of groundwater is very closely associated with other aspects of water quality. Aeration, oxidation, mineral precipitation, temperature changes and degassing of a sample can significantly alter its pH (Weaver *et al*., 2007). Changes to the pH of groundwater will likely affect other constituents as well, as changes in pH affect the degree of dissociation of weak acids and bases. This effect is of special importance because the toxicity of many compounds is affected by their degree of dissociation (DWAF, 1996). Knowledge of the in-situ pH is, therefore, essential to reconstruct the potential mobility of constituents, many chemical equilibria, and encrustation and corrosion potential of the groundwater (Weaver *et al*., 2007).

On-site analyses (Table 6.1) has demonstrated that, on average, the pH levels recorded throughout the study area are at an acceptable range for domestic use. According to DWAF guidelines for drinking water quality (DWAF, 1996), the pH of freshwater should vary from 6.0 to 9.0. In the study area, it varies from 4.0 to 10.0, with an average pH of 7.7 calculated for the entire study area. Those values that fall within the prescribed range do not in any way have direct health consequences to its consumers, however, those falling outside of this prescribed range could prove harmful, where the adverse effects of pH result from the solubility of toxic heavy metals (Weaver *et al*., 2007). At the lower end of the pH range (< 6), the groundwater in certain parts of the study area may have a slightly sour taste. Corrosion of metals that are frequently used in household plumbing (notably lead, zinc and copper) may also occur, which is a major source of metal contamination in drinking water (DWAF, 1996). At the higher end of the pH spectrum (> 9) the water tastes bitter and the probability of toxic effects associated with deprotonated species (e.g. ammonium deprotonating to form ammonia).

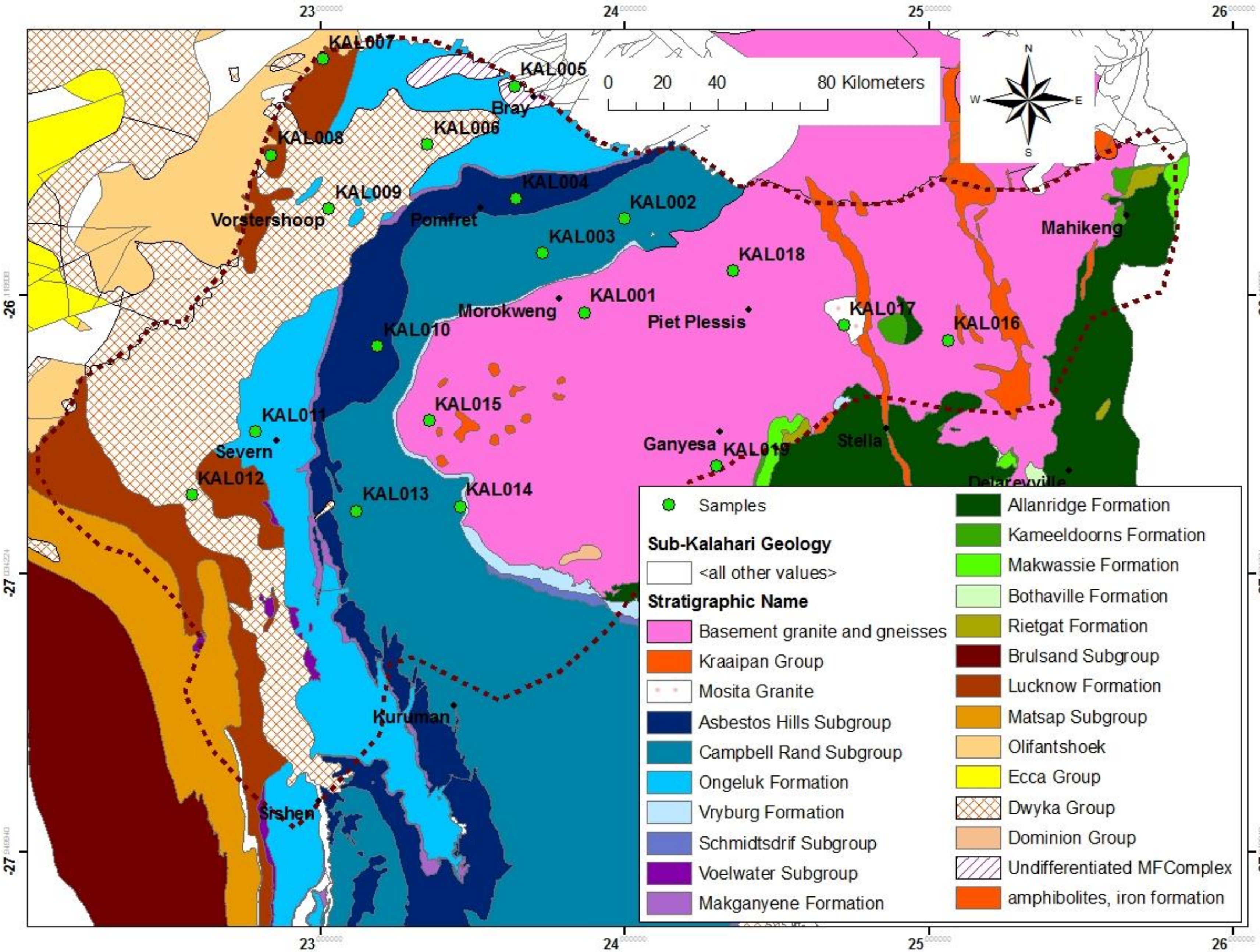

Figure 6.1: The position of samples collected relative to the sub-Kalahari geology

increases sharply. Various metals and pesticides also demonstrate a strong dependence on pH, with high percentages of sorption occurring at pH values of 8 and above (DWAF, 1996).

Table 6.1: The measured physical and chemical parameters of the 19 samples collected

Date Sampled	Time Sampled	Sample Number	Latitute	Longitude	Electrical Conductivity (mS/m)	TDS (mg/l)	pH	Temperature (°C)	Dissolved Oxygen (mg/l)
31-01-2015	10:30	KAL001	-26.17650	23.86636	81.2	522	6.56	24.5	7.46
31-01-2015	12:30	KAL002	-25.86775	23.99736	95.4	613	6.65	25.6	7.80
31-01-2015	15:00	KAL003	-25.98061	23.72919	82.4	533	6.54	25.0	10.68
31-01-2015	16:30	KAL004	-25.80303	23.64231	94.4	606	6.65	25.8	9.50
31-01-2015	17:40	KAL005	-25.43119	23.63625	90.1	575	6.51	25.8	-
31-01-2015	19:15	KAL006	-25.62100	23.35039	188.9	1211	6.64	26.8	9.47
01-02-2015	08:00	KAL007	-25.34075	23.00533	85.7	548	6.82	26.3	10.16
01-02-2015	10:00	KAL008	-25.65744	22.83508	1078	6910	6.73	26.8	9.86
01-02-2015	10:45	KAL009	-25.83578	23.02519	276	1761	6.86	26.9	9.98
01-02-2015	12:45	KAL010	-26.28744	23.18567	40.3	257	6.60	26.7	10.19
01-02-2015	14:30	KAL011	-26.56981	22.78400	104.5	669	6.74	29.1	9.43
06-02-2015	12:30	KAL012	-26.77569	22.57425	145.8	934	6.73	27.2	10.35
06-02-2015	14:38	KAL013	-26.82964	23.11617	92.5	593	6.71	26.8	10.92
06-02-2015	16:00	KAL014	-26.81486	23.45722	71.4	455	6.81	25.4	10.13
06-02-2015	18:40	KAL015	-26.53228	23.35622	270	1735	7.05	26.8	10.75
07-02-2015	12:00	KAL016	-26.26775	25.06492	91.3	584	6.48	27.6	10.45
07-02-2015	13:18	KAL017	-26.21825	24.72119	45.7	293	6.69	24.1	10.28
07-02-2015	20:40	KAL018	-26.03861	24.35519	95.3	611	6.49	26.9	10.54
08-02-2015	16:00	KAL019	-26.68289	24.30322	84.6	541	6.38	22.6	10.48

The geology and geochemistry of the rocks and soils of a particular catchment area are known to affect the pH and alkalinity of the groundwater (DWAF, 1996). In order to determine if such a relationship exists in the study area, the pH values determined in the field were plotted against the sub-Kalahari geological map of Haddon (2005). The data proved far too sparse to make any real correlations and, as such, it was decided to incorporate the pH values from the vast NGANET database of the Department of Water Affairs.

The combined pH values were interpolated using the kriging method to create a groundwater pH surface map of the study area (Figure 6.2), which shows the broad spectrum of pH values ranging from 4.0 to 10.0. The percentage of boreholes with an extreme pH value (> 9.0 and < 6.0) is very low (< 1 %) compared to those with a normal pH ranging between 6.0 and 9.0. It appears that those

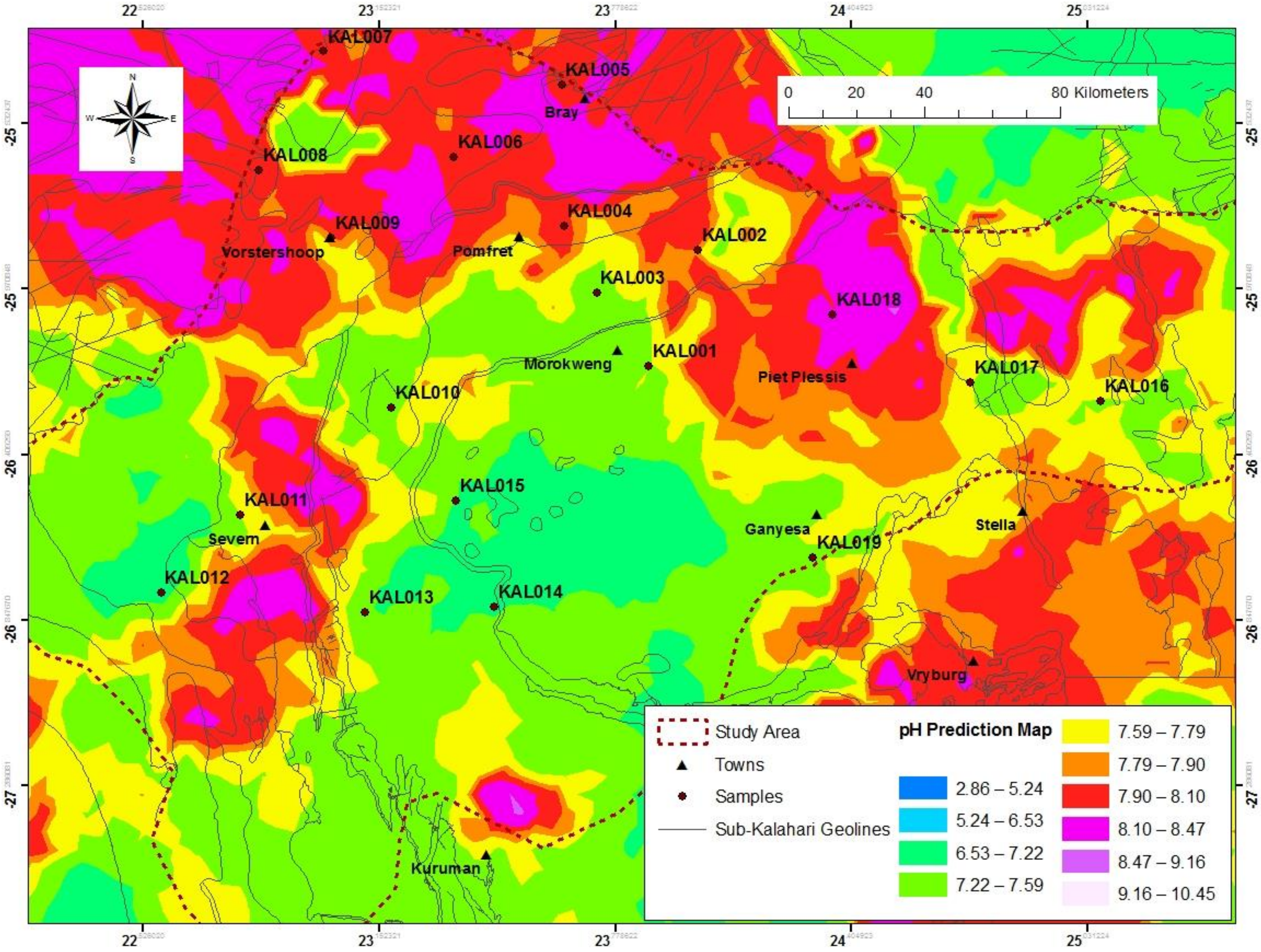

Figure 6.2: pH map of the study area relative to the sub-Kalahari geology (Data sourced from DWAF NGANET)

groundwater samples with a lower pH (< 6) tend to correspond with the Kraaipan and Amalia greenstone terrane (Figure 6.2). The pyrite associated with these assemblages is often a source of SO_4^{2-} when oxidised, which ultimately alters the acid-base equilibria in natural waters and results in a reduced acid-neutralising capacity and hence the lowering of the pH.

Higher values of pH (> 8) tend to be associated with the carbonate rocks (limestone and dolomite) of the Campbell Rand Subgroup (Figure 6.2). Carbonate compounds tend to dominate acid–base reactions in groundwater, with acidic water being "neutralised" by the presence of these compounds. High values of pH also seem to be associated with the deeper Kalahari sediments (Figure 6.2). If the geology of the aquifer containing the groundwater has few carbonate rocks (e.g. sandstones, metamorphic granitic schists and gneisses; volcanic rocks, etc.) the groundwater will tend to remain acidic.

6.2 Temperature

Temperature is an important measurement to be made because it affects many chemical and biological reaction rates and equilibria, in addition to having a strong effect on pH measurements (Weaver *et al*., 2007). Species solubility is temperature controlled i.e. for most species the higher the temperature the more soluble they are. Temperature can also provide a first indication of depth of water interception in confined aquifers as the temperature of groundwater increases with depth, with the temperature gradients in southern Africa ranging between 1 and 3 $^oC/100$ m (Weaver *et al*., 2007).

A relatively narrow range of temperature values (22.6 ^oC to 29.1 ^oC) were recorded during sampling (Table 6.1), with a much wider range of values (7.0 ^oC to 35.0 ^oC) recorded in the NGANET database of the Department of Water Affairs. From the observed values it is apparent that the water in this region is not associated with geothermal fields. Where water circulates to a considerable depth, it attains a substantially higher temperature than water near the land surface, given that rock temperatures increase with depth. With this in mind, it can be assumed that the groundwater in this region is not associated with a substantial depth of flow, nor with fracture zones that penetrate deep into the underlying bedrock. From the groundwater temperature map constructed for the study area (Figure 6.3), it appears that the highest temperature values are typically associated with those boreholes located in the deepest portion of the Kalahari basin, which reaches a maximum depth of 210 m.

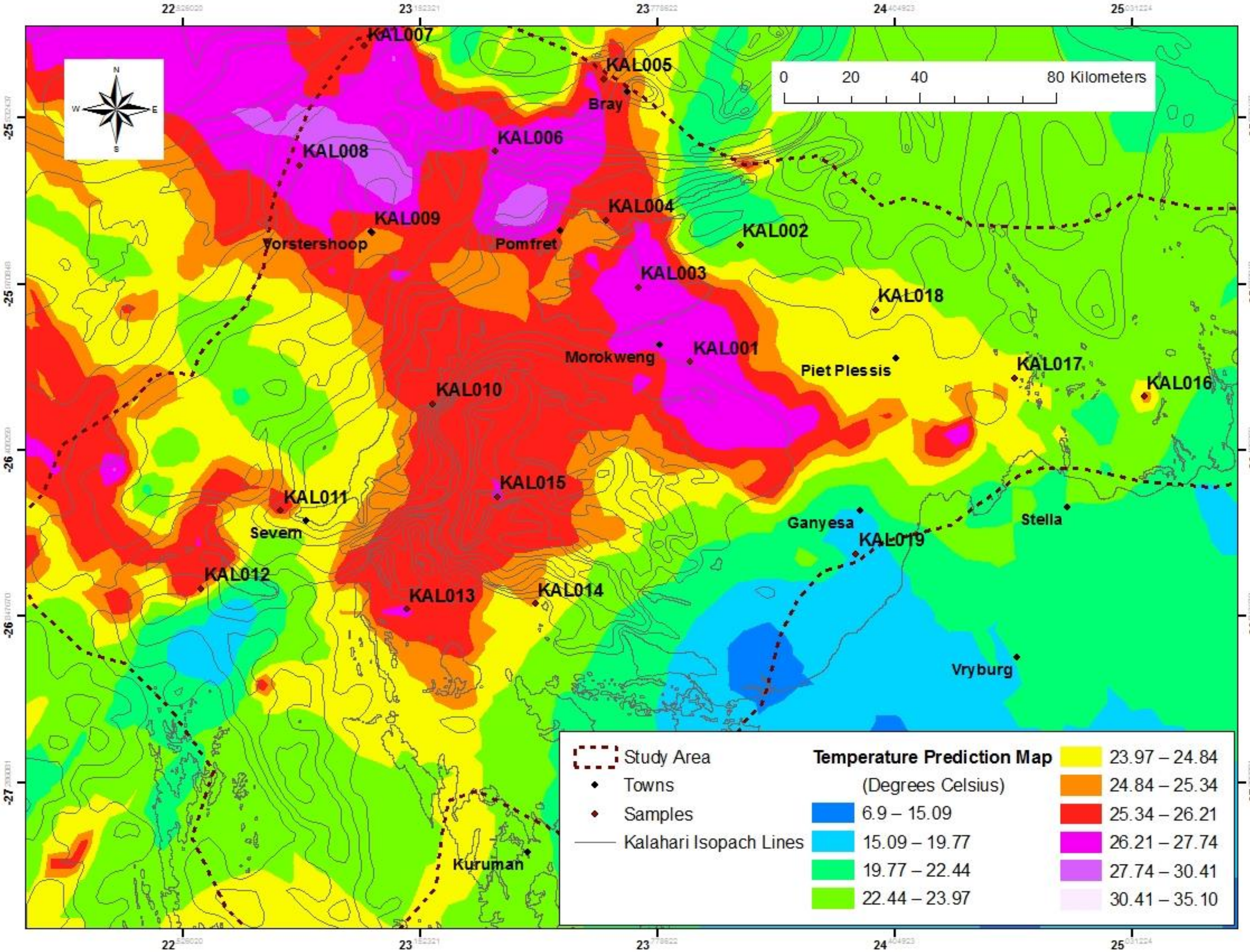

Figure 6.3: Groundwater temperature map of the study area relative to the Kalahari isopach map (Data sourced from DWAF NGANET)

6.3 Electrical Conductivity

Electrical conductivity (EC) is a measure of the ability of an aqueous solution to conduct an electric current. This physical property of water depends on the presence of ions, their total concentration (TDS), mobility, valence, and relative concentrations, and on the temperature of measurement (APHA, 1998). In general, solutions of most inorganic acids, bases, and salts are relatively good conductors. Conversely, molecules of organic compounds that do not dissociate in aqueous solution are poor conductors, if at all (Weaver *et al*., 2007). Given this, electrical conductivity is a very helpful parameter to record during a sampling exercise as it provides an indication of the presence of different water sources (different geological formations), their quality, as well as of contamination that may have occurred from another source.

From the samples collected, it was noted that the EC values vary widely throughout the study area, ranging from 40.3 mS/m to 1078 mS/m (Table 6.1). According to DWAF guidelines for drinking water quality (DWAF, 1996), the taste threshold for dissolved salts in water is in the region of 45 mS/m, with an increased salty taste being detected above this concentration. As expected in this arid region, most of the samples recorded values greater than this taste threshold, with one sample (notably KAL 008) recording an EC value in excess of 1000 mS/m. Although elevated, most of these samples, while not having an aesthetically pleasing taste, pose no health risks should the water be consumed. The use of water, however, from those boreholes recording excessive EC values (> 450 mS/m) should be discontinued for both domestic and livestock consumption. At such high concentrations, noticeable short term health effects can be expected, resulting in disturbances of the body's salt balance (DWAF, 1996). In addition, these elevated EC values could have serious implications on soil quality in the region, further aggravating the issue of food security.

Virtually all natural waters contain varying concentrations of total dissolved solids (TDS), as a consequence of the dissolution of minerals in rocks and soils. The TDS of natural waters and, therefore, its EC is often dependent on the characteristics of the geological formations (DWAF, 1996). With this in mind, the sampled values, in combination with those acquired from the NGANET database, were plotted onto the sub-Kalahari geological and isopach map of Haddon (2005; Figure 6.4 A and B). A trend becomes apparent, with those samples recording the highest EC values typically being associated with the deepest portions of the Kalahari basin, where the Kalahari sequence is at its thickest (> 90 m thick). The high electrical conductivity recorded in these areas is likely attributed to a prolonged rate of evaporation (see Section 6.6), as confirmed by the environmental isotope data analysed for this region (see Section 8.3), with surface water bodies becoming increasingly saline before filtering through to the underlying unconfined groundwater aquifers of the Kalahari Group. Because salts are continuously being added through natural processes, the EC is likely to increase in the groundwater accumulating in these unconfined aquifers, as very little salt is removed by precipitation or natural processes (DWAF, 1996).

A.

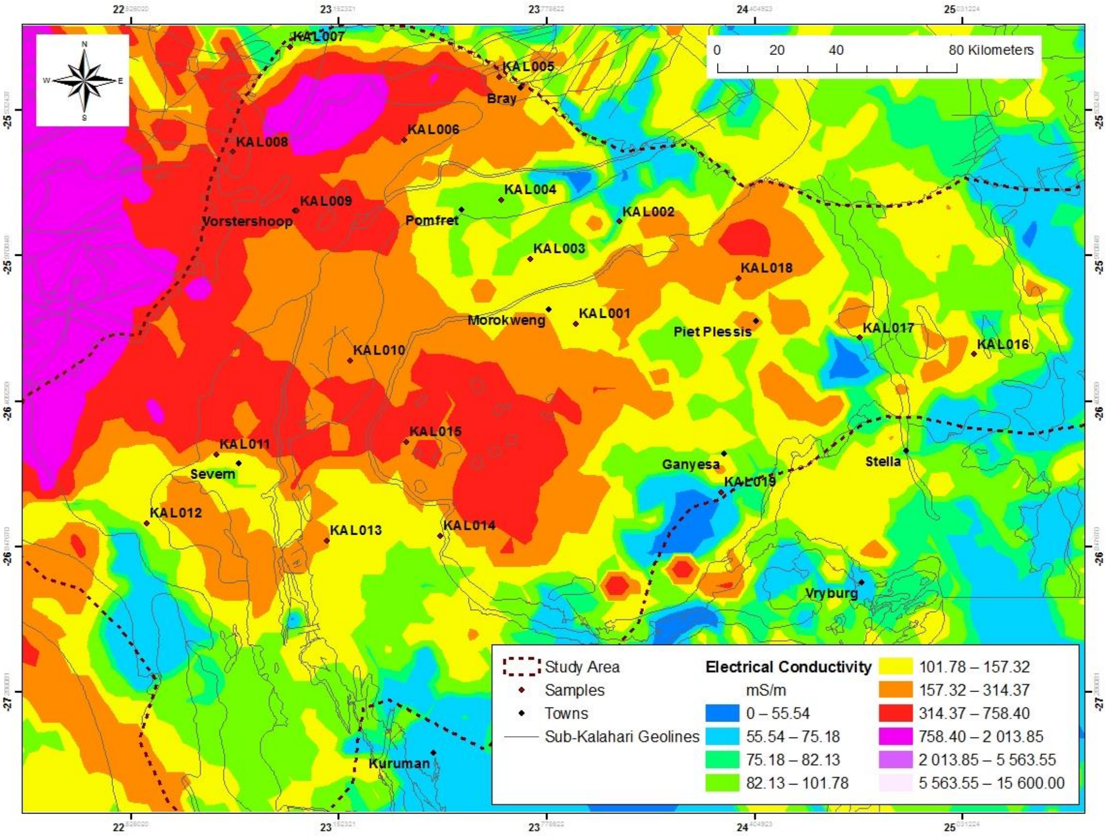

B.

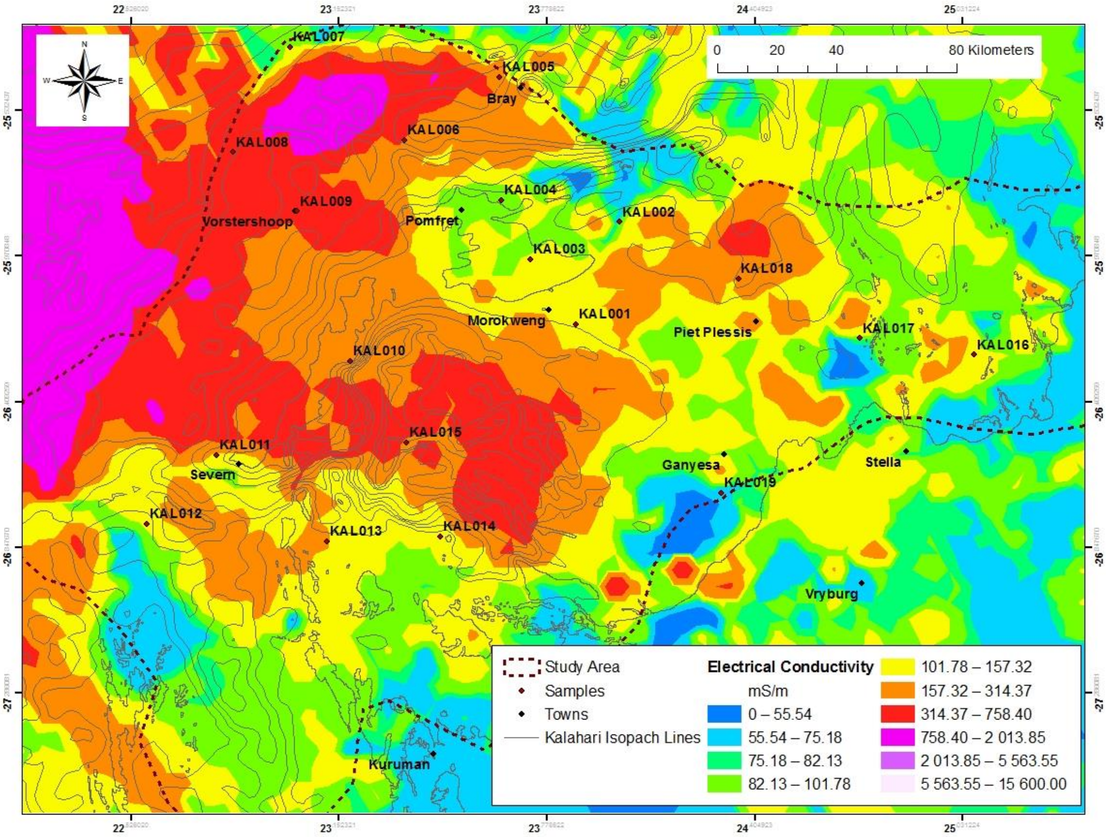

Figure 6.4: Electrical conductivity map relative to the (A) sub-Kalahari geology (B) Kalahari isopach map (Data sourced from DWAF NGANET)

Underlying the deepest portions of the Kalahari basin, where the sediments are at their thickest, are the basal tillites of the Dwyka Group, which also seem to be a source of groundwater given the depth of some of the boreholes drilled in these areas. The Dwyka Group is commonly found to contain saline water (Levin, 1980), which may also account for the high EC values recorded in these borehole samples. Those groundwater samples associated with the shallower portions of the Kalahari basin have typically lower EC values in the range of 40.0 mS/m to 100 mS/m (Figure 6.4 B). These groundwater samples seem to be sourced largely from the underlying basement lithologies, comprising the Archaean granites, Kraaipan - Amalia greenstone belt assemblages, Transvaal sediments and the Ventersdorp volcanics (Figure 6.4 A). These lithologies are typically characterized by confined structural aquifers, with little influence from evapotranspiration (Section 8.3).

6.4 Total Dissolved Solids

Total dissolved solids (TDS) is the measure of the amount of various inorganic salts dissolved in water and it quantitatively provides information about the amount of major ions in water. Given that the electrical conductivity of water also depends on the amount of ions in water, then it is understood why electrical conductivity is routinely used as a proxy to TDS concentration (DWAF, 1996), with many portable measuring tools using EC to calculate TDS concentration. As with electrical conductivity, TDS is an important indicator of water quality, varying as a consequence of contamination and dissolution of minerals in varying geological formations, soils and decomposed plant materials.

The Total Dissolved Solids (TDS) in the sampled boreholes ranged from 257 mg/l to 6910 mg/l (Table 6.1), with most values proving greater than the 0 - 450 mg/l target water quality range defined by DWAF in its guidelines for domestic drinking water quality (DWAF, 1996). Given that a proportional factor of 6 was used by the portable measuring tool to calculate TDS from the EC concentration, the results are indistinguishable. As with EC, the maximum values (notably KAL008) correspond to the deepest portions of the Kalahari basin, with the lower values corresponding to the shallower portions of the Kalahari basin, which are underlain largely by the fractured basement and sedimentary aquifers (Figure 6.4 B).

As mentioned above, the lowest values correspond to the meta-sediments and iron formations of the fractured basement and sedimentary aquifers, as well as those areas underlain by low-solubility, crystalline silicate bedrock i.e. granite. These areas occur at relatively shallow depths (< 30 m). The TDS of groundwater tends to be lowest at shallow depth in recharge areas, where the water has only recently infiltrated from precipitation. Higher TDS values in the region are associated with those waters sourced from boreholes located in the shallow carbonate bedrock (limestone or dolomite) of the Campbell Rand Subgroup. These higher TDS values are typically due to the high solubility of carbonate minerals.

The highest TDS content of all the boreholes tested in the region are those restricted to the thickest portion of the Kalahari Group, which is typically underlain by Dwyka tillite (Figure 6.4A). It is obvious that this water has not been sourced from precipitation that has recently infiltrated into the aquifer, but has more than likely been subjected to a prolonged rate of evaporation prior to infiltration (Section 6.6). This high dissolved solid content may also be due to the concentration of dissolved weathering products in the soil by evaporation, typical of arid climates which are unfavourable for rapid rates of solvent erosion (Abiye, 2015). The higher TDS water occurs where the water filtering from the surface comes into contact with highly soluble minerals over long periods of time. As the water spends more time in the subsurface, inorganic solute concentrations rise, approaching equilibrium levels after long residence times (Fitts, 2002). Although demonstrating on average high TDS values, it appears that fresh water aquifer units are also present within the Kalahari aquifer (Figure 6.4 A). These lenses of fresh water are localised and very limited in extent, occurring mainly along the Molopo River, which seems to be a source of groundwater recharge.

The TDS content is commonly used as a hydrogeological tool to identify the water quality in each aquifer. A review of the TDS content of each of the boreholes sampled has indicated that, although slightly higher than the target water quality range (DWAF, 1996), the groundwater in this region is generally suitable for several uses including recreational and domestic uses. From the results obtained, it is obvious that the basement aquifers in the central and southern parts of the study area have the best quality water, exceeding the water quality of the Kalahari aquifers to the north of the study area, some of which are not suitable for human and livestock consumption. Health effects related to TDS are minimal at concentrations below 2000 - 3000 mg/l, however, high concentrations of salts impart an unpleasant taste to water and may also adversely affect the kidneys (DWAF, 1996).

6.5 Total Hardness

Water hardness is a measure of the relative abundance of bivalent cations that will react with soaps to form a soft precipitate or react in boilers to form a solid scale precipitate (Fitts, 2002). In most waters, the principal cations causing hardness are Ca^{2+} and Mg^{2+}, however, other metals such as strontium, iron, aluminium, zinc and manganese may occasionally contribute to the hardness of water (DWAF, 1996). The hardness represents the equivalent concentration of dissolved $CaCO_3$ that would produce an effect similar to the actual calcium and magnesium concentrations and may be expressed as:

$$\text{Total hardness (mg } CaCO_3\text{ /l)} = 2.497 \times \text{Ca (mg/l)} + 4.118 \times \text{Mg (mg/l)}$$

While the calculation represents the equivalent concentration of dissolved bicarbonates, it must be noted that hardness can also be attributed to other salts such as sulphate and chloride.

A wide range of values (10 mg/l to 3000 mg/l) were recorded in the NGANET database of the Department of Water Affairs, with approximately 94 % of the samples recording values greater than 100 mg/l. According to DWAF guidelines for drinking water quality (DWAF, 1996), the hardness of freshwater should vary from 50 mg/l to 100 mg/l, with the water considered to be “hard” if the value recorded is above 100 mg/l. With almost all of the samples recording values greater than 100 mg/l, much of this water is not ideally suitable for drinking purposes, with the scaling in plumbing and household heating appliances expected throughout the study area.

The natural hardness of water is influenced by the geology of the catchment and the presence of soluble calcium and magnesium minerals. The hardness map constructed for the region (Figure 6.5) shows the variation of hardness throughout the study area, which is superimposed over the underlying geology. Aquifers in the fractured sediments of the Asbestos Hills Subgroup exhibit some of the “lower” values recorded (< 300 mg/l). Higher values, as expected, are typically associated with the water sourced from boreholes located in the shallow carbonate bedrock (limestone or dolomite) of the Campbell Rand Subgroup. These higher values are typically due to the high solubility of the Ca- Mg-carbonate minerals. The bicarbonates and magnesium rich waters in this hydrogeological unit are indicative of recently recharged aquifers.

Of interest in the study area are the elevated values (> 1000 mg/l) associated, once again, with the deeper Kalahari sediments and the underlying Dwyka Group. Interspersed with these higher values of hardness in the Kalahari aquifer are lenses of fresh water, with much lower values of hardness recorded. These fresh water lenses are very limited in extent, occurring mainly along the Molopo River.

6.6 Chloride

Chloride is a common constituent in water and enters an aquifer by the rainfall recharging the aquifer. The chlorides of sodium, potassium, calcium and magnesium are all highly soluble in water. Once in solution these chlorides tend to accumulate, with increasing concentrations resulting from evaporative processes. Increased chloride inputs to groundwater can also arise from the dissolution of aquifer material, from salts contained within the aquifer matrix, or from pollution (irrigation return flows, sewage effluent discharges and various industrial processes) that has entered the aquifer.

Typically, the concentration of chloride in the groundwater within the study area ranges from 1 to 5000 mg/l (Figure 6.6), with approximately 40 % of the recorded values proving greater than 100 mg/l. Ideally, water should record values of between 0 – 100 mg/l (DWAF,1996), with values greater than this being of concern to domestic water supplies. Elevated concentrations impart a salty taste to water, which becomes highly objectionable at values greater than 600 mg/l. At chloride concentrations greater than 2 000 mg/l nausea may occur, while at 10 000 mg/l vomiting and dehydration may be

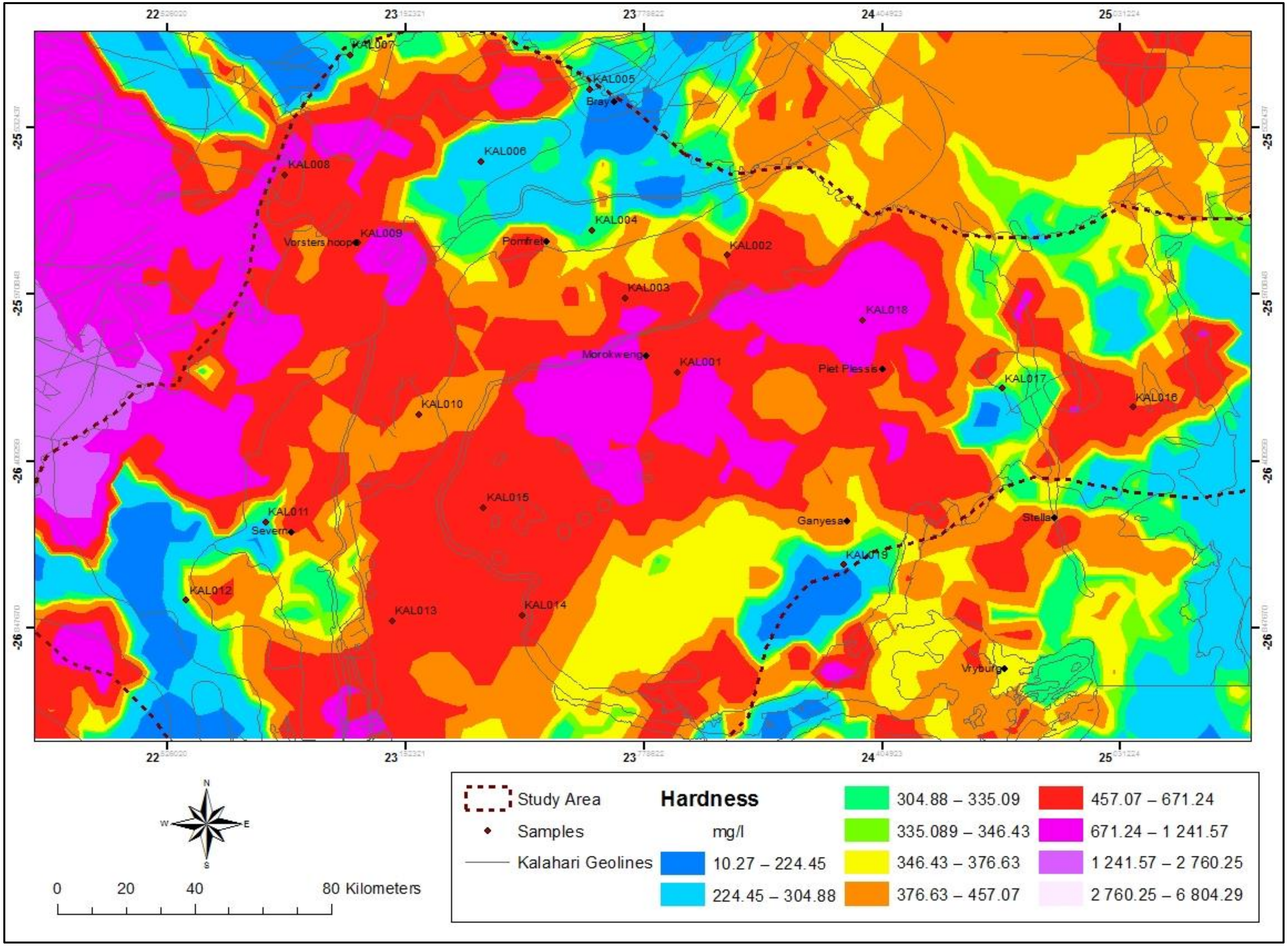

Figure 6.5: Hardness map relative to the sub-Kalahari geology (Data from DWAF NGANET)

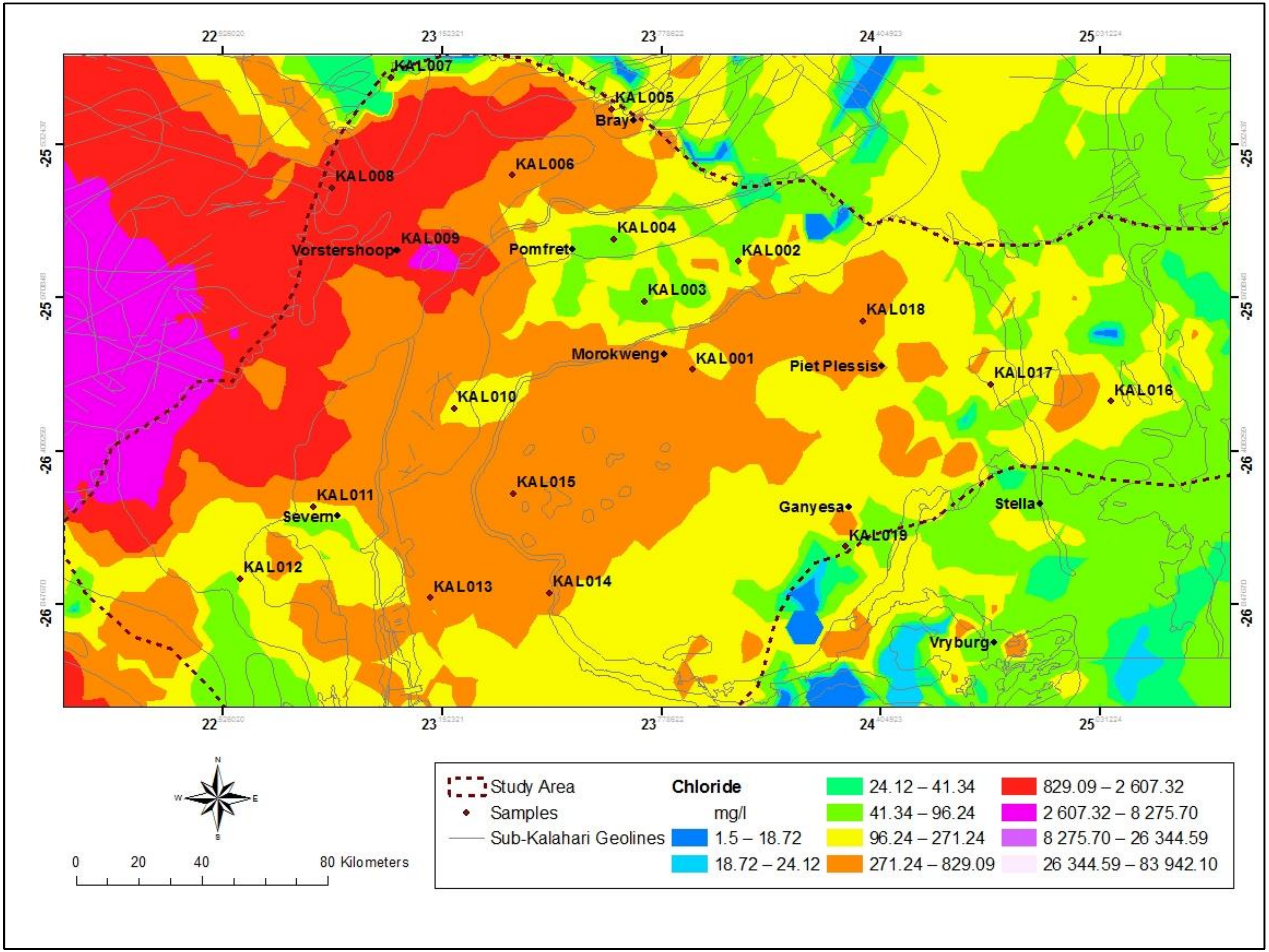

Figure 6.6: Chloride map of the study area relative to the sub-Kalahari geology (Data sourced from DWAF NGANET)

induced (DWAF, 1996). Elevated concentrations also accelerate the corrosion rate of metals, well below the concentration at which it is detectable by taste (> 50 mg/l).

These high concentrations of chloride recorded in the study area, particularly in the groundwater sourced from the unconfined Kalahari Group of sediments (> 500 mg/l; Figure 6.6), indicate the presence of highly saline groundwater in the study area. In an attempt to determine if NaCl has influenced the groundwater chemistry in the study area, the sodium concentrations in the groundwater were plotted relative to its chloride concentrations (Figure 6.7). Because sodium and chloride ions enter solution in equal quantity, an approximately linear relationship may be observed between these ions (Hem, 1985). In particular, if the concentrations are plotted in milliequivalents per litre (meq/l), this linear relationship should be described by a line with a slope equal to one, the distribution of which is displayed in Figure 6.7. From the plotted data (Figure 6.7) it is apparent that there is a clearly defined linear relationship (R^2 of 0.82) between the concentrations of chloride and sodium for the samples sourced from the Kalahari aquifer. This suggests that the source of salinity in the groundwater of the Kalahari aquifer is heavily influenced by sodium and chloride.

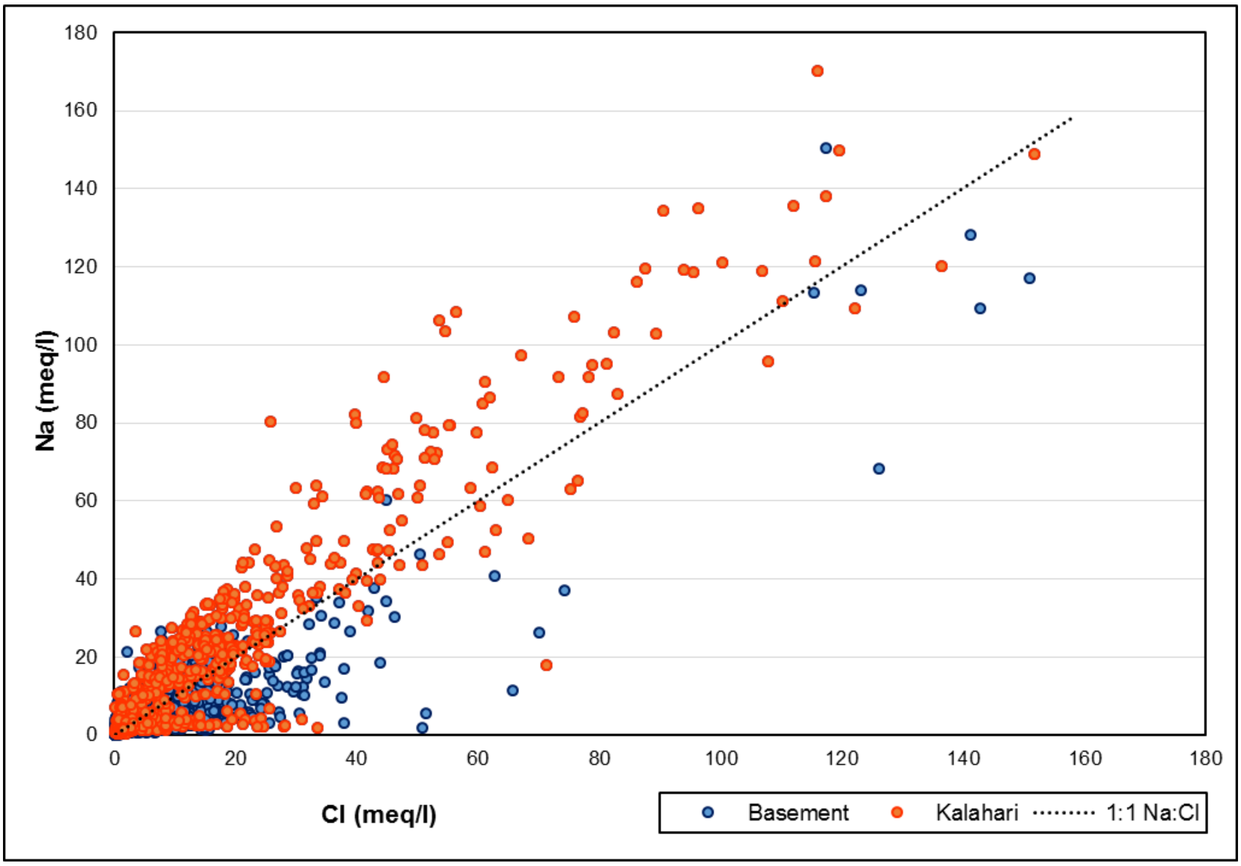

Figure 6.7: A plot of Na against Cl concentrations of groundwater in the region (R^2 of 0.82) relative to the line representing 1:1 Na:Cl

The highly saline groundwater in the Kalahari sediments may be derived from intensive evaporation and and/or water-rock interactions. While some local pollution may be apparent, due to irrigation return flows and effluent discharge, it is firmly believed that the elevated concentrations of chloride in the region are largely attributed to natural hydrological processes, notably evaporation. Correlations between stable isotope content (Section 8.5) and salinity seem to confirm that evaporation is the main cause of salinisation in these unconfined aquifers of the Kalahari Group. In particular, the groundwater sourced from the unconfined Kalahari Group of sediments has seen extensive evaporation and enrichment, with very little recharge.

Some contribution, however, from water-rock interactions is also apparent in some of the basement lithologies, some samples of which show a poor correlation between concentrations of chloride and sodium. Some 35 % of the samples from the study area indicate sodium concentrations that exceed chloride concentrations, suggesting that additional sources of sodium may be present. The leaching of sodium bearing minerals in rocks, particularly felsic rocks, are known to provide an additional source of sodium. A lack of correlation between stable isotope content and evaporation in some of the granite samples (Section 8.5), is consistent with salinisation from dissolution of salts in the aquifer.

6.7 Nitrate (NO_3+NO_2-N)

Nitrates are ubiquitous in soils and in the aquatic environment, with natural concentrations in groundwater originating from the atmosphere and from the breakdown of organic matter and eutrophic conditions (DWAF, 1996). Concentrations of nitrate-nitrite in water are typically less than 5 mg/l, however, increased concentrations in natural water may result from a variety of anthropogenic activities. In particular, high nitrate levels can result from the leaching of industrial and agricultural chemicals/fertilisers, the latter of which are commonly added to cultivated soils (DWAF, 1996). Nitrate is also present in domestic wastewater, with high levels of this constituent often associated with septic systems and treated sewage wastes. Animal manure can also be a source of nitrate in groundwater systems, with high nitrate levels typically detected in the groundwater down gradient from watering points or feedlots (DWAF, 1996; Stadler *et al*., 2012).

High concentrations of nitrate are undesirable in drinking water because of possible health effects. Under oxidising conditions nitrite is converted to nitrate, which is the most stable positive oxidation state of nitrogen and far more common in the aquatic environment than nitrite (DWAF, 1996). However, nitrate in drinking water can readily be converted in the gastrointestinal tract to nitrite as a result of bacterial reduction. Upon absorption, nitrite combines with the oxygen-carrying red blood pigment, haemoglobin, to form methaemoglobin, which is incapable of carrying oxygen. This condition is termed *methaemoglobinaemia*, which is particularly hazardous in infants under three months of age (DWAF, 1996).

High nitrate concentrations are quite common in Kalahari groundwater (Stadler *et al*., 2012). Because many sources of nitrate are associated with agriculture, the Kalahari region offers much potential for nitrogen input into its groundwater as cattle farming and crop irrigation are the most commonly pursued activities in this region. This is seen from the nitrate concentration (average of 12.53 mg/l) associated with the groundwater in this region, the dominant anthropogenic input of which is expected to be from cattle faecal material and local occurrences of human wastes. From the nitrate map (Figure 6.8) it is apparent that even higher concentrations (> 25 mg/l) than average occur. These values seem to be restricted to water sources associated with agricultural practices (notably Tosca – large concentration of irrigation pivots) and runoff from rural settlements (notably Morokweng and Pomfret), which are notorious for their unsewered sanitation.

6.8 Dissolved Oxygen (DO)

The dissolved oxygen (DO) concentration regulates the valence state (and thus the solubility) of trace metals and constrains the bacteriological metabolism of organic compounds in groundwater (Weaver *et al*., 2007). This is largely due to the main characteristic of oxygen, which is its ability to oxidise (that is, accept electrons from) other species in water (Stumm and Morgan 1996). Both electrons and energy are transferred in biological and geochemical oxidation-reduction (redox) reactions. No other naturally occurring constituent of water is a more energetic, or biologically reactive, oxidant than molecular oxygen; therefore aerobic bacteria utilize DO as part of their metabolism (Weaver *et al*., 2007). Given this, the measurement of DO is important for groundwater quality investigations and especially so when dealing with polluted water.

The DO concentration of the samples collected in the study area range between 9.43 and 10.92 mg/l (Table 6.1). The target water quality range for this constituent of groundwater is not available in the water quality guidelines outlined by DWAF (1996), as such, there is no standard with which to compare these values. It is known, however, that in low-salinity water at sea level, the DO content of water saturated with air is typically 9 mg/l at 20 ^{o}C (Weaver *et al*., 2007). This value being dependent on the local atmospheric pressure and inversely related to water temperature and salinity, it seems that the values recorded for the study area are acceptable, with no evidence of pollution.

When groundwater becomes polluted, DO is likely to be absent, even at shallow depths (Weaver *et al*., 2007). The fact that the samples record an average DO concentration of 10.20 mg/l infers the absence or concentration of oxygen-sensitive contaminants such as methane or hydrogen sulphide. As mentioned above, aerobic bacteria utilise DO as part of their metabolism, which results in the oxidation of organic carbon, hydrogen sulphide, ammonium and other reductants (Weaver *et a*l., 2007). An important aspect of these biochemical redox reactions is their irreversibility, as bacterial metabolism always consumes, but never produces oxygen (Weaver *et al*., 2007). The presence of dissolved oxygen within all of the samples hints, therefore, at the absence of bacterial organisms.

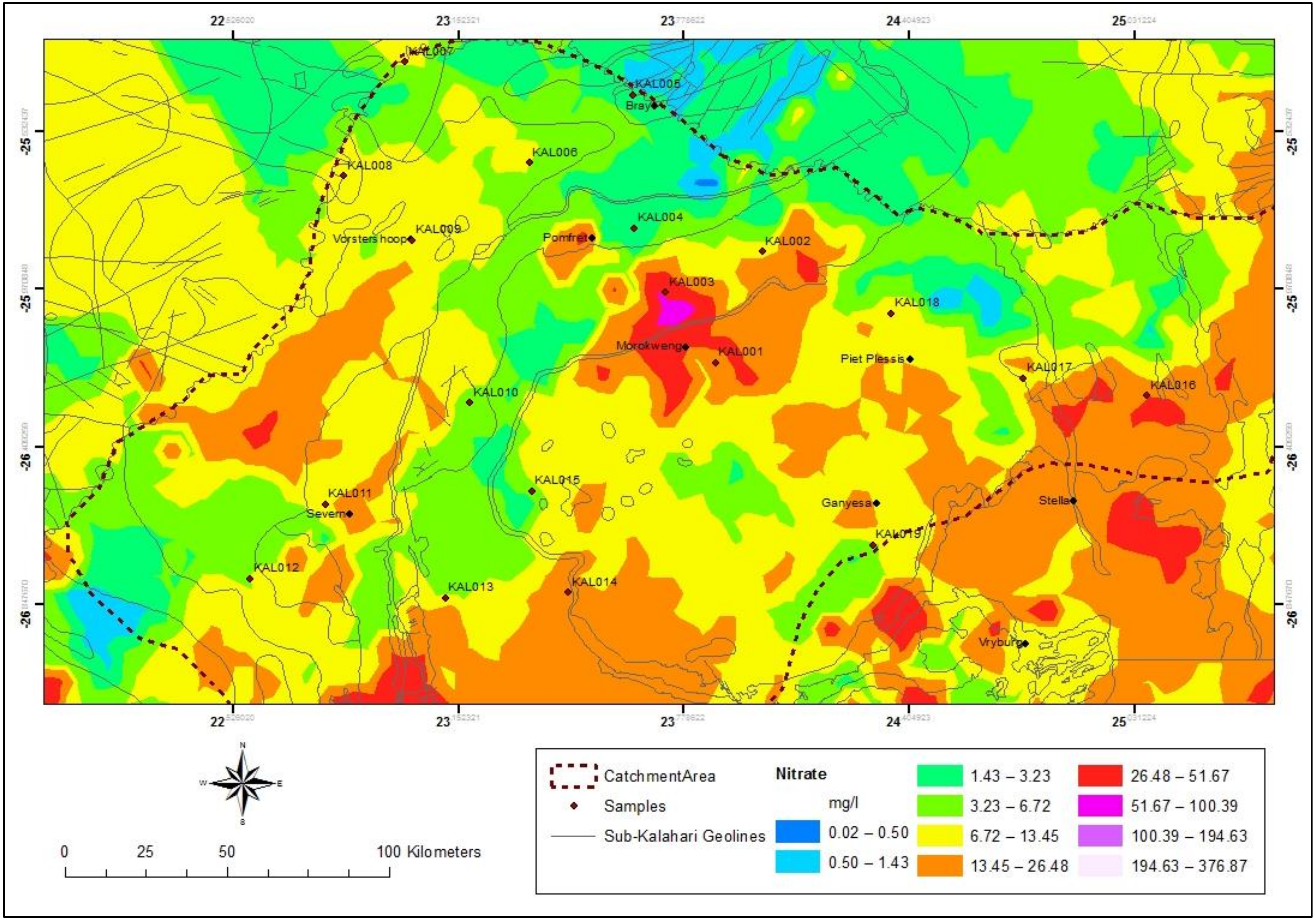

Figure 6.8: Nitrate map of the study area relative to the sub-Kalahari geology (Data sourced from DWAF NGANET)

6.9 Bacterial Analysis

The subsurface environment, both in the vadose zone and the saturated zone, has a huge microbial population and a wide variety of living micro-organisms. These range from health affecting species such as *Giardia lamblia* and *Salmonella typhi* (typhoid fever) to indicator bacteria such as faecal coliforms and to the large variety of species of bacteria that mineralise organic carbon (Weaver *et al*., 2007; Bezuidenhout *et al*., 2013). Despite the huge microbial population of the sub-surface environment, it is impractical and expensive to monitor water supplies for all potential human pathogens, the study of which requires a specialised microbiologist. As such, this investigation focusses largely on the analysis of indicator bacteria that are the most frequent source of health-significant microbial contamination of groundwater supplies and are usually indicative of the presence of other pathogenic microorganisms. This inexpensive and practical method is typically used to determine whether groundwater is fit for use as a drinking water resource, domestic or otherwise (Weaver *et al*., 2007).

Table 6.2: The measured biological parameters of samples collected

Date Sampled	Time Sampled	Sample Number	Latitute	Longitude	E. Coli (cfu/100ml)	Enterobacter Aerogens (cfu/100ml)	Proteus Mirabilis (cfu/100ml)	BOD (mg/l)
31-01-2015	10:30	KAL001	-26.17650	23.86636	0	758	466	14.6
31-01-2015	12:30	KAL002	-25.86775	23.99736	0	0	203	3.1
31-01-2015	15:00	KAL003	-25.98061	23.72919	0	147	0	-
31-01-2015	16:30	KAL004	-25.80303	23.64231	0	816	0	-
31-01-2015	17:40	KAL005	-25.43119	23.63625	0	0	104	-
31-01-2015	19:15	KAL006	-25.62100	23.35039	0	132	49	3.1
01-02-2015	08:00	KAL007	-25.34075	23.00533	0	542	63	-
01-02-2015	10:00	KAL008	-25.65744	22.83508	0	157	0	0.0
01-02-2015	10:45	KAL009	-25.83578	23.02519	0	145	263	0.0
01-02-2015	12:45	KAL010	-26.28744	23.18567	0	0	0	-
01-02-2015	14:30	KAL011	-26.56981	22.78400	0	27	0	-
06-02-2015	12:30	KAL012	-26.77569	22.57425	0	0	0	-
06-02-2015	14:38	KAL013	-26.82964	23.11617	0	13	12	2.2
06-02-2015	16:00	KAL014	-26.81486	23.45722	0	0	0	4.5
06-02-2015	18:40	KAL015	-26.53228	23.35622	0	16	0	2.0
07-02-2015	12:00	KAL016	-26.26775	25.06492	0	92	0	0.3
07-02-2015	13:18	KAL017	-26.21825	24.72119	0	54	0	0.0
07-02-2015	20:40	KAL018	-26.03861	24.35519	0	1	0	-
08-02-2015	16:00	KAL019	-26.68289	24.30322	0	12	0	0.0

Almost all (90 %) of those samples collected from boreholes situated on private farms recorded the presence of either *Enterobacter Aerogens* (88 % of the samples) and/or *Proteus Mirabilis* (40 % of the samples), whereas those samples collected from municipal boreholes (KAL010 and KAL014), supplying surrounding rural communities, proved clear of indicator bacteria (Table 6.2). Some of the bacterial counts recorded for those samples collected on private farms proved high with regard to their bacterial content, particularly given that the Department of Water Affairs (DWAF, 1996) has compliance guidelines for these organisms which state that 100 mℓ of water should be absolutely free from these bacterial species. Caution should; however, be exercised upon interpretation of these results, given that the samples were not analysed within the ideal maximum holding time of 48 hours (See Section 2.3.7) and many of the borehole outlet pipes extended over a few metres in length, making them susceptible to contamination.

While the results remain questionable, it is felt that these compromised samples reflect contamination of the groundwater to some degree. *Enterobacter Aerogens* and *Proteus Mirabilis* are typical members of the bacterial flora of the gastrointestinal tract of humans and other warm-blooded animals and, as such, their presence indicates recent faecal contamination (Grabow, 2003; Lin *et al*., 2012; Bezuidenhout *et al*., 2013; Du Preez *et al*., 2013). With most of the boreholes being sited in or close to livestock watering points, where there is a large volume of animal waste being produced in a limited area, there is little doubt that farming practices have contributed to some degree to these elevated counts.

Transport of faecal microorganisms in groundwater is facilitated primarily by the bulk movement of groundwater, with faecal microorganisms being filtered and immobilised to varying extents by the medium through which they are transported. The extent is dependent on the aquifer type, with groundwater contamination occurring more readily in unconfined coarse alluvial aquifers (such as the overlying Kalahari sand) than in less porous environments, and microorganism size. These factors, coupled with the generally relatively slow movement of groundwater, usually results in a localised impact (Murray *et al*., 2007). Based on this localised impact theory and given that many of the boreholes are sited within the immediate vicinity of faecal pollution, it is believed that bacterial contamination of the groundwater originated from polluted surface runoff that reached the aquifer via the borehole itself. A borehole provides a direct link to the aquifer, and as such, contamination can use the disturbed zone along the outside of the borehole casing as a conduit to reach the aquifer (Murray *et al*., 2007). The outlet pipes from most of the borehole pumps can also be responsible for the contamination observed, as many proved to be a few metres in length, laying open and susceptible to contamination. This is confirmed by the absence of any faecal pollution in the community sited boreholes, each of which was sealed, with no outlet pipe, and covered by a metal shed to protect it from direct access to both people and animals.

Generally, *Enterobacter Aerogens* and *Proteus Mirabilis* are not associated with adverse health effects and are typically responsible for various community acquired infections, which include urinary tract, soft tissue and wound infections (Grabow *et al*., 2003; Lin *et al*., 2012; Bezuidenhout *et al*., 2013; Du Preez *et al*., 2013). While this coliform group of bacteria themselves are not considered to be a severe health risk, their presence can indicate that other, more harmful pathogenic microorganisms such as viruses (enterovirus, adenovirus and hepatitis A & B) and bacteria (*Vibrio cholerae, Shigella* spp. *Yersina* spp. and *Enterocolitica* spp.) may also be present in these water sources (Grabow *et al*., 2003; Lin *et al*., 2012; Bezuidenhout *et al*., 2013; Du Preez *et al*., 2013). Finding this bacterium in the groundwater that is used for domestic and recreational purposes, as well as for drinking by people and livestock, is cause for concern and there can be little doubt that 'hazards' exist that could ultimately impact on human and animal health.

6.10 Biological Oxygen Demand-5 (BOD_5)

In the same way as humans require oxygen, many microorganisms also require oxygen to obtain energy for the decomposition of organic matter. The biochemical oxygen demand results from the respiratory processes of microorganisms and can be determined by measuring this biological phenomenon (OxiTop ® manual). In particular, this respirometric method of BOD_5 determination uses carbon dioxide, rather that oxygen, and measures the change in pressure. Microorganisms consume oxygen and when the oxygen is converted to carbon dioxide by respiration (both of which have the same volume per mole), there is no direct change in pressure (OxiTop ® manual). However, if sodium hydroxide is added to the sample, as performed in this test, the sodium hydroxide and carbon dioxide react chemically to form sodium carbonate ($2NaOH + CO_2 \uparrow \rightarrow Na_2CO_3 \downarrow + H_2O$). This causes the carbon dioxide that was formed to be removed from the gas phase and results in a measurable negative pressure due to the respiration of oxygen. The respirometric measurement is, therefore, a pressure measurement and comes closest to representing the natural conditions of biological degradation. The measured negative pressure is then converted into the BOD_5 value using an equation that was derived from the ideal gas law under the conditions of an additional liquid phase (OxiTop ® manual).

Almost all of the eleven samples tested, excluding KAL001, displayed inhibited oxygen degradation curves (Figure 6.9). In most cases the oxygen degradation is greatly delayed, with almost no oxygen degradation seen in the first few days, whereas in other cases, degradation is reduced throughout the entire testing period. Inhibited samples do not consume oxygen, confirming the absence of micro-organisms which typically consume oxygen for the decomposition of organic matter. This, together with the DO concentrations measured for the groundwater, point to the absence of bacterial organisms in the groundwater, further suggesting that the bacterial analyses' samples collected were possibly compromised. The highly positive bacterial analyses (Section 6.9) seems to point to local contamination effects i.e. contaminated pump outlet pipes, boreholes situated within feeding pens etc. rather than the groundwater aquifers themselves being contaminated.

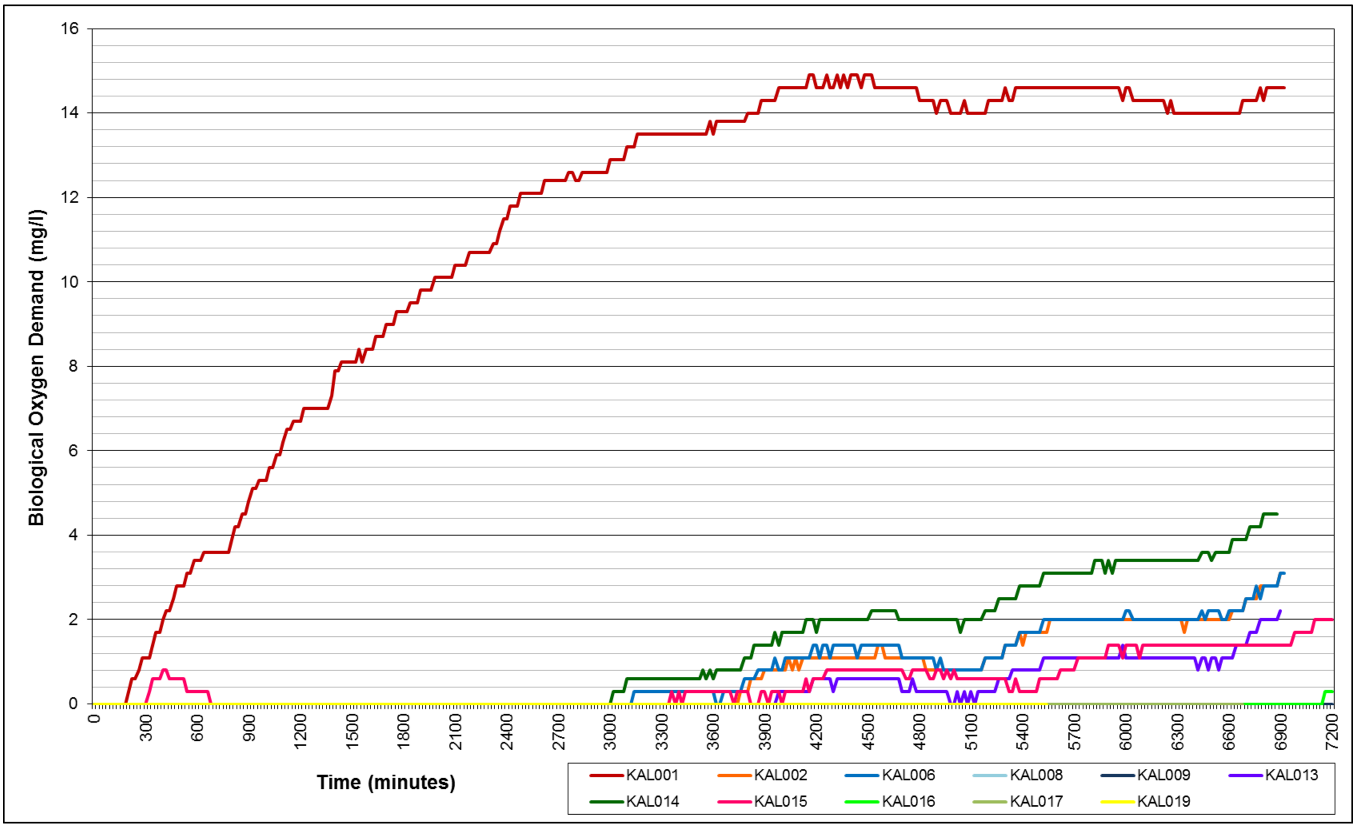

Figure 6.9: Biological oxygen demand over time for those samples collected within the study area

Only one sample (KAL001) recorded a high BOD value of 14.6 mg/l (Table 6.2) and when plotted over time (Figure 6.9) displayed a normal curve from beginning to end. This value exceeded the universal water quality index of 3 mg/l BOD (Lin *et al*., 2012). This seems to point to local contamination of the aquifer. The borehole is typically situated within a feeding pen, within the immediate vicinity of faecal pollution, and sources its groundwater from the unconfined Kalahari sediments. Groundwater contamination occurs more readily in such coarse, unconfined aquifers that are typically porous environments of microorganism size. These factors, coupled with the generally relatively slow movement of groundwater, has resulted in a localised impact, in which the polluted surface water runoff has reached the aquifer, possibly via the borehole itself, and contaminated the groundwater.

7. GROUNDWATER HYDROCHEMISTRY

The assessment of groundwater chemistry is a major step towards understanding the source of the groundwater in the region, its evolution and quality. The chemical variations within an aquifer or chemical differences between aquifers are largely influenced by hydrogeological and anthropogenic controls (Kovalevsky *et al*., 2004). As water flows through geological formations, the progressive interaction between slow moving water and the minerals that are in contact with the water along the flow path, result in the water composition evolving from that initially introduced (dilute rainwater) to concentrated ionic compositions at depth. These specific concentrated ionic compositions, therefore, provide insight into the geology at depth and if contamination was encountered, the nature thereof. The variability observed in the chemical composition of these natural waters can also provide an insight into different aquifer types, aquifer heterogeneity and connectivity, as well as the physical and chemical processes controlling water chemistry (Tessema *et al.,* 2014).

Given the indisputable advantages of assessing groundwater chemistry, it proved essential to identify the existing hydrochemical signature of the groundwater in this region. Grouping the hydrochemical data from the NGIS/CHART archive into its respective Quaternary drainage regions (Figure 7.1; See Section 2.4) allowed for the quick inspection of the results and for the detection of general trends, with the graphs revealing similarities and differences amongst the various drainage regions (Figure 7.1). The ultimate goal was then to divide the samples into similar homogeneous groups, each representing different hydrochemical facies i.e. groups of samples with similar chemical characteristics that could then be correlated with location, geology, topography or aquifer types. The samples with similar chemical characteristics often have similar hydrologic histories, similar recharge areas, infiltration pathways and flow paths in terms of climate, mineralogy and residence time (Tessema *et al*., 2014). In addition, the classification of groundwater into water types on the basis of major ion composition also provided a framework for interpretation of groundwater quality.

7.1 Results

The hydrochemical data covering the study area is shown in Figure 7.1, with the detail provided in Appendix A. In general, the chemical characteristics of the groundwater varies widely across the study area, with the various Piper diagrams showing a larger variability in cations, while the anions show nearly similar patterns (Figure 7.1). In particular, the Mg – Ca and Na – K content varies considerably, with the Mg – Ca content of the groundwater ranging from 0.5 to 50 meq/l in the eastern part of the study area, with more defined populations becoming evident towards the western part of the study area. By contrast, the anion triangles show similar patterns from east to west of the study area, with very little SO_4 present and a wide ranging Cl – HCO_3 content (Figure 7.1).

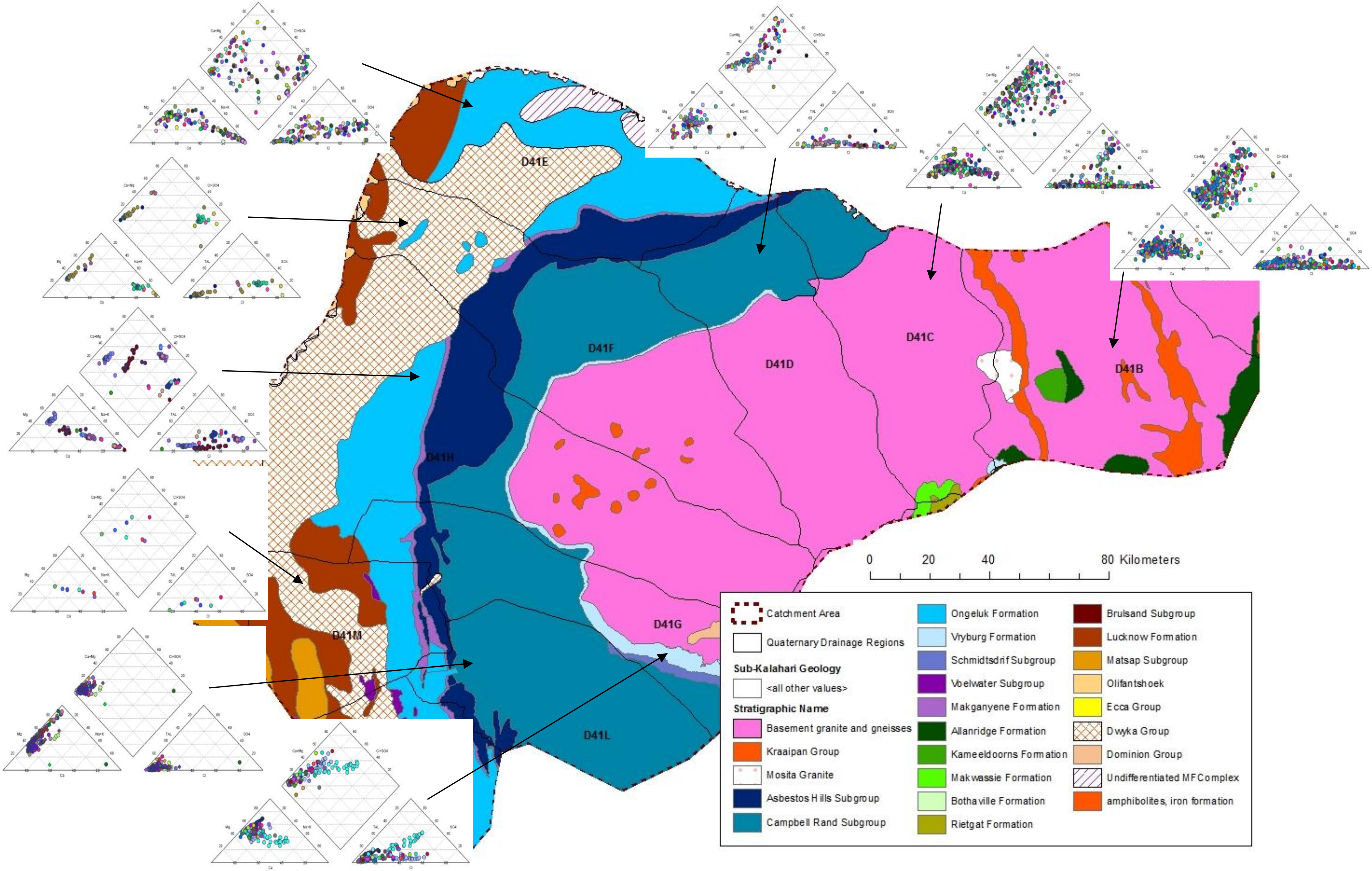

Figure 7.1: The chemistry data (Piper) relative to the Quaternary drainage regions and the sub-Kalahari geology (Chemistry data sourced from DWAF NGANET)

The eastern part of the study area comprises groundwater that is characterised by two populations, with many samples plotting between these two extremes, possibly signifying a variable degree of mixing of different water types (Figure 7.2). One population is characterised by groundwater that is relatively enriched in Ca, Mg and Cl ions, while depleted in Na and HCO_3 ions, with the other extreme characterised by groundwater that is enriched in Na and Cl ions, while depleted in Ca, Mg and HCO_3 ions. The former may be associated with the volcanic and sedimentary rocks of the Kraaipan, Amalia and Ventersdorp Supergroups located along the eastern margin of the study area. The predominance of SO_4 in some of these samples signifies the oxidation of pyrite, the presence of which is commonly associated with the gold deposits of the Kraaipan greenstone belt. The chemical characteristics of this groundwater seems to vary quite considerably compared to that associated with the other extreme population of groundwater enriched in Na and Cl ions. The semi-arid Kalahari environment is typically associated with this hydrochemical facies, where the rate of evaporation is rapid and creates suitable conditions for generating elevated salt content (Na – Cl water type).

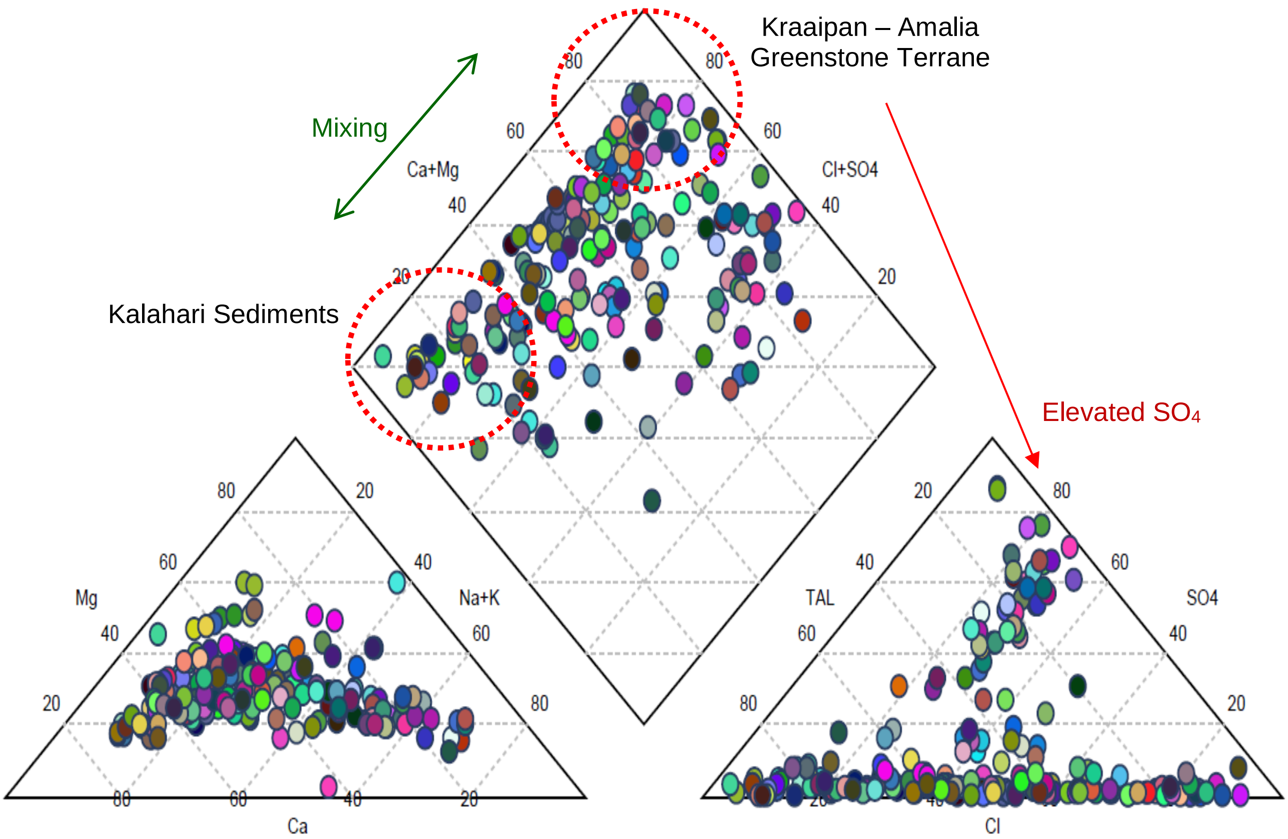

Figure 7.2: The chemistry data (Piper Diagram) characteristic of the eastern portion of the study area

Moving westward towards the central part of the study area, the Kalahari hydrochemical facies remains in place, however, the Ca – Mg – Cl dominant hydrochemical facies of the Kraaipan and Amalia sequence is replaced by groundwater that is dominated by Ca, Mg and HCO_3 ions (Figure 7.3). The dominance in Ca and Mg, with strong HCO_3 content suggests an interaction between groundwater and aquifer material at shallow depth, presumably the carbonate rocks of the Griqualand West sequence, which underlie this portion of the study area and consist of soluble minerals such as Ca and Mg. An intermediate population, which is slightly more mineralised with regard to Cl than this end member population of Ca – Mg – HCO_3, is also visible on the Piper diagrams. This suggests that the boreholes in the central region of the study area are not only tapping water from the carbonates, but also from other fractured rocks that are rich in Ca and Mg (ferromagnesian minerals). The fact that this portion of the study area is characterised by dolomite and limestone that are intercalated with quartzite, shale, dolerite dykes and dolerite sills, seems to account for this slight variation in the groundwater's chemistry.

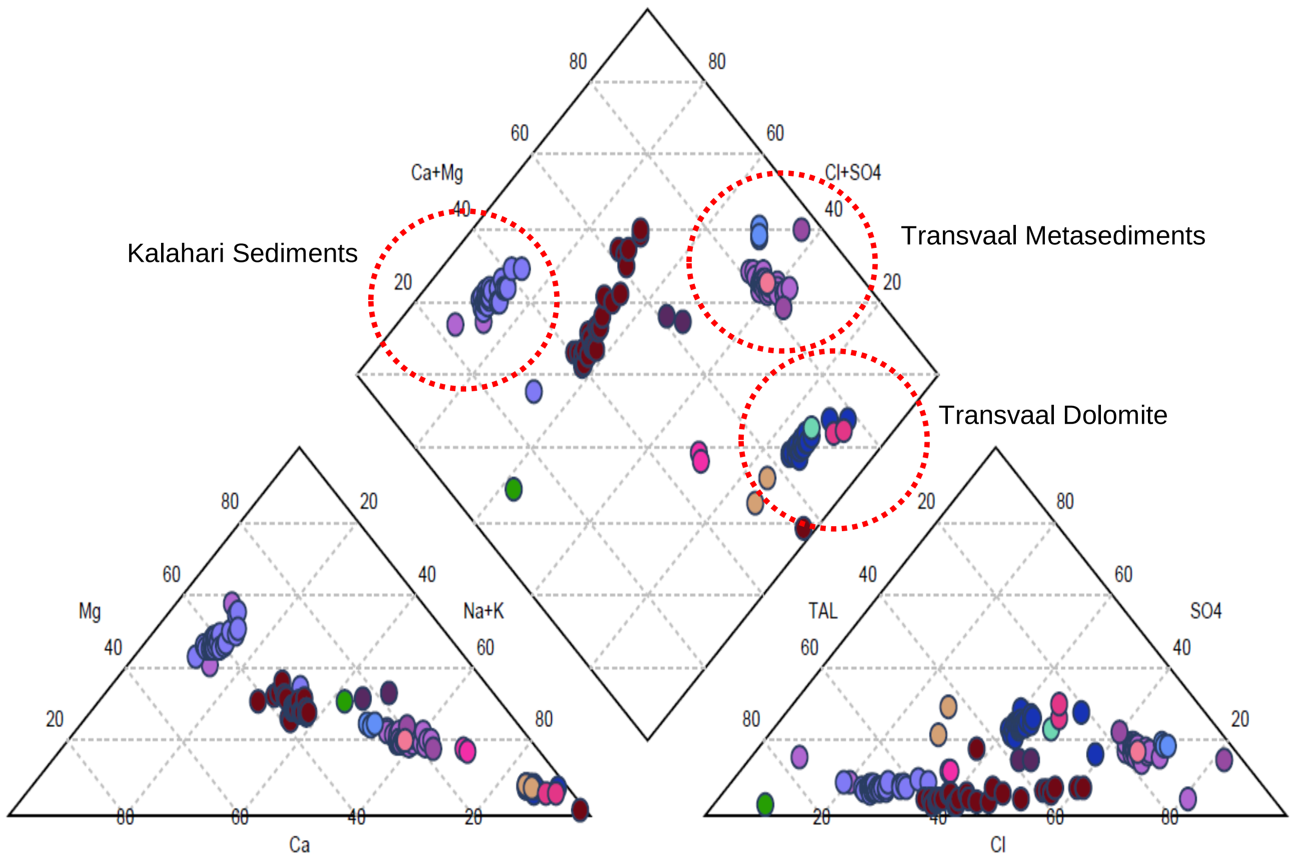

Figure 7.3: The chemistry data (Piper Diagram) characteristic of the central portion of the study area

This portion of the study area is also characterised by samples where the Na content of some samples is significantly more compared to Ca and Mg in the cation triangle. This possibly suggests that silicate minerals (e.g. plagioclase feldspar: albite or hornblende), typical of the granites in the area, are also an important dissolved species in groundwater as compared to carbonate minerals. This hydrochemical facies' signature, however, seems to be subdued by that of the Ca – Mg – HCO_3 population. This is largely due to the fact that groundwater reacts to varying degrees with the minerals in the surrounding aquifer, with silicate minerals typically not reacting as readily as that of the carbonate minerals.

While still present, the dominance of this Ca – Mg – HCO_3 hydrochemical facies diminishes northward and westward, where the hydrochemical facies (Na + K – Cl dominant) typical of semi-arid to arid environments is observed (Figure 7.4). This area is characterised by thick assemblages of Kalahari sediment, where the rate of evaporation is rapid, creating suitable conditions for the generation of elevated salt content in the groundwater. This is confirmed by the elevated TDS and chloride content (Section 6.6) typically associated with groundwater in this portion of the study area, which also shows an evaporative enrichment of the stable isotopes ^{18}O and deuterium (Section 8.3). The Olifantshoek quartzites and the Dwyka tillites are also typically characterised by water that is mainly of the Na - Cl type, partly accounting for the dominant Na - Cl hydrochemical facies seen along the northern and western portions of the study area.

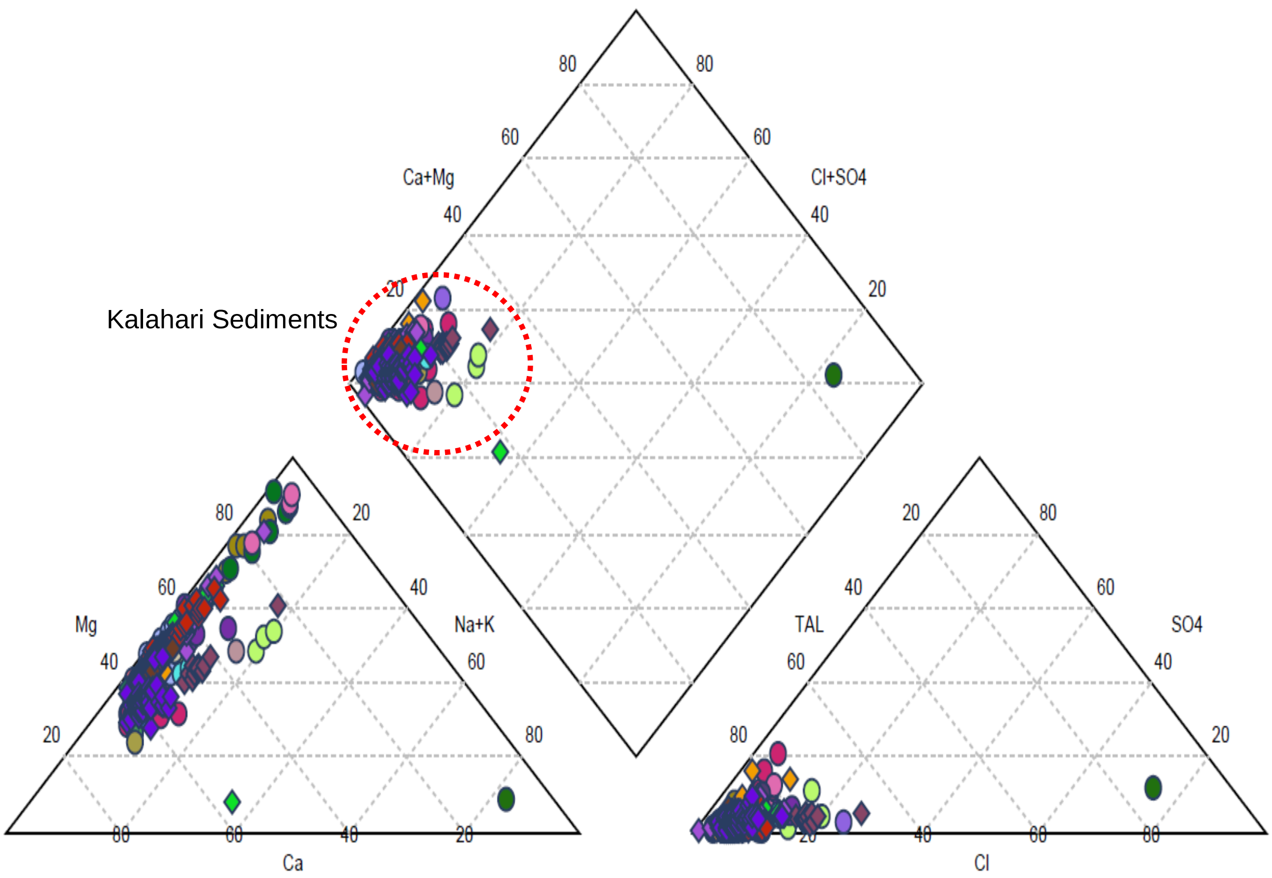

Figure 7.4: The chemistry data (Piper) characteristic of the northern and western portion of the study area

7.2 Discussion

Overall, the hydrochemical analysis of the region can quite easily be linked to distinct hydrogeological systems from which groundwater was extracted, with some degree of mixing between the various water types. In particular, five fundamental groups of aquifers can be identified on the basis of the hydrochemical data. The first group corresponds to the groundwater sourced from the unconfined Kalahari Group of sediments, which is characterised by highly mineralised (Na – Cl dominant) groundwater that has seen extensive evaporation and enrichment, with very little recharge. This is confirmed by the isotopic enrichment of $^{18}O/^{16}O$ and D/H ($^{2}H/^{1}H$) ratios in the groundwater samples sourced from the Kalahari sediments, the signature of which corresponds to evaporation (Section 8.3). An area which has seen extensive enrichment has been identified to the north of the study area, where the Kalahari sequence is at its thickest (> 90 m). This area also records the highest salinities (Section 6.6), making this groundwater unsuitable for human consumption and/or irrigation.

The second group includes the groundwater associated with the carbonate (dolomite and limestone) rocks of the Griqualand West sequence. The homogeneity of this hydrochemical facies (Ca – Mg – HCO_3 dominant) throughout the study area, suggests good water exchange and permeability within each aquifer compartment. This hydrochemical facies can, however, be seen evolving to more Cl dominated types (Group 3), particularly where the dolomite is intercalated with the shales, quartzites and banded iron formations of the Asbestos Hills Subgroup. This chemical evolution suggests some degree of mixing between these two groups of aquifers.

The fourth group is characterised by poorly mineralised groundwater, associated with the weathered zone of the Archaean granites. An identifying characteristic of this hydrochemical facies is the elevated Na – K content of the groundwater, typical of the dissolution of silicate minerals which form an important constituent of the basement granites. The highly mineralised nature of some of these samples suggests a long residence time, with little recharge. The basement aquifer water samples to the east of the study area, with their prevailing chloride and sulphate content, represents the fifth group of aquifers identified.

As seen above, the type of aquifer plays a significant role in determining the evolution of groundwater, with some rocks reacting readily with water, while others do not. While different populations can be clearly defined, some degree of mixing between the various water types is evident. The existence of preferential pathways such as fracture or fault zones could allow groundwater from different aquifer types to mix. In addition, those areas where groundwater storage and flow is predominantly in fractures, the hydrochemical facies may be subdued as the opportunity for water-rock interactions may be restricted due to short residence times and low contact surface area.

8. ENVIRONMENTAL ISOTOPE ANALYSIS

Environmental isotope analysis embraces the measurement of isotope ratios of the elements making up the water molecule (^{18}O, ^{2}H and ^{3}H), elements which are subject to environmental processes and, therefore, change (Abiye, 2013). Not only do the variations in their isotopic composition assist in determining the origins and ages of different water bodies (Levin and Verhagen, 2013), it has the most potential to forecast groundwater recharge based on the relationship between rainfall, abstraction/evapotranspiration and interconnectivity of water resources, information that can be built into a groundwater management plan at the inception of exploitation (Verhagen, 2003; Abiye, 2013). Given its potential, 19 samples were taken at different locations spread across the eastern Kalahari region (See Section 2.5) and assessed for their environmental isotope content, the details of which are provided below.

8.1 Results

8.1.1 Stable Isotope analysis ($^{2}H/^{1}H$ and $^{18}O/^{16}O$)

In order to gain an idea of the isotopic composition of the groundwater within the study area, the $\delta^{18}O$ and δD results of each water sample, the details of which can be viewed in Table 8.1, were plotted on a $\delta^{18}O$ versus δD graph (Figure 8.1). The Global Meteoric Water Line (GMWL), which is commonly used as a reference for interpretation of the isotopic composition of groundwater, was also plotted. While useful, the data associated with the Global Meteoric Water Line is too broad and provides little insight to the unique conditions that are specific to the study area. As such, a Local Meteoric Water Line (LMWL) was also plotted and used for the interpretation of the results. Given that the study area is broadly similar in climatic and physiographic setting to Pretoria, the long-term monitoring data recorded at the Pretoria meteorological station was used as a Local Meteoric Water Line (PLMWL). A rainfall sample collected (KAL020) plots along this local meteoric water line, confirming the validity of using the PLMWL as a reference for interpretation.

Three populations can be distinguished from the plotted data – those data points that plot along the local meteoric water line, those that plot below the meteoric water line along an evaporation trend line of gentler slope than that of the PLMWL and those samples that plot below the evaporation trend line (Figure 8.1). These isotopic results suggest that the study area can be divided into specific groundwater regimes, each of which have their own characteristic variations in terms of recharge, depth to groundwater, hydrochemistry and other hydrogeological properties, the details of which are discussed below.

Table 8.1: Results of the environmental isotopic samples collected

Laboratory Number	Sample Identification	Latitute	Longitude	δ D (‰)	$\delta^{18}O$ (‰)	Tritium (T.U.)		d-excess
WITS 390	Kal001	-26.1765	23.8664	-31.84	-5.32	0.7	±0.2	10.75
WITS 391	Kal002	-25.8678	23.9974	-33.01	-5.51	0.8	±0.2	11.04
WITS 392	Kal003	-25.9806	23.7292	-27.53	-4.62	0.0	±0.2	9.42
WITS 393	Kal004	-25.8030	23.6423	-32.79	-5.64	0.0	±0.2	12.32
WITS 394	Kal005	-25.4312	23.6363	-24.80	-3.65	0.4	±0.2	4.44
WITS 395	Kal006	-25.6210	23.3504	-29.26	-4.95	0.4	±0.2	10.37
WITS 396	Kal007	-25.3408	23.0053	-34.77	-5.82	0.3	±0.2	11.81
WITS 397	Kal008	-25.6574	22.8351	-36.23	-5.90	0.0	±0.2	10.97
WITS 398	Kal009	-25.8358	23.0252	-33.55	-5.59	0.0	±0.2	11.21
WITS 399	Kal010	-26.2874	23.1857	-31.60	-5.66	0.5	±0.2	13.69
WITS 400	Kal011	-26.5698	22.7840	-32.24	-5.86	0.3	±0.2	14.66
WITS 401	Kal012	-26.7757	22.5743	-20.76	-3.76	0.0	±0.2	9.30
WITS 402	Kal013	-26.8296	23.1162	-28.90	-5.66	0.0	±0.2	16.41
WITS 403	Kal014	-26.8149	23.4572	-28.20	-5.93	0.9	±0.2	19.21
WITS 404	Kal015	-26.5323	23.3562	-28.11	-5.17	0.0	±0.2	13.22
WITS 405	Kal016	-26.2678	25.0649	-22.06	-4.39	0.7	±0.2	13.10
WITS 406	Kal017	-26.2183	24.7212	-25.10	-5.01	1.3	±0.3	14.98
WITS 407	Kal018	-26.0386	24.3552	-30.14	-5.68	0.0	±0.2	15.33
WITS 408	Kal019	-26.6829	24.3032	-31.66	-5.92	0.0	±0.2	15.73
WITS 409	Kal020	-26.6829	24.3032	-41.78	-7.86	2.7	±0.3	21.11

8.1.2 Tritium Analysis

Analysis of the 19 samples has revealed groundwater with a tritium content that ranges from 0.0 to 1.3 TU (Table 8.1). The bulk of the tritium values observed in the area of study have relatively low tritium values (0.3 to 0.6 TU) that lie slightly above the limit of detection (0.2 ± 0.2 TU), with almost half of the samples measuring zero tritium content (Figure 8.2). The maximum value of 1.3 TU corresponds to the Mosita Granite to the north of Stella, while the zero values correspond to numerous lithologies spread across the study area. As with the stable isotopic data, a plot of tritium values against $\delta^{18}O$ (Figure 8.2) confirms the presence of differing groundwater regimes with their characteristic variations in source, climatic condition, recharge, depth to groundwater etc., the details of which are discussed below.

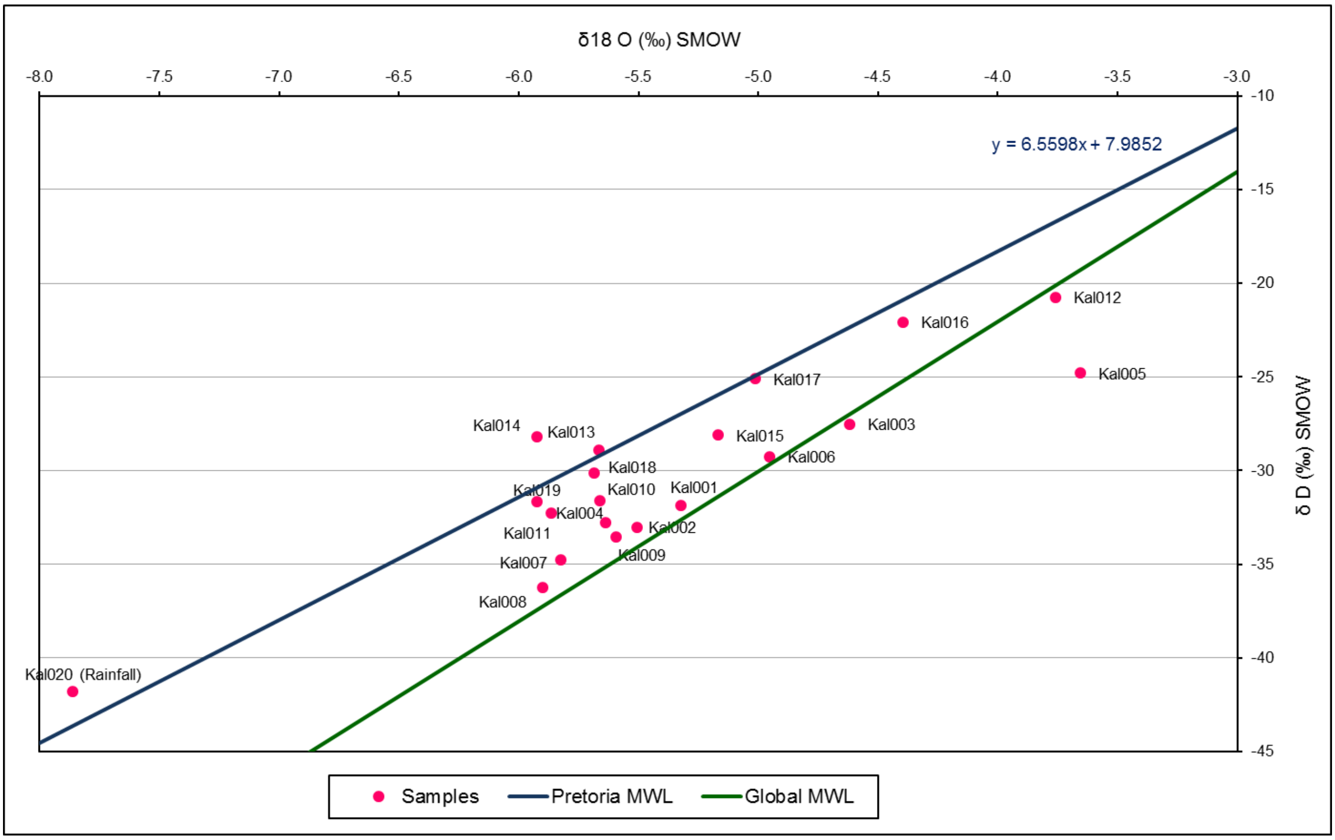

Figure 8.1: Plot of the environmental isotope data on a δ^{18}O versus δD graph, relative to both the Local and Global Meteoric Water Lines

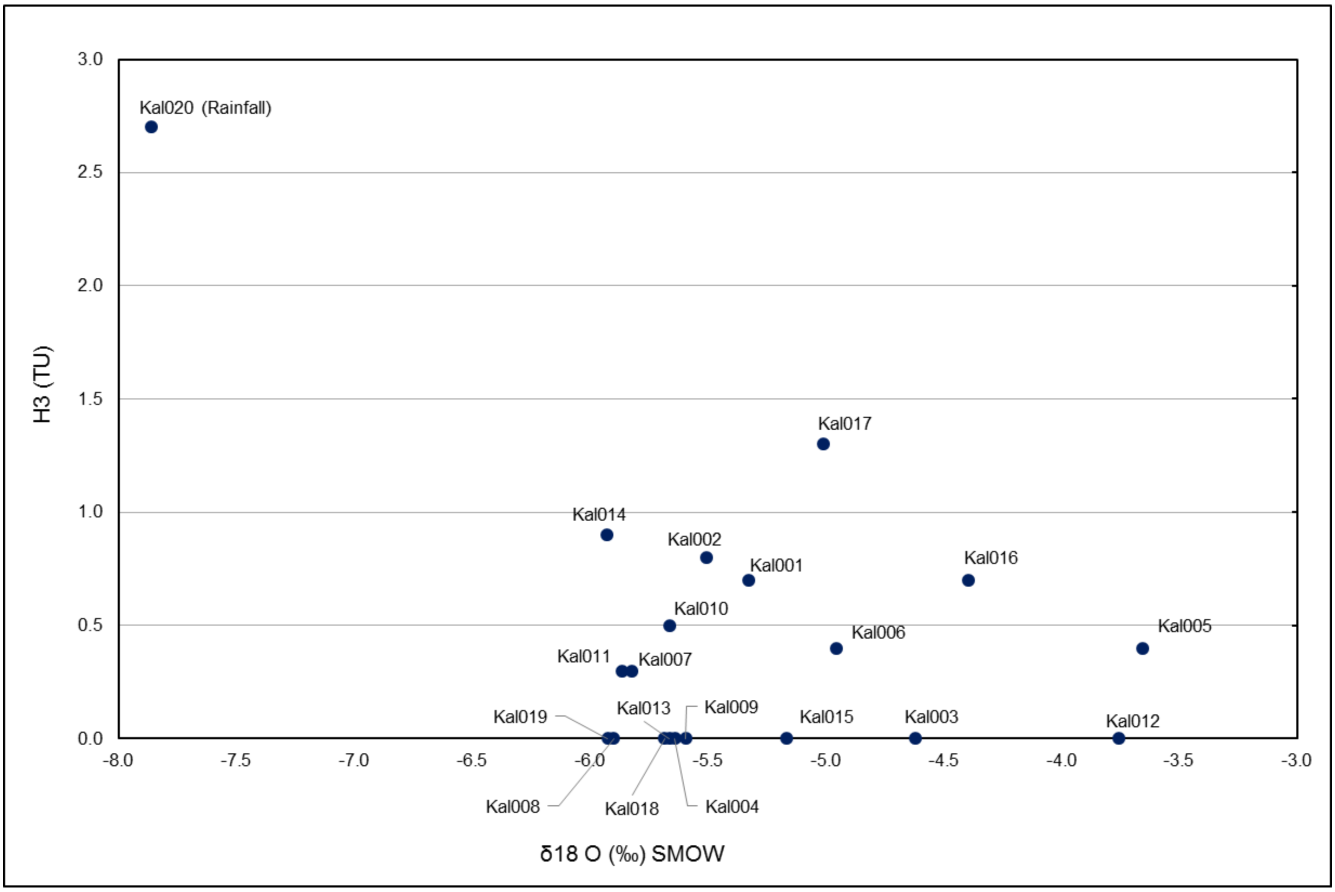

Figure 8.2: Plot of δ^{18}O versus Tritium for the samples collected

8.2 Age Relationships

The residence time of groundwater in an aquifer or the groundwater age is an important parameter in any hydrogeological study. Isotope studies, notably radioactive decay, offers the possibility to determine approximate ages of various groundwaters. In particular, the radiogenic isotope of hydrogen (^3H – tritium), which has a half-life of 12.43 years, is commonly used to evaluate the relative ages or circulation time of groundwater i.e. determining the time elapsed since the infiltration of the water (Geyh, 2001). Tritium is produced naturally in the upper atmosphere from nitrogen by neutron impacts of cosmic radiation and it enters the water cycle by precipitation. Tritium acts as a conservative tracer in the water molecule itself and its content is only influenced by mixing with older water and radioactive decay (Weaver *et al*., 2007). As such, it has the potential of being used to date groundwater 'ages' in the order of decades.

Before the advent of nuclear weapons testing during the 1950s and early 1960s, rainfall tritium values were in the order of 3 to 5 TU. During the period of nuclear weapons testing, rainfall tritium levels reached 5000 TU in the northern hemisphere, while it never exceeded more than 100 TU in the southern hemisphere. Present day rainfall tritium levels in the southern hemisphere have since decreased to pre-bomb values of 3 to 5 TU, while the northern hemisphere still recorded elevated levels of approximately 80 to 100 TU in 2000 (Clark and Fritz 1997, Tessema *et al*., 2012). This major worldwide contamination event has afforded the possibility of using tritium as an indicator of recent (post 1955) recharge. Assuming that piston flow conditions (no dispersion or mixing) are applicable, Clark and Fritz (1997) noted the following guidelines for interpretation of the radiogenic tritium for groundwater investigation:

1. Groundwater with a tritium content of less than 0.8 TU may correspond to recharge prior to 1952.
2. Water with a tritium content ranging from 0.8 to 4 TU may represent a mixture of water that contains components of recharge before and after 1952.
3. Tritium concentrations from about 5 to 15 TU may indicate recharge after about 1987.
4. Tritium concentrations from about 16 to 30 TU are indicative of recharge since 1953, but cannot be used to provide a more specific time of recharge.
5. Water with more than 30 TU is probably from recharge in the 1960's or 1970's.
6. Water with more than 50 TU is predominantly from recharge in the 1960's.

The present study has revealed groundwater with a tritium content that ranges from 0.0 to 1.3 TU (Table 8.1). Based on the guideline of Clark and Fritz (1997), the results suggest that a large proportion of the groundwater resources in the study area have been recharged during former pluvial periods prior to 1952. In particular, a lower limit of a century can be placed on the mean residence time of most of the groundwater in the area (Verhagen, 2013). Those samples recording tritium values equal to and greater than 0.8 TU suggest mixing of components of differing isotopic composition in the boreholes, interpreted as indicating some mixture with recent recharge or the mixing of groundwater of different residence times. Leakage between aquifers may result in the mixture of groundwater of different age or, alternatively, the boreholes from which the samples were derived have accessed water from different aquifers at various depths. The latter is quite feasible given that most of the boreholes sampled were drilled to great depths, many penetrating beneath the Kalahari sediments to the underlying basement lithologies.

The maximum value of 1.3 TU corresponds to a shallow groundwater sample (< 60 m) that was collected to the north of Stella (KAL017), within the Mosita granite. These high tritium values are not only limited to shallow drilled wells, with some shallow groundwater encountered in similar lithologies found to contain little to no tritium. This is interpreted as indicating that significant recharge to both the shallower and deeper groundwater in the area is episodic, i.e. at intervals comparable to the decay time of mean natural tritium values in rain to the detectable limit, i.e. in the order of 50-100 years (Verhagen, 2013). Only certain shallow aquifers, as with the sample recording 1.3 TU of tritium, with its highly weathered and thus permeable nature, seem to record the more ongoing, but lesser recharge events.

8.3 Origin

Despite the great complexity of different components of the hydrological cycle, oxygen and hydrogen isotope labels are generally very conservative underground, once the water has recharged beyond a few metres depth in an aquifer (Weaver *et al*., 2007). As such, they form unique characteristic groundwater tracers that can provide information about the origin and movement of groundwater and its dissolved constituents, allowing for the quantitative evaluation of mixing of different groundwater components (Weaver *et al*., 2007). Variations in the stable isotope compositions of oxygen and hydrogen in the groundwater can also be used to describe the numerous physical processes to which the water has been subjected during the course of the hydrological cycle, prior to recharge.

There are numerous physical processes associated with the hydrological cycle which produce variations in the isotopic compositions of oxygen and hydrogen, namely diffusion, evaporation, condensation, melting etc. (Geyh, 2001). For most of the physical processes listed above, ^{18}O and deuterium variations occur in parallel, resulting in a fixed relation of 8 between the deuterium and ^{18}O isotope ratios in the water, resulting in the Global, or else Local Meteoric Water Lines. According to Craig (1961), this correlation can be expressed as: $\delta D = 8\delta^{18}O + 10$ ‰. This relationship can also be presented in a more generalised expression as: $\delta D = s\ \delta^{18}O + d$, where '*s*' is the slope and '*d*' is the deuterium excess (*d*-excess). The slope '*s'* depends on many factors, but most importantly on the relative humidity of vapour source, evaporation and mixing. By contrast, the *d*-excess is an important parameter in describing the relative magnitude of kinetic fractionation and has been used extensively for investigation of recharge pathways, flow regimes and correlating groundwater with palaeo-climate

(Gupta and Deshpande, 2005). Given the above relationships, it proves useful to plot the $\delta^{18}O$ and δD values of the sampling points, as it provides insight into the numerous physical processes to which the groundwater has been subjected.

A plot of the $\delta^{18}O$ and δD values for the samples collected (Figure 8.1), reveals three fundamental groups - those data points that plot along the local meteoric water line, those that plot below the meteoric water line along an evaporation trend line of gentler slope than that of the PLMWL and those samples that plot below the evaporation trend line. One sample (KAL 014) was found to have an enriched isotopic signature that plots above the meteoric water line. According to Kendall and McDonnel (1998), it is rare to find precipitation or groundwater that plots above the LMWL. The re-evaporation of precipitated water under low-humidity regions is thought to create vapour masses with an isotopic content that plots above the LMWL.

The first group of sampling points that plot along the local meteoric water line represent groundwater which is isotopically similar to that of present meteoric water, confirming the validity of using the PLMWL as a reference for interpretation of the stable isotopic variations of groundwater in the study area. While some of these samples comprise higher tritium values (0.7 – 1.3 TU), which is indicative of more recent recharge, others reveal zero tritium content (Figure 8.2). This suggests that the stable isotope composition of precipitation in the study area has remained relatively constant over the last few decades, having been precipitated during similar climatic conditions to those prevailing at present.

In arid regions evaporation is regarded as one of the most significant physical processes influencing the isotopic composition of groundwater prior to recharge. Its influence on the groundwater in this semi-arid region can be seen from those samples plotting below the local meteoric water line, along a trend line of gentler slope. In general, evaporation of water from open water bodies, such as lakes, pans, rivers, and the like, results in enrichment (i.e. increase) of both isotope ratios of the water remaining in the reservoir, because the heavier isotopes preferentially tend to stay with the more condense phase in any fractionation process (Gupta and Deshpande, 2005). A plot of δD versus $\delta^{18}O$ will, therefore, show a gentler slope relative to the LMWL, generally of gradient 4 to 6, and is a relatively easy means by which evaporating water can readily be identified (Weaver *et al*., 2007). Taking all into consideration, the environmental isotope signature of the study area indicates an evaporation effect, with most of the samples falling on an evaporation trend line of slope 4.9 (Figure 8.1), a trend which has been observed in numerous cases elsewhere in the Kalahari (Verhagen, 1984; Verhagen, 2013). It can, therefore, be assumed that significant portions of the study area have been recharged from precipitation that has undergone evaporation prior to infiltration. The evaporation effect could also be due to near-surface evaporation during the natural recharge processes.

The third group of sampling points exhibit isotopic signatures that plot below the evaporation trend line. Their stable isotopic contents diverge clearly from that of recent precipitation. The evaporation effect seems to be lower for these samples, as indicated by the lower spread of the d-excess values for these samples (10.75 – 12.30 ‰, Table 8.1). This lower spread of d-excess values would have been caused by variations in the air circulation pattern and rainout regime prevailing at the time (Froehlich *et al*., 2007).

8.4 Geology and Aquifer Connectivity

Isotope exchange between groundwater and minerals at temperatures of common, non-thermal groundwater bodies is slow, with water-rock interactions occurring during groundwater recharge within days/weeks and during flow in the aquifer within years to even millions of years (Geyh, 2001). Chemical data, in combination with isotopic data, can therefore be used to distinguish between different aquifer types, with environmental isotopes being used extensively to address the dynamics and interconnections of groundwater systems (Geyh, 2001).

Based on the hydrochemical analyses, the groundwater in the study area can quite easily be linked to the five distinct aquifer types (Section 5.1) from which the water was extracted, with some degree of mixing between the various water types. This classification can also be verified in certain places by the environmental isotopic data (Figure 8.3). In general, the unconfined Kalahari Group of sediments, which are characterised by highly mineralised (Na – Cl dominant) groundwater, typically have isotopic ratios that exhibit extensive evaporation, with water characterised by limited recharge from recent rainfall (0 – 0.7 TU). In particular, an area to the north and west of the study area has been identified, where the Kalahari sequence is at its thickest (> 90 m), which records the highest salinities, in addition to the most enriched isotopic signatures ($\delta^{18}O$ > -3.7 ‰; Table 8.1). The second group of aquifers, which are associated with the Transvaal meta-sediments, define a narrow range of $\delta^{18}O$ values (-5.64 – -5.66 ‰) in places, which suggests good water exchange and permeability within the aquifer. Their stable isotopic contents are relatively depleted and diverge clearly from that of recent precipitation (Figure 8.3).

The isotopic data for the karstic aquifers (Campbell Rand dolomites) do not show a clear trend, with many of the $\delta^{18}O$ and δD values spread over the entire range, with some samples plotting above the PLMWL, some plotting below the meteoric water line and others along the evaporation trend line (Figure 8.3). Their tritium contents are also highly variable (0 – 0.9 TU). This suggests poor water exchange and permeability within the aquifer, which may largely be attributed to major structural deformations (faulting) and intrusions (dykes), as well as impervious sedimentary layers (carbonaceous shale and quartzite), within the limestones and dolomites. These structural features are notoriously known to divide this hydrogeological unit into semi-autonomous groundwater units or "compartments", which may differ significantly with regard to their isotopic signature.

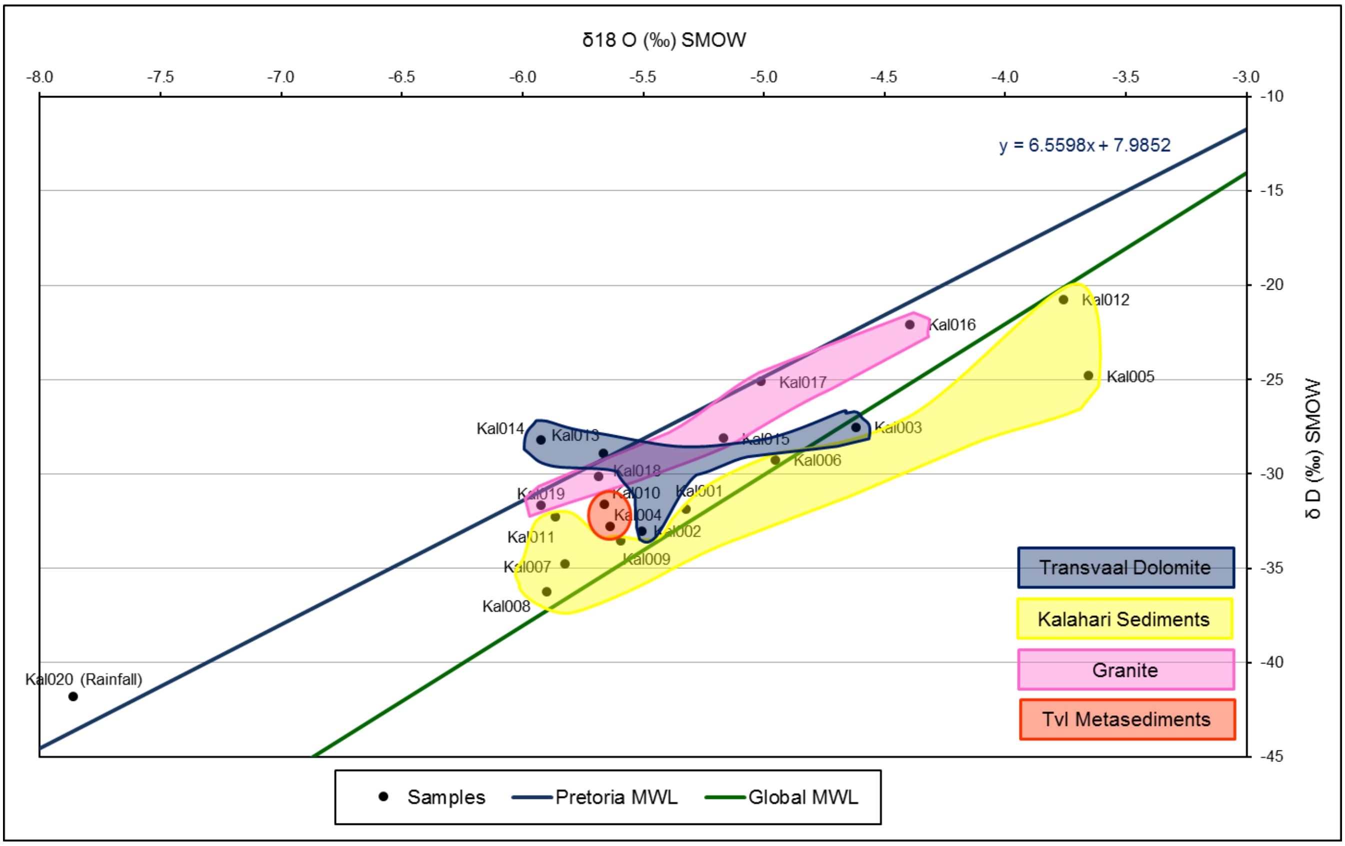

Figure 8.3: Plot of $\delta^{18}O$ versus δD for the samples collected, linked to the various aquifer types

The fourth aquifer type, which is associated with the weathered and fractured zone of the Archaean granites, is also typically characterised by relatively depleted isotopic signatures ($\delta^{18}O$ < -4.39 ‰), that plot on or close to the local meteoric water line (Figure 8.3). The fact that some of the groundwater sampled from these weathered aquifers recorded zero tritium may indicate that the weathered zone is not necessarily connected with the surface alluvium in places, with groundwater possibly sourced from deeper fracture zones, which have had much longer residence times. The basement aquifers (Kraaipan - Amalia greenstone assemblages and Ventersdorp Supergroup) to the east of the study area, also seem to be characterised by old groundwater, with long residence times that have not particularly been subject to evaporation.

The comparison of the stable isotope signature between the various regions emphasises the influence of local geographic and physiographic conditions on the stable isotope composition of the groundwater. This regional dependence of stable isotope data has been observed during numerous studies undertaken across the Kalahari region (SGAB, 1988; Geoflux, 1993; WCS, 1993; BRGM, 1993; Verhagen, 2013). While this classification can often be verified in certain places by the environmental isotopic data, the latter does not always show clear contrasts between different lithological units, as with the Campbell Rand dolomites. The frequency distribution of $\delta^{18}O$ values in the project area is shown in Figure 8.4, with the lithological associations of the samples also shown in the histogram. The range of $\delta^{18}O$ values shown is relatively narrow, which is striking given the extent of the project area. The distribution can be seen as uni-modal, with the maximum lying between -5.8 ‰ and -5.9 ‰. The isotopic data does not show clear contrasts between the different lithological units, with many of the $\delta^{18}O$ values for a particular lithology being spread over the entire range. This leads to the conclusion that the $\delta^{18}O$ values are controlled more by physiographic differences and variable rainfall selectivity, than by lithology. It also suggests that the various recharge points are not very far apart (given the limited range of $\delta^{18}O$ values), possibly taking place from the surrounding high ground, where surface and structural controls are responsible for the regional hydraulic continuity.

This is further confirmed by the tritium values observed throughout the study area. Within the study area, there are examples in which the tritium values recorded for samples sourced from both the deeper and shallower drilled holes both proved to be zero. In addition, samples collected from different boreholes sited within the same lithological unit have recorded very different tritium values, some showing zero tritium and others showing a degree of mixing with younger groundwater. This suggests that the aquifers are not exclusively controlled by lithology, but rather by structural controls allowing some aquifers to be hydraulically connected.

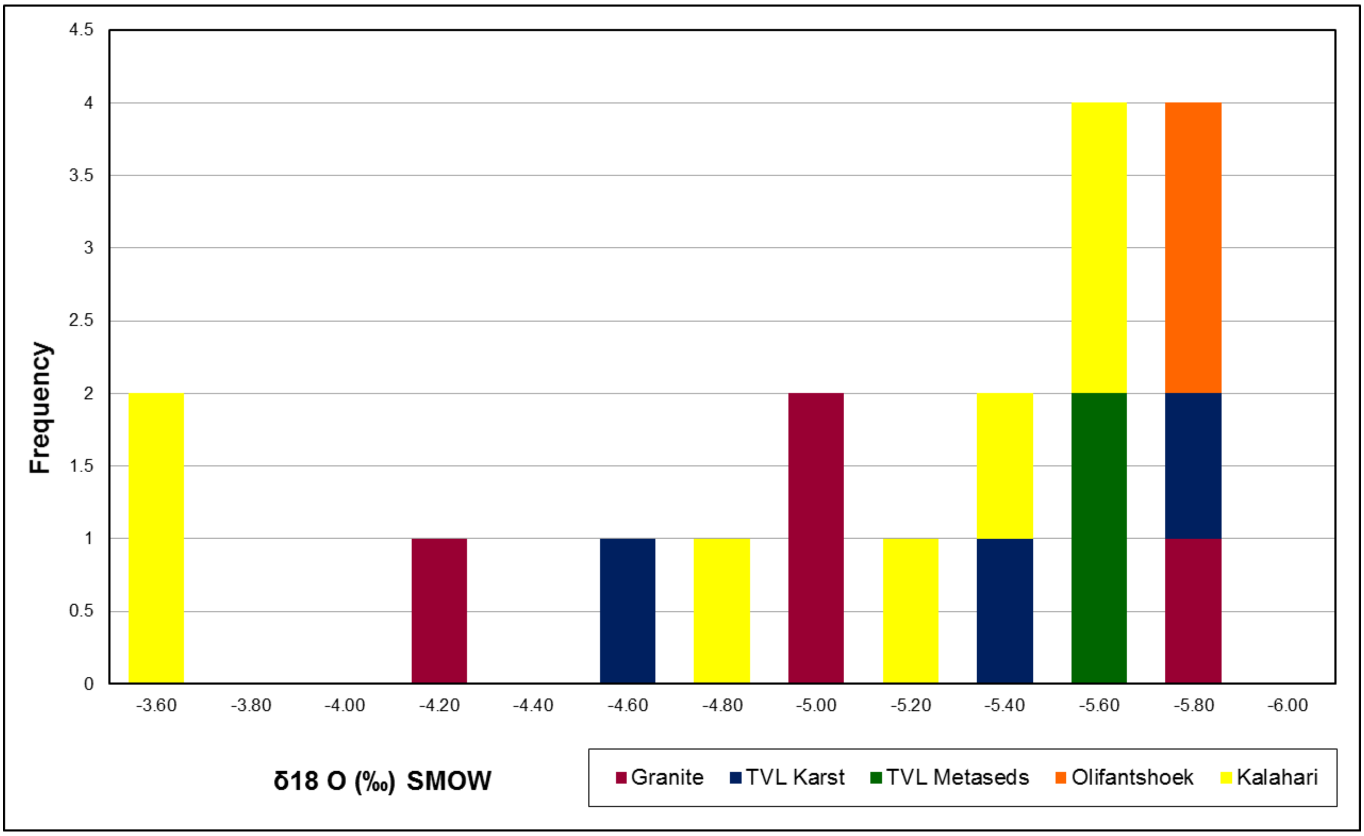

Figure 8.4: The frequency distribution of $\delta^{18}O$ values in the project area relative to the various lithological units encountered

8.5 Recharge

A lively debate has continued for almost a century regarding the question of whether the Kalahari aquifers are being replenished at all under present climatic conditions. Environmental tracer studies and groundwater flow modelling along the eastern fringe of the Kalahari (De Vries *et al*. 2000) have indicated that present-day recharge is taking place in the order of 5 mm/yr, where annual rainfall is between 300 - 400 mm. Figures in the order of 1 mm were obtained from the central Kalahari, which is characterised by lower precipitation values of 100 mm/yr (De Vries *et al*., 2000). Since no clear changes in morphological conditions could account for this different recharge rate, it was suggested that the decrease in recharge reflects the rainfall pattern, which decreases from about 450 mm at the edge of the Kalahari to less than 350 mm in the centre.

Situated on the southern fringe of the greater Kalahari basin, with an average rainfall of between 350 - 450 mm (Section 9.2.1), it can be expected that the study area will also reflect similar recharge rates of between 1 mm to 5 mm per year. An attempt to estimate the recharge rates in the study area is presented in Section 9.2. What is known from the environmental isotope data is that a small degree of modern recharge has taken place in some portions of the study area. Those samples recording tritium values equal to and greater than 0.8 TU suggest mixing of groundwater of differing isotopic composition, implying a small component of modern recharge. Many of the samples, however, record negligible tritium, indicating the absence of modern recharge in these areas.

Isotopic indications are that recharge events in the study area are most probably episodic, both in terms of recent recharge (of the order of several decades) and major recharge inputs (pluvial periods). In particular, this is confirmed by samples collected from different boreholes sited within the same lithological unit which record very different tritium values, some showing zero tritium, while others show a degree of mixing.

In addition to the rate of recharge, isotope techniques also provide one of the best approaches that can be used to determine the area of recharge, providing critical information for the management of groundwater resources (Geyh, 2001). On a regional scale, the natural variation of the environmental isotope composition of ^{18}O and ^{2}H, taking the tritium content into consideration as well, has defined numerous areas which have differing potential of being recharge areas (Figure 8.5).

Within the study area, many of the samples that plot below the local meteoric water line along an evaporation trend line are largely restricted to the north-north western part of the study area, north of the resistant ridge of Asbestos Hill's iron formations. As such, it can be assumed that much of the groundwater associated with this area, which is dominated by thick successions of Kalahari sediments, has been recharged from precipitation that has undergone evaporation prior to infiltration. Much of this recharge can be associated with evaporated salt pans, which are common in this portion

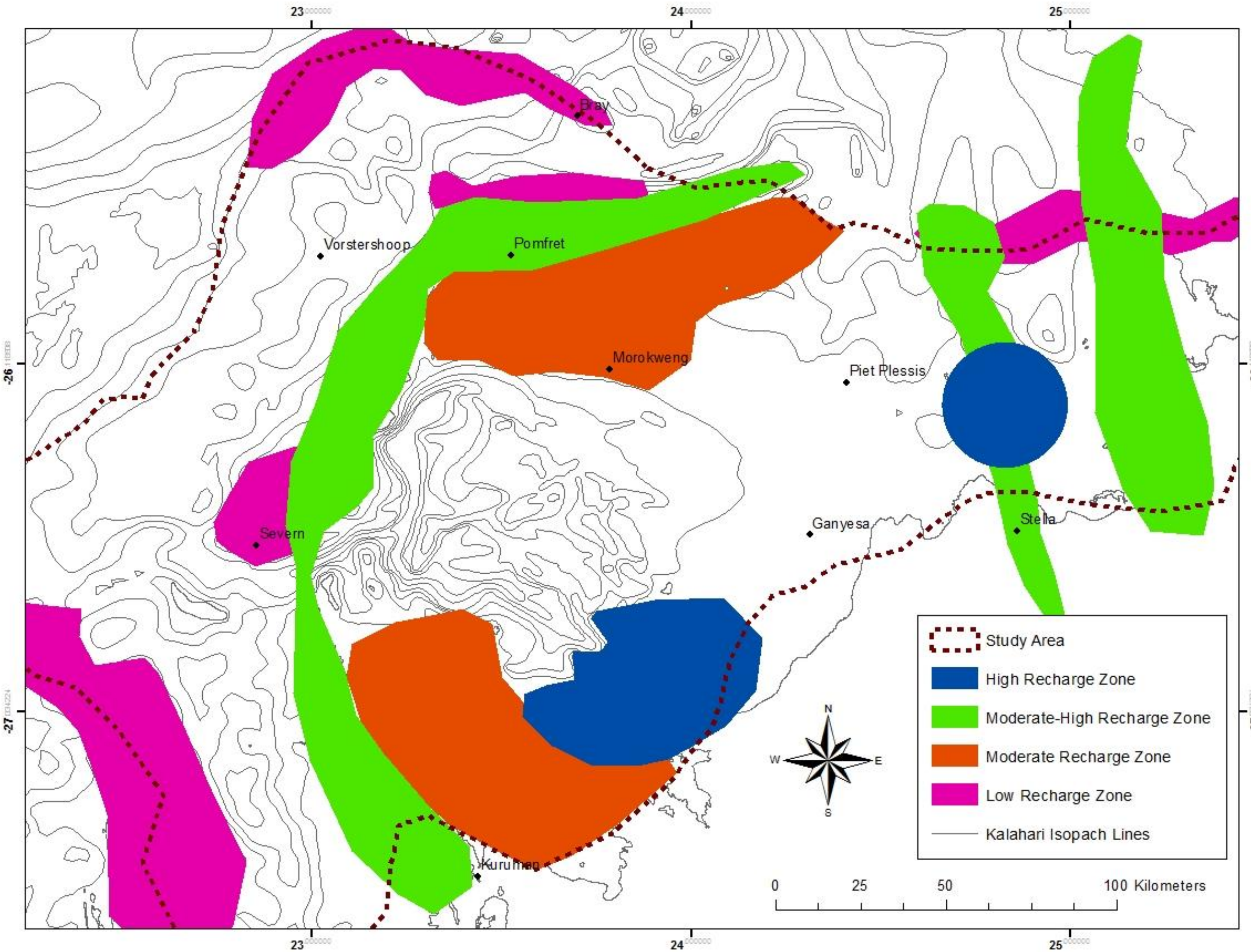

Figure 8.5: Potential areas of recharge based on the environmental isotope data collected for the region

of the Kalahari, given the high chloride concentrations recorded for this region (Section 6.6). It is firmly believed, however, given the zero to low tritium values recorded, that little to no recharge is occurring in this area, particularly in those areas where the Kalahari sediments are at their thickest (Figure 8.5). What precipitation there might be, will be depleted through transpiration by deep rooting *Acacias* from depths of tens of metres. In addition, water losses from greater depths (up to 20 m) by capillary transport may occur from perched water tables in areas of enhanced recharge, such as depressions and fractured duricrust surfaces (De Vries *et al*., 2000).

A more likely source of recharge in this region is restricted to a narrow zone (Figure 8.5) adjacent to the Molopo River, where groundwater is recharged following flood events. Following flooding, the flow of water in the Molopo River eventually stagnates, with the water ultimately drying up through extensive evaporation and seepage underground. The influence of the Molopo River and its tributaries on the groundwater in the region, however, is relatively isolated. Numerous samples collected adjacent to the Molopo River and its tributaries have recorded zero tritium content, suggesting that groundwater recharge in these areas have not occurred during a recent flooding event (early 2014 – last recorded flow event), but rather points to an older recharge event that underwent evaporation prior to infiltration. A similar situation was noted in the Palla Road region of Botswana (Verhagen, 2013), with the stable isotope data suggesting recharge mainly through non-vadose processes, such as occasional flooding of a neighbouring river bed or overland sheet flow during exceptional rainfall events.

The isotopic signature of the Transvaal meta-sediments (shales and BIFS) reflect a more restricted recharge regime. In particular, the relatively narrow range (-5.64 – -5.93 ‰) of $\delta^{18}O$ values seems to suggest that the various recharge points are not very far apart, possibly taking place from the surrounding high ground, where surface and structural controls are responsible for the regional hydraulic continuity. The isotopic data also seems to signify direct recharge from precipitation with minimal impact from evaporative fractionation. The availability of fractures allows for fast percolation of rainwater prior to the modification of its isotopic composition. Given the similarities between this hydrogeological unit and that of the Kraaipan - Amalia greenstone terrane (Section 5.1), it may be assumed that the latter is similarly recharged.

Isotopic evidence suggests that recharge to the karstic aquifers is taking place, with tritium values ranging from 0 to 0.9 TU. The higher tritium samples (> 0.9 TU) with depleted $\delta^{18}O$ signatures are indicative of more recent recharge, with groundwater flow within the karstic aquifers having responded quickly to precipitation. Those samples with lower tritium values (0 TU), some of which have an evaporative $\delta^{18}O$ signature, may be indicative of base flow within the aquifer, which typically exhibits much longer mean residence times. Although there is isotopic evidence of recharge within this hydrogeological unit, this particular aquifer does not display hydraulic continuity, both within the aquifer nor with adjacent aquifers. The near-surface vertical and sub-vertical fractures associated with the

Transvaal meta-sediments and the Kraaipan - Amalia greenstone terrane, typically provide recharge to both the underlying and adjacent aquifers. This is not true of the karstic aquifers, the “compartmentalisation” of which means that recharge is site specific, the rate and amount depending on the structural controls of that particular compartment.

Samples to the south and east of the study area have a broad range of isotopic signatures that seem to plot along or close to the PLMWL (Figure 8.3). Given this, it is understood that these samples to the south of the study area did not undergo extensive evaporation and may indicate fast recharge through vertical fractures or through highly permeable media (Figure 8.5). The highly fractured and weathered granite basement in the area may account for the relatively fast rate of recharge, with very little associated evaporation. This is typically seen in the sample located within the Mosita granite, which points to rapid recharge from recent precipitation (tritium content of 1.3 TU). Some samples located within the basement granites, however, recorded zero tritium content. These results indicate that the granites may be considered as completely mixed reservoirs. Their isotopic distribution reflects the geological structure and morphology, as tectonic zones and faults act as regional groundwater drainage systems (Geyh, 2001).

Taking all into consideration, the environmental isotope signatures have indicated that much of the study area has been recharged from numerous rainfall events, many of which have not been recent. Recharge to the confined systems (Transvaal meta-sediments and basement granites) has taken place quickly after heavy rains in the recharge areas, without substantial evaporation, while the recharge to the unconfined aquifers of the Kalahari Group has been generally slower and often accompanied by extensive evaporation.

9. GROUNDWATER POTENTIAL

Groundwater occurrence depends primarily on geology, geomorphology/weathering and effective rainfall (both current and historic). The interplay of these three factors give rise to complex hydrogeological environments with innumerable variations in aquifer transmissivity, effective porosity, saturated thickness and groundwater recharge (MacDonald *et al*., 2012). The careful characterisation of these specific hydrogeological units within the study area (Section 5) has allowed for the quantitative calculation of groundwater storage and recharge within this arid region, the details of which are discussed below. These calculations provide a realistic assessment of water security and water stress in the area, guiding investments in water supply and allowing the resource to be managed by minimising environmental degradation and widespread depletion (MacDonald *et al*., 2012).

9.1 Groundwater Storage

Estimates of the volume of groundwater held in storage were made for each hydrogeological unit (See Section 2.7), the details of which are provided in Table 9.1, with a quantitative map of aquifer storage for the entire study area presented in Figure 9.1.

The interpretation of the overall aquifer storage map generated (Figure 9.1) is quite difficult, as the Kalahari sediments, which vary considerably in thickness throughout the study area, are eroded into and superimposed over many portions of the other hydrogeological units. As such, certain aquifer types play a role at a specific depth, however, where covered in places by thick Kalahari sediments they do not contribute at all to the groundwater storage at that specific depth. Given this, it was decided to calculate the groundwater storage for the study area in 30 m depth intervals (Table 9.2 A - H), establishing which of the hydrogeological units contribute to groundwater storage at that specific depth interval. The maps of aquifer storage for each of the 30 m depth intervals are shown in Figure 9.2 (A - H). Three geological cross sections (Figures 5.9 A, B and C) were also constructed across the study area, allowing for the distribution of each hydrogeological unit to be visualised with depth.

Table 9.1: The storage volume calculated for the various lithological units

Lithostratigraphic Domain	Lithology	Total Area (km^2)	Average Water Level (mbgl)	Average Aquifer Base (mbgl)	Saturated Thickness (m)	Storativity/ Specific Yield	Volume Groundwater Stored in aquifer		
							Total (Mm^3)	Unit (m^3/km^2)	% Total Volume
Kalahari	Sandstone	18973.24	92.25	150.00	57.75	0.005	5478.52	288750.00	43.26%
Dwyka	Tillite	7788.80	101.15	225.00	123.85	0.0002	192.93	24770.00	1.52%
Olifantshoek	Quartzites	4819.63	84.45	175.00	90.55	0.0007	305.49	63385.00	2.41%
Ventersdorp	Andesite/Quartz Porphyry	1609.43	17.28	45.00	27.72	0.0004	17.85	11088.00	0.14%
Transvaal	Shale/BIF	3194.76	64.39	120.00	55.61	0.0009	159.89	50049.00	1.26%
Transvaal	Andesite	5344.14	83.47	225.00	141.53	0.0004	302.54	56612.00	2.39%
Transvaal	Dolomite	8758.74	25.33	180.00	154.67	0.002	2709.43	309340.00	21.40%
Archaean Basement	Granite (Weathered)	15498.43	28.11	90.00	61.89	0.003	2877.59	185670.00	22.72%
Archaean Basement	Granite (Fractured)	19628.80	90.00	240.00	150.00	0.0002	588.86	30000.00	4.65%
Kraaipan - Amalia	Meta-arenaceous sediments	1006.34	29.59	105.00	75.41	0.0004	30.36	30164.00	0.24%
TOTAL		**86622.32**					**12663.47**	**104982.80**	**100.00%**

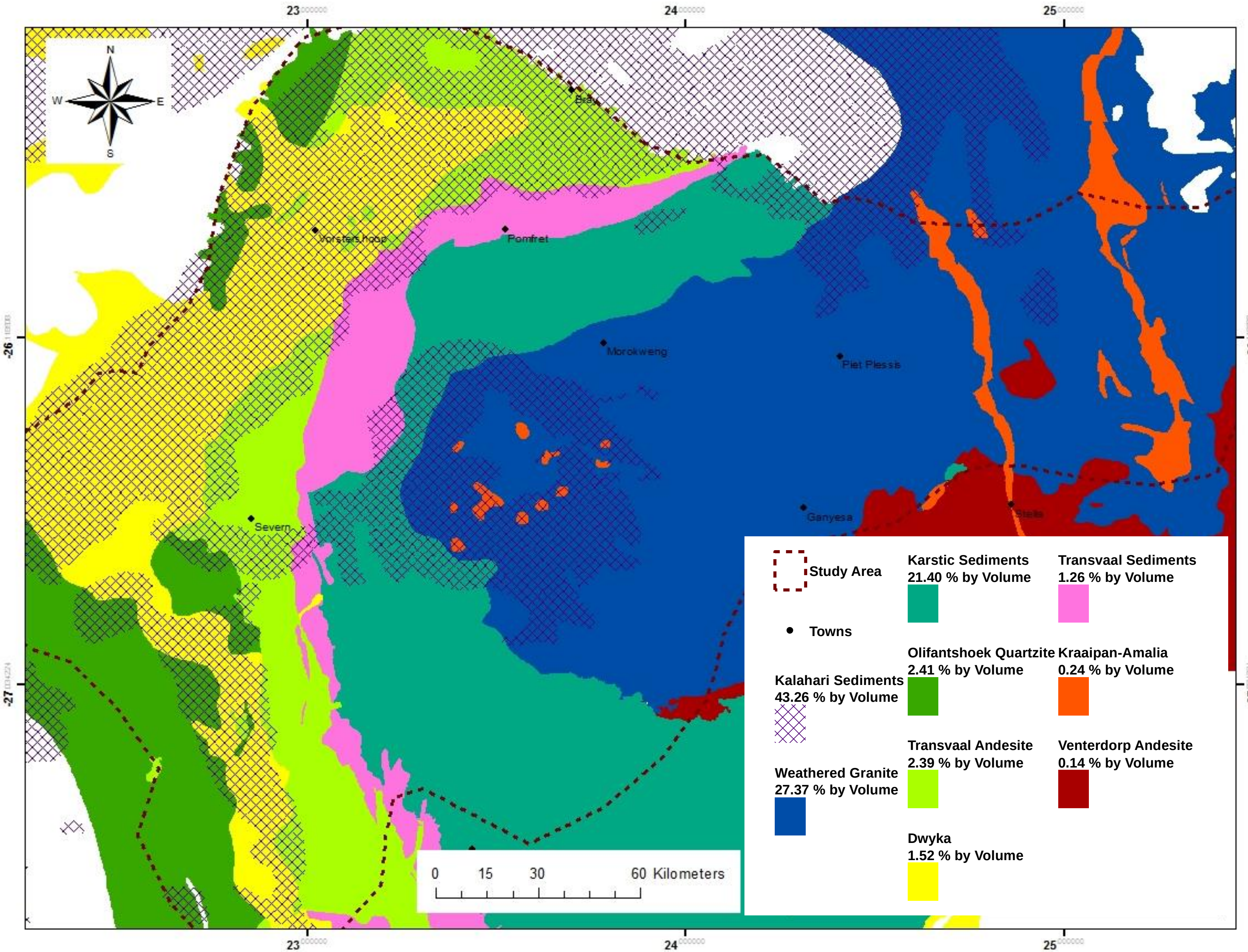

Figure 9.1: The percent by volume held in storage by the respective hydrogeological units

(A)

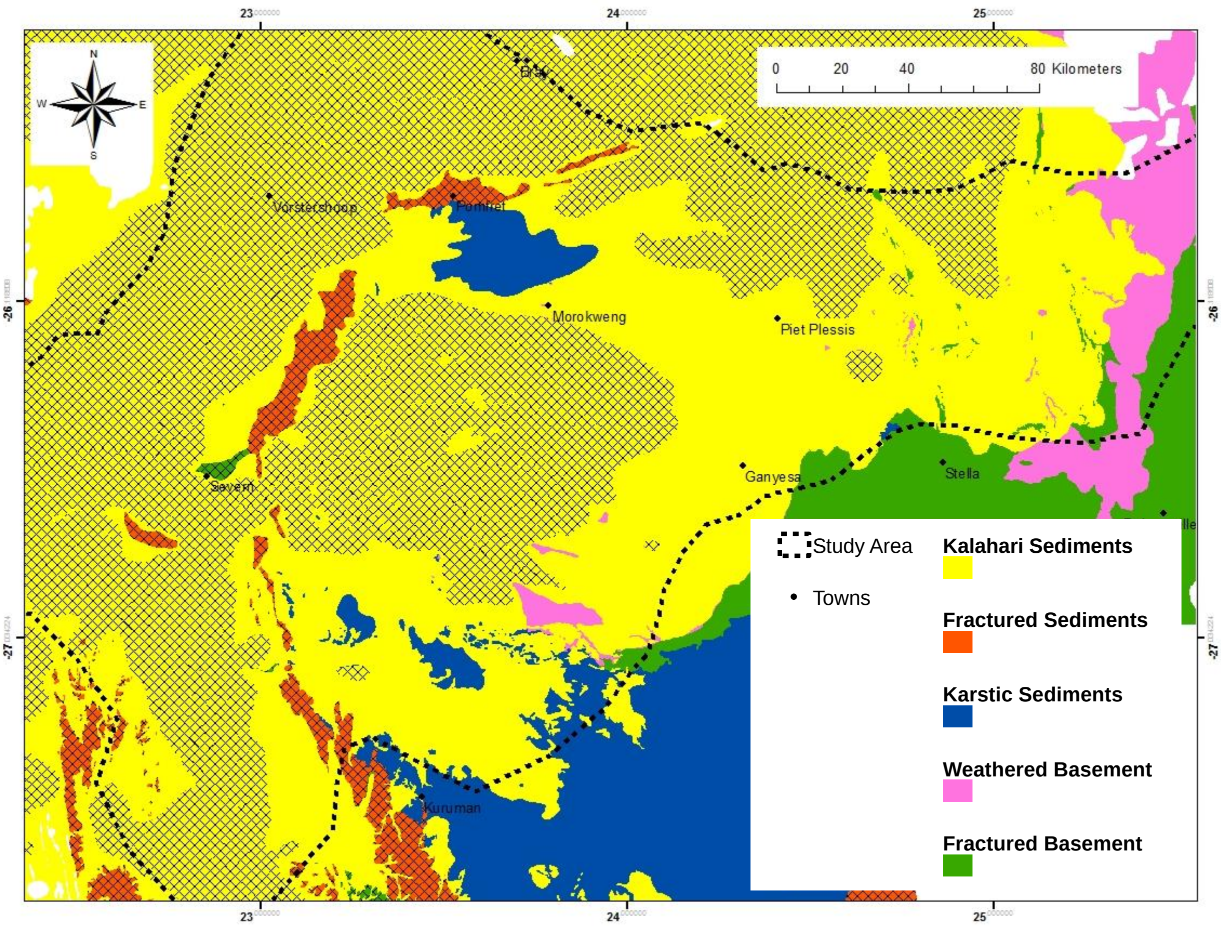

Figure 9.2 (A): 0 – 30 m Aquifer storage map. Crosshatched areas are not saturated at this specific depth interval

Depth Interval	Lithostratigraphic Domain	Lithology	Total Area (km^2)	Average Water Level (mbgl)	Average Aquifer Base (mbgl)	Saturated Thickness (m)	Storativity/ Specific Yield	Volume Groundwater Stored in Aquifer		
								Total (Mm^3)	Unit (m^3/km^2)	% Total Volume
0 - 30 metres	Kalahari	Sandstone	17492.53	17.64	30.00	12.36	0.005	1081.04	61800.00	96.92%
	Dwyka	Tillite	-	-	30.00	0.00	0.0002	0.00	0.00	0.00%
	Olifantshoek	Quartzites	145.84	-	30.00	0.00	0.0007	0.00	0.00	0.00%
	Ventersdorp	Andesite/Quartz Porphyry	1420.23	17.28	30.00	12.72	0.0004	7.23	5088.00	0.65%
	Transvaal	Shale/BIF	1152.50	-	30.00	0.00	0.0009	0.00	0.00	0.00%
	Transvaal	Andesite	53.74	-	30.00	0.00	0.0004	0.00	0.00	0.00%
	Transvaal	Dolomite	1783.80	25.33	30.00	4.67	0.002	16.66	9340.00	1.49%
	Archaean Basement	Granite (Weathered)	1833.17	28.11	30.00	1.89	0.003	10.39	5670.00	0.93%
	Archaean Basement	Granite (Fractured)	-	-	30.00	0.00	0.0002	0.00	0.00	0.00%
	Kraaipan - Amalia	Meta arenaceous sediments	272.75	29.59	30.00	0.41	0.0004	0.04	164.00	0.00%
	TOTAL		**24154.56**					**1115.36**	**8206.20**	**100.00%**

Table 9.2 (A): The storage volume calculated for the various lithological units within the depth interval 0 – 30m

(B)

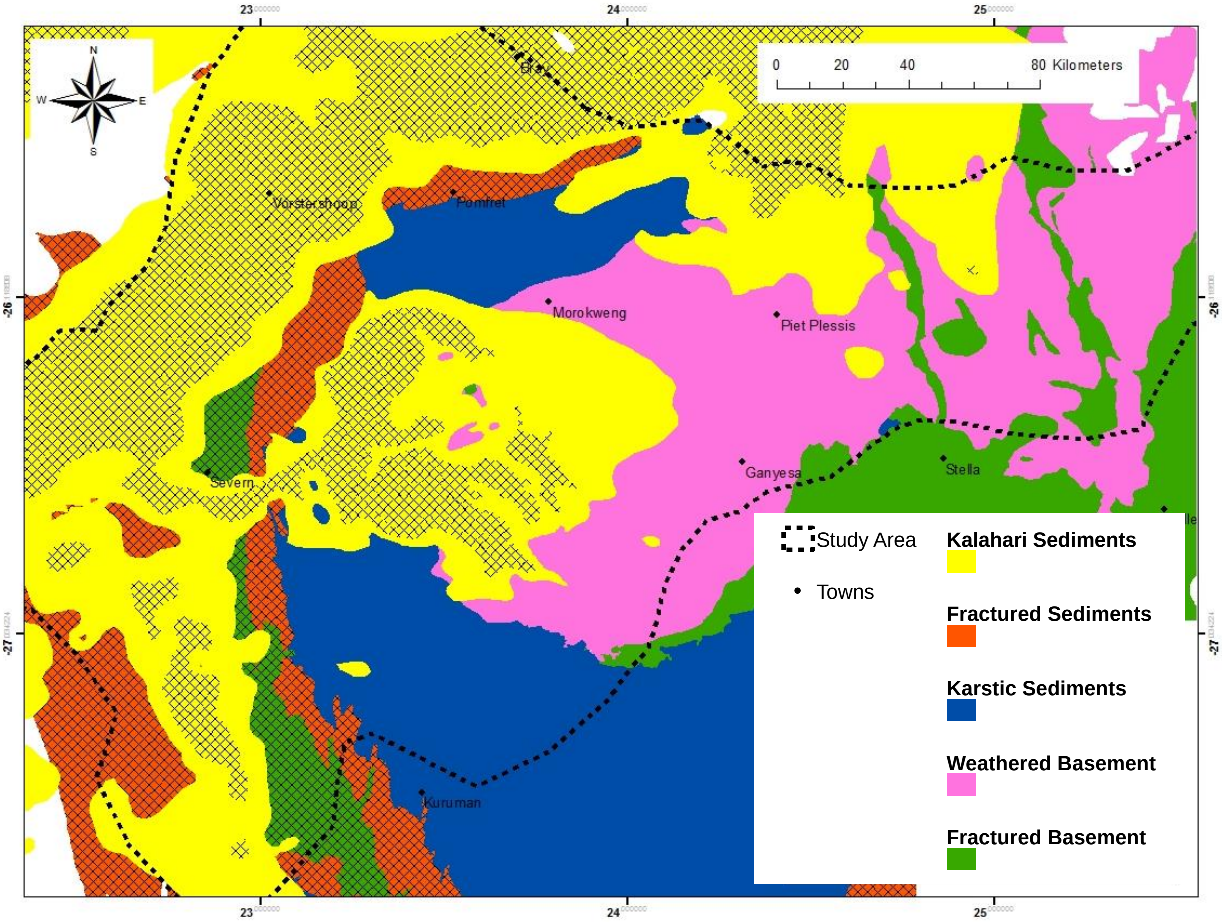

Figure 9.2 (B): 30 – 60 m Aquifer storage map. Crosshatched areas are not saturated at this specific depth interval

Depth Interval	Lithostratigraphic Domain	Lithology	Total Area (km^2)	Average Water Level (mbgl)	Average Aquifer Base (mbgl)	Saturated Thickness (m)	Storativity/ Specific Yield	Volume Groundwater Stored in Aquifer		
								Total (Mm^3)	Unit (m^3/km^2)	% Total Volume
30 - 60 metres	Kalahari	Sandstone	15286.72	33.31	60.00	26.69	0.005	2040.01	133450.00	57.98%
	Dwyka	Tillite	-	-	60.00	0.00	0.0002	0.00	0.00	0.00%
	Olifantshoek	Quartzites	1110.05	-	60.00	0.00	0.0007	0.00	0.00	0.00%
	Ventersdorp	Andesite/Quartz Porphyry	1609.43	30.00	45.00	15.00	0.0004	9.66	6000.00	0.27%
	Transvaal	Shale/BIF	1981.00	-	60.00	0.00	0.0009	0.00	0.00	0.00%
	Transvaal	Andesite	1349.97	-	60.00	0.00	0.0004	0.00	0.00	0.00%
	Transvaal	Dolomite	6154.04	30.00	60.00	30.00	0.002	369.24	60000.00	10.50%
	Archaean Basement	Granite (Weathered)	12080.47	30.00	60.00	30.00	0.003	1087.24	90000.00	30.90%
	Archaean Basement	Granite (Fractured)	-	-	60.00	0.00	0.0002	0.00	0.00	0.00%
	Kraaipan - Amalia	Meta arenaceous sediments	1006.34	30.00	60.00	30.00	0.0004	12.08	12000.00	0.34%
	TOTAL		**40578.01**					**3518.23**	**30145.00**	**100.00%**

Table 9.2 (B): The storage volume calculated for the various lithological units within the depth interval 30 – 60m

(C)

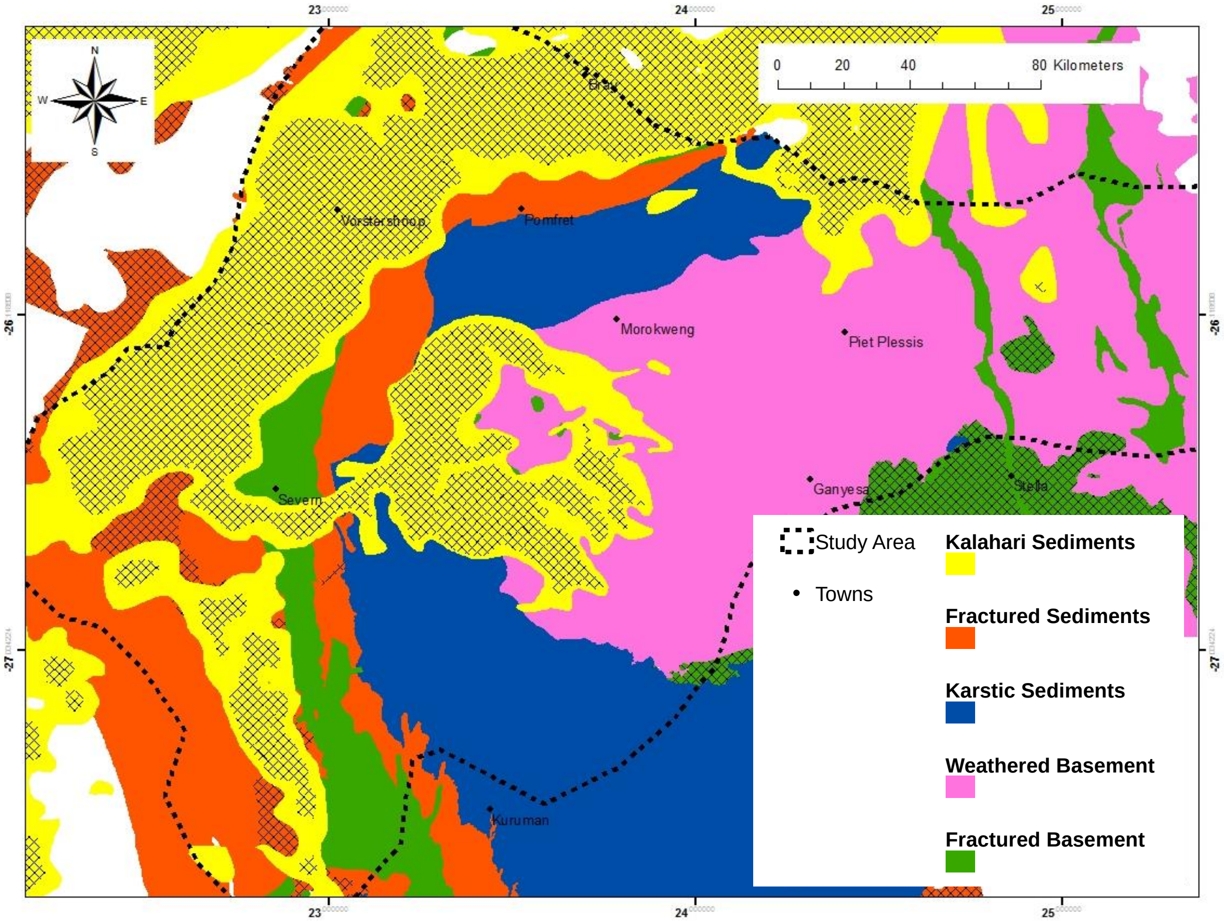

Figure 9.2 (C): 60 – 90 m Aquifer storage map. Crosshatched areas are not saturated at this specific depth interval

Depth Interval	Lithostratigraphic Domain	Lithology	Total Area (km^2)	Average Water Level (mbgl)	Average Aquifer Base (mbgl)	Saturated Thickness (m)	Storativity/ Specific Yield	Volume Groundwater Stored in Aquifer		
								Total (Mm^3)	Unit (m^3/km^2)	% Total Volume
60 - 90 metres	Kalahari	Sandstone	6831.64	60.00	90.00	30.00	0.005	1024.75	150000.00	35.29%
	Dwyka	Tillite	600.54	-	90.00	0.00	0.0002	0.00	0.00	0.00%
	Olifantshoek	Quartzites	2688.79	84.45	90.00	5.55	0.0007	10.45	3885.00	0.36%
	Ventersdorp	Andesite/Quartz Porphyry	-	-	90.00	0.00	0.0004	0.00	0.00	0.00%
	Transvaal	Shale/BIF	2492.95	64.39	90.00	25.61	0.0009	57.46	23049.00	1.98%
	Transvaal	Andesite	2269.21	83.47	90.00	6.53	0.0004	5.93	2612.00	0.20%
	Transvaal	Dolomite	6839.03	60.00	90.00	30.00	0.002	410.34	60000.00	14.13%
	Archaean Basement	Granite (Weathered)	15362.36	60.00	90.00	30.00	0.003	1382.61	90000.00	47.62%
	Archaean Basement	Granite (Fractured)	-	-	90.00	0.00	0.0002	0.00	0.00	0.00%
	Kraaipan - Amalia	Meta arenaceous sediments	1006.34	60.00	90.00	30.00	0.0004	12.08	12000.00	0.42%
	TOTAL		**38090.85**					**2903.61**	**34154.60**	**100.00%**

Table 9.2 (C): The storage volume calculated for the various lithological units within the depth interval 60 – 90m

(D)

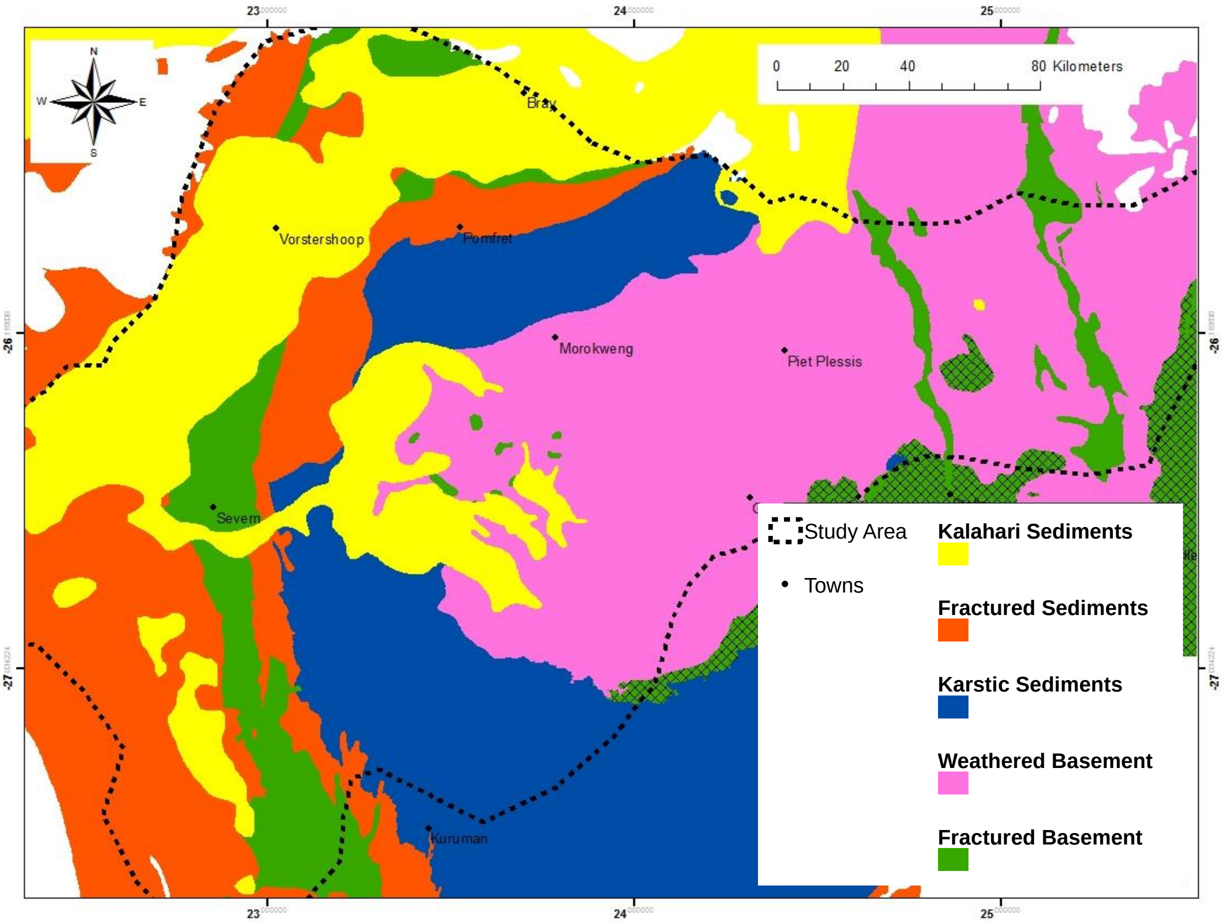

Figure 9.2 (D): 90 – 120 m Aquifer storage map. Crosshatched areas are not saturated at this specific depth interval

Depth Interval	Lithostratigraphic Domain	Lithology	Total Area (km^2)	Average Water Level (mbgl)	Average Aquifer Base (mbgl)	Saturated Thickness (m)	Storativity/ Specific Yield	Volume Groundwater Stored in Aquifer		
								Total (Mm^3)	Unit (m^3/km^2)	% Total Volume
90 - 120 metres	Kalahari	Sandstone	11301.99	90.00	120.00	30.00	0.005	1695.30	150000.00	69.01%
	Dwyka	Tillite	2086.01	101.15	120.00	18.85	0.0002	7.86	3770.00	0.32%
	Olifantshoek	Quartzites	4348.16	90.00	120.00	30.00	0.0007	91.31	21000.00	3.72%
	Ventersdorp	Andesite/Quartz Porphyry	-	-	120.00	0.00	0.0004	0.00	0.00	0.00%
	Transvaal	Shale/BIF	2785.47	90.00	120.00	30.00	0.0009	75.21	27000.00	3.06%
	Transvaal	Andesite	3546.65	90.00	120.00	30.00	0.0004	42.56	12000.00	1.73%
	Transvaal	Dolomite	7304.13	90.00	120.00	30.00	0.002	438.25	60000.00	17.84%
	Archaean Basement	Granite (Weathered)	-	-	120.00	0.00	0.003	0.00	0.00	0.00%
	Archaean Basement	Granite (Fractured)	16674.70	90.00	120.00	30.00	0.0002	100.05	6000.00	4.07%
	Kraaipan - Amalia	Meta arenaceous sediments	1006.34	90.00	105.00	15.00	0.0004	6.04	6000.00	0.25%
	TOTAL		**49053.45**					**2456.58**	**28577.00**	**100.00%**

Table 9.2 (D): The storage volume calculated for the various lithological units within the depth interval 90 – 120m

(E)

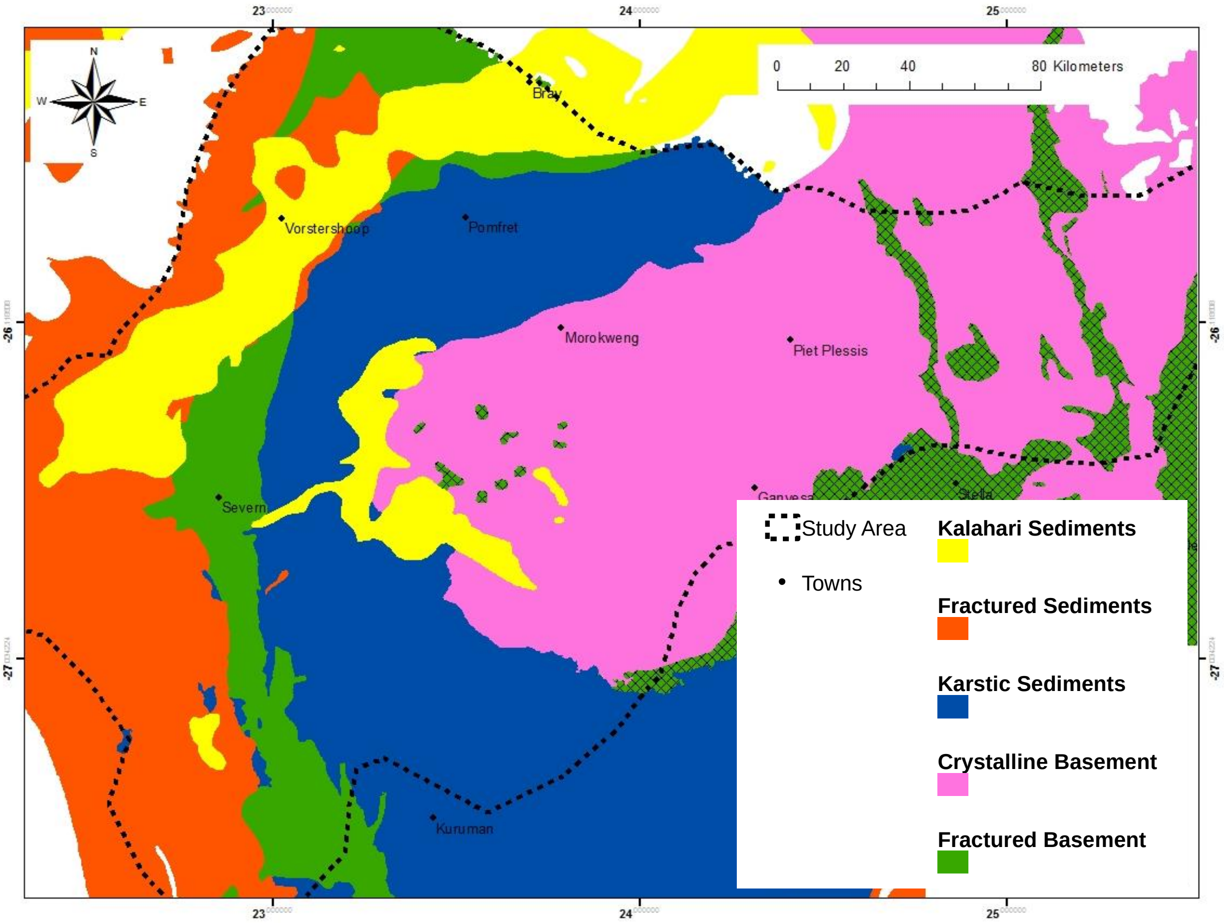

Figure 9.2 (E): 120 – 150 m Aquifer storage map. Crosshatched areas are not saturated at this specific depth interval

Depth Interval	Lithostratigraphic Domain	Lithology	Total Area (km^2)	Average Water Level (mbgl)	Average Aquifer Base (mbgl)	Saturated Thickness (m)	Storativity/ Specific Yield	Volume Groundwater Stored in Aquifer		
								Total (Mm^3)	Unit (m^3/km^2)	% Total Volume
120 - 150 metres	Kalahari	Sandstone	5885.66	120.00	150.00	30.00	0.005	882.85	150000.00	48.35%
	Dwyka	Tillite	4147.41	120.00	150.00	30.00	0.0002	24.88	6000.00	1.36%
	Olifantshoek	Quartzites	4819.63	120.00	150.00	30.00	0.0007	101.21	21000.00	5.54%
	Ventersdorp	Andesite/Quartz Porphyry	-	-	150.00	0.00	0.0004	0.00	0.00	0.00%
	Transvaal	Shale/BIF	-	-	150.00	0.00	0.0009	0.00	0.00	0.00%
	Transvaal	Andesite	4471.65	120.00	150.00	30.00	0.0004	53.66	12000.00	2.94%
	Transvaal	Dolomite	10826.16	120.00	150.00	30.00	0.002	649.57	60000.00	35.57%
	Archaean Basement	Granite (Weathered)	-	-	150.00	0.00	0.003	0.00	0.00	0.00%
	Archaean Basement	Granite (Fractured)	18976.40	120.00	150.00	30.00	0.0002	113.86	6000.00	6.24%
	Kraaipan - Amalia	Meta arenaceous sediments	-	-	150.00	0.00	0.0004	0.00	0.00	0.00%
	TOTAL		**49126.91**					**1826.03**	**25500.00**	**100.00%**

Table 9.2 (E): The storage volume calculated for the various lithological units within the depth interval 120 – 150m

(F)

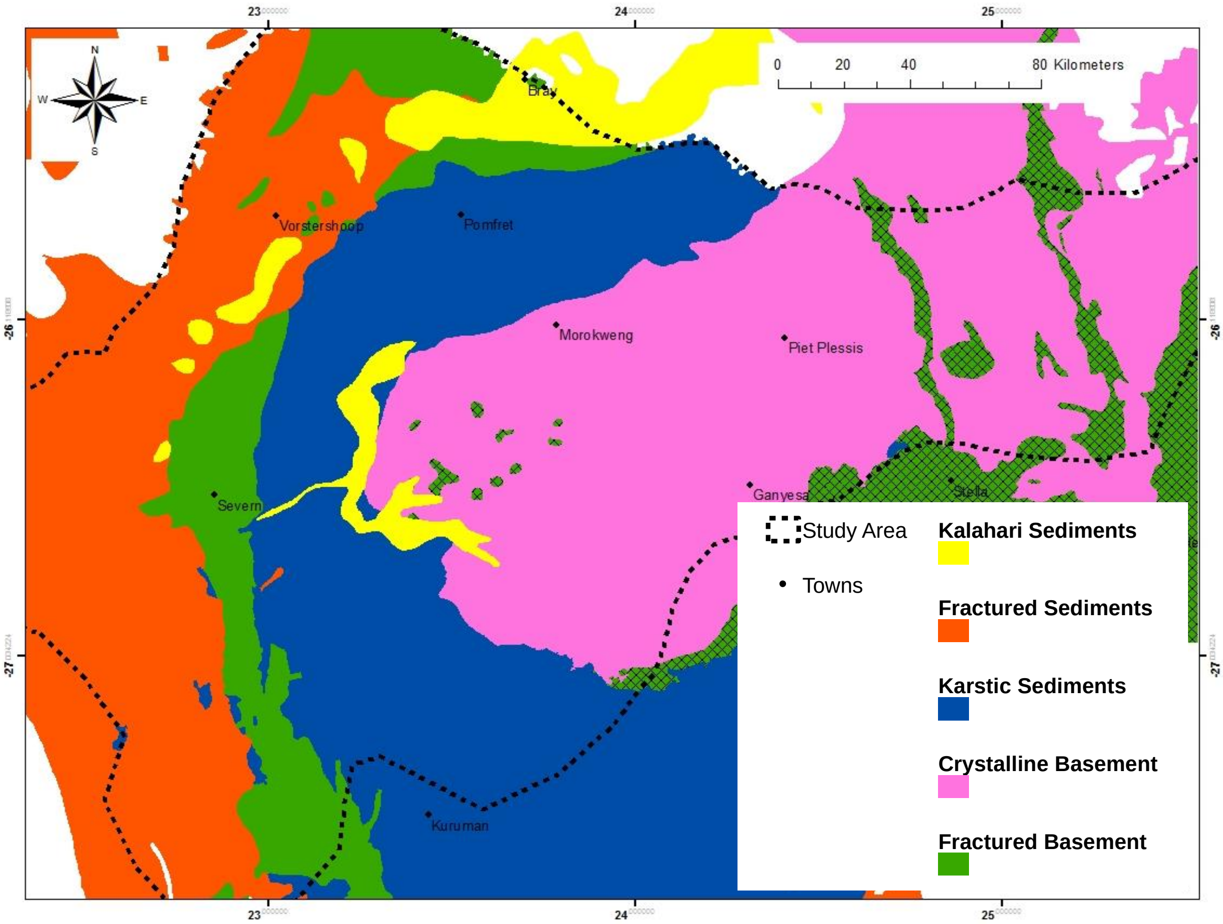

Figure 9.2 (F): 150 – 180 m Aquifer storage map. Crosshatched areas are not saturated at this specific depth interval

Depth Interval	Lithostratigraphic Domain	Lithology	Total Area (km²)	Average Water Level (mbgl)	Average Aquifer Base (mbgl)	Saturated Thickness (m)	Storativity/ Specific Yield	Volume Groundwater Stored in Aquifer		
								Total (Mm³)	Unit (m³/km²)	% Total Volume
150 - 180 metres	Kalahari	Sandstone	1915.82	150.00	180.00	30.00	0.005	287.37	150000.00	22.54%
	Dwyka	Tillite	7140.41	150.00	180.00	30.00	0.0002	42.84	6000.00	3.36%
	Olifantshoek	Quartzites	4819.63	150.00	175.00	25.00	0.0007	84.34	17500.00	6.61%
	Ventersdorp	Andesite/Quartz Porphyry	-	-	180.00	0.00	0.0004	0.00	0.00	0.00%
	Transvaal	Shale/BIF	-	-	180.00	0.00	0.0009	0.00	0.00	0.00%
	Transvaal	Andesite	4824.81	150.00	180.00	30.00	0.0004	57.90	12000.00	4.54%
	Transvaal	Dolomite	11441.22	150.00	180.00	30.00	0.002	686.47	60000.00	53.84%
	Archaean Basement	Granite (Weathered)	-	-	180.00	0.00	0.003	0.00	0.00	0.00%
	Archaean Basement	Granite (Fractured)	19360.80	150.00	180.00	30.00	0.0002	116.16	6000.00	9.11%
	Kraaipan - Amalia	Meta arenaceous sediments	-	-	180.00	0.00	0.0004	0.00	0.00	0.00%
	TOTAL		**49502.69**					**1275.10**	**25150.00**	**100.00%**

Table 9.2 (F): The storage volume calculated for the various lithological units within the depth interval 150 – 180m

(G)

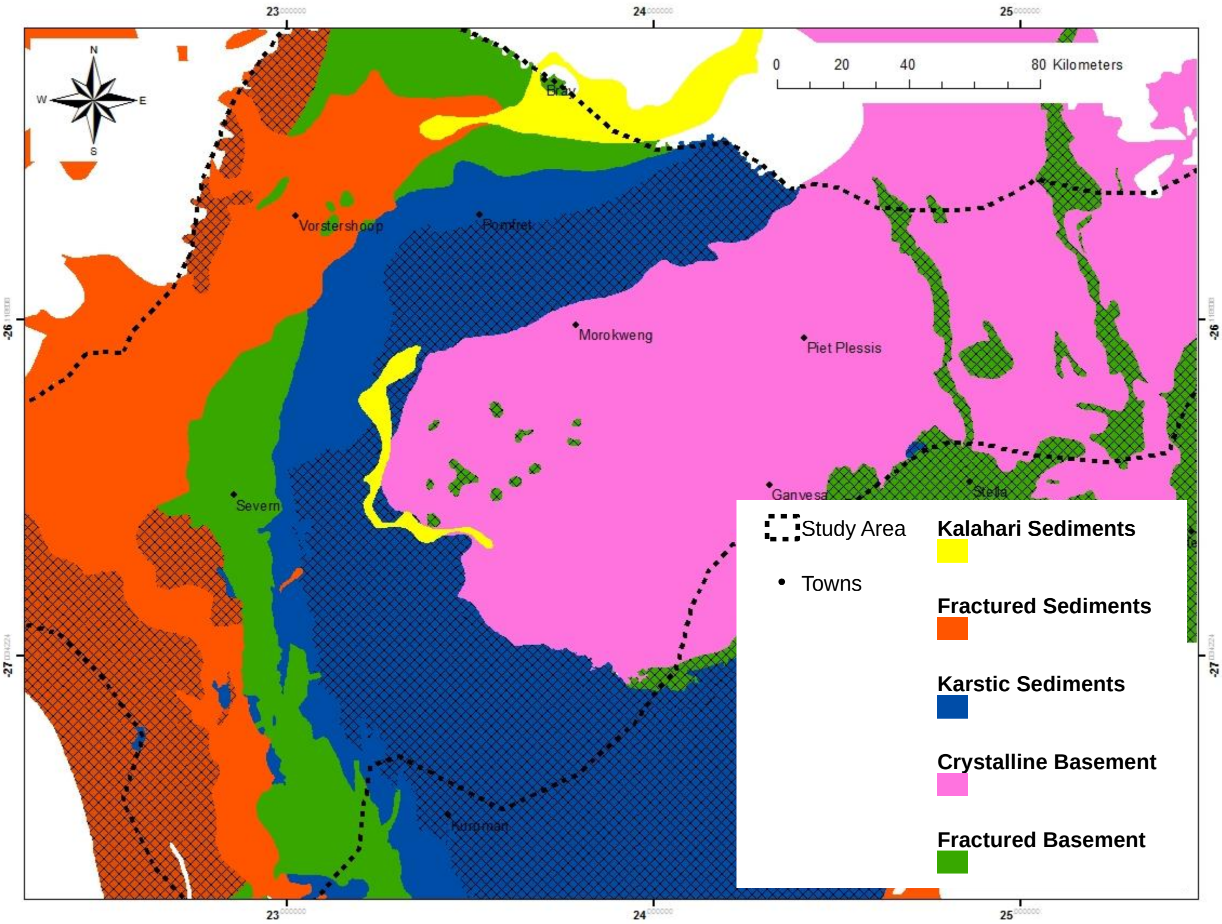

Figure 9.2 (G): 180 – 210 m Aquifer storage map. Crosshatched areas are not saturated at this specific depth interval

Depth Interval	Lithostratigraphic Domain	Lithology	Total Area (km^2)	Average Water Level (mbgl)	Average Aquifer Base (mbgl)	Saturated Thickness (m)	Storativity/ Specific Yield	Volume Groundwater Stored in Aquifer		
								Total (Mm^3)	Unit (m^3/km^2)	% Total Volume
180 - 210 metres	Kalahari	Sandstone	778.95	180.00	210.00	30.00	0.005	116.84	150000.00	23.45%
	Dwyka	Tillite	7701.39	180.00	210.00	30.00	0.0002	46.21	6000.00	9.27%
	Olifantshoek	Quartzites	-	-	210.00	0.00	0.0007	0.00	0.00	0.00%
	Ventersdorp	Andesite/Quartz Porphyry	-	-	210.00	0.00	0.0004	0.00	0.00	0.00%
	Transvaal	Shale/BIF	-	-	210.00	0.00	0.0009	0.00	0.00	0.00%
	Transvaal	Andesite	5019.54	180.00	210.00	30.00	0.0004	60.23	12000.00	12.09%
	Transvaal	Dolomite	3149.04	180.00	205.00	25.00	0.002	157.45	50000.00	31.60%
	Archaean Basement	Granite (Weathered)	-	-	210.00	0.00	0.003	0.00	0.00	0.00%
	Archaean Basement	Granite (Fractured)	19592.63	180.00	210.00	30.00	0.0002	117.56	6000.00	23.59%
	Kraaipan - Amalia	Meta arenaceous sediments	-	-	210.00	0.00	0.0004	0.00	0.00	0.00%
	TOTAL		**36241.55**					**498.29**	**22400.00**	**100.00%**

Table 9.2 (G): The storage volume calculated for the various lithological units within the depth interval 180 – 210m

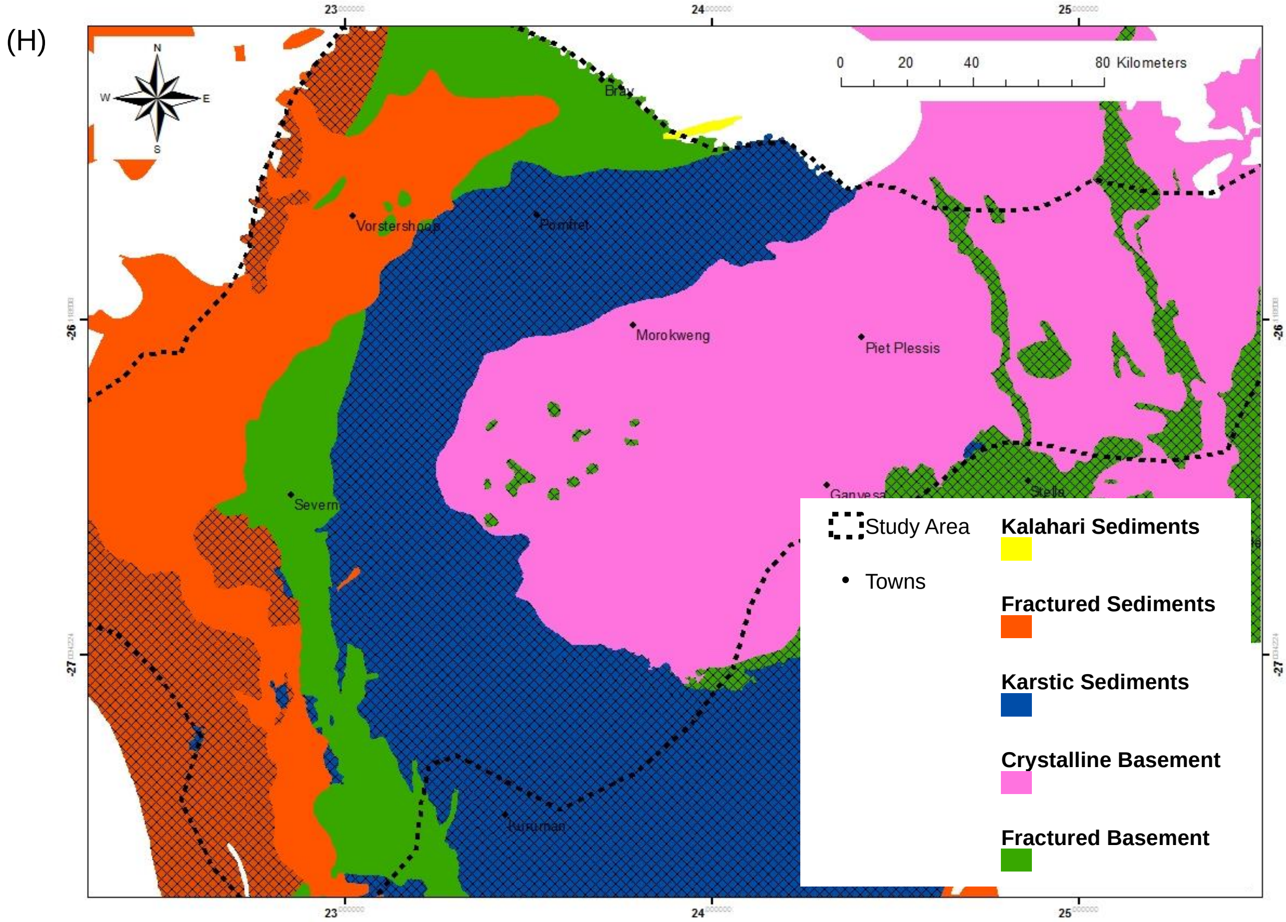

Figure 9.2 (H): 210 – 240 m Aquifer storage map. Crosshatched areas are not saturated at this specific depth interval

Depth Interval	Lithostratigraphic Domain	Lithology	Total Area (km^2)	Average Water Level (mbgl)	Average Aquifer Base (mbgl)	Saturated Thickness (m)	Storativity/ Specific Yield	Volume Groundwater Stored in Aquifer		
								Total (Mm^3)	Unit (m^3/km^2)	% Total Volume
210 - 240 metres	Kalahari	Sandstone	10.60	210.00	240.00	30.00	0.005	1.59	150000.00	0.91%
	Dwyka	Tillite	7788.80	210.00	225.00	15.00	0.0002	23.37	3000.00	13.37%
	Olifantshoek	Quartzites	-	-	240.00	0.00	0.0007	0.00	0.00	0.00%
	Ventersdorp	Andesite/Quartz Porphyry	-	-	240.00	0.00	0.0004	0.00	0.00	0.00%
	Transvaal	Shale/BIF	-	-	240.00	0.00	0.0009	0.00	0.00	0.00%
	Transvaal	Andesite	5333.54	210.00	225.00	15.00	0.0004	32.00	6000.00	18.31%
	Transvaal	Dolomite	-	-	240.00	0.00	0.002	0.00	0.00	0.00%
	Archaean Basement	Granite (Weathered)	-	-	240.00	0.00	0.003	0.00	0.00	0.00%
	Archaean Basement	Granite (Fractured)	19628.80	210.00	240.00	30.00	0.0002	117.77	6000.00	67.40%
	Kraaipan - Amalia	Meta arenaceous sediments	-	-	240.00	0.00	0.0004	0.00	0.00	0.00%
	TOTAL		**32761.74**					**174.73**	**16500.00**	**100.00%**

Table 9.2 (H): The storage volume calculated for the various lithological units within the depth interval 210 – 240m

Upon calculating the groundwater storage in 30 m depth intervals (Table 9.2 A - H), the total storage volume for the study area was determined by adding the volumes calculated for each of the 30 m depth intervals, a summary of which is presented in Table 9.3. These estimates of storage for each lithological unit tend to be slightly lower than that calculated when using the average saturated thickness for each unit (Table 9.1), however, the total storage volume proved greater than that estimated in Table 9.1. This is largely due to the increased contribution from the shallower Kalahari sediments (0 – 60 m), the areal extent and the average saturated thickness of which were not taken into consideration when calculating the storage volume for this aquifer (Table 9.1).

Table 9.3: The storage volumes determined for the different lithological units by summing the volumes calculated for each of the 30 m depth intervals

Lithostratigraphic Domain	Lithology	Total Area (km^2)	Volume Groundwater Stored in Aquifer		
			Total (Mm^3)	Unit (m^3/km^2)	% Total Volume
Kalahari	Sandstone	44002.99	7129.75	162028.73	51.79%
Dwyka	Tillite	7788.80	145.17	18637.78	1.05%
Olifantshoek	Quartzites	4819.63	287.31	59613.06	2.09%
Ventersdorp	Andesite/Quartz Porphyry	1609.43	16.88	10489.88	0.12%
Transvaal	Shale/BIF	3194.76	132.67	41526.65	0.96%
Transvaal	Andesite	5344.14	252.28	47206.86	1.83%
Transvaal	Dolomite	8758.74	2727.99	311458.85	19.81%
Archaean Basement	Granite (Weathered)	15498.43	2480.25	160032.21	18.01%
Archaean Basement	Granite (Fractured)	19628.80	565.40	28804.61	4.11%
Kraaipan - Amalia	Meta arenaceous sediments	1006.34	30.24	30044.45	0.22%
TOTAL			**13767.93**	**86984.31**	**100.00%**

Aquifers with the least storage in the study area generally comprise the fractured basement rocks of the Kraaipan - Amalia greenstone belt and the Ventersdorp Lavas, where average groundwater volumes are estimated to be 30.24 x 10^6 m^3 and 16.88 x 10^6 m^3, respectively (Table 9.3). Within the study area, these assemblages are not very extensive in area, largely accounting for the lower storage volumes calculated. Similar poor storage volumes were expected for the andesites of the Ongeluk Formation (Griqualand West Sequence) given their poor storativity values, however, their greater areal extent and deeper saturated thicknesses have resulted in slightly greater storage volumes of 252.28 x 10^6 m^3 being calculated (Table 9.3). While of limited storage, these aquifers, particularly the Kraaipan - Amalia greenstone terrane, can prove useful and highly significant in this arid region, as they play a significant role in recharging the adjacent granitic aquifers (Section 8.6).

The groundwater storage for the fractured sedimentary aquifers was calculated at a total of 565.15 x 10^6 m^3 (Table 9.3), a depleted value given the low intrinsic primary permeability and porosity of this hard bedrock, with groundwater movement controlled by zones of faulting, fracturing and jointing. The bulk of this water is stored in the quartzites of the Olifantshoek Supergroup (287.31 x 10^6 m^3), with the least being stored in the fractured sediments of the Asbestos Hills Subgroup (132.67 x 10^6 m^3). The storage volume of groundwater found in the Dwyka Group (145.17 x 10^6 km^3) is slightly higher than that of the Asbestos Hills Subgroup, given its greater areal extent (Table 9.3). This deep aquifer unit, with its low storativity and associated low borehole yields, is limited with regard to its ability to transmit water within the host formation. This and the saline water commonly associated with the Dwyka Formation make it a poor aquifer, not regarded to be viable for the exploitation of groundwater.

From the geological cross sections constructed for the region (Figures 5.9 A, B and C) it is apparent that many of the holes drilled in the Asbestos Hills Subgroup have passed through this relatively thin layer of sediments (~ 125 m thick) and have penetrated the underlying dolomites of the Campbell Rand Subgroup. From the various depth interval maps (Figures 9.2 A - H), it would seem that the Asbestos Hills Subgroup plays a significant role between depths of 60 to 120 m, with holes drilled deeper than this sourcing their water from the underlying dolomites. While very restricted with regard to its storage potential, these fractured lithologies play a significant role with regard to recharging the underlying dolomites (Section 8.5).

Compared to the volume of water stored within the hard rock of the fractured sedimentary aquifers, the storage in the adjacent granitic aquifers is much greater, with large volumes of water stored in both an upper weathered – jointed zone (2480.25 x 10^6 m^3) and a deeper, fractured zone (565.40 x 10^6 m^3; Table 9.3). When viewing the water strike levels for this aquifer unit (Figure 5.10 i), most of the water strike levels in the Archaean granites are shallow (30 – 90 m, weathered zone), with a small component (< 30 %) showing much deeper water strike levels (90 m - 240 m, fractured zone). When plotted across the aquifer, it is apparent that these deeper storage zones are largely restricted to the Morokweng Meteorite Impact crater and areas where the granites are covered by thick deposits of Kalahari sediments. The Morokweng deformation event seems to have had a significant impact on the hydrogeological parameters of this region, with the fractures penetrating much deeper than the structural features usually associated with the rest of this crystalline basement.

An aquifer containing a considerable proportion of the study area's groundwater (19.81 %; Table 9.3) is the dolomites of the Campbell Rand Subgroup. Taking into consideration the hydrogeological character of the karst in the study area and its associated secondary porosity (Section 5), an average groundwater storage volume of 2727.99 x 10^6 m^3 was calculated for this aquifer unit (Table 9.3). This storage volume takes into consideration its extent below the fractured sediments of the Asbestos Hills Subgroup (120 – 205 m), whereas the storage volume (2709.43 x 10^6 m^3) calculated from the average saturated thickness does not (Table 9.1), accounting for the lower storage volumes calculated for the latter. While not contributing as much per volume as the granites (22.12 %) and Kalahari sediments (51.79 %), this unit demonstrates one of the highest volumes available per square kilometre (311.46 x 10^3 m^3/km^2).

The large intergranular sedimentary aquifer of the Kalahari Group contains the largest proportion of the study area's groundwater (51.79 %), with an estimated groundwater storage volume of 5478.52 x 10^6 m^3 (Table 9.1) calculated using its average saturated thickness. The calculation of this average thickness (Section 5.3) gave precedence to the thicker and deeper deposits, since most of the shallower Kalahari sediments (< 60 m) are rarely utilised within the study area. If the entire sedimentary aquifer, however, was to be taken into consideration, the total maximum storage of this aquifer is estimated at 7129.75 x 10^6 m^3 (Table 9.3), 1.3 times more than what is currently being exploited at present. The storage capabilities of the Kalahari Group are of particular significance and it has been estimated that its storage capabilities are more than twice that of the dolomite (Table 9.3). This significant storage space can allow groundwater recharge to be stored for several decades, thereby providing a vital buffer against variable climates. The only problem is that this aquifer is not actively recharged, with portions having been recharged when the climate of the area was wetter (Section 8.5). It must also be noted, that this calculation is based on groundwater that generally occurs under phreatic conditions, however, as noted by the geological cross sections generated (Figure 5.9 A, B and C), these sandstones can also occur under semi-confined conditions owing to the presence of inter-fingering clay horizons. This can impact significantly on the transmissivities of this unit, resulting in low yields and the Kalahari being regarded as insignificant. As such, although showing the most potential for storage, exploitation of this resource is restricted.

It must be reiterated that the value of 13767.93 x 10^6 m^3 (Table 9.3) calculated for groundwater storage within the study area represents an average value that may either increase or decrease depending on numerous factors. In particular, not all of this groundwater storage is available for abstraction, as the volume of water that is released from an aquifer through pumping is often less than the effective porosity. In addition, the groundwater storage reflects the spatial distribution and morphology of the structural features present, the distribution of which varies considerably within each hydrogeological unit and throughout the study area, making the calculation of groundwater storage extremely difficult.

The confidence in a result is a function of the number of components used in the various calculations and the accuracy of the data used. Given the large scale of the study area, site specific data was not always available (Section 5), with some vital information proving scarce for this region. As such, some generalisations had to be made. Despite this, it is with a moderate degree of confidence that the storage volumes calculated are considered to be representative of the study area.

9.2 Recharge

The quantification of recharge is increasingly given attention in the management of groundwater, particularly in this semi-arid region where the average rainfall is generally low and the evapotranspiration rates high. To ensure the long-term sustainability of this resource, it proved essential that the groundwater recharge be estimated (See Section 2.6). Recharge estimates were calculated across the study area, with an attempt made to determine if quantitative estimates of recharge could be defined for different geological formations and/or aquifers.

9.2.1 Mean Annual Precipitation (MAP)

Of the four historical rainfall datasets acquired, two were accessed from the Department of Water Affairs, while the other two were sourced from local farmers (See Section 2.6), the distribution of which is shown in Figure 9.3. The results, detailed in Appendix B, seem to range from 350 mm in the southwest to 500 mm in the northeast (Figure 9.3), with a mean annual rainfall of approximately 400 mm falling almost entirely during the summer season between October and April. This average of 400 mm is thought to be representative of the entire region, taking into consideration the altitude, distance from sea, aspect, terrain roughness and the direction of prevailing rain-bearing winds.

9.2.2 Concentration of Chloride in Rainfall and Groundwater

Reliable (accurate laboratory analysis) and spatially representative chloride concentration data in groundwater is essential to enable assessment of recharge. Such data, the distribution of which is presented in Figure 9.4, was accessed from the NGANET archive (See Section 2.6). In order to assess recharge at a local scale, representative groundwater chloride concentrations were also identified for each of the hydrogeological units described in Section 5.1 (Table 9.4).

Table 9.4: Representative groundwater chloride concentrations for the study area

Lithostratigraphic Domain	Lithology	Average Groundwater Chloride (mg/l)
Kalahari	Sandstone	358.26
Olifantshoek	Quartzites	132.68
Ventersdorp	Andesite/Quartz Porphyry	91.37
Transvaal	Shale/BIF	75.36
Transvaal	Andesite	128.25
Transvaal	Dolomite	87.34
Archaean Crystalline Basement	Granite (Weathered)	67.84
Kraaipan - Amalia	Meta arenaceous sediments	66.38

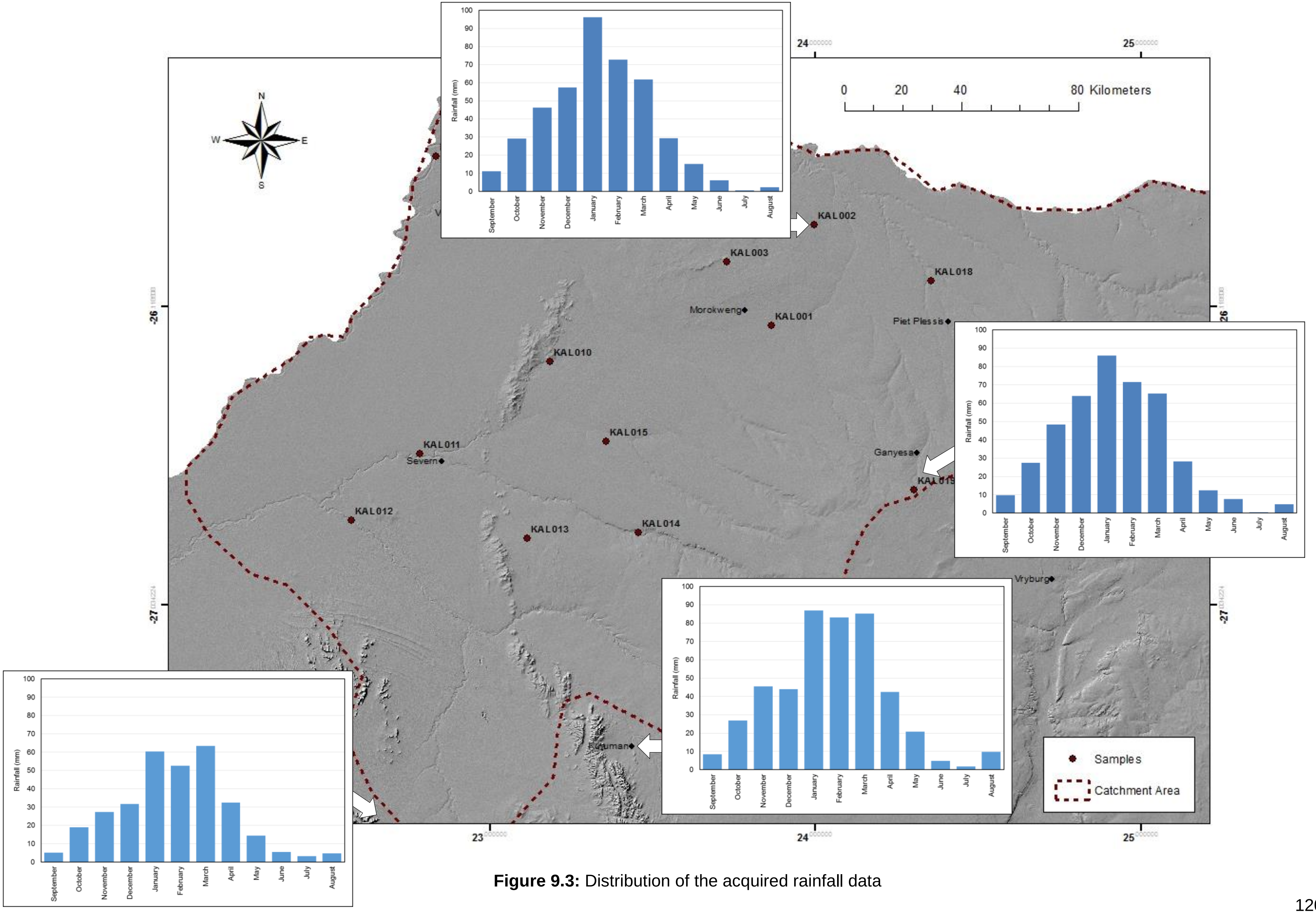

Figure 9.3: Distribution of the acquired rainfall data

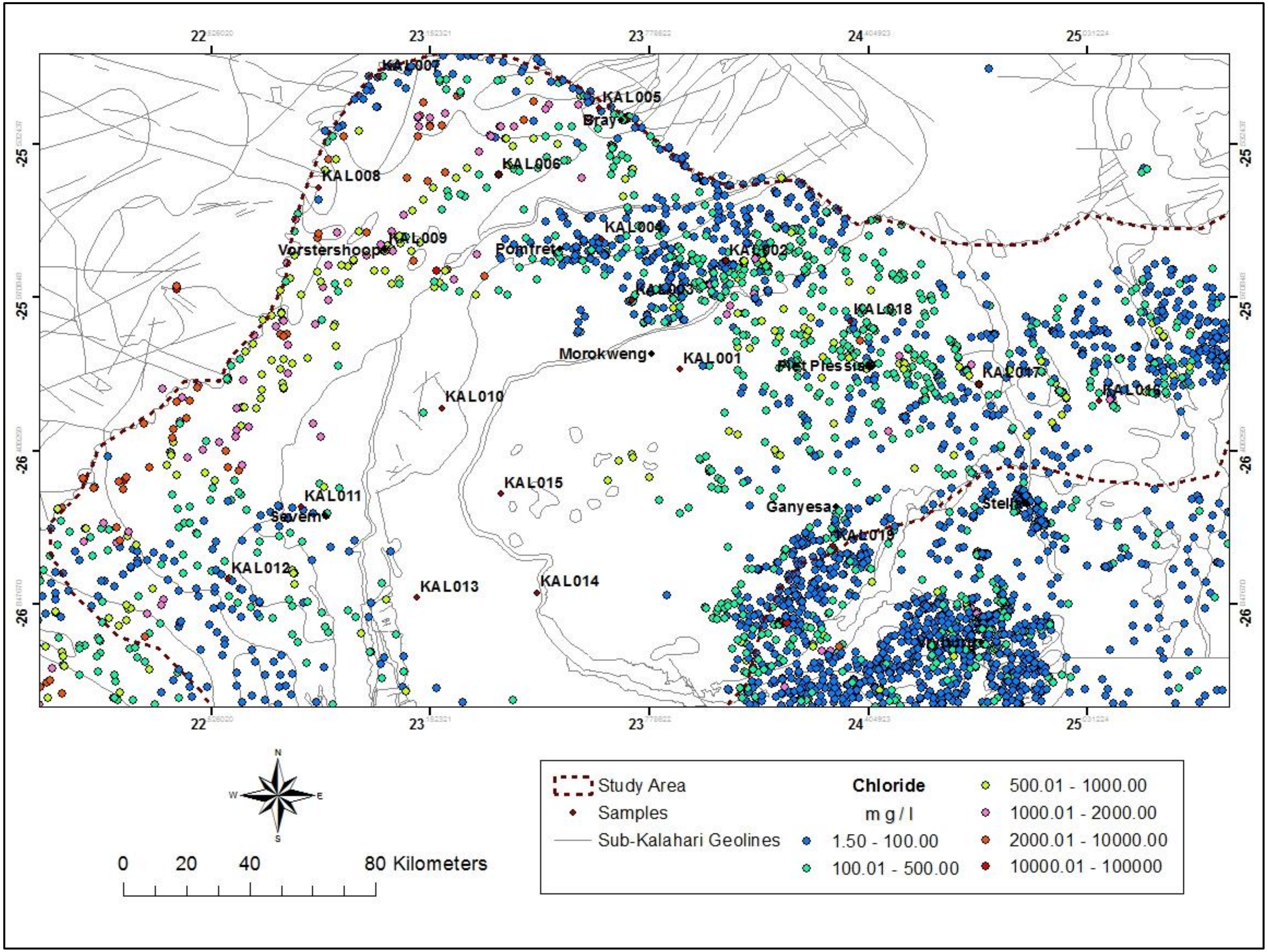

Figure 9.4: Distribution of the groundwater chloride data accessed from the NGANET

Reliable, time-related chloride data for all of the rainfall stations in the area would have also proved valuable, however, such data does not exist. Within South Africa there is a lack of rainwater chloride concentration data. The currently accepted concentration of chloride in rainfall for the study area is approximately 0.80 mg/l. This is based on the chloride concentrations that were extracted from the rainfall chloride map created during the GRAII study of South Africa (DWAF, 2006). This value of 0.80 mg/l was also calculated by relating rainfall chloride to MAP and geographical setting, using the same formula as that used during the GRAII study (DWAF, 2006).

It is fully understood that there is much more variation in the actual rainfall chloride content and better definition of this content is required. However, in the absence of data, it is firmly believed that this average value will provide an adequate first approximation of recharge.

9.2.3 Chloride Mass Balance Calculation and Discussion

The recharge was calculated for each groundwater chloride point (See Section 2.6), the values of which were interpolated using the kriging method to create a groundwater recharge surface map (Figure 9.5). The recharge was also calculated for each of the hydrogeological units identified (Table 9.5), using the representative groundwater chloride concentrations extracted for each unit (Table 9.4). In general, the generated map indicates that the eastern portions of the study area, characterised by thin Kalahari sand cover and shallow water levels, have the highest recharge rates, which decrease steadily to the west as the Kalahari cover thickens and the water levels deepen. Overall, the recharge values calculated correspond reasonably well with other recharge assessments conducted in the Kalahari region (Verhagen 2003; Verhagen, 2013).

It is obvious that recharge in the areas covered by thick Kalahari sediments is negligible, with an average recharge of 0.89 mm/a being calculated (Table 9.5). Isolated areas of higher recharge are evident, particularly in close proximity to the upper reaches of the Molopo River. These higher values are directly linked to recharge that occurs infrequently at times when floodwater reaches as far as Mokopong, following which there appears to be no contribution from the lower reaches of the river. At a regional scale, recharge via the river bed is of limited importance, with the dominant recharge mechanism being that of local, diffuse recharge, which is typically characterised by poor quantitative estimates. These poor estimates of recharge are largely attributed to the geological nature of the Kalahari Group, with the clay-dominated sands capable of absorbing large volumes of rainwater, but poor at transmitting the water through the unsaturated zone. This leads to a loss of water by evaporation and transpiration by dense vegetation before it percolates and recharges the underlying permeable units. This is consistent with the sparse distribution of drainage lines within the Kalahari Group, indicating a high infiltration rate and storage retention, compared to limited surface runoff.

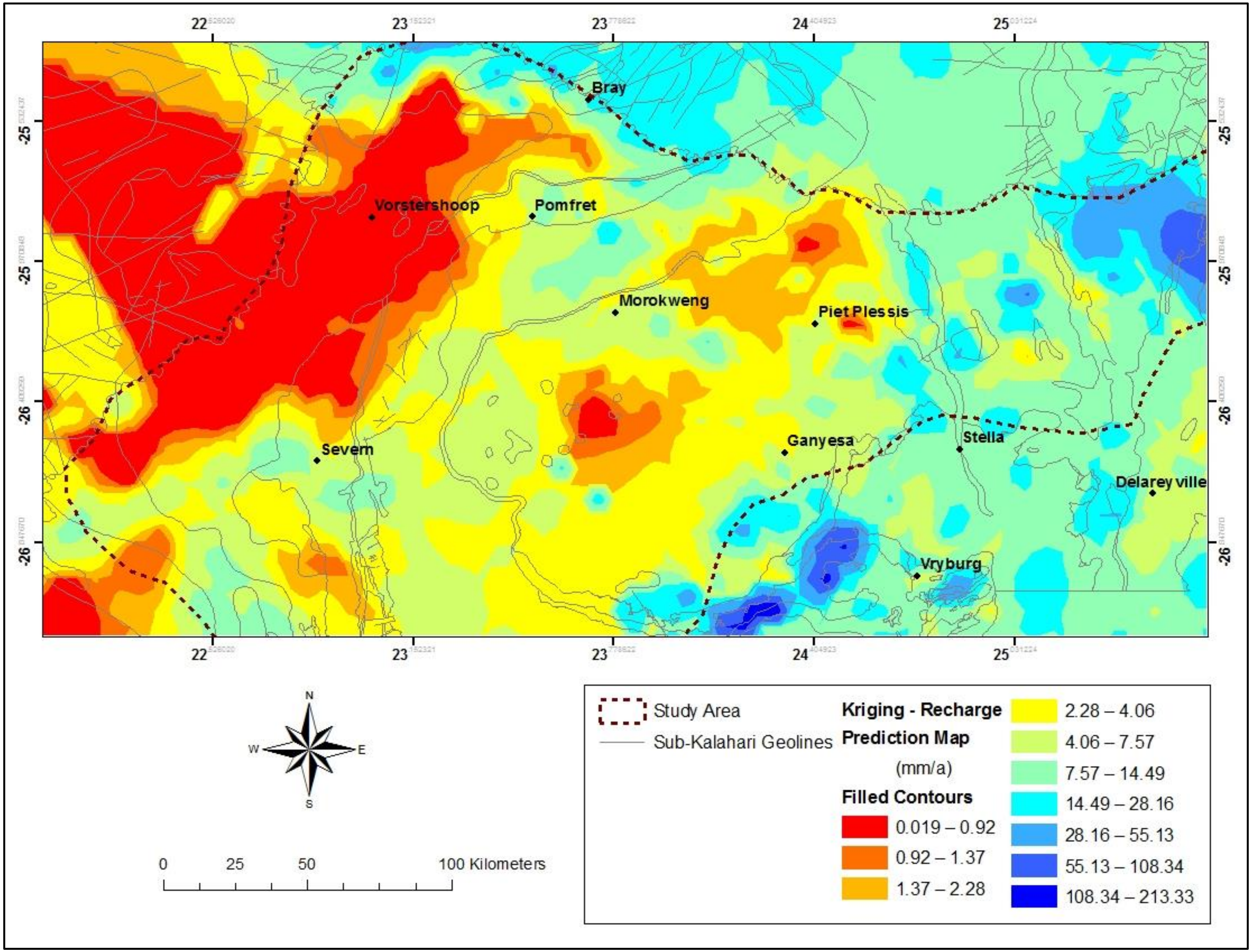

Figure 9.5: Groundwater recharge surface map relative to the sub-Kalahari geology

Table 9.5: Recharge values calculated for each of the hydrogeological units identified

Lithostratigraphic Domain	Lithology	Total Area (km^2)	MAP (mm/a)	Average Groundwater Chloride (mg/l)	Average Rainfall Chloride (mg/l)	Recharge (%)	Recharge (mm/a)	Recharge (Mm^3/a)	Annual Recharge (m^3/km^2)
Kalahari	Sandstone	44002.99	400	358.26	0.80	0.22	0.89	39.30	893.21
Dwyka	Tillite	7788.80	400	358.26	0.80	0.22	0.89	6.96	893.21
Olifantshoek	Quartzites	4819.63	400	132.68	0.80	0.60	2.41	11.62	2411.84
Ventersdorp	Andesite/Quartz Porphyry	1609.43	400	91.37	0.80	0.88	3.50	5.64	3502.21
Transvaal	Shale/BIF	3194.76	400	75.36	0.80	1.06	4.25	13.57	4246.45
Transvaal	Andesite	5344.14	400	128.25	0.80	0.62	2.50	13.33	2495.13
Transvaal	Dolomite	8758.74	400	87.34	0.80	0.92	3.66	32.09	3663.84
Archaean Basement	Granite (Weathered)	15498.43	400	67.84	0.80	1.18	4.72	73.11	4716.98
Archaean Basement	Granite (Fractured)	19628.80	400	67.84	0.80	1.18	4.72	92.59	4716.98
Kraaipan - Amalia	Meta-arenaceous sediments	1006.34	400	66.38	0.80	1.21	4.82	4.85	4820.73

The fractured sediments of the Kraaipan - Amalia greenstone terrane and the Asbestos Hills Subgroup, offer some of the best recharge areas within the study area, with a recharge rate of 4.82 mm/a and 4.25 mm/a calculated, respectively (Table 9.5). These outcropping lithologies are rarely covered by thick deposits of Kalahari sediments, with their water levels proving to be relatively shallow. As such, little loss to evapotranspiration is expected from these aquifers. Under favourable conditions, given the multifaceted nature of fractured rocks, these aquifers not only contain a viable resource of groundwater, but may also recharge the underlying granitic and karstic aquifers, where local structures enable limited lateral and vertical displacement.

The granite in the study area is regularly being recharged in view of the average recharge value of 4.72 mm/a calculated for this hydrogeological unit. More than 70 % of the investigated area, however, is overlain by thick deposits (> 15 m) of Kalahari sediments and, as confirmed by the tritium values, the recharge in these areas will be low as a result of the retention of potential recharge in the unsaturated zone, from where it is lost by evapotranspiration. Recharge is expected where the overburden of unsaturated material is thin. In particular, it appears that this aquifer receives most of its recharge from the outcropping areas of the aquifer, notably the Mosita and Middlekop granites, and relatively little from infiltration through the Kalahari sediments (Nijsten and Beekman 1997). This is confirmed by higher recharge rates of ± 13.3 mm/a calculated for the Middlekop granite near Stella (Nel, 2001).

Groundwater recharge to the karstic aquifers also appears moderate, with an average recharge rate of 3.66 mm/a calculated. Many mechanisms of recharge to this aquifer have been suggested, with recharge occurring via geological lineaments (generally faults, less dykes), through shallow outcrop and sub-outcrop of dolomite, through the banded ironstone formations of the Asbestos Hills Subgroup and through the alluvial channels of the Molopo river, when in flood (Van Dyk, 2005). It has been suggested that the presence of dissolution channels within the karstified carbonate rocks play a more important role in groundwater flow and storage than lineament-intersection frequency (Tessema *et al*., 2012). Nevertheless, given the “compartmentalisation” of this karstic aquifer, each with its varying degree of fracture density and weathering, the recharge rate is expected to vary considerably throughout the aquifer.

The spatial variability of recharge over a range of scales presents significant difficulty in any recharge investigation, particularly if based on point estimates that have been extrapolated over an entire region. One of the concerns regarding the use of this model to predict groundwater recharge is that it does not take into account the geological complexity and preferred flow paths along which groundwater recharge occurs. Rainfall variability and intensity (depth), which are significant contributing factors in this area characterised by episodic rainfall events, have also not been taken into account. As such, it must be appreciated that the estimations of groundwater recharge stated above are associated with high levels of uncertainty. Nonetheless, it provides a useful base with which to manage the water resources of the region.

9.3 Groundwater Potential

Only once an attempt was made to understand the various controls on groundwater in the region, with the recharge history being modelled, coupled with the geological model of the region and chemical testing of the groundwater, has it proved possible to determine the potential of this region to host significant groundwater reserves. Fundamental to this project, was the quantification of the groundwater potential and the “exploitability” of this resource, the former of which provides an assessment of the resource based on recharge and storage capacity, whereas the latter provides an estimation of the availability of groundwater based on the transmissivity of the aquifer. Both assessments not only provide an indication of the size of the resource, but an indication of how the resource can be exploited on a sustainable basis without “mining” the resource. This knowledge is extremely useful to regulate and optimize water use without adversely impacting the water resource for future use.

9.3.1 Groundwater Resource Potential

The Groundwater Resource Potential for the entire study area and for each of the hydrogeological units described in Section 5.1 is presented in Table 9.6. The total resource potential for the entire study area is estimated at 10127.29 x 10^6 m^3/a (Table 9.6), with the Kalahari aquifer showing the greatest potential in the study area, comprising 50.67 % of the total resource (Table 9.6). Aquifers with the least potential in the study area generally comprise the fractured basement rocks of the Kraaipan - Amalia greenstone belt and the Ventersdorp lavas, where average groundwater potential is estimated to be 26.45 x 10^6 m^3/a and 17.70 x 10^6 m^3/a, respectively (Table 9.6). Trends in the calculated groundwater potential values mirror that of aquifer storage (Section 9.1), given that the latter is fundamental to the assessment of groundwater potential.

As mentioned above, the values calculated represent the potential capacity of each aquifer, without abstraction. If each aquifer could be fully utilised, a considerable volume of water is available for sustainable abstraction, at an assurance of supply similar to that of surface water. Notwithstanding the uncertainties of quality, the estimated groundwater potential represents a water resource that is of a different magnitude to all other freshwater resources.

Table 9.6: Groundwater Resource Potential calculated for each of the hydrogeological units identified within the study area

Lithostratigraphic Domain	Lithology	Total Area (km^2)	Groundwater Storage (Mm^3)	Drought Index (years)	Recharge (Mm^3/a)	Groundwater Resource Potential (Mm^3/a)	Annual Groundwater Resource Potential (m^3/km^2)
Kalahari	Sandstone	44002.99	7129.75	1.40	39.30	5131.98	116628.01
Dwyka	Tillite	7788.80	145.17	1.40	6.96	110.65	14205.91
Olifantshoek	Quartzites	4819.63	287.31	1.40	11.62	216.85	44992.59
Ventersdorp	Andesite/Quartz Porphyry	1609.43	16.88	1.40	5.64	17.70	10994.98
Transvaal	Shale/BIF	3194.76	132.67	1.40	13.57	108.33	33908.35
Transvaal	Andesite	5344.14	252.28	1.40	13.33	193.53	36214.32
Transvaal	Dolomite	8758.74	2727.99	1.40	32.09	1980.65	226134.45
Archaean Basement	Granite (Weathered)	15498.43	2480.25	1.40	73.11	1844.71	119025.71
Archaean Basement	Granite (Fractured)	19628.80	565.40	1.40	92.59	496.45	25291.70
Kraaipan - Amalia	Meta-arenaceous sediments	1006.34	30.24	1.40	4.85	26.45	26281.05
TOTAL		**111652.08**	**13767.93**		**293.06**	**10127.29**	**65367.71**

9.3.2 Groundwater Availability and Exploitation

Direct measurements of transmissivity and borehole yield for each of the aquifers types identified proved impossible, given the scope of the project (See Section 2.7). As such, a number of pumping tests throughout the study area were analysed and used to determine a range of possible values for each identified hydrogeological domain (based on lithology); as well as the various structural features present within the study area. Table 9.7 provides a summary of the transmissivities and borehole yields that can reasonably be expected in each of the hydrogeological units. This information was used to determine the likely availability of accessible groundwater per borehole and per km^2 in each of the hydrogeological domains (Table 9.8). The impacts of various pumping rates encountered within each aquifer unit were also assessed to ensure that the quantities extracted were considered sustainable. Localised effects on borehole yield, such as impermeable boundaries and fracture zones were also taken into consideration, the details of which are discussed below.

Table 9.7: Borehole yield and transmissivity values assigned to each hydrogeological unit

Lithostratigraphic Domain	Lithology	Transmissivity (m^2/d)	Borehole Yield Range (l/s)	Average Borehole Yield (m^3/a)
Kalahari Group	Sandstone, Shale, Gravel	4 - 70	0.5 - 2.0	39420.00
Dwyka	Tillite	< 5	0.1 - 2.0	31536.00
	Associated Fractures	< 22	2.0 - 5.0	-
Olifantshoek	Quartzites	20 - 40	0.1 - 2.0	31536.00
	Associated Fractures	-	> 5.0	-
Ventersdorp	Andesite/Quartz Porphyry	< 10	0.1 - 0.5	15768.00
	Associated Fractures	-	< 2.0	-
Transvaal	Shale/BIF	5 - 50	0.1 - 5.0	78840.00
	Associated Fractures	> 100	15 - 30	-
Transvaal	Dolomite	100 - 250	0.1 - 5.0	78840.00
	Associated Fractures/Dykes	> 300	> 10	-
Archaean Crystalline Basement	Granite	25 - 350	0.1 - 5.0	78840.00
	Associated Fractures	< 2000	10 - 25	157680.00
Kraaipan - Amalia	Meta-arenaceous sediments	5 - 50	0.1 - 2.0	31536.00
	Associated Fractures	>100	< 15	-

Table 9.8: The likely availability of accessible groundwater per borehole and per km² in each of the hydrogeological domains

Lithostratigraphic Domain	Lithology	Total Area (km²)	Recharge (Mm³/a)	Groundwater Resource Potential (Mm³/a)	Groundwater Availability			
					Average Borehole Yield (m³/a)	Annual Borehole Yield (m³/km²)	% of Recharge	% of Resource Potential
Kalahari	Sandstone	44002.99	39.30	5131.98	39420.0	0.896	0.10%	0.001%
Dwyka	Tillite	7788.80	6.96	110.65	31536.0	4.049	0.45%	0.029%
Olifantshoek	Quartzites	4819.63	11.62	216.85	31536.0	6.543	0.27%	0.015%
Ventersdorp	Andesite/Quartz Porphyry	1609.43	5.64	17.70	15768.0	9.797	0.28%	0.089%
Transvaal	Shale/BIF	3194.76	13.57	108.33	78840.0	24.678	0.58%	0.073%
Transvaal	Andesite	5344.14	13.33	193.53	15768.0	2.951	0.12%	0.008%
Transvaal	Dolomite	8758.74	32.09	1980.65	78840.0	9.001	0.25%	0.004%
Archaean Basement	Granite (Weathered)	15498.43	73.11	1844.71	157680.0	10.174	0.22%	0.009%
Archaean Basement	Granite (Fractured)	19628.80	92.59	496.45	78840.0	4.017	0.09%	0.016%
Kraaipan - Amalia	Meta-arenaceous sediments	1006.34	4.85	26.45	31536.0	31.337	0.65%	0.119%

9.3.2.1 Fractured Basement Volcanic Aquifers

Kraaipan – Amalia Greenstone Terrane: No site specific pumping tests could be found within the Kraaipan - Amalia greenstone terrane. As such, an attempt was made to find a proxy for this transmissivity value, with the flow and storage characteristics of known lithologies in the Limpopo Province being compared and related to that of the study area. The greenstone belts associated with the Limpopo Province typically exhibited an average transmissivity value of 35 m^2/d (Holland 2011; 2012). Amphibolites, which are the dominating lithological unit contributing to these transmissivity values, are only rarely exposed in the study area, with iron formations (magnetite quartzites, banded ferruginous cherts, jaspilites, and iron formation breccias) being the main Archaean rock types exposed throughout the Kraaipan - Amalia region. As such, it was felt that a lower range of transmissivity values, typical of that of banded iron formations (5 – 50 m^2/d) should be assigned to this hydrogeological unit.

Generally, these aquifers are characterized by borehole yields that vary from 0.1 to 5.0 l/s, with the higher yields corresponding to meta-argillaceous sediments consisting of slate, siltstone and dolomite which are located approximately 40 km south of the town of Stella (Tessema *et al*., 2012). The productivity of these aquifers is also largely dependent on the nature of the fissure system. A statistical correlation between borehole yield and lineament density by Tessema *et al*. (2012; 2014) revealed that high borehole yields in these hard rock terranes are typically associated with areas that exhibit high concentration of fissures, fractures and joints. In addition, the results of this statistical correlation provided supporting evidence regarding the significance of cross cutting structures in controlling groundwater distribution. The intersection of the NE-SW and NW-SE striking lineaments located in this portion of the study area are typical examples of where high borehole yields may be expected, presumably enhanced by fracture connectivity (Tessema *et al*., 2014). This is confirmed by records of high yielding boreholes (> 15.0 l/s) in the greenstone assemblages (Nel, 2001), typically associated with near-surface vertical and sub-vertical fractures.

Given the small storage volume of this hydrogeological unit, there is a concern that the higher yields associated with structural features in this area, may have a negative effect on the resource. A borehole suitably sited within an area that exhibits a high concentration of structural features (average yield of 10.0 l/s), pumped for 24 hours in a full year will abstract 6.5 % of the potential recharge and 1.19 % of the total resource, with no more than 83 boreholes being able to operate at the same yield, per year for fear of depleting the resource. This is a challenge given the large mining presence in this region. The resource potential of this aquifer unit is also highly dependent on recharge, with the recharge forming 18.26 % of the total resource potential for this aquifer unit (Table 9.8). The inability of this aquifer to store large volumes of water (Table 9.1), given that the host rock is considered an aquitard and the associated fractures are generally not conduits for large scale water volumes, means that any excess recharge will be directed to the surrounding granitic aquifers. If over-exploited, this recharge will be not be able to sustain the aquifer through droughts.

Ventersdorp and Transvaal Andesites: The basic extrusive rocks (andesitic and basaltic lavas) of the Ventersdorp Supergroup and the Ongeluk Formation (Griqualand West Sequence) are typically characterised by transmissivities of 1 – 10 m^2/d (Dondo *et al*., 2010). A significant number of low yielding boreholes (0.1 - 0.5 l/s) are typically associated with these andesites (Van Veelen *et al*., 2009; Nel *et al*., 2014), with boreholes in excess of 2.0 l/s proving rare, the productivity being largely dependent on the nature of the fissure system.

There are no indications that the average rate at which water is currently withdrawn from these areas (0.5 l/s) has a negative effect on the resource, given that one borehole pumped for 24 hours in a full year will only abstract 0.08 % of the potential recharge and 0.01 % of the total resource (Table 9.8). These low transmissivities and yields ensure that abstraction remains sustainable, however, they make it impractical to utilise all of the resource available since an excessive number of low yielding boreholes would be required for its abstraction. In general, these volcanic aquifers offer poor prospects of securing groundwater, as they have limited porosity due to the solid nature of the rock and are generally resistant to the development of secondary porosity. These aquifers should, however, prove sufficient for community water supplies, if fitted with hand pumps that can be sustained by borehole yields of 0.5 l/s and greater (MacDonald *et al*., 2012).

9.3.2.2 Fractured and Weathered Crystalline Basement Aquifers

Granitoid bodies themselves have very poor hydrogeological aspects, such as transmissivity, porosity etc. to deem them of significant importance in groundwater exploitation. Their importance in contributing to the groundwater reserve is largely controlled by the availability of cross-cutting structures and the thickness of weathered horizons. Work by Nel (2001) and Botha and Van Wyk, (1995) on fractured and intergranular granite in the Stella and Louwna districts, respectively, provided matrix transmissivity values of between 100 and 200 m^2/day and fracture transmissivity estimates of 2000 m^2/day. These widely ranging transmissivity values reflect the spatial distribution and morphology of the structural features present, including the thickness of the weathered zone, which varies considerably from place to place.

Borehole yields in this hydrogeological unit vary from 0.1 to 5.0 l/s (Tessema *et al*., 2014). The lower yields are typically associated with areas that demonstrate a lack of hydraulic permeability in their exfoliation fractures. In particular, weathered aquifers associated with very small fracture apertures (width/length ratio) and a lack of interconnection, in which the percolation threshold of the fracture system is not reached, are of little influence to groundwater flow and storage (Stauffer and Aharony, 1994). The influence to groundwater flow and storage is increased with increased fracture interconnectivity. This may be attributed in some areas to a faster rate of weathering, which has proved sufficient enough to initiate loss of cohesion and the formation of interconnected fractures. Moore and Hollyday's (1975) have also suggested that the stronger the surface expression and the longer the lineament, the more significant the lineament is to groundwater. An example of one such higher yielding region occurs in the Middelkop area. Granites in the region are associated with a series of near-horizontal fracture zones at a depth of 20 – 45m, which are responsible for yields of up to 25 l/s (Nel, 2001).

This region with its higher yields and transmissivities is notoriously known for its intensive irrigated agriculture, particularly in Louwna, with its large number of boreholes that are unevenly distributed over the accessible portion of the aquifer. A standard central irrigation pivot of 30 ha generally requires a borehole that can supply approximately 50 l/s (WSU Calculator), which if pumped for 24 hours for a full year would deplete 0.09 % of the total resource and 2.16 % of the recharge potential. Given this rate of abstraction, the total resource would be completely depleted within a year if 1170 irrigation pivots were sited within this aquifer. More than 100 central irrigation pivots were identified in the Louwna area alone (Google Earth), which only occupies a small area of this vast aquifer, suggesting that the current number of irrigation pivots spread across the entire aquifer must be very close to the number required to completely deplete this resource.

After abstraction by agricultural irrigation, the remainder of this resource would need to be shared amongst local communities and livestock farmers, which means that if this aquifer is to be utilised sustainably, the remaining boreholes would ideally need to be evenly distributed over this relatively large surface area. This may prove quite challenging, which compels a person to call for stricter controls on the volume of water abstracted by irrigated agriculture, in so doing protecting the aquifer and ensuring its use for future generations. If unexploited, this aquifer should be able to sustainably meet the current needs of local communities and livestock farmers. The groundwater levels are also sufficiently shallow, making this resource well sought after, particularly by communities that can only access groundwater using a hand pump.

9.3.2.3 Fractured Sedimentary Rocks

The fundamental characteristic of fractured rock aquifer systems is their extreme spatial variability in hydrogeological properties and, therefore, groundwater flow regimes (Cook, 2003). The transmissivity of a fractured rock aquifer can vary widely over short distances, both with depth below surface and laterally across the aquifer, which makes it extremely difficult to characterize. This spatial variability can also been seen across the different fractured sedimentary units identified within the study area, the details of which are discussed below.

Asbestos Hills Subgroup: The transmissivities associated with the banded iron formations/shales of the Asbestos Hills Subgroup typically range between 5 – 50 m^2/d, with borehole yields of between 1.0 – 5.0 l/s being recorded (Golder Associates, 2014). Drilling has indicated, however, that the contact between dolomite and banded iron formations forms a reliable, higher yielding secondary aquifer (Van Dyk, 1993). Where boreholes are located adjacent to regional fault zones, dolerite intrusions, or on limbs of folds where changes in bedding dip occur, the yield is also generally found to be significantly higher than the yields of boreholes located where no structural deformation can be observed (Sami, 1996). In particular, a geophysical investigation of this region by Golder Associates (2014), recognised the N-S striking thrust faults along the western margin of the Asbestos Hills Subgroup as the best targets for groundwater abstraction (Figure 5.7), as these geological structures could act as preferential groundwater flow paths. The importance of dolerite dykes was also investigated, as the intrusion of dolerite typically creates zones of local metamorphism at the contact zones, which can also create fractures on both sides of the dolerite body. The weathering of these zones is an important process that enhances the permeability of the lithological unit, yielding exploitable quantities of groundwater (Nel *et al*., 2014). In particular, yields of between 6 and 30 l/s were recorded in shale and BIF bedrock where intruded by dolerite dykes (Golder Associates, 2014), with transmissivities of over 100 m^2/d recorded in places.

The nature of most fractured rock aquifers is that the water residing in these aquifers is generally abstracted at a relatively low yield. For any single borehole operating at 2.0 l/s continuously for a year, only 0.06 % of the resource would be utilised, necessitating a large number of boreholes to be spread over a very wide area to access the entire resource. Given the small surface area of this aquifer and the associated rugged terrain, this may prove impractical. Knowing that the yield associated with structural features is generally found to be significantly higher than the yields of boreholes located where no structural deformation can be observed, it may be felt that regional groundwater abstraction schemes should give preference to well-known structures in the region. It must be noted, however, that transmissivity and borehole drilling yields on major structural features vary significantly at both local and regional scales, dependent largely on the regional interconnection of fractures. If the fracture network is not well connected, the groundwater in these structural features (faults and dykes), which are not conduits for large-scale groundwater flow, will be depleted and the water will be drawn largely from the relatively limited storage within the aquifer (Dondo *et al*., 2010).

Olifantshoek Supergroup: The quartzites and shales of the Olifantshoek sequence are typically associated with low transmissivity values of 20 - 40 m^2d (Dondo *et al*., 2010). Similarly, the borehole yields are low and range in value from 0.1 to 2.0 l/s, with high yielding boreholes (> 2.0 l/s) proving rare (Van Veelen *et al*., 2009). Although not regarded viable for large-scale exploitation (irrigation, urban cities), a redeeming feature of the low transmissivities associated with this hard rock aquifer is that it makes small quantities of water available (31536 m^3/a) in the dug wells or boreholes spread across the aquifer. These quantities are suitable for drinking purposes, with farmers able to water their livestock without causing harmful mutual interference (Kovalevsky *et al*., 2004). The low transmissivities also help in retarding the outflow and regulating the availability of water in individual wells, so much so that the aquifer is able to sustain abstraction through inter-annual variations in recharge i.e. drought.

Dwyka Group: Transmissivity values of the Dwyka Group are typically less than 5 m^2/d, with values of up to 22 m^2/day being recorded in boreholes located adjacent to structural features, such as dykes (Dondo *et al*., 2010). Borehole yields are generally low and range from 0.1 to 2.0 l/s (Van Veelen *et al*., 2009), with higher yields of 2.0 – 5.0 l/s typically occurring in those tillites located adjacent to dykes (Dondo *et al*., 2010). These low yields show that the ability to transmit water within the host formation is limited. This and the saline water commonly associated with this lithological unit make it a poor aquifer, not regarded to be viable for exploitation of groundwater.

9.3.2.4 Karstified Sedimentary Rocks

Based on numerous pump tests conducted within the dolomites of the study area, an average transmissivity of 200 m^2/d was assigned to this hydrogeological unit (Godfrey and Van Dyk, 2002; Van Veelen *et al*., 2009). The spatial arrangement of the groundwater flow systems in karstified rocks, however, differs from locality to locality and is controlled by the geological and morphological evolution of the rocks (Geyh, 2001). The structural and tectonic history of the region also plays a significant role in determining the behaviour of carbonate aquifers. Major structural deformations (faulting) and intrusions (dykes), as well as impervious sedimentary layers (carbonaceous shale and quartzite), within the limestones and dolomites divide this hydrogeological unit into semi-autonomous groundwater units or “compartments”, each of differing hydrogeological character i.e. transmissivity. Variations in the chert content of the dolomite can also largely influence its hydrogeological character, with transmissivity estimates of between 50 and 80 m^2/d recorded for chert poor zones and 800 to 8000 m^2/day recorded for chert rich zones (Nel *et al*., 2014).

The dolomites in the study area are characterised by typical yields of between 0.5 - 5 l/s (Van Dyk, 2005). It seems that the lower yields are typically associated with channel systems that are poorly interconnected and partly obstructed. Weathering of the dolomite may have been limited by overburden, with aquifer characteristics becoming poor with depth (Cobbing *et al*., 2014). Higher yielding boreholes (> 10 l/s) are also recorded in the study area (Golder Associates, 2014). They are typically located against barriers, such as dykes and impervious sedimentary layers within the dolomite, which impound the aquifers (Martini, 2006). While dykes and faults are of importance in karstic carbonate rocks, a study by Tessema *et al*. (2012)

revealed that the presence of dissolution channels within karstified carbonate rocks is more important than lineament-intersection frequency for groundwater flow and storage. As such, in pursuit of higher yielding boreholes, the boreholes should be sighted within permeable carbonate rocks with interconnected channel systems, the discovery of which may prove challenging in this arid region.

The dolomitic aquifers are probably the only areas within the study area where recharge can fully be exploited, where abstractability and potential are of the same magnitude (Middleton and Bailey, 2008). Caution should, however, be exercised within these regions over how much of the groundwater can in fact be abstracted to ensure sustainable groundwater exploitation. Due to the large transmissivities, particularly in relation to structures, it could prove quite easy to draw water tables down on a regional scale. This was noted in the Tosca area (Van Dyk, 2005), where regional water levels in the Kalahari sediments were impacted i.e. depleted by increased abstraction from the underlying dolomitic aquifers.

Although this area shows potential for higher yielding boreholes (> 5 l/s), it is firmly believed that pumping rates should probably not exceed 5 l/s. A borehole with a pumping rate of 5 l/s will only deplete 0.49 % of the recharge potential in a year. This seems minor in relation to the entire resource available, however, the problem with these aquifers is that due to their high transmissivities, they cannot sustain abstraction through periods of drought, there being no natural regulation to their outflow. Limited recharge can pose a serious problem, with the aquifers lifetime being shortened to 2 years, with the previous year's entire recharge resource being depleted if the same abstraction rate is maintained by 100 boreholes.

This is further aggravated by the fact that the aquifers are compartmentalised, which means that a borehole sited within a particular compartment will only have access to that volume of water stored in the compartment. If there is no interconnectivity between compartments, the groundwater in this compartment will be depleted quickly during periods of drought as the borehole will be unable to draw more water from the overall resource. The delineation of dykes that may compartmentalize dolomite aquifers is, therefore, critical to ensure sustainable use. The distribution of dykes encountered within the karstic aquifer is presented in Figure 5.7, from which specific compartments can be distinguished.

9.3.2.5 Intergranular Sedimentary Rocks

Transmissivity values of between 4 and 70 m^2/day are expected for this hydrogeological unit, with an average of 25 m^2/day having been reported (Nel *et al*., 2014). The variability of these values depend on the combination of sediment type present at a particular site, ranging from boulders, through to sand to clay size particles, with an increase in the latter resulting in poorer transmissivities. Similarly, borehole yields for this aquifer type also depend on particle size distribution and sorting, with borehole yields ranging from 0.1 to 2.0 l/s, with the sandstones of the Eden Formation recording some of the higher borehole yields (Tessema *et al*., 2012; Golder Associates, 2014). The borehole yield corresponding to the lower two Kalahari Group formations, namely the Wessel and Budin Formations, are much lower due to the lack of primary porosity (Tessema *et al*., 2012), with the formations found to commonly contain brackish to saline water, particularly when in contact with saline water from the Dwyka Group (Levin, 1980).

The Kalahari Group aquifers, although not of the highest yielding aquifers, are an important source of water in this semi-arid region, particularly where faulting has lowered the Kalahari Group of rocks below the water table (Simmonds and Smalley, 2000). The faults themselves, however, do not seem to have a significant influence on borehole yield. A statistical correlation between borehole yield and lineament density in the Kalahari Group did not show the influence of lineaments on borehole productivity (Tessema *et al*., 2012). Of importance to groundwater potential, however, seems to be the proximity of the Kalahari sediments to river channels, with moderate to good groundwater potential zones found close to the Molopo River. Very little groundwater is available from this formation away from the river, where the thickness of the sediments decrease (Godfrey and Van Dyk, 2002).

While of significant potential (5131.98 x 10^6 m^3/a), strategies to utilise the Kalahari aquifers for irrigation or rapidly increasing towns may prove unsuccessful. Their low transmissivities restrict possibilities to access this excess water, with an excessive number of low yielding boreholes required for such abstraction, making this impractical and uneconomical. Even those regions of greater potential close to the Molopo River, which can accommodate higher yielding boreholes, are often far from population centres, also making them costly to develop. Depth to groundwater is another important factor controlling accessibility and cost of accessing this groundwater. These aquifers typically associated with their deep water levels (> 50m) will not be able to be accessed easily by a hand pump. At depths greater than 100 m the cost of borehole drilling increases significantly due to the requirement of more sophisticated drilling equipment (MacDonald *et al*., 2012).

Large scale abstraction aside, for many users (farmers and local communities) the Kalahari aquifers have proven essential to their livelihood, the supply of water proving sufficient to meet their needs. A redeeming quality of the Kalahari aquifers is that, in this arid area, where recharge is low and groundwater tables are deep, the groundwater flow is relatively steady. This hydrogeological unit contains sufficient storage to provide a natural buffer against climate variability and is, therefore, able to sustain abstraction through inter-annual variations in recharge and through periods of drought. In the absence of recharge and given an average borehole yield of 1.0 l/s, the total resource would be able to sustain abstraction from 10000 boreholes for a total of 16 years.

Where in hydraulic connectivity with the underlying aquifers, particularly that of dolomite, the storage capabilities of the Kalahari may prove useful. The storage capabilities of the Kalahari Group are more than twice that of dolomite (Table 9.1), which means that during times of significant recharge the Kalahari sediments may be able to store excess water derived from the high yielding dolomites. This can also work to its disadvantage, as noted above, where regional water levels in the Kalahari sediments can be depleted by increased abstraction from the underlying dolomitic aquifers.

10. DISCUSSION

In an attempt to quantitatively and spatially characterise the groundwater resource in the region, all of the hydrogeological factors at play were examined, integrating existing research with that already known. The geology of the region, structural controls, water quality and recharge history were among the most important controlling factors that were examined. Environmental isotope methods were also employed in an attempt to identify the provenance of different water masses, their transport and interconnectivity. The interplay of all these various factors gave rise to the identification of complex hydrogeological environments within the study area, with the generation of appropriate quantitative estimates of potential for each of the aquifers identified, a summary of which is discussed below. Differences in their fracture set populations, coupled with contrasts in aquifer transmissivity, effective porosity and saturated thickness have significantly contributed to the variability in groundwater potential values calculated for each of the aquifer units identified. This information has also allowed for the implementation of strategies as to how each resource can adapt to growing water demand associated not only with population growth, but also with climate variability and change.

10.1 Fractured Basement Aquifers (volcanic and meta-sedimentary)

Much of the south-eastern portion of the study area, which is dominated by the basement aquifers of the Kraaipan - Amalia greenstone terrane and the Ventersdorp Supergroup, offer poor prospects of securing large volumes of groundwater. These rocks have limited porosity, with the groundwater primarily confined to their fracture systems. Given their vast geological past, the depth to which they and their associated fracture systems are regarded as being permeable (saturated thickness) is also restricted. This, in combination with their small surface area, accounts for the lower storage volumes and resource potential values calculated for these aquifers. While generally restricted, some high borehole yields have been recorded for these aquifers, typically associated with the intersection of the NE-SW and NW-SE striking lineaments located in this portion of the study area, the yield presumably enhanced by fracture connectivity. While it would seem unwise to drill a large number of these high yielding production boreholes in these regions, given the small storage volume of this hydrogeological unit, the limited storage of these aquifers can prove useful and highly significant in this arid region, proving adequate for use by livestock farmers and rural households.

While the inability of these aquifers to store large volumes of groundwater is understood, these aquifers offer some of the best recharge areas within the study area, particularly the fractured sediments of the Kraaipan - Amalia greenstone terrane. Their isotopic signature seems to suggest that recharge is taking place from the surrounding high ground, where surface and structural controls are responsible for the regional hydraulic continuity. Under favourable conditions these aquifers may also recharge the adjacent granitic aquifers, where local structures enable limited lateral and vertical displacement.

The isotopic data support the idea of sporadic or eventful recharge in the area, with the recharge occurring directly from precipitation with minimal impact from evaporative fractionation. These outcropping lithologies are rarely covered by thick deposits of Kalahari sediments, with available fractures allowing for fast percolation of rainwater prior to the modification of its isotopic composition. The recently infiltrated water, which tends to be relatively shallow in recharge areas, is also characterised by groundwater of relatively good quality, with a low TDS content. The only problem with the quality of water from the Kraaipan and Amalia greenstone terrane is the associated low pH (< 6) values in some areas. The pyrite associated with these assemblages is often a source of SO_4^{2-} when oxidised, which ultimately alters the acid-base equilibria in natural waters and results in a reduced acid-neutralising capacity and hence the lowering of the pH.

While of greater areal extent than the other basement aquifers (Kraaipan - Amalia and Ventersdorp), the andesitic lavas of the Griqualand West Sequence also offer a poor prospect of securing large volumes of groundwater. The andesitic lavas generally have limited porosity due to the solid nature of the rock and are largely resistant to the development of secondary porosity. As such, a significant number of low yielding boreholes are typically associated with these andesites, the productivity of which is largely dependent on the nature of the fissure system. These low transmissivities and yields ensure that abstraction remains sustainable, however, they make it impractical to utilise all of the resource available, particularly for supply to cities/towns or agricultural irrigation. These aquifers should, however, prove sufficient for rural community water supplies, if fitted with hand pumps that can be sustained by borehole yields of 0.3 l/s and greater.

10.2 Fractured and Weathered Crystalline Basement Aquifers

The granitic rocks of the Archaean basement within the south-central portion of the study area show favourable resource potential, largely owing to the formation of secondary porosity due to weathering, fracturing and jointing. This hydrogeological unit is typically characterised by unconfined, shallow groundwater circulation in the zone of weathering and fracturing, which only reaches a depth of some 90 metres, covering a thicker zone of groundwater circulation, confined to fractures penetrating much deeper than those structural features usually associated with the weathered crystalline basement rocks. Despite having a shallower and varying depth of saturation, the weathered zone offers the greatest resource potential of the two, typically associated with higher yields. Unfortunately, however, it is this shallow, weathered horizon that is commonly exploited, particularly for intensive irrigated agriculture, which is usually associated with a large number of boreholes that are unevenly distributed over the accessible portion of the aquifer. If this aquifer is to be utilised sustainably, stricter controls need to be placed on the volume of water abstracted by irrigated agriculture, in so doing protecting the aquifer and ensuring its use for future generations.

The groundwater quality within this aquifer unit is also of relatively good quality, typically associated with low TDS contents and neutral pH levels, making this resource even more sought after. Isotopic data suggests that much of the water in this aquifer did not undergo extensive evaporation and may indicate fast recharge through vertical fractures or through highly permeable media. In particular, it appears that this aquifer receives most of its recharge from the outcropping areas of the aquifer (notably the Mosita and Middlekop granites) and nothing from infiltration through the overlying Kalahari sediments. The problem, however, is that more than 70 % of the investigated area is overlain by thicker deposits (> 15 m) of Kalahari sediments and, as confirmed by the tritium values, some portions of this aquifer have not been recently recharged, with any potential recharge being retained in the overlying Kalahari sediments, from where it is lost by evapotranspiration. The groundwater with a longer residence time in the granitic aquifer, with very little associated recharge, is typically characterised by highly mineralised groundwater, elevated with regard to its Na – K content.

10.3 Fractured Sedimentary Aquifers

The Asbestos Hills Subgroup, which comprises banded iron-formation, jaspillite, quartzite, shale and siltstone in a band stretching across the central portion of the study area, is very similar in its hydrogeological properties to that of the Kraaipan - Amalia greenstone terrane, both of which have good quality water, yet limited storage and resource potential. While the inability of this aquifer to store large volumes of groundwater is understood, given that the host rock is considered an aquitard and the associated fractures are generally not conduits for large scale water volumes, this aquifer, as with the Kraaipan - Amalia aquifer, offers some of the best recharge areas within the study area, recharging the underlying dolomite in places as well. The isotopic signature of the Transvaal meta-sediments reflect a more restricted recharge regime, with the relatively narrow range of $\delta^{18}O$ values suggesting that the various recharge points are not very far apart, possibly taking place from the surrounding high ground. The isotopic data also seems to signify direct recharge from precipitation with minimal impact from evaporative fractionation, where surface and structural controls are responsible for the fast percolation of rainwater prior to the modification of its isotopic composition.

Of the fractured sedimentary aquifers in the region, the quartzites of the Olifantshoek sequence offer better estimates of storage and resource potential, however, the values calculated are insignificant compared to that of the other aquifer types in the study area. While offering better quality water, the quartzites are typically associated with low transmissivity values and similarly low borehole yields. Although not regarded viable for large-scale exploitation (irrigation, urban cities), a redeeming feature of the low transmissivities associated with this hard rock aquifer is that it makes small quantities of water available in the dug wells or boreholes spread across the aquifer. These quantities are suitable for drinking purposes, with farmers able to water their livestock without causing harmful mutual interference. The low transmissivities also help in retarding the outflow and regulating the availability of water in individual wells, so much so that the aquifer is able to sustain abstraction through inter-annual variations in recharge i.e. drought.

The Dwyka tillites are buried deep beneath the Kalahari Group of sediments, confined to the same palaeo-valley (adjacent to the Molopo river) as that occupied by the thickest portion of the Kalahari Group. Recharge to these deeply buried sediments is believed to be negligible, similar to the rate at which the overlying Kalahari sediments are recharged. Transmissivity values and corresponding borehole yields are also generally low for this aquifer unit, demonstrating that the ability of the host formation to transmit water is limited. This and the saline water commonly associated with this lithological unit make it a poor aquifer, not regarded to be viable for the exploitation of groundwater.

10.4 Karstic Aquifers

The limestones and dolomites of the Campbell Rand and Schmidtsdrif Subgroups are considered as the most prospective water bearing formations in the study area, supporting not only valuable irrigated agricultural activities, but also underpinning the water supply to several towns, including Vryburg. While the primary porosity and hydraulic conductivity of dolomite is poor, weathering and karstification have made them prolific aquifers, aiding significantly in their resource potential. Since the structural and morphological evolution of the rocks play a significant role in determining the behaviour of carbonate aquifers, varying yields are expected throughout the aquifer, which is commonly divided by dykes/faults into semi-autonomous groundwater units or “compartments”, each of differing hydrogeological character i.e. transmissivity. Although this area shows potential for higher yielding boreholes (> 5 l/s), caution should be exercised over how much of the groundwater can in fact be abstracted, as these aquifers cannot sustain abstraction through periods of drought, there being no natural regulation to their outflow. The dolomitic aquifers are probably the only areas within the study area where recharge can fully be exploited, where abstractability and potential are of the same magnitude.

Many mechanisms of recharge to this aquifer have been suggested, with recharge occurring via geological lineaments (generally faults, less dykes), through shallow outcrop and sub-outcrop of dolomite, through the banded ironstone formations of the Asbestos Hills Subgroup and through the alluvial channels of the Molopo river, when in flood. Although there is isotopic evidence of recharge within this hydrogeological unit, this particular aquifer does not display hydraulic continuity. The isotopic data for the karstic aquifers do not show a clear trend, with many of the $\delta^{18}O$ and δD values spread over the entire range, with some samples plotting above the PLMWL, some plotting below the meteoric water line and others along the evaporation trend line. Their tritium contents are also highly variable (0 – 0.9 TU). This suggests poor water exchange and permeability within the aquifer, which may largely be attributed to the division of this hydrogeological unit into “compartments”, which differ significantly with regard to their isotopic signature. The “compartmentalisation” of this aquifer means that recharge is site specific, the rate and amount depending on the structural controls of that particular compartment.

The groundwater associated with the carbonate (dolomite and limestone) rocks of the Transvaal Supergroup are dominated by a Ca – Mg – HCO_3 hydrochemical facies, which are typically associated with numerous water quality challenges. The presence of soluble calcium and magnesium minerals means that the groundwater is typically "hard". Higher values of pH (> 8) also tend to be associated with these carbonate rocks, since carbonate compounds tend to dominate acid–base reactions in groundwater, with acidic water being "neutralised" by the presence of these compounds. Higher TDS values are also associated with groundwater sourced from the shallow carbonate bedrock, the higher values typically being due to the high solubility of carbonate minerals.

10.5 Intergranular Sedimentary Aquifers

An intergranular sedimentary aquifer that exhibits the most potential in the study area is the sediments of the Kalahari Group. Usually sandstones are suitable aquifers, often proving to be very efficient aquifers as their porosity and permeability are usually high. Inter-fingering layers of clay, as well as calcrete within this hydrogeological unit have decreased the permeability of this unit somewhat, resulting in decreased yields. Nevertheless, the Kalahari Group aquifer remains an important source of water in this semi-arid region, the storage capabilities of which are estimated to be more than twice that of the dolomite. Usually the calculation of storage and resource potential within this aquifer has given precedence to the thicker and deeper deposits, since most of the shallower Kalahari sediments (< 60 m) are rarely utilised within the study area. If the entire sedimentary aquifer, however, was to be taken into consideration, the storage and resource potential of this aquifer is estimated to be almost 1.5 times more than what is currently being exploited at present. This significant storage space can allow groundwater recharge to be stored for several decades, thereby providing a vital buffer against variable climates.

Despite having such great potential, the aquifer is not actively recharged, with portions having been recharged when the climate of the area was wetter. It is obvious from the isotopic data and Chloride Mass Balance calculations that recharge in the areas covered by Kalahari sediments is negligible. Isolated areas of higher recharge are evident, particularly in close proximity to the upper reaches of the Molopo River, where recharge occurs infrequently at times when the river is in flood. At a regional scale, however, recharge via the river bed is of limited importance, with the dominant recharge mechanism being that of local, diffuse recharge, which is typically characterised by poor quantitative estimates. These poor estimates of recharge are largely attributed to the geological nature of the Kalahari Group, with the clay-dominated sands capable of absorbing large volumes of rainwater, but poor at transmitting the water through the unsaturated zone. This leads to a loss of water by evaporation and transpiration by dense vegetation before it percolates and recharges the underlying permeable units. As such, although showing the most potential for storage, exploitation of this resource is restricted.

An additional challenge to utilising this sizeable resource is the poor quality of the groundwater. The highest TDS content of all the boreholes tested in the region are those restricted to the thickest portion of the Kalahari Group, some of which are so high that the groundwater is not suitable for human and livestock consumption. Some fresh water aquifer units seem to be present within the Kalahari aquifer, however, these lenses of fresh water are localised and very limited in extent, occurring mainly along the Molopo River. The water in the Kalahari aquifer is also “hard”, with the water hardness in these regions caused by non-bicarbonate salts, such as chloride, the presence of which is further indicative of highly saline groundwater in the study area. Numerous chemical plots have indicated that the source of salinity in the groundwater of the Kalahari aquifer is heavily influenced by the dissolution of sodium and chloride, both of which were largely derived from intensive evaporation processes. Correlations between stable isotope content and salinity also seem to confirm that evaporation is the main cause of salinisation in these unconfined aquifers of the Kalahari Group.

High bacterial counts (*Enterobacter Aerogens and Proteus Mirabilis*) and uninhibited oxygen degradation curves for boreholes sourcing the Kalahari aquifer are an additional concern. Results, however, seem to point to local contamination effects, rather than the groundwater aquifers themselves being contaminated. Boreholes within the study area are typically situated within or close to watering troughs/feeding pens, within the immediate vicinity of faecal pollution. The coarse, unconfined aquifer of the Kalahari Group are typically porous environments of microorganism size, making them susceptible to groundwater contamination. These factors, coupled with the generally relatively slow movement of groundwater, has resulted in a localised impact, in which the polluted surface water runoff has reached the aquifer, possibly via the borehole itself, and contaminated the groundwater.

11. CONCLUSIONS AND RECOMMENDATIONS

Droughts throughout South Africa have been the phenomena of great concern during the last few years (2012 – 2016), inflicting devastating effects on both the agricultural and local communities. The eastern Kalahari region of South Africa is no exception and is one of those vulnerable areas to be severely affected by drought during the last year (2015 – 2016), with many of the towns and villages in the area faced with water restrictions, including the farmers in the area who have complained of boreholes drying up. The main source of water in this arid region is invariably the groundwater resources, which suffer from pumping rates that often exceed the natural recharge rate, or from human or naturally induced salinisation and pollution. Such groundwater exploitation usually occurs as a result of insufficient knowledge of the hydrogeological processes at work, with the aquifers finite geometry and properties often being ignored. The best way to ensure that an aquifer will not exceed its sustainable yield is to quantitatively and spatially characterise the resource. This was attempted in the study area by examining all of the hydrogeological factors at play, integrating existing research with that already known, all aimed at understanding the resource potential of the region.

The study area can be divided into zones of high and low potential. The low potential zones, as defined by the Resource Potential calculations, are represented by the fractured basement volcanic (Kraaipan - Amalia greenstone terrane, Ventersdorp volcanics and Ongeluk lavas) and fractured sedimentary aquifers (Asbestos Hills meta-sediments, Olifantshoek quartzites and Dwyka tillites). These may be regarded as minor aquifer systems, formations with negligible permeability that are generally regarded as not containing groundwater in exploitable quantities. The water quality of some of these aquifers is such that it renders the aquifer unusable. While these aquifers offer poor prospects of securing large volumes of groundwater, they offer some of the best recharge areas within the study area, recharging the adjacent karstic and granitic aquifers.

Although of great resource potential, with significant storage space to allow groundwater recharge to be stored for several decades, the sediments of the Kalahari Group also represent a poor to minor aquifer system. The water quality is variable, with some water proving so saline that it is not suitable for human and livestock consumption. The aquifer also rarely produces large quantities of water, the recharge of which is minimal. As such, although showing the most potential for storage, exploitation of this resource is restricted.

High zones of potential include the weathered crystalline basement and karstic aquifers, both of which may be regarded as major aquifer systems. These are characterised by highly permeable formations, with a known presence of significant fracturing that are highly productive and able to support large abstractions for public supply and other purposes. Unfortunately, however, it is these aquifers that are commonly exploited, particularly for intensive irrigated agriculture. If they are to be utilised sustainably and their use ensured for future generations, stricter controls need to be placed on the volume of water abstracted. Additional caution needs to be exercised when utilising the karstic aquifers. Despite being of favourable potential, the karstic aquifers do not display hydraulic continuity, with poor water exchange between compartments, resulting in variations in yield and the amount of recharge available. Unlike the Kalahari, these aquifers cannot sustain abstraction through periods of drought, there being no natural regulation to their outflow, as such, care must be taken on how much of the groundwater can in fact be abstracted from this aquifer

It is important to note that there are numerous factors that play a significant role in determining the behaviour of each aquifer type. While some generalisations had to be made, it must be noted that the range of variation among so many interdependent and independent factors is so wide that the same aquifer will not always exhibit identical characteristics. Strategies to use groundwater from a particular aquifer should, therefore, not be based upon expectation, but should rather recognise that a detailed knowledge of the local groundwater conditions is required. As such, a detailed hydrogeological investigation is suggested for any areas of interest, one which should unravel the unique hydrogeological controls governing groundwater movement in that particular area. Since the most important and common controlling factor of groundwater occurrence and potential in the study area appears to be the presence of structural features and their connectivity, any exploration targets or abstraction schemes should give preference to the identified structures within the area.

Knowledge of the quality of groundwater in the study area should also guide future exploration and abstraction schemes. Besides the presence of sulphate, typically associated with the pyrites of the Kraaipan - Amalia greenstone terrane, chloride and its associated high TDS content in the unconfined sediments of the Kalahari Group seem to be the largest negative factor influencing the quality of water in the region. This impacts negatively on livestock production and has serious implications on soil quality, with the salinisation of soils reducing the carrying capacity thereof and eventually rendering it unproductive. If salinity levels become such that additional treatment is required then this will add cost to such operations, having further implications on food affordability and security. As such, a detailed analysis of the water quality for any areas of interest should be conducted, creating awareness on how to better use, manage and protect the groundwater without adversely affecting its future quality.

The shallow, intergranular sediments of the Kalahari Group are the most vulnerable to surface contamination, with some of the groundwater samples showing elevated nitrate and microbiological content. Given the associated health risks, it is essential that faecal pollution of the groundwater sources be addressed and appropriate action be taken by adhering to a few fundamental groundwater management aspects. Aside from treating the water, which may prove impractical given the large volumes required daily for the watering of livestock, protection can be achieved by equipping any vulnerable boreholes with a sanitary seal and by preventing unnecessary access to the boreholes by animals and people (Murray *et al*., 2007).

The uncertainties of water quality aside, the estimated groundwater storage and resource potential within the study area represents a water resource that is of a different magnitude to all other freshwater resources in the area. It must be emphasised that the volume of groundwater estimated gives an indication of the availability and distribution of groundwater resources on a regional scale. Detailed studies are still required to quantify, develop and exploit individual groundwater abstraction schemes. Nevertheless, groundwater without a doubt offers a major source of water to this semi-arid region that, if properly managed, could be economically, effectively and sustainably utilised. The emphasis is placed on "sustainably utilised", as groundwater in this region is not invulnerable to degradation and exploitation. Areas of over-exploitation (Louwna and Tosca agricultural irrigation schemes), where groundwater development seems to exceed declining levels of recharge, have already been identified. The key challenge relates to the management of the resource, with all role players involved in this complex system working together to achieve the goal of maintaining the quality of the water and ensuring that it is used sustainably, protecting it for future generations.

12. REFERENCES

Abiye, T. A. (ed), 2013: *The use of isotope hydrology to characterize and assess water resources in South(ern) Africa*, Water Research Commission, Pretoria, WRC Report No. TT 570/13, 211 pp.

Abiye, T. A., 2015: Introduction to hydrogeology – Lecture Notes, School of Geosciences, University of the Witwatersrand, Johannesburg.

Alker, M., 2008: The Stampriet artesian aquifer basin. In Scheumann, W. and Herrfahrdt-Pahle, E., (eds): *Conceptualizing co-operation for Africa's transboundary aquifer systems*, German Development Institute, pp 165 – 203.

Altermann, W. and Hälbich, I. W., 1991: Structural history of the southwestern corner of the Kaapvaal Craton and the adjacent Namaqua realm: new observations and a reappraisal, *Precambrian Research*, 52, pp. 133-166.

Altermann, W. and Siegfried, H. P., 1997: Sedimentology and facies development of an Archaean shelf: carbonate platform transition in the Kaapvaal Craton as deduced from a deep borehole at Kathu, South Africa, *Journal of African Earth Sciences*, 24 (3), pp. 391-410.

Andreoli, M. A. G., Ashwal, L. D., Smith, C. B., Webb, S. J., Tredoux, M., Gabrielli, F., Cox, R. M., Hambleton-Jones, B. B., 1995: The impact origin of the Morokweng ring structure, southern Kalahari, South Africa, *Centennial Congress*, Geological Society of South Africa, Johannesburg, Abstracts, 1, pp. 541-544.

Anhaeusser, C. R., 2006: Ultramafic and mafic intrusions of the Kaapvaal craton. In Johnson, M. R., Anhaeusser, C. R. and Thomas, R. J. (eds): *The Geology of South Africa*, Geological Society of South Africa/Council for Geosciences, pp 95 - 134.

Anhaeusser, C. R. and Walraven, F., 1997: Polyphase crustal evolution of the Archaean Kraaipan granite-greenstone terrane, Kaapvaal Craton, South Africa, *Inform. Circ. Economic Geology Research Institute,* University of the Witwatersrand, Johannesburg, No. 313, 27 pp.

Anhaeusser, C. R. and Walraven, F., 1999: Episodic granitoid emplacement in the western Kaapvaal Craton: Evidence from the Archaean Kraaipan granite-greenstone terrane, South Africa, *Journal of African Earth Sciences*, Vol. 28 (2), pp 289 – 309.

Anhaeusser, C. R., Stettler, E., Gibson, R. L. and Cooper, G. R. J., 2010: A possible Mesoarchaean impact structure at Setlagole, North West Province, South Africa: Aeromagnetic and field evidence, *South African Journal of Geology*, Vol. 113.4, pp 413 – 436.

APHA, 1998: *Standard Methods for the examination of water and wastewater (20th Ed)*, American Public Health Association, Washington DC.

Armstrong, R. A., 1987: *Geochronological studies on Archaean and Proterozoic formations of the foreland of the Namaqua Front and possible correlates on the Kaapvaal Craton*, Unpublished PhD thesis, University of the Witwatersrand, Johannesburg, South Africa, 274 pp.

Astier, R. J., 1987: The development of crystalline basement aquifers in a tropical environment, *Quaternary Journal of Engineering Geology*, 20, pp. 265 – 272.

Baron, J., Seward, P. and Seymour, A., 1998: *The groundwater harvest potential map of the Republic of South Africa*, Technical Report GH 3917, Directorate Geohydrology, Department of Water Affairs and Forestry, Pretoria, 19 pp.

Bean, J. A., 2003: *A critical review of recharge estimation methods used in southern Africa*, Unpubl. PhD Thesis, Faculty of Natural and Agricultural Sciences, Department of Geohydrology, University of the Free State, Bloemfontein, South Africa.

Bean, J., Van Tonder, G. and Dennis, I., 2004: A new method for the estimation of episodic recharge. In Stephenson, D., Shemang, E. M. and Chaoka, T. R. (eds): *Water resources of arid areas*, Taylor and Francis Group, London, ISBN 04 1535 913 9, pp 92 – 98.

Beekman, H. E. and Xu, Y., 2003: Review of groundwater recharge estimation in arid and semi-arid southern Africa. In Xu, Y. and Beekman, H. E. (eds): *Groundwater recharge estimation in Southern Africa*, UNESCO IHP Series No. 64, UNESCO Paris, ISBN 92-9220-000-3, pp 3 – 16.

Beukes, N. J., 1979: Litostratigrafiese onderverdeling van die Schmidtsdrif-Subgroep van die Ghaap-Groep in Noord-Kaapland, *Transactions of the Geological Society of South Africa*, 82, pp. 313 – 327.

Beukes, N. J., 1980: Lithofacies and stratigraphy of the Kuruman and Griquatown iron-formations, Northern Cape Province, South Africa, *Transactions of the Geological Society of South Africa*, 83, pp 69 - 86.

Beukes, N. J., 1984: Sedimentology of the Kuruman and Griquatown iron-Formations, Transvaal Supergroup, Griqualand West, South Africa. *Precambrian Research*, 24, pp. 47-84.

Beukes, N. J., 1986: The Transvaal Sequence in Griqualand West. In Anhaeusser, C. R. and Maske, S. (eds): *Mineral Deposits of Southern Africa*, Geological Society of South Africa, Johannesburg, pp. 819-828.

Beukes, N. J. and Smit, C. A., 1987: New evidence for thrust faulting in Griqualand West, South Africa: implications for stratigraphy and the age of red beds, *South African Journal of Geology*, 90, pp. 378 - 398.

Bezuidenhout, C. C. and the North-West University Team, 2013: *A large-scale study of microbial and physico-chemical quality of selected groundwaters and surface waters in the North West Province, South Africa*, Water Research Commission, Pretoria, WRC Report No TT 1966/1/13, 175 pp.

Bredenkamp, D. B., Botha, L. J., Van Tonder, G. J. and Van Rensburg, H. J., 1995: *Manual on quantitative estimation of groundwater recharge and aquifer storativity*, Water Research Commission, Pretoria, 407 pp.

Bootsman, C. S., 1998: *The evolution of the Molopo drainage*. Unpublished PhD Thesis, University of the Witwatersrand, Johannesburg, South Africa, 262 pp.

Botha, L. J. and Bredenkamp, D. B., 1992: *Quantitative estimation of recharge and aquifer storativity of the Louwna – Coetzersdam aquifer system*, Department of Water Affairs, Pretoria, Report No. GH 3786, 25 pp.

Botha, L. J. and Van Wyk, E., 1995: Louwna – Coetzersdam: Re-evaluation of groundwater potential, Department of Water Affairs, Pretoria, Report No. GH 3860, 7 pp.

BRGM, 1993: *Mmamabula groundwater resources investigation phase II - Khurutshe area*, Appendix 4: Recharge Study, Department of Geological Survey, Botswana.

Burke, K., Kidd, W. S. F., Kusky, T. M., 1985: Is the Ventersdorp system of southern Africa related to continental collision between the Kaapvaal and Zimbabwe cratons at 2.64 Ga ago?, *Tectonophysics*, 115, pp. 1 - 24.

Butler, M. J., Malinga, O. H. T. and Mabitsela, M., 2015: *Environmental isotope analysis on twenty (20) water samples collected in the eastern Kalahari region, South Africa*, Environmental Isotope Laboratory, iThemba Laboratories, Johannesburg, Report No. WGEO038, 5 pp.

Clark, I. D. and Fritz, P., 1997: *Environmental isotopes in hydrology*, Lewis, New York, 328 pp.

Cobbing, J., Eales, K., Gibson, J., Lenkoe, K. and Rossouw, T., 2014*: An appraisal of diverse factors influencing long-term success of groundwater schemes for domestic water supplies, focusing on priority areas in South Africa*, Water Research Commission, Pretoria, WRC Report No. TT 2158/1/14, 152 pp.

Connelly, R. J., Abrams, L. J. and Schultz, C. B., 1989: *An Investigation into rainfall recharge to groundwater*, Water Research Commission, Pretoria, WRC Report No. TT 149/1/89, 188 pp.

Cook, P. G., 2003: *A guide in regional groundwater flow in fractured aquifers*, CISRO Technical Report, CSIRO Glen Osmond Land and Water, South Australia, pp. 1 – 5.

Cornell, D. H., 1987: Stratigraphy and petrography of the Hartley Basalt Formation, northern Cape Province, *South African Journal of Geology*, 90, pp. 7 – 24.

Cornell, D. H., Armstrong, R. A. and Walraven, F., 1998: Geochronology of the Hartley Formation, South Africa: Constraints on the Kheis tectogenesis and the Kaapvaal Craton's earliest Wilson Cycle, *Journal of African Earth Sciences*, 26, pp 5 – 27.

Cornell, D. H., Schutte, S. S. and Eglington, B. L., 1996: The Ongeluk basaltic andesite formation in Griqualand West, South Africa: submarine alteration in a 2222 Ma Proterozoic sea, *Precambrian Research*, 79, pp. 101-123.

Corner, B., Reimold, W. U., Brandt, D. and Koeberl, C., 1996: Morokweng impact structure, North West Province, South Africa: Geophysical imaging and shock petrographic studies, *Earth Planetary Science Letters*, 146, pp 351 – 364.

Craig, H., 1961: Isotopic variations in meteoric waters, *Science*, 133, pp. 1702–1703.

De Villiers, P. R. and Visser, J. N. J., 1977: The glacial beds of the Griqualand West Super Group as revealed by four deep boreholes between Postmasburg and Sishen, *Transactions of the Geological Society of South Africa*, 80, pp. 1-8.

De Vries, J. J., Selaolo, E. T. and Beekman, H. E., 2000: Groundwater recharge in the Kalahari, with reference to paleo-hydrologic conditions, *Journal of Hydrology*, 238, pp 110 – 123.

Dondo, C., Chevallier, L., Woodford, A. C., Murray, R., Nhleko, L. O., Nomnganga, A. and Gqiba, D., 2010: *Flow conceptualisation, recharge and storativity determination in Karoo aquifers, with special emphasis on Mzimvubu – Keiskamma and Mvoti - Umzimkulu water management areas in the*

Eastern Cape and KwaZulu-Natal provinces of South Africa, Water Research Commission, Pretoria, WRC Report No. 1565/1/10, 250 pp.

Du Preez, M., Van der Merwe, M., Le Roux, W., Nel, J., Meyer, R., Murray, K., Paramoer, E., Steyl, G. and Velly, C., 2013: *Investigation of the fate and transport of selected microorganisms in two simulated aquifer conditions in the laboratory and in the field*, Water Research Commission, Pretoria, WRC Report No. TT 1905/1/12, 131 pp.

Du Toit, A. L., 1954: *The Geology of South Africa (3rd ed.)*, Oliver and Boyd, Edinburgh.

DWAF: Department of Water and Forestry, 1996: *South African water quality guidelines, Volume 1: Domestic use,* 2nd Edition, DWAF, Pretoria, South Africa, 175 pp.

DWAF: Department of Water Affairs and Forestry, 2006: *Groundwater Resources Assessment II*, Task 1 – 5, Version 2, DWAF, Pretoria, South Africa.

DWAF: Department of Water Affairs and Forestry, 2009: *Intermediate Reserve Determination Study for the Integrated Vaal River System: Lower Vaal Water Management Area, Groundwater Component,* Compiled by Raath, C. J. D (AGES) for DWAF, Pretoria, 168 pp.

Eglington, B. M. and Armstrong, R. A., 2004: The Kaapvaal Craton and adjacent orogenism southern Africa: A geochronological database and overview of the geological development of the craton, *South African Journal of Geology*, Vol 107, No.1/2, pp 13 – 32.

Eriksson, P. G., Altermann, W. and Hartzer, F. J., 2006: The Transvaal Supergroup and its Precursors. In Johnson, M. R., Anhaeusser, C. R. and Thomas, R. J. (eds): *The Geology of South Africa*, Geological Society of South Africa, Johannesburg/Council for Geoscience, Pretoria, pp. 237 - 260.

Fitts, C. R., 2002: *Groundwater Science*, Academic Press, London, 452 pp.

Foster, S. S. D., Bath, A. H., Farr, J. L. and Lewis, W. J., 1982: The likelihood of active groundwater recharge in the Botswana Kalahari, *Journal of Hydrology*, 55, pp 113 – 136.

Frakes, L. A. and Crowell, J. C., 1970: Late Palaeozoic Glaciation: III Africa exclusive of the Karoo Basin, *Bulletin of the Geological Society of America*, 81, pp. 2261-2286.

Froehlich, K., Aggarwal, P. K. and Garner, W. A., 2007: An integrated approach in evaluating isotope data of the Nubian Sandstone Aquifer System (NSAS) in Egypt (IAEA–CN–151/167). In: *Advances* *in isotope hydrology and its role in sustainable water resources management (IHS-2007)*, Vol 1, International Atomic Energy Agency, Vienna, Austria, pp. 31 – 46.

Geoflux, 1993: *Toteng/Sehitwa TGLP groundwater resources investigation*, Department of Geological Survey, Botswana.

Geyh, M. (Ed), 2001: Groundwater saturated and unsaturated zone, *Environmental Isotopes in the Hydrological Cycle: Principles and Applications,* Vol. 4, International Atomic Energy Agency and United Nations Educational, Scientific and Cultural Organization, pp. 308 – 424.

Gibbs, R. J., 1970: Mechanism controlling world water chemistry, *Science*, Vol. 170, pp. 1088 – 1090.

Godfrey, L. and Van Dyk, G., 2002: *Reserve determination for the Pomfret - Vergelegen dolomitic aquifer, North West Province*, Department of Water Affairs, Pretoria, Report No ENV-P-C 2002-031, 26 pp.

Golder Associates, 2014: *Groundwater assessment and development for the Vaal Gamagara Pipeline Scheme - SD4 Area*, Golder Associates Africa (Pty) Ltd, Pretoria, Report Number 11613568-12578-03, 93 pp.

Gould, D., Rathbone, P. A., Kimbell, G. S., 1987: The geology of the Molopo Farms Complex, southern Botswana, *Geological Survey of Botswana*, Bulletin, 23, 178 pp.

Grabow, W. O. K., Müller, E. E., Ehlers, M. M., De Wet, C. M. E., Uys, M. and Clay, C. G., 2003: *Occurrence of Ecoli 0157:H7 and other pathogenic Ecoli strains in water sources intended for direct and indirect human consumption*, Water Research Commission, Pretoria, WRC Report No. 1068/1/03, 80 pp.

Grobbelaar, W. S., Burger, M. A., Pretorius, A. I., Marais, W., Van Niekerk, I. J. M., 1995: Stratigraphic and structural setting of the Griqualand West and the Olifantshoek Sequences at Black Rock, Beeshoek and Rooinekke Mines, Griqualand West, South Africa, *Mineralium Deposita*, 30, pp. 152 - 161.

Grobler, N. J. and Botha, B. J. V., 1976: Pillow-lavas and hyaloclastic in the Ongeluk Andesite Formation in a road-cutting west of Griquatown, South Africa, *Transactions of the Geological Society of South Africa*, 79 (1), pp. 53-57.

Gupta, S. K. and Deshpande, R. D., 2005: Groundwater isotopic investigations in India: What has been learned?, *Current Science*, 89, pp. 825-835.

Haddon, I. G., 2005: *The sub-Kalahari geology and tectonic evolution of the Kalahari basin, Southern Africa*, University of the Witwatersrand, Johannesburg, PhD thesis, 343 pp.

Haddon, I. G. and McCarthy, T. S., 2005: The Mesozoic - Cenozoic interior sag basins of Central Africa: The Late-Cretaceous - Cenozoic Kalahari and Okavango basins, *Journal of African Earth Sciences,* 43, pp 316 – 333.

Hälbich, I. W., Scheepers, R., Lamprecht, D., Van Deventer, J. L., De Kock, N. J., 1993: The Transvaal-Griqualand West banded iron formation: geology, genesis, iron exploitation, *Journal of African Earth Sciences*, 16 (1,2), pp. 63-120.

Hart, R. J., Andreoli, M. A. G., Tredoux, M., Moser, D., Ashwal, L. D., Eide, E. A., Webb, S. J., Brandt, D., 1997: Late Jurassic age for the Morokweng impact structure, southern Africa, *Earth and Planetary Science Letter*, 147, pp. 25-35.

Hartzer, F. J., 1998: *A stratigraphic table of the SADC countries*, Council for Geoscience, Pretoria, South Africa.

Hem, J. D., 1985: *Study and interpretation of the chemical characteristics of natural water (3rd Ed.)*, U.S. Geological Survey, Water Supply Paper 2254.

Henkel, H., Reimold, W. U. and Koeberl, C., 2002: Magnetic model of the Morokweng impact structure, North West Province, South Africa, *Journal of Applied Geophysics*, 49, pp. 129 – 147.

Holland, M., 2011: *Hydrogeological characterisation of crystalline basement aquifers within the Limpopo Province, South Africa*, PhD Thesis, University of Pretoria, 163 pp.

Holland, M., 2012: Evaluation of factors influencing transmissivity in fractured hard-rock aquifers of the Limpopo Province, *Water SA*, Vol. 38, No. 3, pp. 379 – 390.

Hunter, D. R. and Reid, D. L., 1987: Mafic dyke swarms in southern Africa. In Halls, H. C. and Fahrig, W. F. (eds): Mafic dyke swarms, *Special Paper Geological Association of Canada*, 34, pp. 445 – 456.

Hunter, D. R., Johnson, M. R., Anhaeusser, C. R. and Thomas, R. J., 2006: Introduction. In Johnson, M. R., Anhaeusser, C. R. and Thomas, R. J. (eds): *The Geology of South Africa*, Geological Society of South Africa/Council for Geosciences, pp 1 - 7.

Jahn, B., Bertrand-Sarfati, J., Morin, N. and Mace, J., 1990: Direct dating of stromatolitic carbonates from the Schmidtsdrif Formation (Transvaal dolomite), South Africa, with implications on the age of the Ventersdorp Supergroup, *Geology*, 18, pp. 1211-1214.

Jones, I. M. and Anhaeusser, C. R., 1991: The Kraaipan Group – Amalia Greenstone Belt, Southwestern Transvaal. In Anhaeusser, C. R. (ed): *The Archaean Kraaipan Group volcano-sedimentary rocks and associated granites and gneisses of the southwestern Transvaal, northwestern Cape Province and Bophuthatswana: Excursion guidebook*, Inform. Circ. Economic Geology Research Institute, University of the Witwatersrand, Johannesburg, Vol. 244, 45 pp.

Kendall, C., McDonnel, J., 1998: *Isotope tracers in catchment hydrology*, Elsevier Science, Amsterdam, pp. 51-86.

Keyser, N., 1998: The geology and geochemistry of the Ventersdorp Supergroup in the area between Vryburg, Ottosdal and Mafikeng, *Bulletin of the Geological Survey of South Africa*, Council for Geoscience, Pretoria, Bulletin No. 122, 117 pp.

Kirchner, J. and Van Tonder, G.J., 1995: Proposed guidelines for the execution, evaluation and interpretation of pumping tests in fractured rock formations, *Water SA*, Vol. 21, No. 3, pp 187 – 200.

Koeberl, C., Armstrong, R. A. and Reimold, W. U., 1997: Morokweng, South Africa: A large impact structure of Jurassic-Cretaceous boundary age, *Geology*, 25, pp. 731 – 734.

Kovalevsky, V. S., Kruseman, G. P. and Rushton, K. R., 2004: *Groundwater Studies: An international guide for hydrogeological investigations*, IHP-VI Series on Groundwater No. 3, United Nations Educational, Scientific and Cultural Organization, Paris, 430 pp.

Külls, C., 2000: *Groundwater of the north-western Kalahari, Namibia: Estimation of recharge and quantification of the flow systems*, Julius-Maximilian University of Würzburg, Würzburg, PhD thesis, 165 pp.

Levin, M., 1980: *A geological and hydrogeochemical investigation of the uranium potential of an area between the Orange and Kuruman rivers, northwestern Cape Province*, Atomic Energy Board, Pelindaba, PEL-272, 1, 65 pp.

Levin, M. and Verhagen, B. Th., 2013: Application of isotope techniques to trace location of leakage from dams and reservoirs. In Abiye, T. (ed): *The use of isotope hydrology to characterize and assess water resources in South(ern) Africa*, Water Research Commission, Pretoria, WRC Report No. TT 570/13, pp 9 – 23.

Lin, J., Ganesh, A. and Singh, M., 2012: *Microbial pathogens in the Umgeni River, South Africa*, Water Research Commission, Pretoria, WRC Report No. KV 303/12, 125 pp.

MacDonald, A. M., Bonsor, H. C., Dochartaigh, B. E. O. and Taylor, R. G., 2012: Quantitative maps of groundwater resources in Africa, *Environmental Research Letters*, 7 024009, 7 pp.

Mapeo, R. B. M., Armstrong, R. A., Kampunzu, A. B. and Ramokate, L. V., 2004: SHRIMP U-Pb zircon ages of granitoids from the western domain of the Kaapvaal Craton, *South African Journal of Geology*, Vol. 107, No. 1/2, pp 219 – 232.

Martinelli, E., 1975: Geophysical exploration for potable groundwater supplies in the Kalahari Gemsbok National Park, *Water SA*, Vol. 1, No. 2, pp. 53 – 56.

Martini, J. E. J., 2006: Karst and Caves. In Johnson, M. R., Anhaeusser, C. R. and Thomas, R. J. (eds): *The Geology of South Africa*, Geological Society of South Africa, Johannesburg/Council for Geoscience, Pretoria, 661 – 668.

Middleton, B. J. and Bailey, A. K., 2008: *Water resources of South Africa, 2005 (WR 2005),* Water Research Commission, Pretoria, WRC Report No. TT 380/08, 179 pp.

Moen, H. F. G., 2006: The Olifantshoek Supergroup. In Johnson, M. R., Anhauesser, C. R. and Thomas, R. J. (eds): *The Geology of South Africa*, Geological Society of South Africa/Council for Geosciences, pp 319 – 324.

Mook, W. G. (Ed), 2001: Introduction, Theory, Methods, Review, *Environmental Isotopes in the Hydrological Cycle: Principles and Applications,* Vol. 1, International Atomic Energy Agency and United Nations Educational, Scientific and Cultural Organization, pp. 1 - 164.

Moore, I. D., 1993: Hydrologic modelling and GIS. In Goodchild, M. F., Parks, B., Johnston, C. and Glendinning, S. (eds): *Environmental modelling and GIS II*, GIS World.

Moore, G. K. and Hollyday, E. F., 1975: Prospecting for groundwater with SKYLAB photographs, central Tennessee, *Remote Sensing Earth Resources*, 4, pp. 499 – 519.

Murray, R., Baker, K., Ravenscroft, P., Musekiwa, C. and Dennis, R., 2012: A groundwater-planning toolkit for the main Karoo basin: Identifying and quantifying groundwater-development options incorporating the concept of wellfield yields and aquifer firm yields, *Water SA*, Vol. 38 No. 3 International Conference on Groundwater Special Edition, pp. 407 – 416.

Murray, K., Du Preez, M. and Meyer, R., 2007: *National microbial monitoring programme for groundwater, Implementation manual*, Water Research Commission, Pretoria, WRC Report No. TT 312/07, 117 pp.

Nel, J. M., 2001: *Assessment of the groundwater potential of the Middlekop/Appleby aquifer, Stella district, Northwest region*, Department of Water Affairs, Pretoria, Report No. GH 3965, 78 pp.

Nel, J., Nel, M., Dustay, S., Siwana, S. and Mbali, S., 2014: *Towards a guideline for the delineation of groundwater protection zones in complex aquifer settings*, Water Research Commission, Pretoria, WRC Report No. TT 2288/1/14, 88 pp.

Nijsten, G. J. and Beekman, H. E., 1997: Groundwater flow study in the Llethlakeng-Botlhapatlou area, *Gress II Technical report : Groundwater recharge and resources in the Botswana Kalahari*.

Oksane, J. and Sarjakoski, T., 2005: Error propagation analysis of DEM-based drainage basin delineation, *International Journal of Remote Sensing*, 26 (14), pp 3085 – 3102.

Opere, A. O., Awuor, V. O., Kooke, S. O. and Omoto, W. O., 2003: Rainfall characteristics in semi-arid Kitui district of Kenya. In Stephenson, D., Shemang, E. M. and Chaoka, T. R. (eds): *Water resources of arid areas*, Taylor and Francis Group, London, ISBN 04 1535 913 9, pp 43 – 59.

Parsons, R., 1995: *A South African aquifer system management classification*, Water Research Commission, Pretoria, WRC Report No. KV 77/95, 46 pp.

Partridge, T. C., Botha, G. A. and Haddon, I. G., 2006: Cenozoic deposits of the interior. In Johnson, M. R., Anhaeusser, C. R. and Thomas, R. J. (eds): *The Geology of South Africa*, Geological Society of South Africa/Council for Geosciences, pp 585 - 604.

Peck, H., 2009: *The preliminary study of the Stampriet transboundary aquifer in the south east Kalahari/Karoo basin*, Unpubl. MSc thesis, University of the Western Cape, Cape Town, 93 pp.

Poujol, M., Anhaeusser, C. R. and Armstrong, R. A., 2000: Episodic Archaean granitoid emplacement in the Amalia-Kraaipan terrane, South Africa: New evidence from single U-Pb geochronology with implications for the age of the western Kaapvaal Craton, *Information Circular Economic Geology Research Unit,* University of the Witwatersrand, Johannesburg, 346, 21 pp.

Poujol, M., Anhaeusser, C. R. and Armstrong, R. A., 2002: Episodic Archaean granitoid emplacement in the Amalia-Kraaipan terrane, South Africa: New evidence from single U-Pb geochronology with implications for the age of the western Kaapvaal Craton, *Journal of African Earth Sciences*, 35, pp 147 – 161.

Poujol, M., Robb, L. J., Anhaeusser, C. R. and Gericke, B., 2003: A review of the geochronological constraints on the evolution of the Kaapvaal Craton, South Africa, *Precambrian Research*, 127, pp 181 – 213.

Poujol, M., Kiefer, R., Robb, L. J., Anhaeusser, C. R. and Armstrong, R. A., 2005: New U-Pb data on zircons from the Amalia greenstone belt, southern Africa: insights into the Neoarchaean evolution of the Kaapvaal Craton, *South African Journal of Geology*, Vol 108, pp 317 – 332.

Reeves, C. V. and Hutchins, D. G., 1982: A progress report on the geophysical exploration of the Kalahari in Botswana, *Geoexploration*, 20, pp. 209-224.

Reichardt, F.J., 1994: The Molopo Farms Complex, Botswana: history, stratigraphy, petrography, petrochemistry and Ni-Cu-PGM mineralization, *Exploration and Mining Geology*, 3, pp. 263 – 284.

Reimold, W. U., Armstrong, R.A. and Koeberl, C., 2002: A deep drillcore from the Morokweng impact structure, South Africa: Petrography, geochemistry, and constraints on the crater size, *Earth and Planetary Science Letters*, 201, pp 221 – 232.

Richards, D. J., 1979: Airborne geophysics in the Northern Cape Province of South Africa. In: McEwan, G., (Ed): The proceedings of a seminar on geophysics and the exploration of the Kalahari, *Geological Survey of Botswana Bulletin*, 22, pp. 141-157.

Robb, L. J., Brandl, G., Anhaeusser, C. R. and Poujol, M., 2006: Archaean granitoid intrusions of the Kaapvaal Craton. In Johnson, M. R., Anhaeusser, C. R. and Thomas, R. J. (eds): *The Geology of South Africa*, Geological Society of South Africa/Council for Geosciences, pp 57 – 94.

Roering, C., Barton, J. M. and Winter, H. de la R., 1990: The Vredefort structure: perspective with regard to new tectonic data from adjoining terranes, *Tectonophysics*, 171, pp. 7 - 22.

Sami, K., 1996: Evaluation of the variations in borehole yield from a fractured Karoo aquifer, South Africa, *Groundwater*, 34, pp. 114 – 120.

Seymour, A. and Seward, P., 1996: *Groundwater harvest potential map of the Republic of South Africa*, Department of Water Affairs and Forestry, Pretoria, South Africa.

SGAB, 1988: *Serowe groundwater resources evaluation project, final report,* CTB No. 10/2/7/84-85, Department of Geological Survey, Botswana.

Simmonds, A. L. E. and Smalley, T. J., 2000: Kalahari aquifers in the Gam area of north-eastern Namibia*, Communications Geological Survey of Namibia*, 12, pp. 409 - 414.

South African Committee for Stratigraphy (SACS), 1980: Stratigraphy of South Africa, Part 1, In Kent, L. E. (ed): *Lithostratigraphy of the Republic of South Africa, South West Africa/Namibia, and the Republics of Bophuthatswana, Transkei and Venda, Handbook*, Geological Survey of South Africa, Handbook 8, 690 pp.

Stadler, S., Talma, A. S., Tredoux, G and Wrabel, J., 2012: Identification of sources and infiltration regimes of nitrate in the semi-arid Kalahari: Regional differences and implications for groundwater management, *Water SA*, Vol. 38, No. 2, pp 213 – 224.

Stauffer, D. and Aharony, A., 1994: *Introduction to percolation theory, 2nd Edition*, Taylor and Francis, London, 181 pp.

Stephenson, D., Shemang, E. M. and Chaoka, T. R. (eds), 2003: *Water resources of arid areas*, Taylor and Francis Group, London, ISBN 04 1535 913 9, 740 pp.

Stumm, W. and Morgan, J. J., 1996: *Aquatic chemistry (3rd Ed)*, John Wiley & Sons, New York.

Talma, A. S., Verhagen, B. Th. and Tredoux, G., 2013: Kalahari Groundwater Isotope Synthesis. In Abiye, T. (Ed): *The Use of Isotope Hydrology to Characterize and Assess Water Resources in South(ern) Africa,* Water Research Commission, Pretoria, WRC Report No. TT 570/13, pp 111 - 122.

Tessema, A., Mengistu, H., Chirenje, E., Abiye, T. A. and Demlie, M. B., 2012: The relationship between lineaments and borehole yield in North West Province, South Africa: results from geophysical studies, *Hydrogeology Journal*, 20, pp 351 – 368.

Tessema, A., Nzotta, U. and Chirenje, E., 2014: *Assessment of Groundwater Potential in Fractured Hard Rocks around Vryburg, North West Province, South Africa*, Water Research Commission, Pretoria, WRC Report No. 2055/1/13, 152 pp.

Thomas, M. A., 1981: *The geology of the Kalahari in the Northern Cape Province (areas 2620 and 2720)*, Unpublished MSc thesis, University of the Orange Free State, Bloemfontein, 138 pp.

Uken, R. and Watkeys, M. K., 1997: An interpretation of mafic dyke swarms and their relationship with major magmatic events on the Kaapvaal Craton and Limpopo Belt, *South African Journal of Geology*, 100, pp. 341 - 348.

USGS: www.p*ubs.usgs.gov/wri/wri014210.* Belcher, W. R., Elliot, P. E. and Geldon, A. L., 2002: Hydraulic-Property Estimates for Use With a Transient Ground-Water Flow Model of the Death Valley Regional Ground-Water Flow System, Nevada and California, USGS, WRIR 01-4210*.*

Van der Westhuizen, W. A., De Bruiyn, H. and Meintjes, P. G., 2006: The Ventersdorp Supergroup. In Johnson, M. R., Anhaeusser, C. R. and Thomas, R. J. (eds): *The Geology of South Africa*, Geological Society of South Africa/Council for Geosciences, pp 187 - 208.

Van DYK, G. S., 1993: *Geohydrological investigation for SADF Pomfret, District Vryburg, Drainage Region D410*, Department of Water Affairs, Pretoria, GH 3813, 28 pp.

Van Dyk, G. S., 2005: *Managing the impact of irrigation on the Tosca-Molopo groundwater resource*, Department of Water Affairs, Pretoria, GH 4023, 122 pp.

Van Heerden, J. and Hurry, L., 1992: *Southern Africa's Weather Patterns: An Introductory Guide*, Acacia, Pretoria, 95 pp.

Van Tonder, G. J. and Bean, J., 2003: Challenges in estimating groundwater recharge. In Xu, Y. and Beekman, H. E. (eds): *Groundwater recharge estimation in southern Africa*, UNESCO IHP Series No. 64, UNESCO, Paris, ISBN 92-9220-000-3, pp 19 – 29.

Van Wyk, E., Van Tonder, G. J. and Vermeulen, D., 2012: Characteristics of local groundwater recharge cycles in South African semi-arid hard rock terrains: Rainfall - groundwater interaction, *Water SA*, Vol. 38, pp 747 – 754.

Van Veelen, M., Baker, T., Mulale, K., Bron, A., Fanta, A., Jonker, V., Mullins, W. and Schoeman, H., 2009: *Feasibility study of the potential for sustainable water resources development in the Molopo-Nossob watercourse*, Orange Senqu River Commission, Report No. 007/209, 106 pp.

Veevers, J. J., Cole, D. I., Cowan, E. J., 1994: Southern Africa: Karoo Basin and Cape Fold Belt. In Veevers, J. J. and Powell, C., (eds.): Permian-Triassic Pangean Basins and Foldbelts along the Panthalassan Margin of Gonwanaland, *Geological Society of America Memoir*, 184, pp. 223-279.

Vegter, J. R., 1995: *An explanation of a set of national groundwater maps*, Water Research Commission, Pretoria, Report No. TT 74/95.

Verhagen, B. Th., 1984: Environmental isotope study of a groundwater supply project in the Kalahari of Gordonia, *Isotope Hydrology*, 1983, IAEA Vienna, pp. 415- 432.

Verhagen, B. Th., 2003: Recharge quantified with radiocarbon in three studies of Karoo aquifers in the Kalahari and independent corroboration. In Xu, Y. and Beekman, H. E. (eds): *Groundwater recharge estimation in Southern Africa*, UNESCO IHP Series No. 64, UNESCO Paris, ISBN 92-9220-000-3, pp 51 – 60.

Verhagen, B. Th., 2013: Environmental isotope contribution to a multi-disciplinary groundwater resource assessment in eastern Botswana. In Abiye, T. A. (ed): *The use of isotope hydrology to characterize and assess water resources in South(ern) Africa*, Water Research Commission, Pretoria, WRC Report No. TT 570/13, pp. 123 - 132.

Verhagen, B. Th., Bredenkamp, D. B. and Botha, L. J., 2001: Hydrogeological and isotopic assessment of the response of a fractured multi-layered aquifer to long term abstraction in a semi-arid environment, Water Research Commission, Pretoria, WRC Report No. 565/1/01, 62 pp.

Visser, D. J. L., 1956: The geology of the Barberton area*, Special Publication Geological Survey of South Africa*, 15, 253 pp.

Visser, J. N. J., 1983: An analysis of the Permo-Carboniferous glaciation in the marine Kalahari basin, southern Africa, *Palaeogeography, Palaeoclimatology, Palaeoecology*, 44, pp. 295-315.

Visser, J. N. J., 1989: The Permo-Carboniferous Dwyka Formation of southern Africa: deposition by a predominantly subpolar marine ice sheet, *Palaeogeography, Palaeoclimatology, Palaeoecology*, 70, pp. 377-391.

Visser, J. N. J. and Praekelt, H. E., 1996: Subduction, mega-shear systems and Late Palaeozoic basin development in the African segment of Gondwana, *Geologische Rundschau*, 85, pp. 632-646.

Visser, J. N. J., Van Niekerk, B. N., Van der Merwe, S. W., 1997: Sediment transport of the Late Proterozoic glacial Dwyka Group in the southwestern Karoo Basin, *South African Journal of Geology*, 100, pp. 223-236.

Walraven, F. and Martini, J., 2005: Zircon Pb-evaporation age determinations of the Oaktree Formation, Chuniespoort Group, Transvaal Sequence: implications for Transvaal-Griqualand West basin correlations, *South African Journal of Geology*, 98, pp 58 – 67.

Walraven, F., Armstrong, R. A. and Kruger, F. J., 1990: A chronostratigraphic framework for the north-central Kaapvaal Craton, the Bushveld Complex and Vredefort structure, *Tectonophysics*, 171, pp 23 – 48.

WCS, 1993: *Trans-Kalahari road groundwater potential study*, Report to the Department of Water Affairs, Botswana.

Weaver, J. M. C., Cave, L. and Talma, A. S., 2007: *Groundwater sampling: A comprehensive guide for sampling methods*, Water Research Commission, Pretoria, WRC Report No. TT 303/07, 168 pp.

Winter, H. de la R., 1976: A lithostratigraphic classification of the Ventersdorp succession, *Transactions of Geological Society of South Africa*, Vol. 79, pp. 31-48.

Witthüser, K. T., Holland, M., Rossouw, T. G., Rambau, E., Bumby, A. J., Petzer, K. J., Dennis, I., Beekman, H., Van Rooy, J. L., Dippenaar, M. and De Wit, M., 2011: *Hydrogeology of basement aquifers in the Limpopo Province*, Water Research Commission, Pretoria, WRC Report No. TT 1693/1/10, 104 pp.

Wood, W. W., 1981: Guidelines for collection and field analysis of groundwater samples for selected unstable constituents, *Techniques of Water Resources Investigation*, Chapter D2, US Geological Survey.

WSU Calculator: http://irrigation.wsu.edu/calculators

Xu, Y. and Beekman, H. E. (eds), 2003: *Groundwater recharge estimation in Southern Africa*, UNESCO IHP Series No. 64, UNESCO Paris, ISBN 92-9220-000-3, 207 pp.

Zhang, J., Murray, R. and Tredoux, G., 2004: Regional fractured aquifer modelling using telescopic mesh refinement (TMR) method, *Proceedings of the 2004 Water Institute of Southern Africa (WISA) Biennial Conference 2*, Cape Town, ISBN: 1-920-01728-3, pp. 351 – 359.

Zimmermann, O. T., 1994: *Aspects of the geology of the Kraaipan Group in the Northern Cape Province and the Republic of Botswana*, MSc thesis (unpubl.).

13. APPENDICES

APPENDIX A

(i) Piper, (ii) Durov and (iii) Schoeller graphs for the respective Quaternary drainage regions within the study area

Quaternary Drainage Region D41B

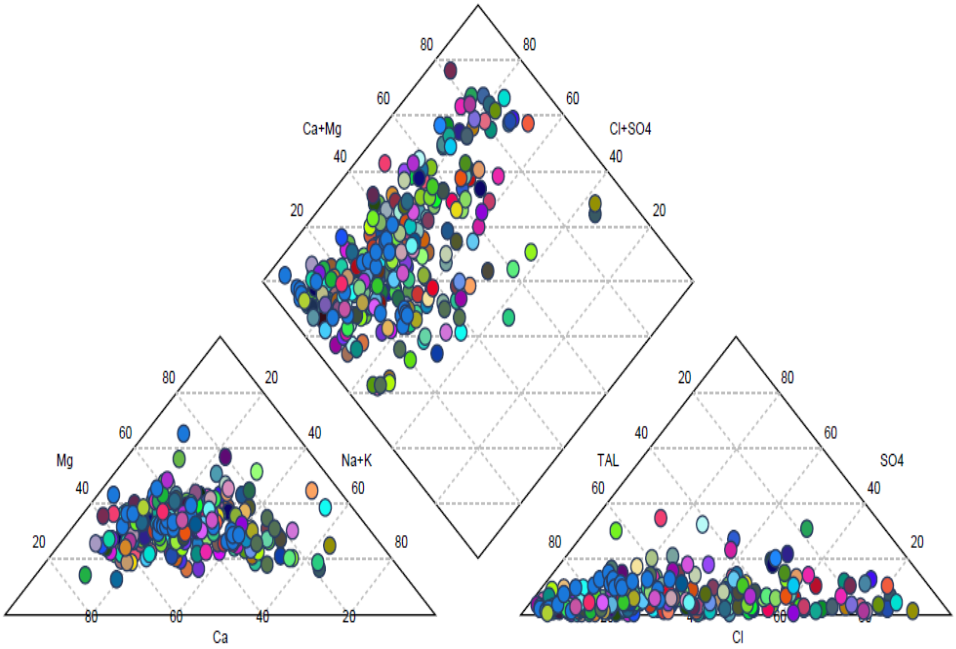

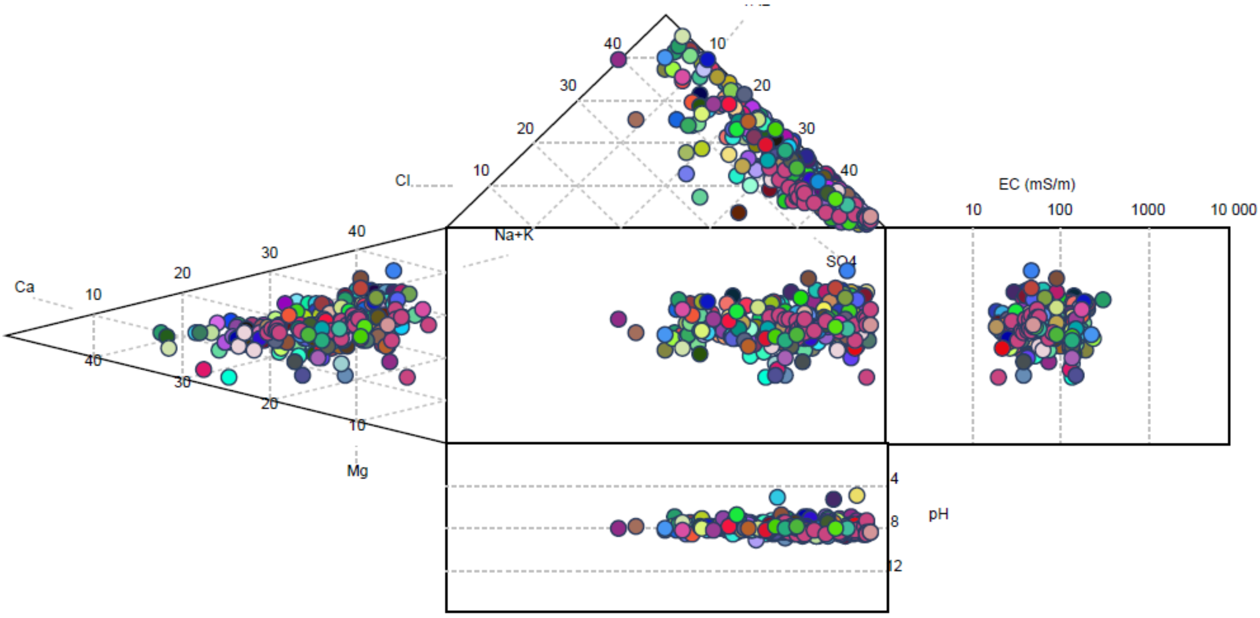

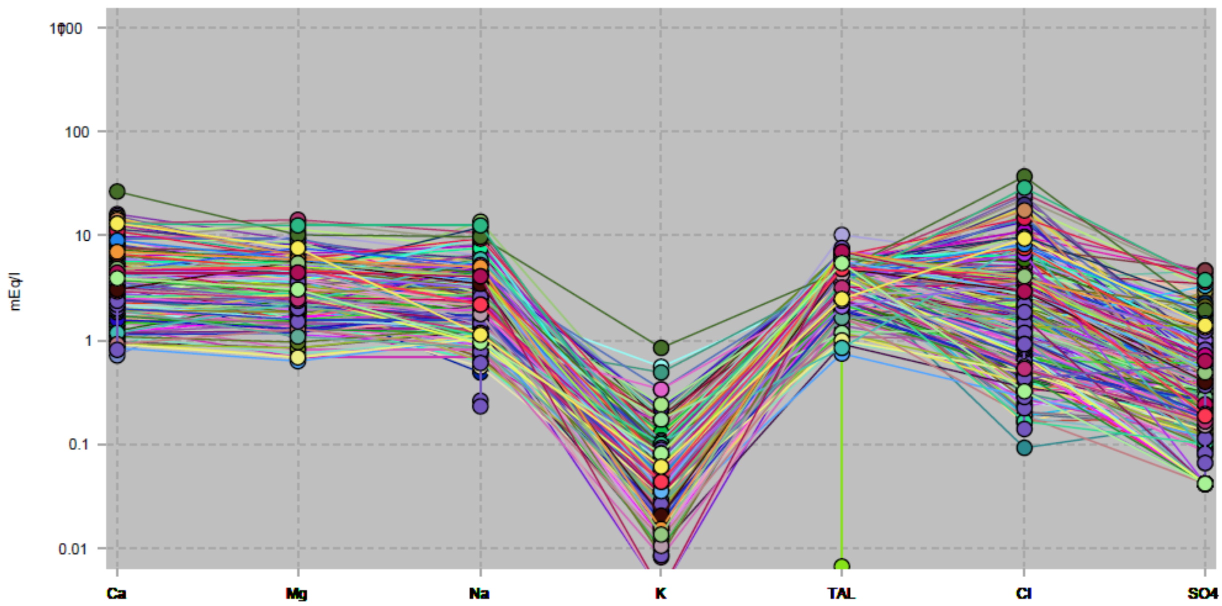

Quaternary Drainage Region D41C

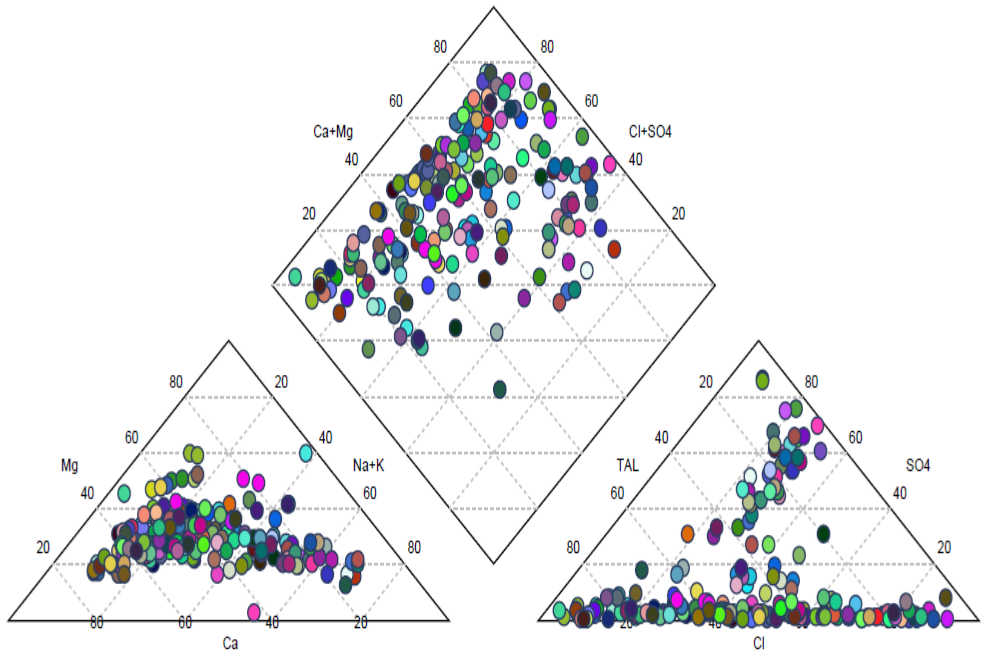

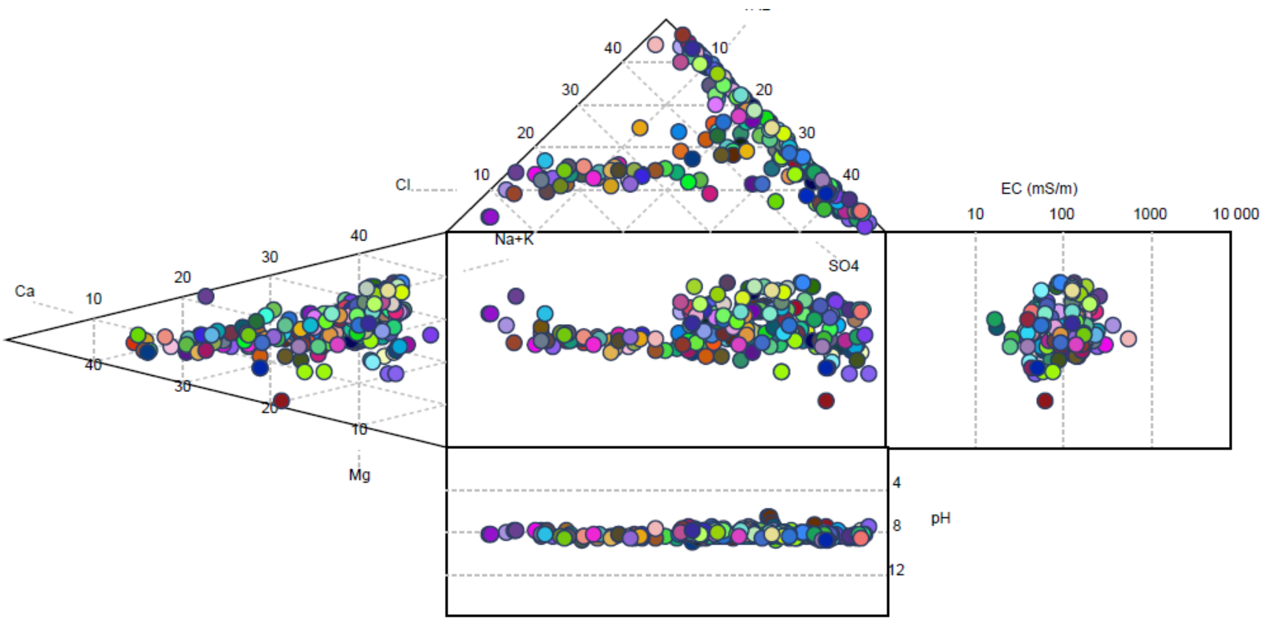

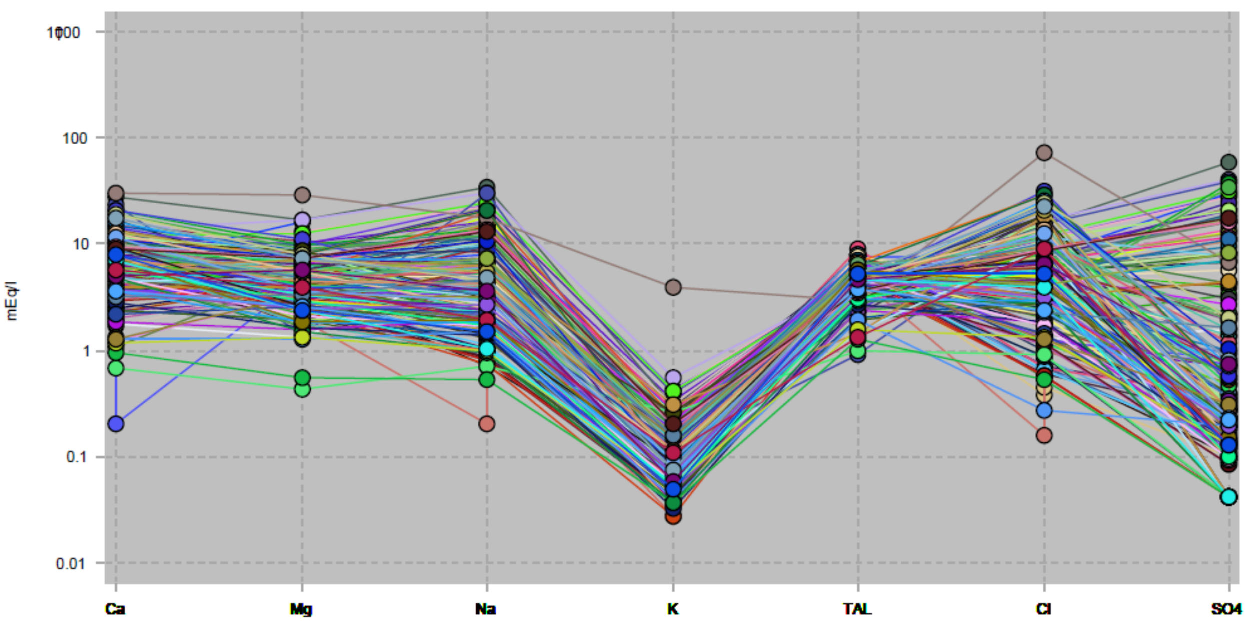

Quaternary Drainage Region D41D

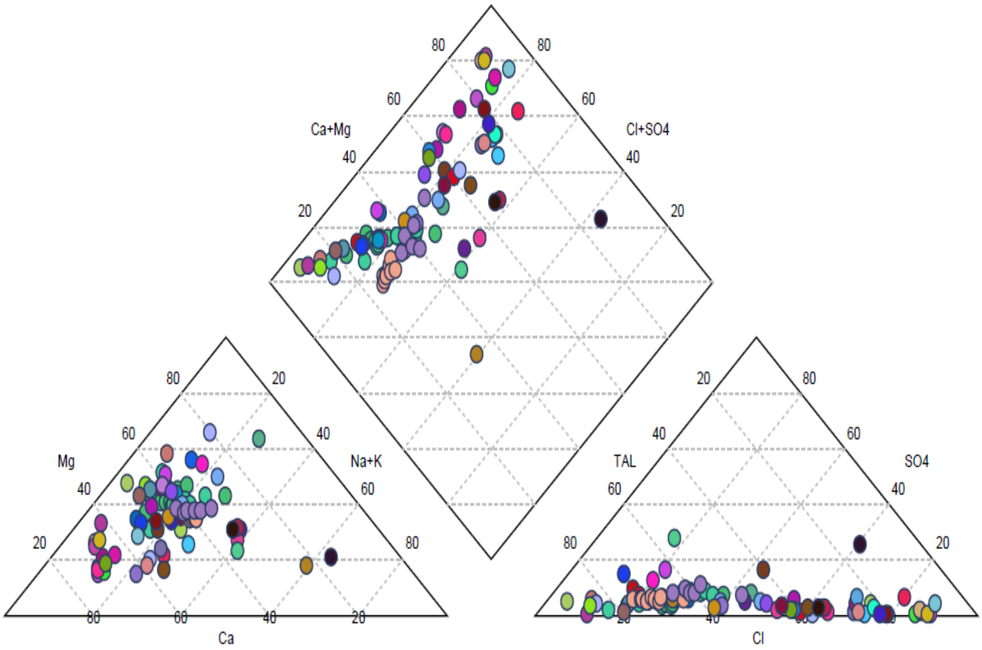

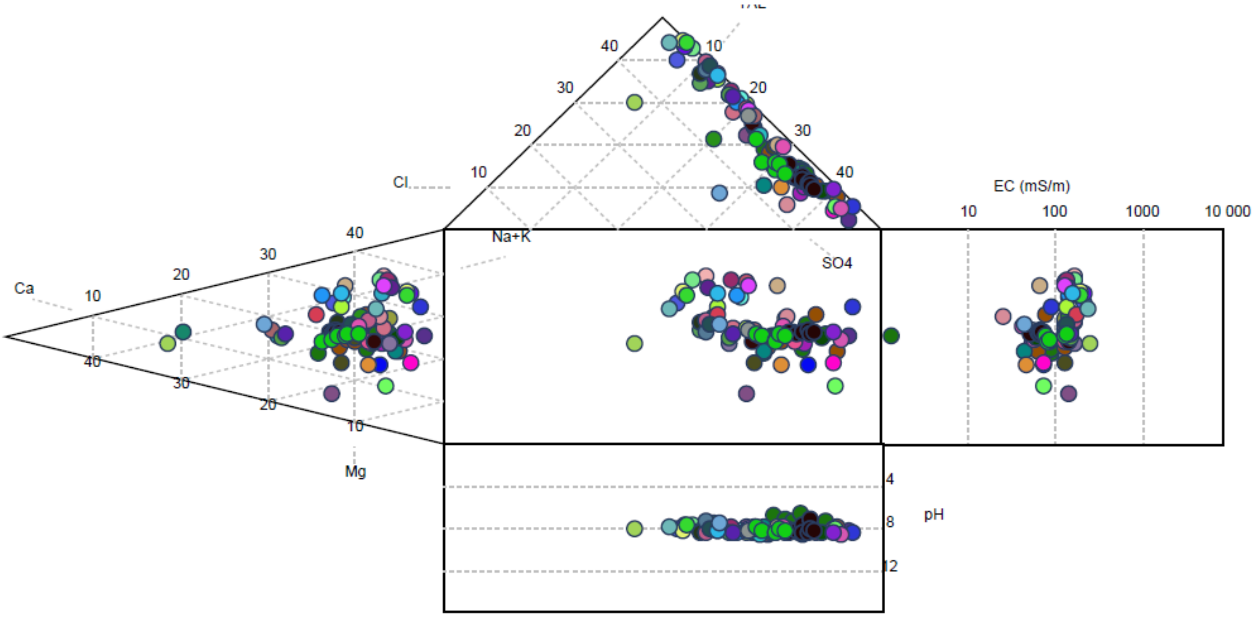

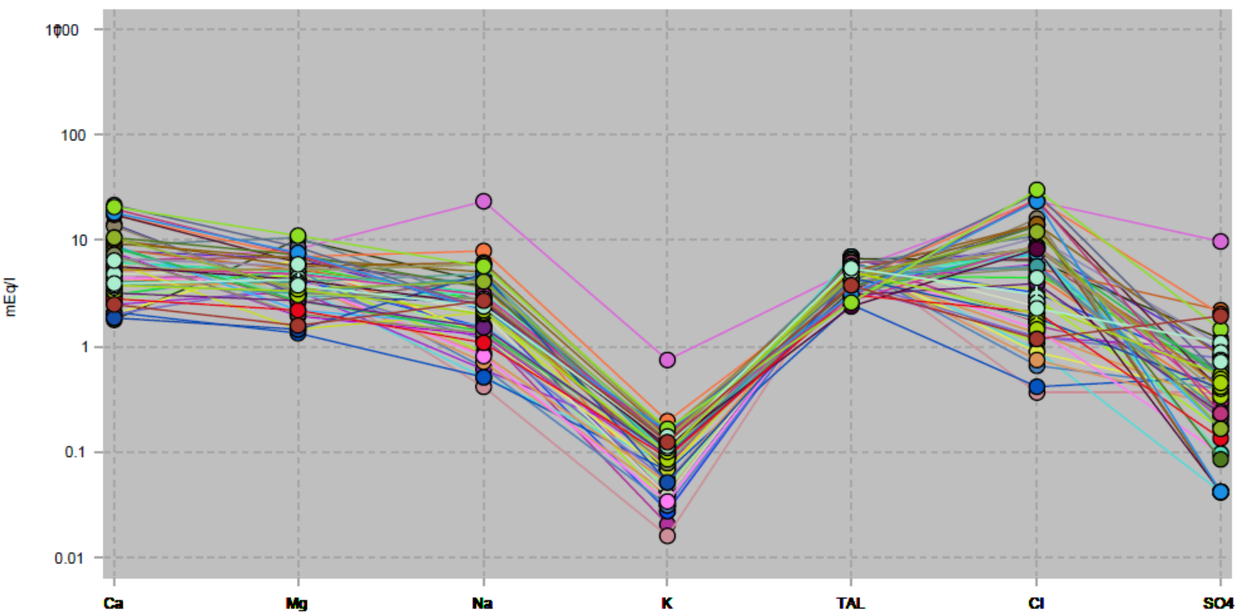

Quaternary Drainage Region D41E

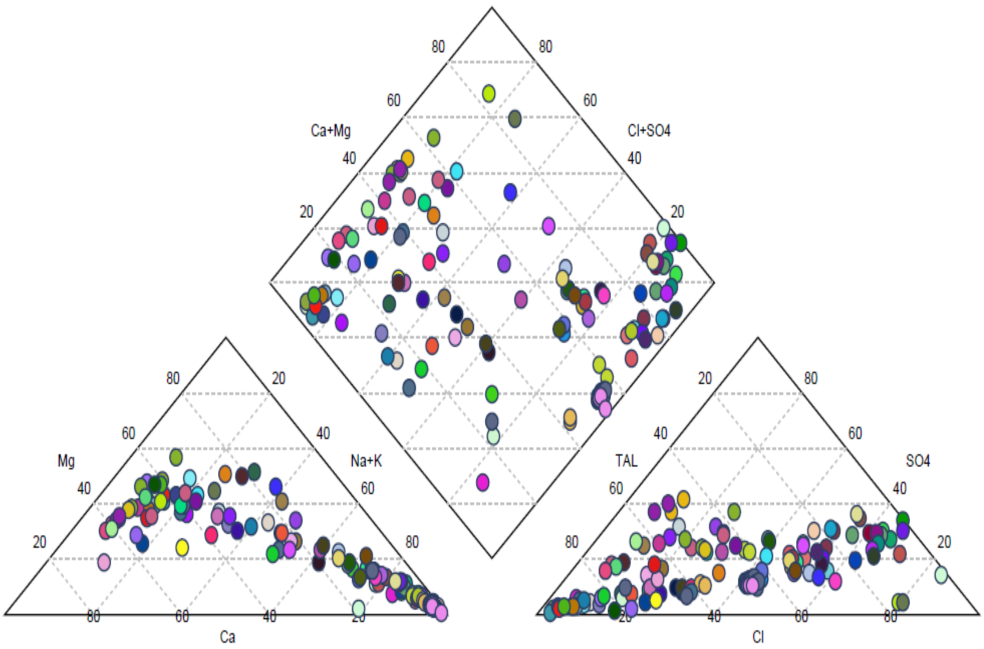

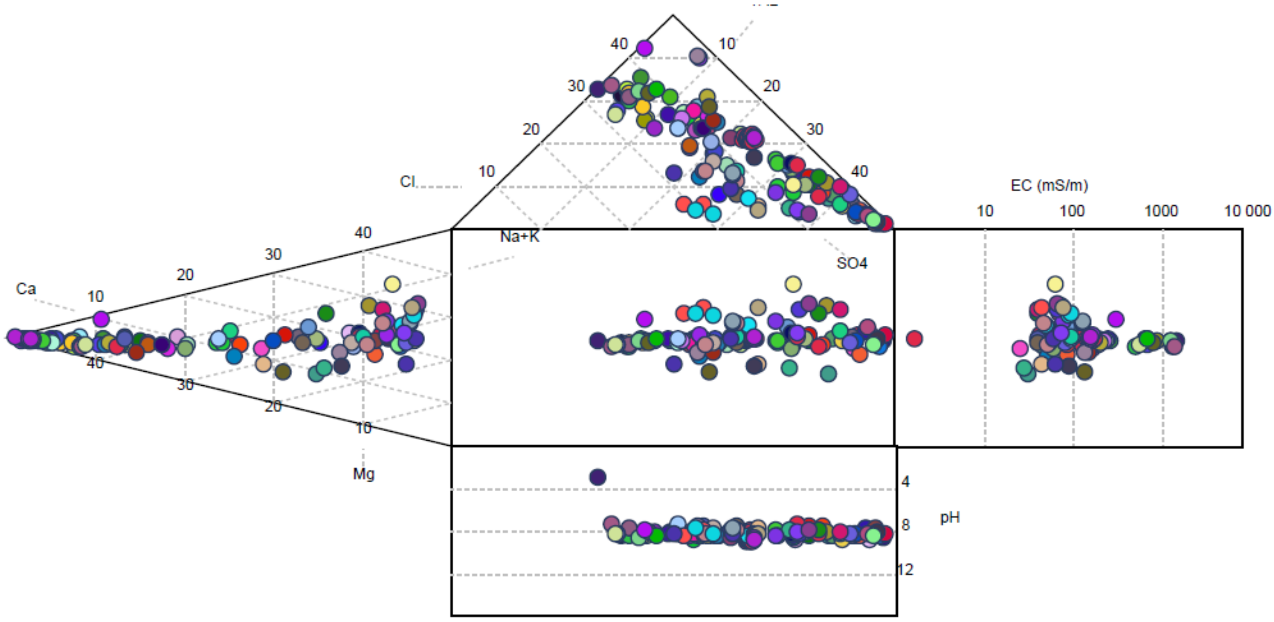

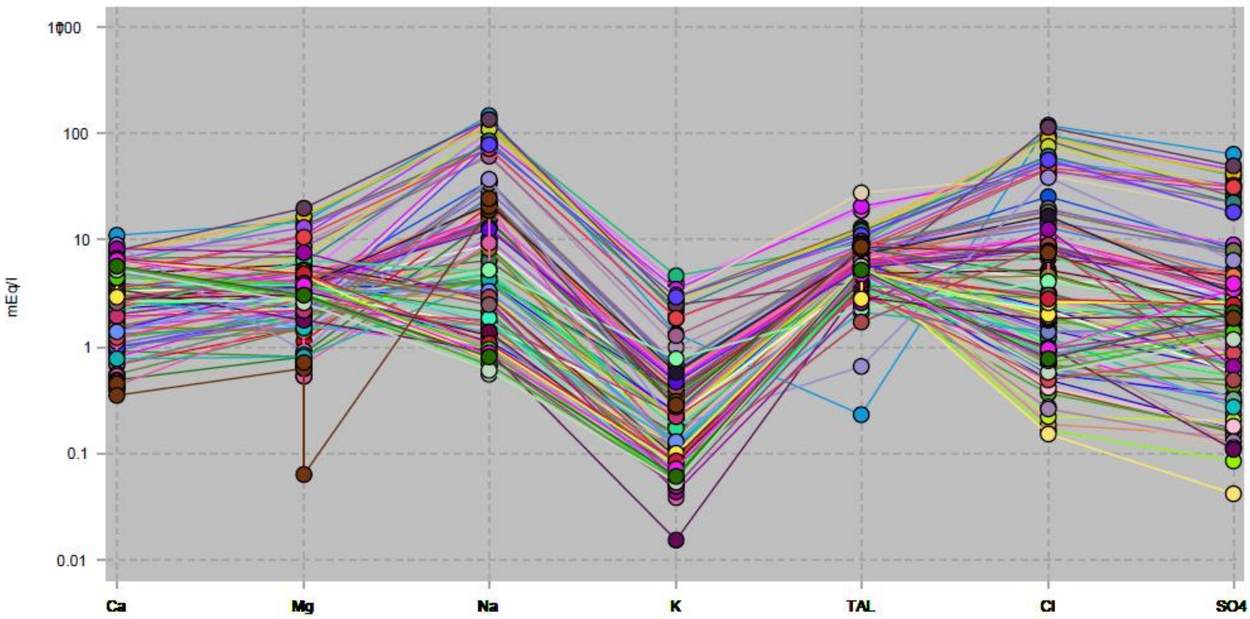

Quaternary Drainage Region D41F

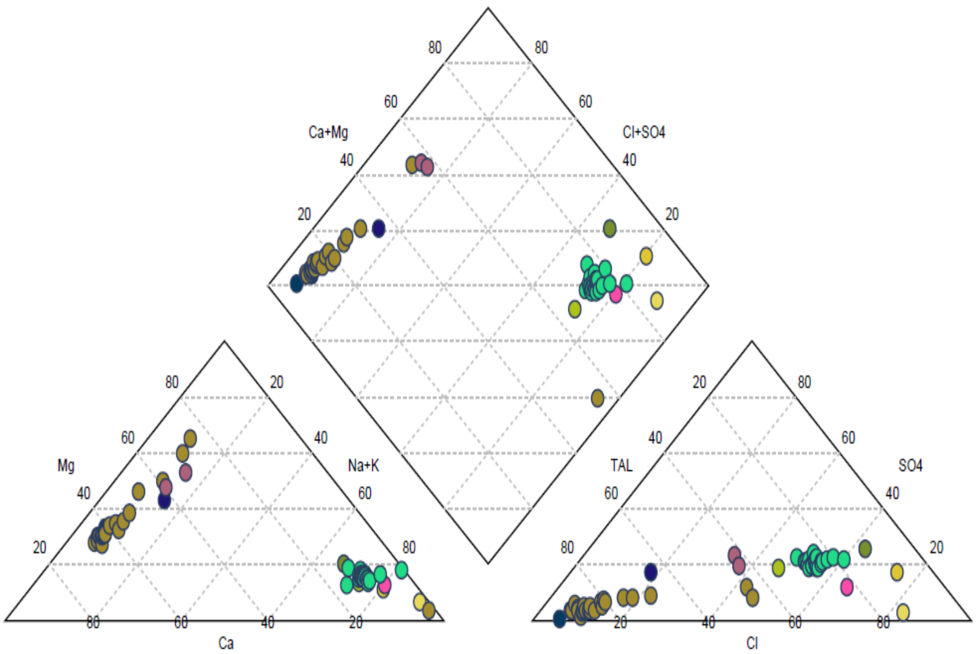

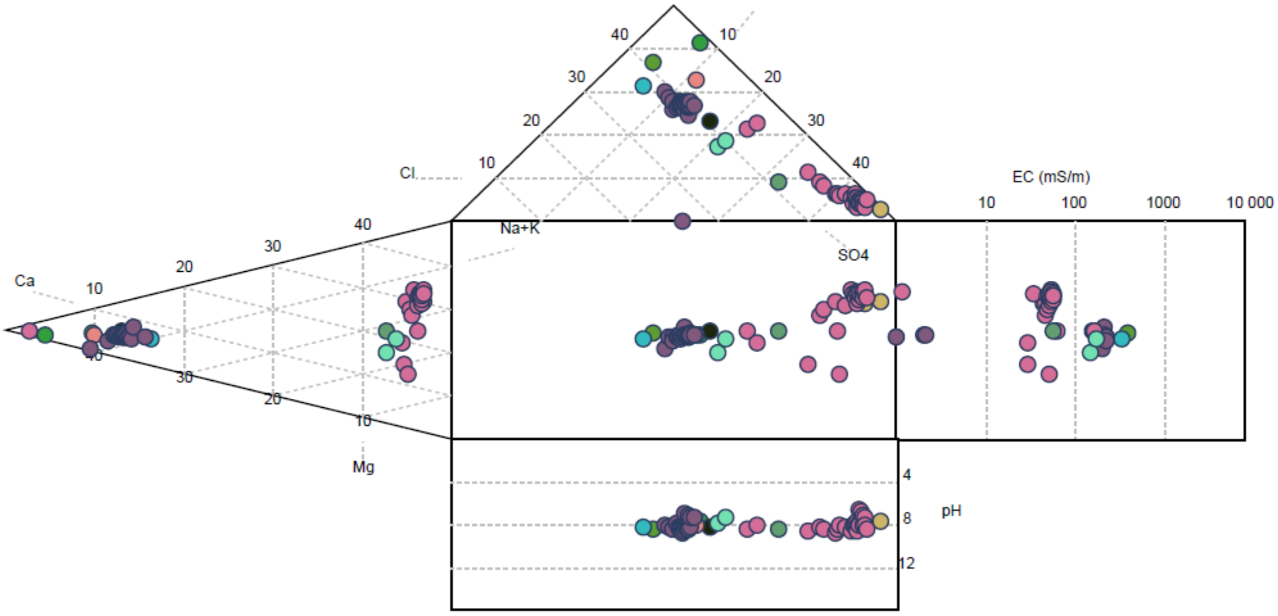

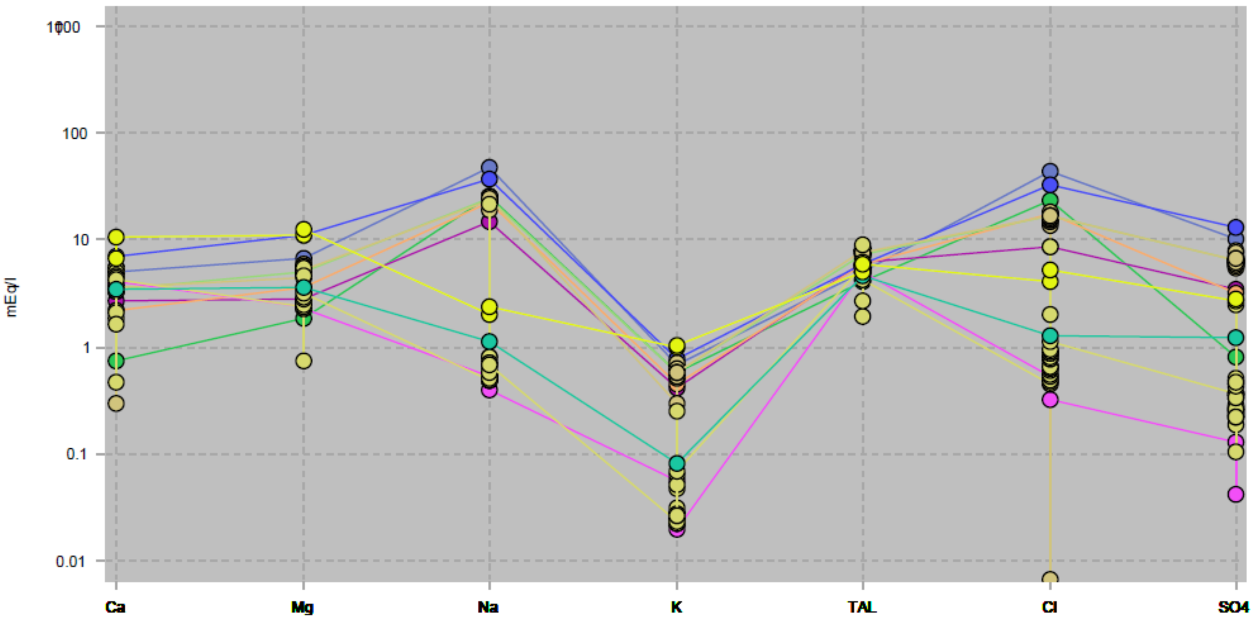

Quaternary Drainage Region D41G

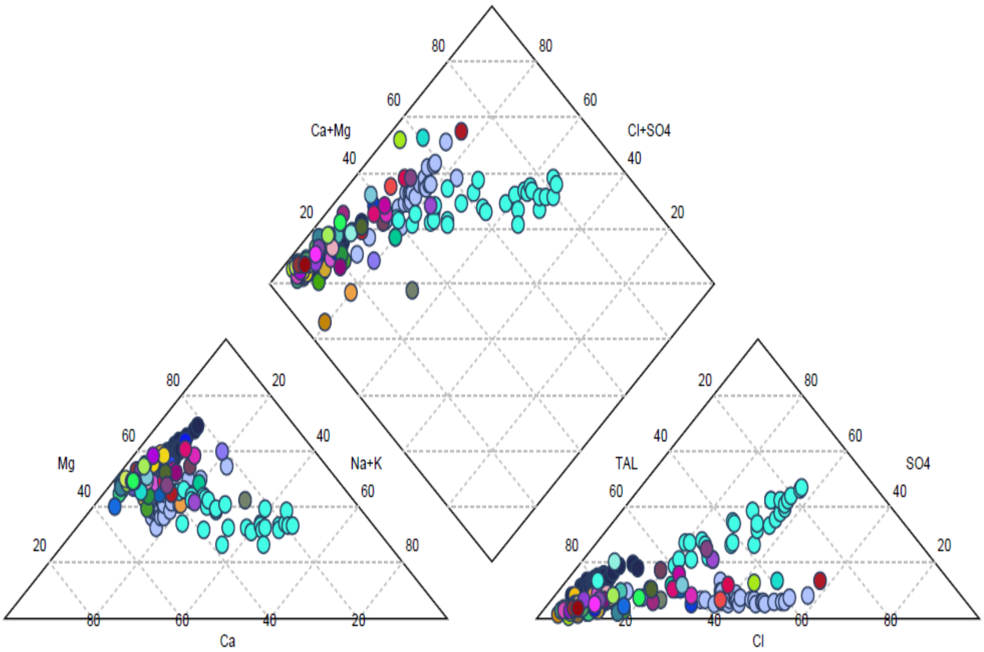

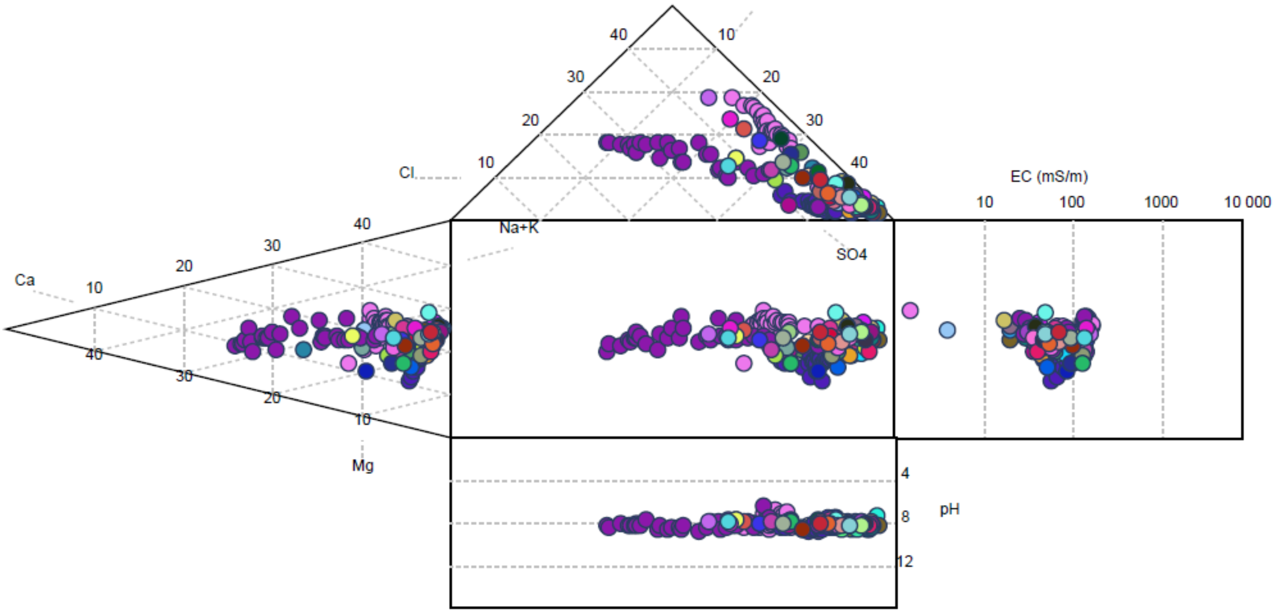

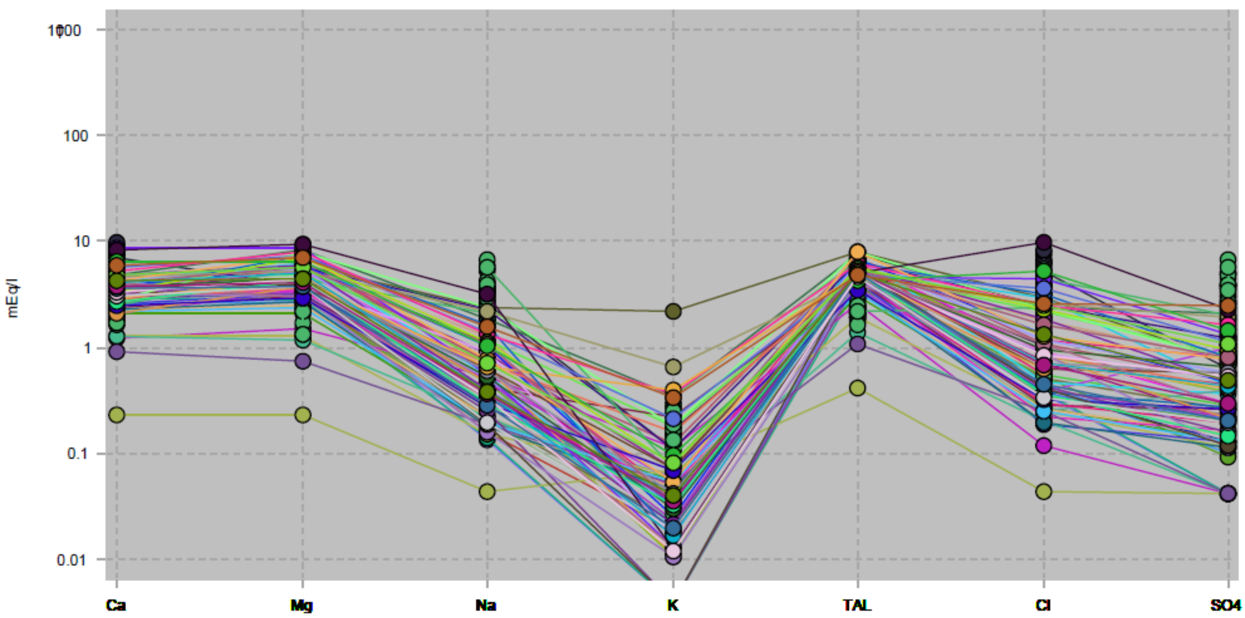

Quaternary Drainage Region D41H

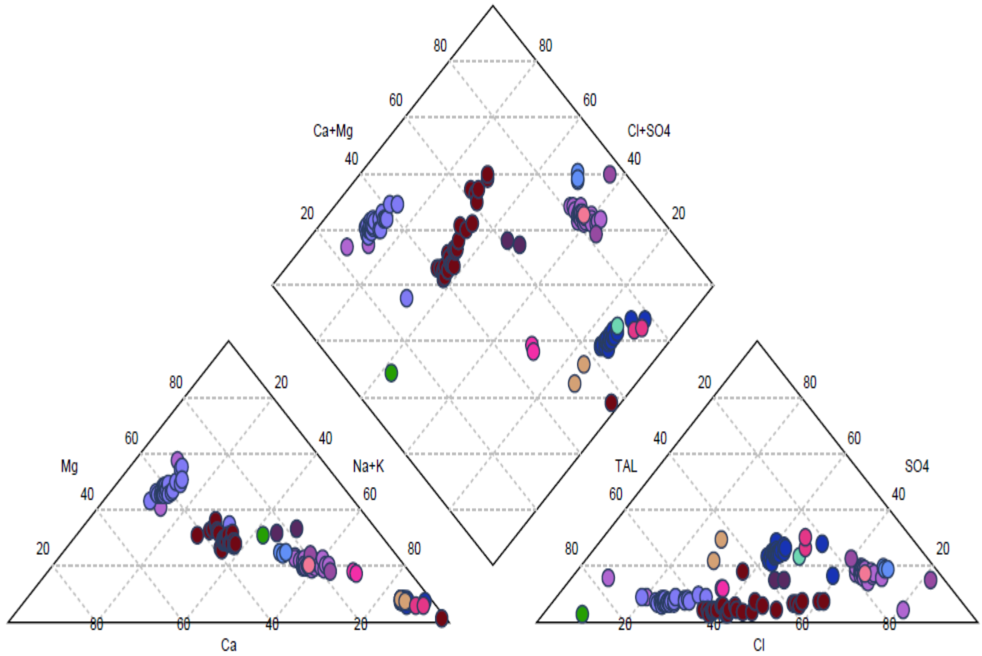

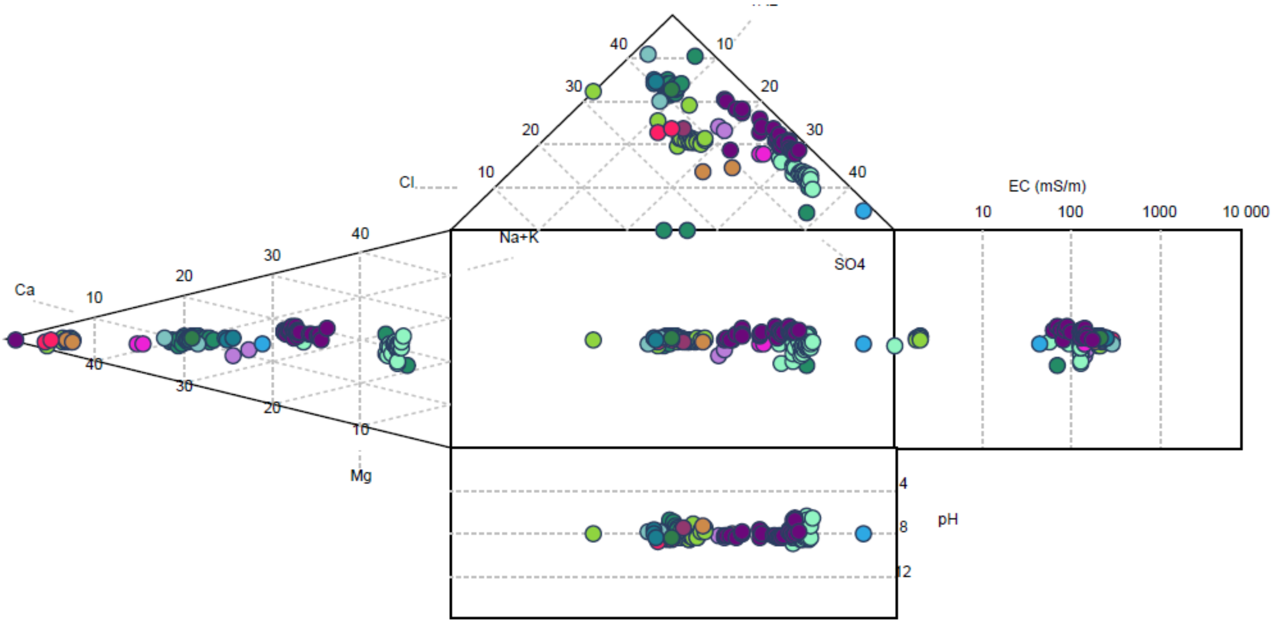

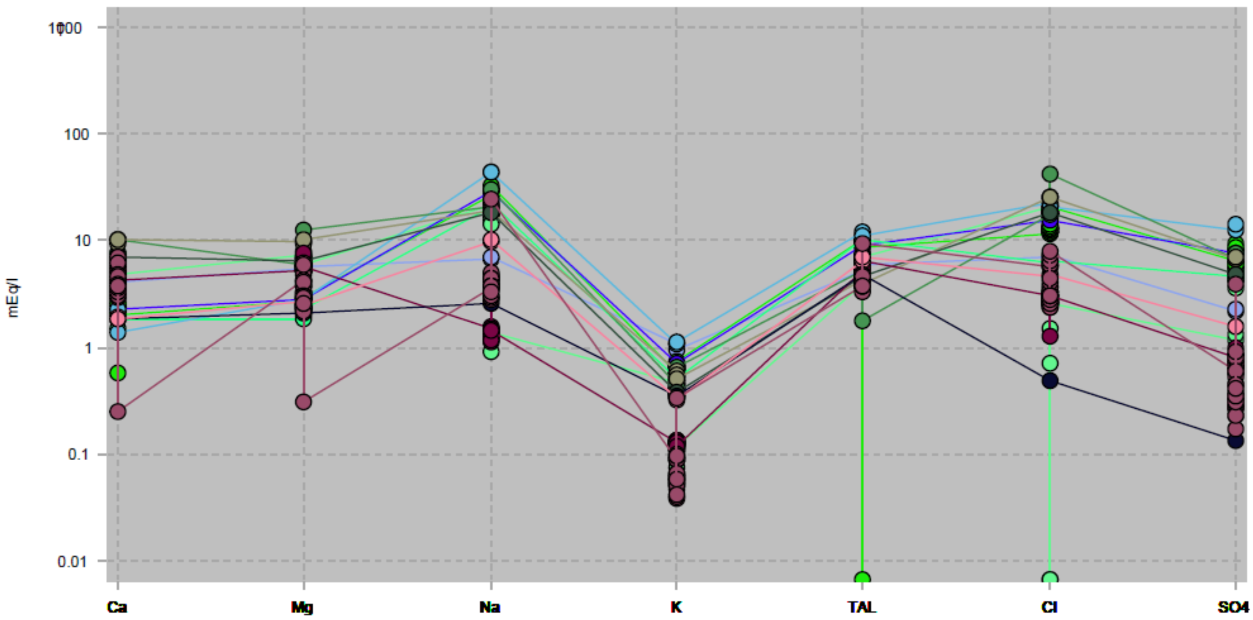

Quaternary Drainage Region D41K

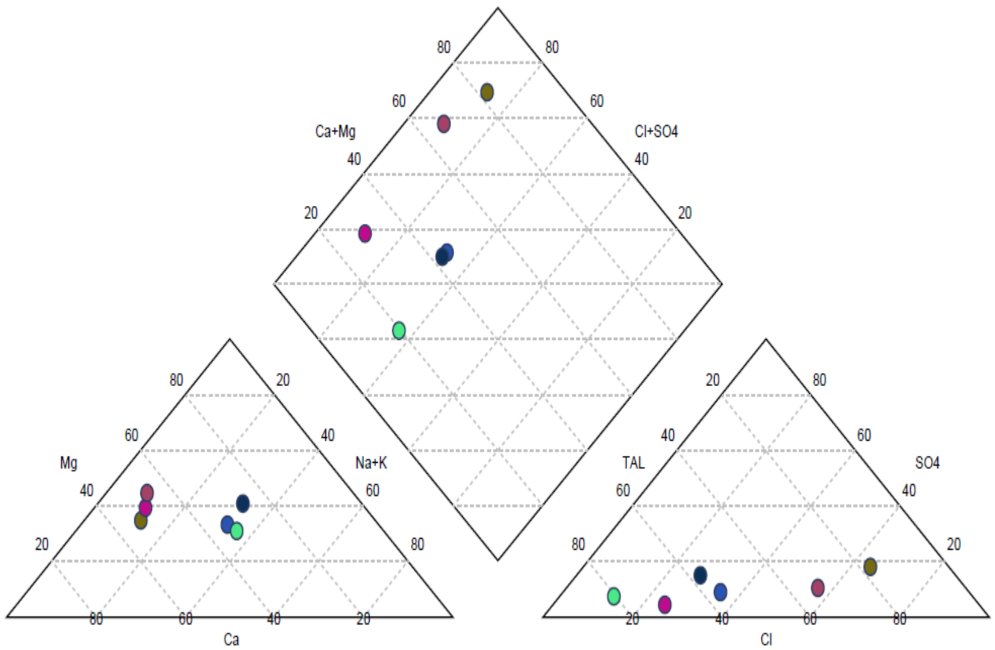

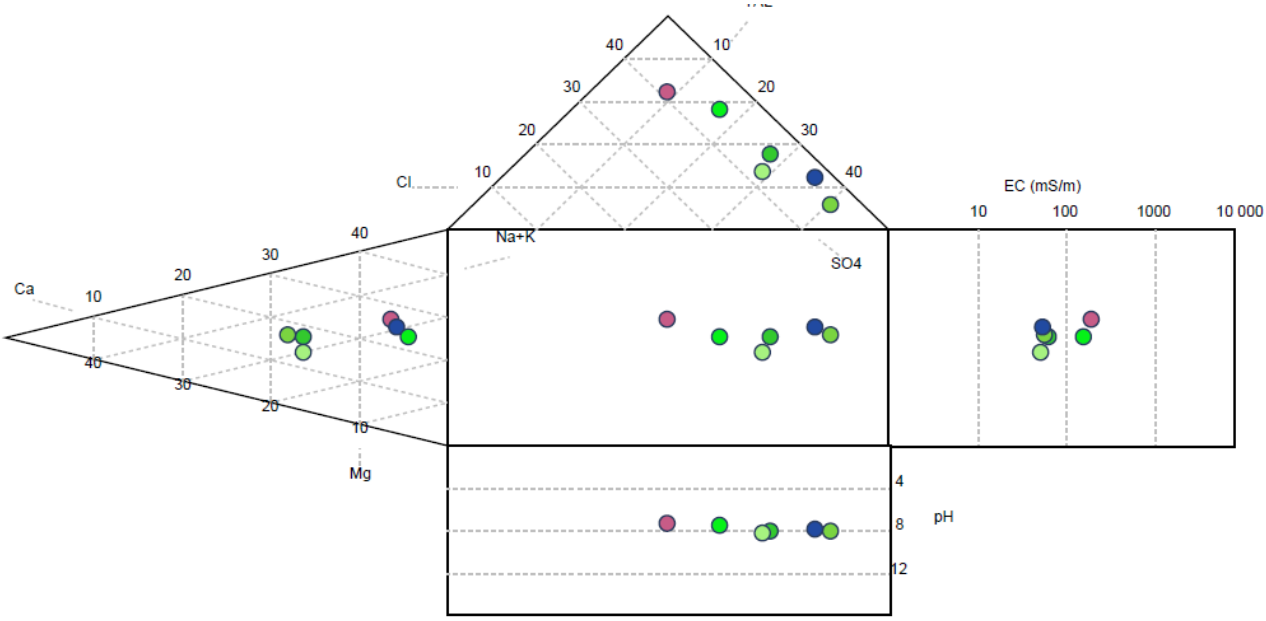

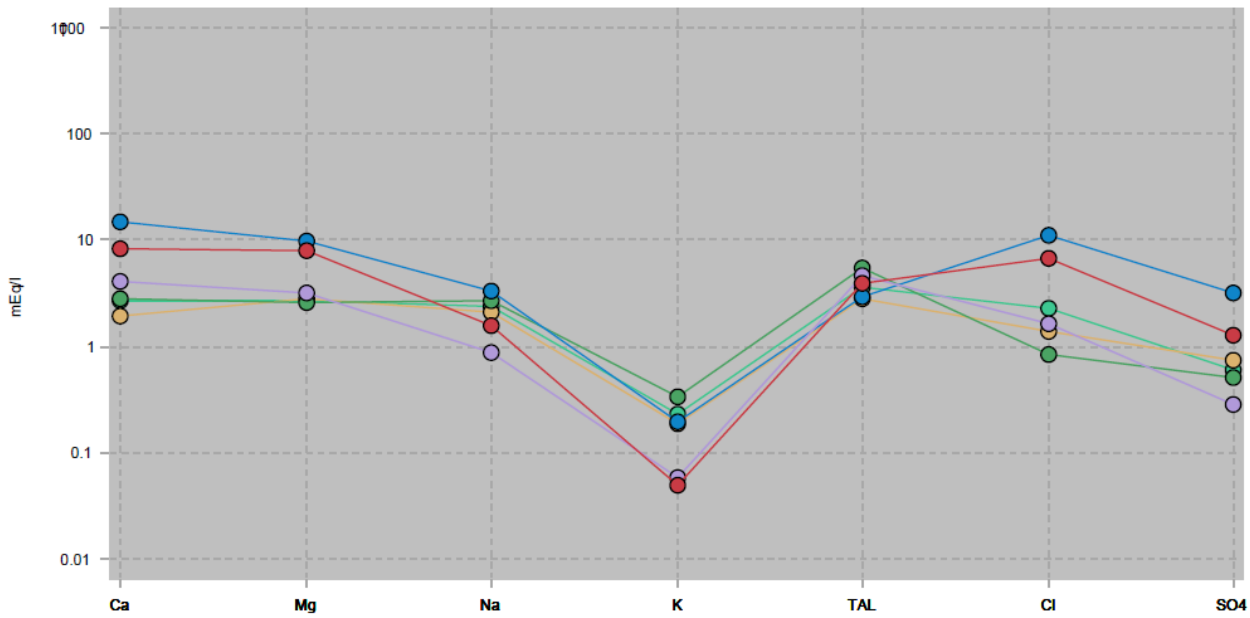

Quaternary Drainage Region D41L

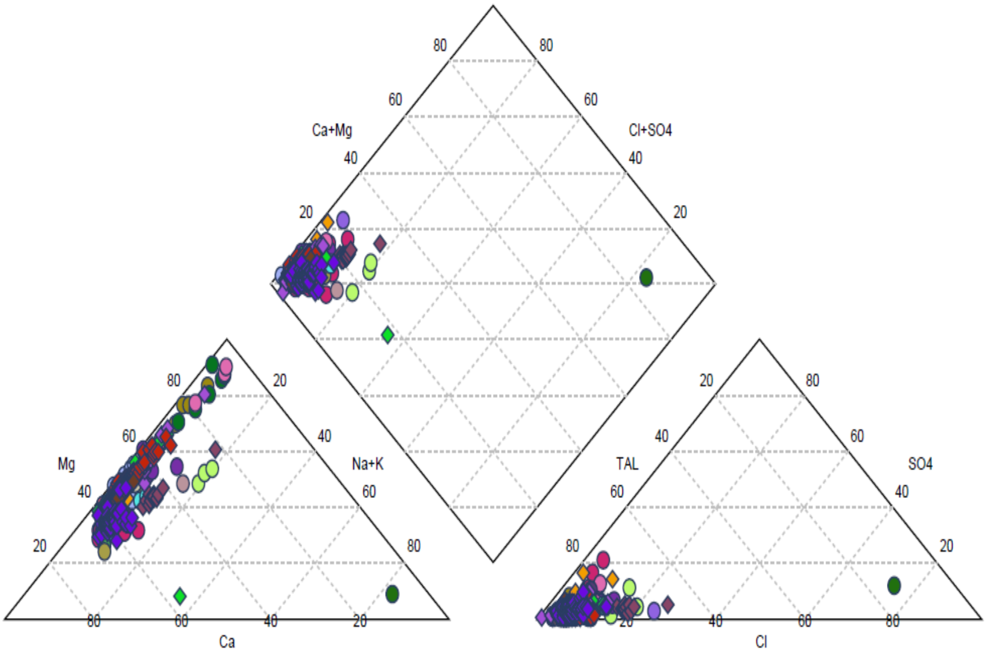

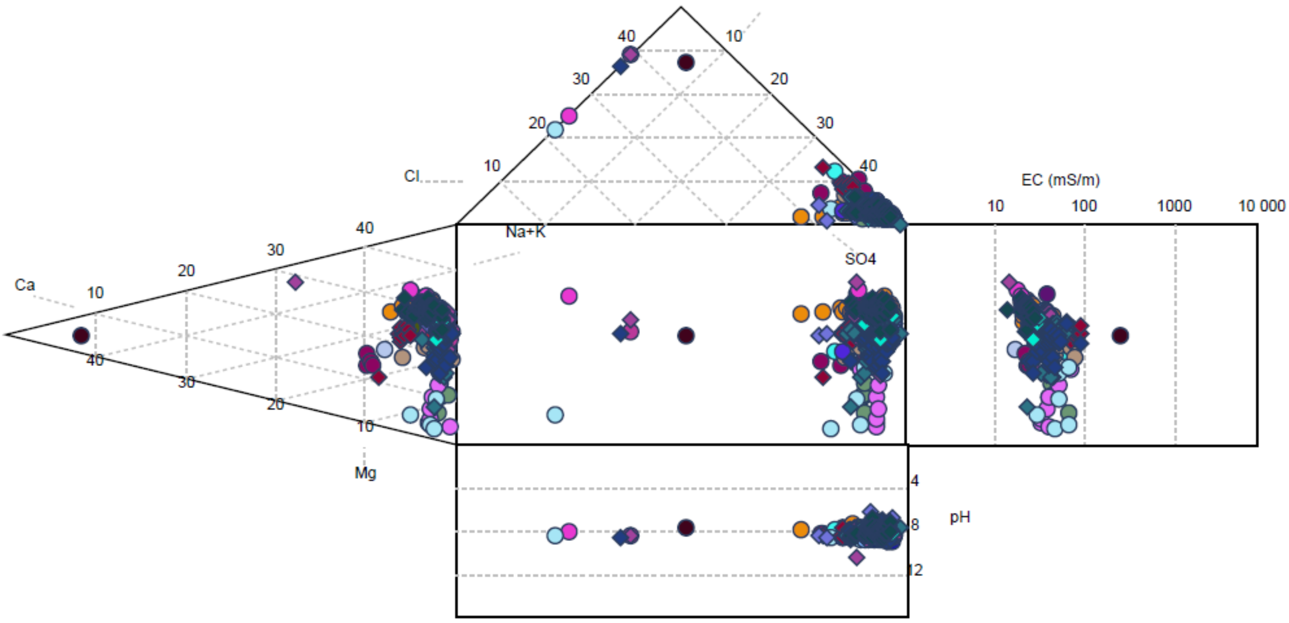

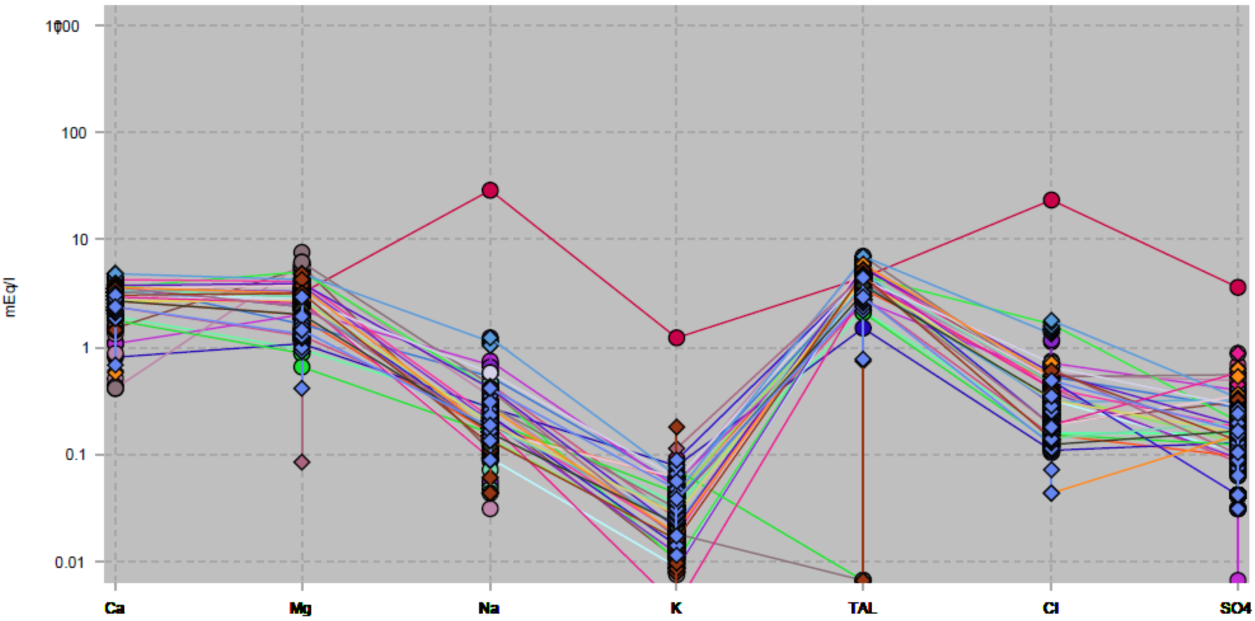

Quaternary Drainage Region D41M

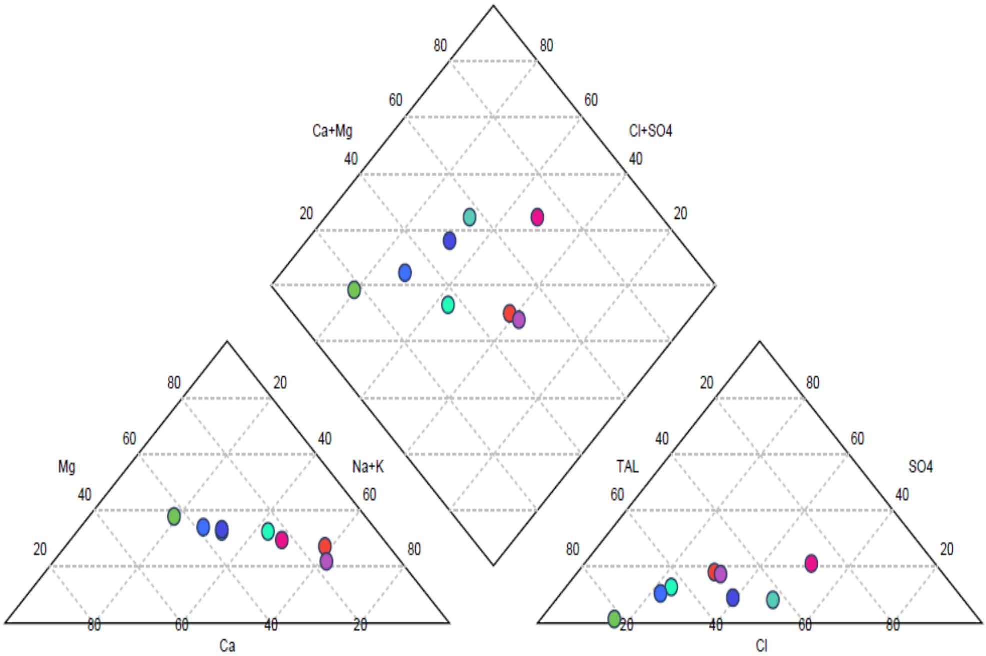

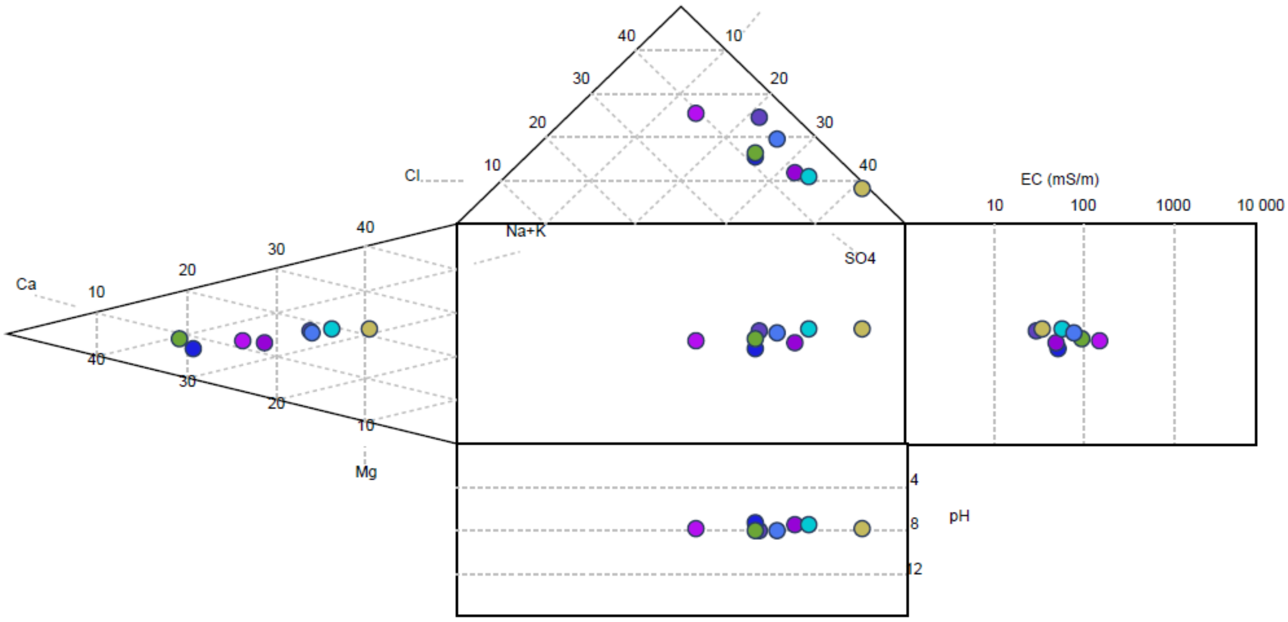

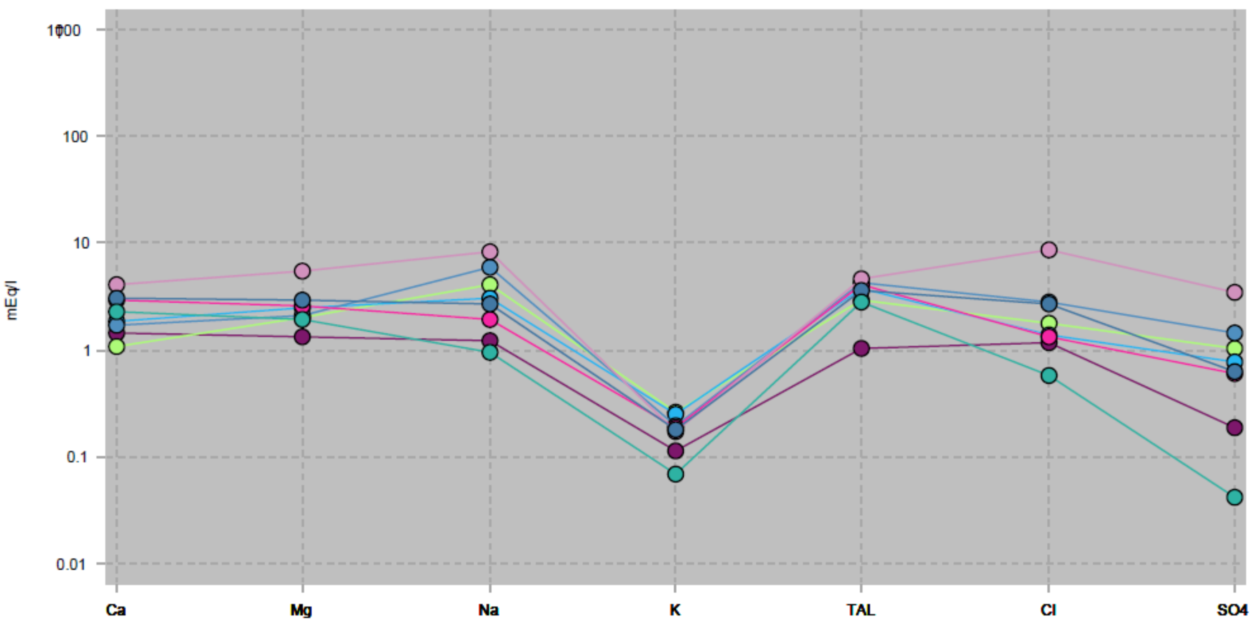

APPENDIX B

Historical Rainfall Data

Historical Rainfall Data from DWAF for the Kuruman Monitoring Point (D4E004)

YEAR	September	October	November	December	January	February	March	April	May	June	July	August	TOTAL
1961-1962	0.00	0.00	118.10	14.00	34.00	95.80	59.40	26.90	0.00	0.00	0.00	2.30	**350.50**
1962-1963	0.00	14.00	77.20	54.10	0.00	27.70	93.00	50.50	28.70	16.00	2.30	4.60	**368.10**
1963-1964	0.00	17.00	101.60	13.50	1.50	31.20	54.90	12.40	2.30	12.40	0.00	2.00	**248.80**
1964-1965	0.00	59.40	3.60	21.30	0.00	0.00	19.00	30.00	0.00	1.50	11.70	0.50	**147.00**
1965-1966	7.10	1.00	39.40	4.30	125.00	107.40	15.00	18.30	7.40	13.00	0.00	0.00	**337.90**
1966-1967	1.80	14.00	0.30	62.70	113.00	65.30	30.70	109.70	65.00	1.50	0.00	4.30	**468.30**
1967-1968	8.40	25.10	33.80	30.00	16.50	3.60	77.50	57.20	66.00	4.60	0.50	0.50	**323.70**
1968-1969	0.50	30.50	16.00	31.00	19.60	189.70	40.60	86.40	21.10	0.00	0.00	9.70	**445.10**
1969-1970	0.00	66.30	0.60	28.40	23.60	32.70	7.10	43.80	102.80	13.50	8.00	4.00	**330.80**
1970-1971	14.00	10.50	15.20	90.70	78.60	130.80	91.20	16.00	40.20	2.20	4.50	2.40	**496.30**
1971-1972	0.00	37.00	17.30	59.50	311.59	48.10	131.90	44.80	1.00	1.10	0.20	0.00	**652.49**
1972-1973	0.00	12.50	23.70	1.20	9.70	86.50	72.50	36.80	9.70	0.40	1.50	1.60	**256.10**
1973-1974	15.50	17.30	27.00	181.00	278.70	214.90	214.50	50.20	26.50	0.00	0.00	47.50	**1073.10**
1974-1975	2.80	27.50	55.50	43.00	124.10	85.60	245.40	35.30	3.00	1.90	1.90	0.50	**626.50**
1975-1976	8.90	21.00	74.70	174.00	316.41	131.90	187.20	78.10	23.80	12.10	1.50	0.40	**1030.01**
1976-1977	21.50	38.30	33.80	0.00	161.90	116.40	218.80	39.40	12.20	0.00	0.00	0.00	**642.30**
1977-1978	65.80	11.70	118.20	8.50	0.00	58.00	83.20	55.20	0.00	2.00	0.00	1.50	**404.10**
1978-1979	11.50	53.60	26.00	24.10	0.00	136.60	16.50	24.70	30.60	0.00	6.20	63.30	**393.10**
1979-1980	0.00	45.20	43.00	13.20	31.60	47.00	84.30	62.10	0.00	1.00	0.00	15.00	**342.40**
1980-1981	28.70	2.70	60.20	50.60	224.10	71.00	64.40	9.00	0.00	12.20	0.00	55.80	**578.70**
1981-1982	0.00	25.70	95.20	37.00	36.00	141.90	29.00	35.20	2.70	1.70	0.00	0.00	**404.40**
1982-1983	0.80	61.90	20.30	23.30	3.70	5.90	38.60	13.50	14.00	10.20	0.80	0.00	**193.00**
Average	**8.51**	**26.92**	**45.49**	**43.88**	**86.80**	**83.09**	**85.21**	**42.52**	**20.77**	**4.88**	**1.78**	**9.81**	**459.67**
											Median		**398.60**
											20 th Percentile		**296.66**
											Drought Index		**1.34**

Historical Rainfall Data from DWAF for the Olifantshoek Monitoring Point (D4E002)

YEAR	September	October	November	December	January	February	March	April	May	June	July	August	TOTAL
1960-1961	0.00	6.10	19.30	11.90	65.00	31.20	77.70	90.40	59.20	36.60	33.30	0.00	**430.70**
1961-1962	0.00	0.00	73.40	18.30	26.20	109.00	25.40	18.00	0.00	0.00	0.00	0.80	**271.10**
1962-1963	4.30	7.40	60.50	49.30	212.90	18.80	127.00	72.40	58.40	2.50	1.50	0.00	**615.00**
1963-1964	0.00	37.10	89.20	82.30	4.30	10.20	39.40	8.60	2.50	13.70	0.00	0.00	**287.30**
1964-1965	0.00	39.90	10.40	73.40	19.00	6.10	28.40	48.30	0.00	0.00	13.70	2.50	**241.70**
1965-1966	1.30	12.70	35.60	0.00	35.10	62.00	16.00	22.90	0.00	6.10	0.00	0.00	**191.70**
1966-1967	2.00	16.50	0.00	0.00	0.00	0.00	23.90	0.00	32.00	4.80	0.00	6.60	**85.80**
1967-1968	7.10	0.00	13.50	21.30	19.30	0.00	59.70	12.40	28.20	5.60	0.00	0.00	**167.10**
1968-1969	0.00	58.20	32.30	16.00	15.00	134.10	60.70	32.80	26.20	3.80	0.00	0.00	**379.10**
1969-1970	0.00	42.70	17.80	13.70	42.70	36.30	0.00	11.20	26.70	19.10	0.00	17.50	**227.70**
1970-1971	0.00	7.60	20.10	46.20	97.30	65.50	20.60	16.80	59.90	3.60	0.00	0.30	**337.90**
1971-1972	0.00	57.40	15.50	4.60	208.60	0.00	152.40	104.40	0.00	0.00	0.00	0.00	**542.90**
1972-1973	0.00	2.50	19.80	7.10	2.80	107.40	56.40	106.90	0.00	0.00	11.20	1.00	**315.10**
1973-1974	10.00	43.20	30.00	194.79	277.91	217.70	242.30	60.50	38.60	0.00	0.00	63.20	**1178.20**
1974-1975	2.00	25.10	47.80	47.20	9.70	46.70	181.10	79.20	9.00	5.70	0.00	0.00	**453.50**
1976-1977	44.20	23.10	0.00	0.00	145.50	75.70	82.00	38.10	0.00	0.00	0.00	0.00	**408.60**
1977-1978	21.09	7.00	18.00	38.60	56.40	0.00	80.00	50.50	0.00	6.00	0.00	15.00	**292.59**
1978-1979	12.50	14.20	12.00	0.00	42.91	61.50	8.20	49.80	30.00	0.00	0.00	48.30	**279.41**
1979-1980	0.00	21.80	0.00	0.00	29.60	21.10	56.40	19.60	0.00	0.00	0.00	20.10	**168.60**
1980-1981	0.00	0.00	11.20	76.70	62.00	0.00	52.09	0.00	0.00	11.90	0.00	8.00	**221.89**
1981-1982	0.00	0.00	20.80	0.00	9.40	31.80	22.40	26.90	0.00	0.00	23.91	0.00	**135.21**

YEAR	September	October	November	December	January	February	March	April	May	June	July	August	TOTAL
1982-1983	0.00	38.40	27.90	0.00	33.50	0.00	12.40	24.90	0.00	0.00	0.00	0.00	**137.10**
1983-1984	0.00	0.00	71.60	53.00	39.00	42.00	0.00	0.00	0.00	0.00	0.00	0.00	**205.60**
1984-1985	0.00	0.00	0.00	0.00	0.00	57.50	43.00	13.00	0.00	0.00	0.00	0.00	**113.50**
1985-1986	7.00	0.00	66.00	14.50	56.50	21.50	13.00	8.30	0.00	9.30	0.00	0.00	**196.10**
1986-1987	0.00	14.00	30.90	8.50	0.00	44.00	33.50	17.00	0.00	0.00	17.20	0.00	**165.10**
1987-1988	47.60	7.80	21.00	0.00	0.00	178.20	141.00	130.10	0.00	2.60	0.00	0.00	**528.30**
1988-1989	22.00	43.20	71.50	35.50	186.00	107.40	33.50	38.30	34.80	0.00	0.00	0.00	**572.20**
1989-1990	9.20	0.00	22.10	0.00	30.00	121.60	38.30	38.70	4.00	8.00	0.00	0.00	**271.90**
1990-1991	0.00	0.00	0.00	27.80	153.00	146.39	189.11	0.00	0.00	67.50	0.00	0.00	**583.80**
1991-1992	4.00	83.00	12.00	0.00	0.00	28.60	46.40	5.00	0.00	0.00	0.00	0.00	**179.00**
1993-1994	0.00	65.10	41.90	36.00	68.50	105.70	32.90	3.20	0.00	3.20	3.40	0.00	**359.90**
1994-1995	0.00	4.60	27.00	8.30	16.60	23.40	159.60	0.00	19.00	0.00	0.00	0.80	**259.30**
1995-1996	0.80	3.60	75.90	131.60	47.70	23.00	0.60	31.00	5.60	0.00	15.00	0.00	**334.80**
1996-1997	0.60	5.40	56.40	74.20	130.00	14.40	150.40	2.80	27.60	2.20	1.40	0.00	**465.40**
1997-1998	0.00	0.00	2.40	12.80	20.00	43.10	75.80	3.20	1.00	0.00	3.20	7.00	**168.50**
1998-1999	1.20	0.00	19.00	13.60	88.20	7.00	52.00	31.80	105.80	0.00	3.20	0.00	**321.80**
1999-2000	0.00	71.00	1.60	147.40	161.60	107.80	103.20	78.20	4.00	0.30	1.00	0.00	**676.10**
Average	**5.18**	**19.96**	**28.80**	**33.28**	**63.48**	**55.44**	**66.76**	**34.08**	**15.07**	**5.59**	**3.37**	**5.03**	**336.04**
											Median		**283.36**
											20 th Percentile		**168.58**
											Drought Index		**1.68**

Historical Rainfall Data from the Farm Thornthwaite (Tosca)

YEAR	September	October	November	December	January	February	March	April	May	June	July	August	TOTAL
1991-1992	25.0	49.0	9.0	14.5	17.0	32.5	42.0	7.0	0.0	0.0	0.0	0.0	**196.0**
1992-1993	0.0	10.0	111.5	11.5	30.0	121.0	18.5	8.0	0.0	6.5	0.0	0.0	**317.0**
1993-1994	0.0	58.0	48.0	40.5	75.0	69.0	11.5	15.0	0.0	0.0	0.0	0.0	**317.0**
1994-1995	0.0	5.0	25.0	75.0	77.5	15.0	116.5	11.0	7.0	0.0	0.0	0.0	**332.0**
1995-1996	15.5	25.0	61.5	75.5	73.5	106.0	8.0	21.0	29.5	0.0	9.0	0.0	**424.5**
1996-1997	8.0	9.0	88.5	151.5	50.0	75.0	117.5	81.0	23.5	0.0	0.0	0.0	**604.0**
1997-1998	41.0	24.0	12.0	48.0	106.5	101.5	111.0	3.0	0.0	0.0	0.0	0.0	**447.0**
1998-1999	5.0	42.0	61.0	86.5	84.0	18.0	9.0	0.0	18.0	0.0	0.0	0.0	**323.5**
1999-2000	0.0	36.0	33.5	129.5	133.0	35.5	102.0	25.5	33.5	0.0	0.0	0.0	**528.5**
2000-2001	8.5	32.0	88.5	36.5	21.5	51.5	102.0	110.5	62.0	0.0	0.0	0.0	**513.0**
2001-2002	62.5	34.0	77.0	86.0	92.0	7.0	27.0	6.0	30.0	0.0	0.0	38.0	**459.5**
2002-2003	3.0	28.0	11.3	83.5	54.0	64.0	52.0	18.0	6.0	0.0	0.0	0.0	**319.8**
2003-2004	0.0	15.0	46.5	5.5	71.5	55.0	51.5	35.5	0.0	0.0	0.0	0.0	**280.5**
2004-2005	2.0	14.0	6.5	58.0	76.5	25.5	20.0	72.5	0.0	0.0	0.0	0.0	**275.0**
2005-2006	0.0	18.0	98.0	0.0	110.5	186.0	94.5	47.5	3.5	0.0	0.0	0.0	**558.0**
2006-2007	0.0	26.5	41.0	25.5	26.5	9.5	13.5	26.5	0.0	12.0	0.0	0.0	**181.0**
2007-2008	65.0	46.0	32.0	78.5	216.0	42.0	149.0	3.0	42.5	0.0	0.0	0.0	**674.0**
2008-2009	0.0	14.5	30.5	10.0	205.0	86.0	56.0	15.0	18.5	82.0	3.0	0.0	**520.5**
2009-2010	0.0	130.5	61.0	19.0	244.5	104.5	122.5	69.0	22.0	0.0	0.0	0.0	**773.0**
2010-2011	0.0	6.0	63.0	64.0	185.5	86.5	47.5	44.0	16.0	33.0	0.0	0.0	**545.5**
2012-2013	9.0	10.5	13.0	106.0	84.0	36.5	28.0	12.5	0.0	0.0	0.0	0.0	**299.5**
2013-2014	0.0	8.0	0.0	59.0	82.5	274.0	62.0	13.0	20.0	0.0	0.0	11.5	**530.0**
Average	**11.1**	**29.1**	**46.3**	**57.5**	**96.2**	**72.8**	**61.9**	**29.3**	**15.1**	**6.1**	**0.5**	**2.3**	**428.1**

Median	**435.75**
20 th Percentile	**291.90**
Drought Index	**1.49**

Historical Rainfall Data from the farm Damplaas (Ganyesa)

YEAR	September	October	November	December	January	February	March	April	May	June	July	August	TOTAL
1972-1973	0.0	0.0	53.0	3.0	41.0	109.8	5.8	39.3	0.0	0.0	0.0	0.0	**251.8**
1973-1974	40.0	7.5	123.8	80.0	91.0	100.0	205.0	25.0	0.0	0.0	0.0	0.0	**672.3**
1974-1975	0.0	23.8	63.0	26.8	125.5	100.0	124.0	12.0	20.0	0.0	0.0	0.0	**495.0**
1975-1976	0.0	16.3	22.5	127.8	258.0	141.3	118.8	80.0	18.0	1.3	0.0	0.0	**783.8**
1976-1977	11.3	87.3	17.5	73.8	130.3	44.3	86.0	30.0	0.0	0.0	0.0	0.0	**480.3**
1977-1978	18.0	27.5	16.3	137.8	107.5	25.0	95.8	50.0	0.0	0.0	0.0	0.0	**477.8**
1978-1979	17.5	30.3	28.8	26.5	47.8	28.8	0.0	36.3	10.5	5.0	0.0	65.8	**297.0**
1979-1980	2.5	44.3	61.3	34.5	40.0	64.3	0.0	0.0	0.0	0.0	0.0	7.5	**254.3**
1980-1981	12.0	0.0	95.8	26.5	93.5	74.5	27.5	0.0	0.0	0.0	0.0	47.5	**377.3**
1981-1982	0.0	2.5	57.0	146.0	0.0	0.0	25.0	64.5	0.0	0.0	0.0	0.0	**295.0**
1982-1983	0.0	78.0	16.8	25.3	101.3	5.0	29.3	0.0	25.0	32.5	10.0	0.0	**323.0**
1983-1984	0.0	18.8	35.5	51.5	11.3	10.0	128.5	0.0	30.0	13.8	0.0	0.0	**299.3**
1984-1985	0.0	21.8	29.5	22.8	49.3	55.0	50.3	6.5	0.0	0.0	0.0	0.0	**235.0**
1985-1986	5.0	56.8	48.8	45.3	65.8	35.0	14.3	0.0	0.0	0.0	0.0	0.0	**270.8**
1986-1987	20.0	75.3	113.3	34.8	16.3	55.3	45.0	0.0	0.0	0.0	0.0	0.0	**359.8**
1987-1988	43.8	16.3	67.3	57.8	24.0	294.5	59.3	0.0	0.0	0.0	0.0	0.0	**562.8**
1988-1989	0.0	0.0	0.0	10.0	60.5	93.5	18.3	42.5	23.5	7.5	0.0	13.5	**269.3**
1989-1990	0.0	0.0	28.8	48.3	27.8	45.0	55.5	63.0	0.0	0.0	0.0	0.0	**268.3**
1990-1991	0.0	0.0	0.0	34.0	150.0	30.0	93.0	0.0	0.0	0.0	0.0	0.0	**307.0**
1991-1992	27.0	79.0	24.0	71.0	0.0	39.0	45.0	22.0	0.0	0.0	0.0	0.0	**307.0**
1992-1993	0.0	0.0	67.0	74.0	20.0	136.0	37.0	9.0	0.0	0.0	0.0	0.0	**343.0**
1993-1994	0.0	93.0	29.0	9.0	134.0	87.0	37.5	0.0	0.0	0.0	0.0	0.0	**389.5**
1994-1995	0.0	8.0	29.0	9.0	91.0	9.0	135.0	0.0	11.0	0.0	0.0	0.0	**292.0**

YEAR	September	October	November	December	January	February	March	April	May	June	July	August	TOTAL
1996-1997	0.0	0.0	96.0	148.0	71.0	18.0	162.0	75.0	32.0	0.0	5.0	0.0	**607.0**
1997-1998	21.0	27.0	30.0	11.0	82.0	116.0	92.0	53.0	0.0	0.0	0.0	0.0	**432.0**
1998-1999	10.0	33.0	98.0	93.0	80.0	40.5	54.0	26.0	86.5	0.0	0.0	0.0	**521.0**
1999-2000	0.0	22.0	18.0	152.0	206.0	38.0	31.0	19.0	27.0	0.0	0.0	0.0	**513.0**
2000-2001	0.0	40.5	83.0	85.0	9.0	88.0	91.0	120.5	55.0	48.0	0.0	5.0	**625.0**
2001-2002	92.0	58.0	113.0	104.5	158.0	76.0	0.0	6.5	20.0	6.0	0.0	52.0	**686.0**
2002-2003	0.0	60.0	8.0	79.0	78.0	127.0	44.0	19.0	2.0	0.0	0.0	0.0	**417.0**
2003-2004	0.0	15.0	28.0	14.0	133.0	56.0	56.0	0.0	0.0	0.0	0.0	0.0	**302.0**
2004-2005	0.0	0.0	9.0	59.0	113.0	25.0	60.0	67.0	0.0	0.0	0.0	0.0	**333.0**
2005-2006	0.0	10.0	70.0	27.0	123.0	266.0	200.0	137.0	0.0	0.0	3.0	0.0	**836.0**
2006-2007	0.0	45.0	71.0	69.0	11.0	0.0	40.0	0.0	0.0	31.5	0.0	0.0	**267.5**
2007-2008	76.0	49.0	62.0	64.0	189.0	58.0	95.0	0.0	78.0	0.0	0.0	0.0	**671.0**
2008-2009	0.0	14.0	111.0	35.0	102.0	31.0	32.0	6.0	6.0	66.0	0.0	0.0	**403.0**
2009-2010	14.0	63.0	27.0	4.0	181.0	89.0	34.0	39.0	27.0	0.0	0.0	0.0	**478.0**
2010-2011	0.0	0.0	29.0	90.0	131.0	81.0	103.0	84.0	33.0	55.0	0.0	0.0	**606.0**
2011-2012	0.0	0.0	27.0	166.0	59.0	68.0	38.0	0.0	0.0	19.0	0.0	0.0	**377.0**
2012-2013	0.0	14.0	16.0	110.0	42.0	34.0	39.0	29.0	0.0	0.0	0.0	0.0	**284.0**
2013-2014	3.0	6.0	40.0	59.0	83.0	202.0	77.0	5.0	15.0	0.0	0.0	11.0	**501.0**
2014-2015	0.0	12.0	69.0	142.0	71.0	8.0	57.0	14.0	0.0	34.0	0.0	0.0	**407.0**
Average	**9.8**	**27.5**	**48.4**	**64.0**	**85.9**	**71.5**	**65.3**	**28.1**	**12.4**	**7.6**	**0.4**	**4.8**	**425.6**
											Median		**424.50**
											20 th Percentile		**305.00**
											Drought Index		**1.39**